2006-37

Final Report

Application of Precast Decks and Other Elements to Bridge Structures

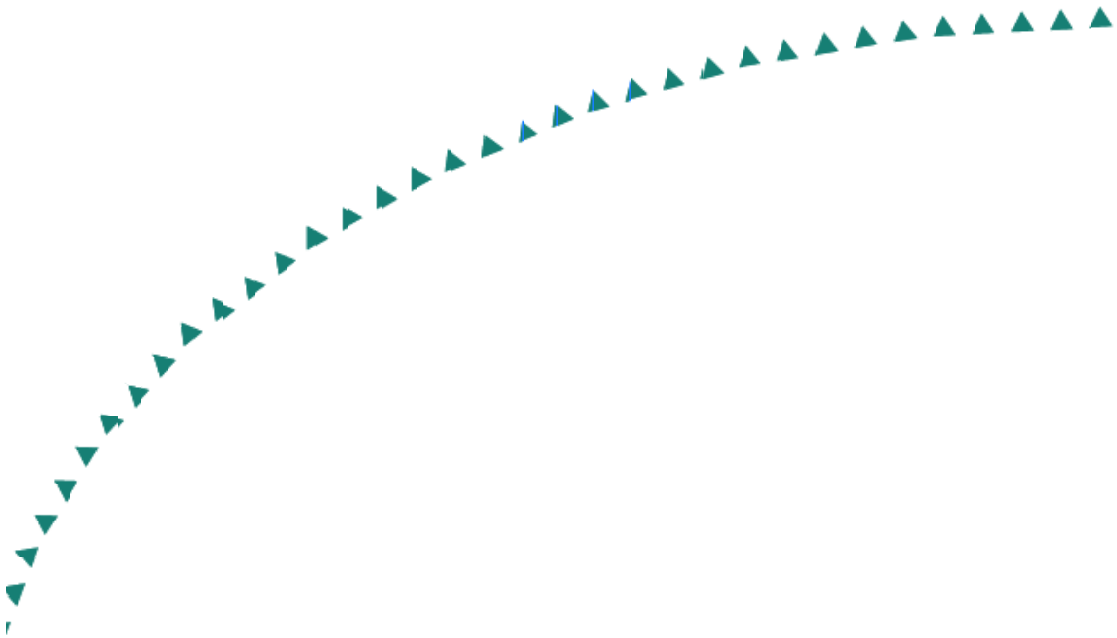

Research

Technical Report Documentation Page

1. Report No. MN/RC-2006-37	2.	3. Recipients Accession No.
4. Title and Subtitle Application of Precast Decks and other Elements to Bridge Structures		5. Report Date September 2006 6.
7. Author(s) Charles M. Bell II Catherine E. French Carol K. Shield		8. Performing Organization Report No.
9. Performing Organization Name and Address University of Minnesota Department of Civil Engineering 500 Pillsbury Drive, S.E. Minneapolis, MN 55455		10. Project/Task/Work Unit No. 11. Contract (C) or Grant (G) No. (c) 81655 (wo) 146
12. Sponsoring Organization Name and Address Minnesota Department of Transportation Research Services Section 395 John Ireland Boulevard Mail Stop 330 St. Paul, Minnesota 55155		13. Type of Report and Period Covered Final Report 14. Sponsoring Agency Code
15. Supplementary Notes http://www.lrrb.org/PDF/200637.pdf		

16. Abstract (Limit: 200 words)

A number of countries have incorporated precast components in bridge superstructures and substructures. Precast components include deck, abutment, and wall elements. Benefits of using precast elements in bridge construction include the high level of quality control that can be achieved in plant cast production compared to field cast operations and speed of construction afforded by the assembly of precast elements at the site rather than the time consuming on site forming and casting required in cast-in-place construction. Key components in the application of precast concrete to bridge structures are the connection elements. Connection details include the use of post-tensioning systems, and various connection details such as weld plates, studs in grout pockets, and shear keys. The Minnesota Department of Transportation (Mn/DOT) constructed a bridge incorporating precast elements to enable rapid construction. The objective of this study was to develop an instrumentation plan to enable investigation of the performance of this bridge. Researchers developed an instrumentation plan based on information provided by the Mn/DOT bridge office regarding the specific bridge details and behaviors to be investigated. The instrumentation plan included the types and locations of the instruments.

17. Document Analysis/Descriptors		18. Availability Statement	
Rapid construction Pourte Dalle	Slab span Precast deck	No restrictions. Document available from: National Technical Information Services, Springfield, Virginia 22161	
19. Security Class (this report) Unclassified	20. Security Class (this page) Unclassified	21. No. of Pages 271	22. Price

Application of Precast Decks and Other Elements to Bridge Structures

Final Report

Prepared by:

Charles Bell III

Carol K. Shield

Catherine French

Department of Civil Engineering
University of Minnesota

September 2006

Published by:

Minnesota Department of Transportation
Research Services Section
395 John Ireland Boulevard, MS 330
St. Paul, Minnesota 55155-1899

Acknowledgements

The work chronicled within this thesis was largely a team effort. A special thank you is also extended to Matthew Smith for his assistance throughout the project, specifically with the installation of instrumentation and set up of the data acquisition system. The following people are also greatly appreciated for the assistance they provided during the installation of instrumentation: Paul Bergson, Scott Nesvold, Justin Ocel, and Brian Runzel.

I would also like to thank the Minnesota Department of Transportation (Mn/DOT) and Lunda Construction for their contributions during this project. Mn/DOT provided all of the funding for this project. In addition, several Mn/DOT engineers and site inspectors provided assistance during the installation of instrumentation and preparation of the final report. The construction crew from Lunda Construction, the general contractor for the construction of Mn/DOT Bridge No. 13004, was very accommodating and cooperative during the entire installation of instrumentation process. Their patience and hospitality was crucial for the success of this project and therefore was greatly appreciated.

Table of Contents

List of Tables

List of Figures

Executive Summary

Prefabricated bridge construction presents many advantages over conventional construction methods. In prefabricated construction, elements are cast off-site and then brought to the site ready to be erected in-place. This eliminates major-time consuming tasks from the project timeline, such as erection and removal of formwork, placement of steel reinforcement and concrete, and curing of the concrete. The result is shorter construction time and a reduction in traffic disruption.

Many existing prefabricated bridge systems used in the United States have durability issues, such as longitudinal reflective cracking, which result in significant maintenance or replacement costs. This takes away from the advantages that would otherwise be associated with these types of systems. This has led to numerous research programs for the development of more durable prefabricated bridge systems.

In April of 2004, the Federal Highway Administration (FHWA) and the American Association of State Highway and Transportation Officials (AASHTO) initiated a scanning tour to explore the state-of-the-art technologies for rapid construction already being implemented in other industrial countries. During this scanning tour, a team of eleven members visited Japan, the Netherlands, Belgium, Germany, and France to identify international uses of prefabricated bridge elements.

The Minnesota Department of Transportation (Mn/DOT) developed a prefabricated superstructure system based on the Poutre Dalle system that was observed in France during the scanning tour. The Poutre Dalle system consisted of inverted-T precast members placed adjacent to one another and then topped with cast-in-place (CIP) concrete. The shape of these sections eliminates the need for formwork for the CIP concrete and provides a working surface for the placement of steel reinforcement and pouring of the CIP concrete.

The precast members of the Poutre Dalle system have transverse hooks that extend out of the vertical sides of the webs. Once in place, the hooks from adjacent sections extend over the longitudinal joints that exist between the adjacent precast sections and overlap with the hooks from the adjacent sections. Thus once the CIP concrete has cured these hooks tie the adjacent sections together.

The system that Mn/DOT developed, the Mn/DOT Inverted-T Precast Slab System, utilized two main design features of the Poutre Dalle system. These two features include the inverted-T precast section shape and the transverse hooks that extend from the vertical sides of the web of the precast sections. Mn/DOT used these features as the basis of their design; however modifications were made to increase the durability, performance, and constructibility of the design.

The largest concern affecting the durability of the system was the potential development of longitudinal reflective cracking above the longitudinal joints between adjacent precast sections. Thus, in addition to the transverse hooks crossing the precast longitudinal joint, a reinforcement cage was added to the CIP concrete directly above the joint. This increased the amount of reinforcement above this joint and therefore increased the load sharing capabilities of the CIP concrete at this location. The intent was to reduce the stresses in the CIP concrete and thus reduce the potential for the development of reflective cracking at these locations. The corners of the flanges and webs of the precast sections were also chamfered to reduce the stress concentrations at those locations and again reduce the potential for the development of reflective cracking.

Another issue of concern was the continuity of the superstructure system. The system was designed to be continuous for live load over the interior piers after the CIP concrete had cured, thus modifications were made to ensure that the system would provide adequate continuity. Continuity was achieved through the use of conventional deck reinforcement and concrete between adjacent precast sections above the piers. Additional reinforcement over the piers was added directly above the flanges of the precast sections to provide a positive moment connection in case a positive restraint moment was to develop above the piers over time.

The design of the Mn/DOT inverted-T Precast Slab System was tailored to the needs of two projects with different span arrangements with the idea that the precast section would be developed for short span ranges of 20 ft. minimum and 65 ft. maximum. One of the bridges (Mn/DOT Bridge No. 13004) was located in Center City, Minnesota about 40 miles northeast of Minneapolis. Instrumentation was installed in this bridge to monitor the behavior of the bridge over time. The main goal of the instrumentation plan was to investigate for the development of longitudinal reflective cracking of the CIP concrete above the precast longitudinal joints and above the precast section web corners. Several vibrating wire (VW) embedment strain gages oriented in the transverse direction were installed above the precast longitudinal joints and precast section web corners at three different locations within the bridge deck. These gages were used to monitor the development and propagation of cracks as would be evident by reading large local increases in strain. If a crack were to develop these gages could then be used to monitor the behavior of the crack over time.

The instrumentation plan also included several vibrating wire (VW) spot-weldable strain gages on the longitudinal reinforcement at different locations within the bridge deck to investigate the continuous behavior of the bridge over the interior piers for live load. At most of these locations, either two or three of these gages were installed so that the curvature of the bridge deck at that location could be determined. The majority of the information provided from these gages was to be obtained during a truck load test to be performed sometime during the two-year monitoring period of this bridge.

The results of this investigation will be used to verify some of the design assumptions and to determine if further modifications need to be made to the design of the Mn/DOT Inverted-T Precast Slab System to improve the performance of the system for future projects.

Chapter 1
Introduction

1.1 Background of Prefabricated Bridge Construction

Prefabricated bridge construction typically consists of fabricating bridge elements off-site and delivering them to the project location ready to be erected. This can include entire superstructure or substructure systems, or elements of each system. There are many prefabricated superstructure systems that consist of both prefabricated and cast-in-place (CIP) elements. Prefabricated bridge construction has been developed because it presents many advantages over conventional bridge construction including speed of erection and improved quality control due to plant fabrication. However, many current systems have durability issues, such as the development of cracking, which reduce the benefits of this type of system. Thus, new systems are constantly being developed to produce systems with improved durability.

1.2 Advantages of Prefabricated Bridge Construction

Prefabricated bridge construction presents many advantages over conventional bridge construction. First, major time-consuming tasks such as the erection and removal of formwork, placement of steel reinforcement and concrete, and concrete curing need not be accomplished in the work zone. The elements can be prefabricated off-site or adjacent to the site, concurrently with the on-site construction, then brought to the site and quickly erected into place. This can significantly compress the construction project timeline and reduce traffic disruption (Ralls et al., 2002). This is especially important in colder climate states, like Minnesota, which must concentrate a large number of projects into the few months available for construction (Hagen et al., 2005).

At construction sites, workers are often exposed to dangerous situations such as working close to traffic, near power lines, or over water. Fabricating the elements off-site, in a safe environment reduces the amount of time workers are exposed to these potentially dangerous situations (Ralls et al., 2002).

The erection and removal of formwork for placement of steel reinforcement and concrete in conventional bridge construction requires significant access to the underside of the bridge for workers and equipment. This can have a negative impact on the environment adjacent to the bridge. The use of prefabricated elements gives contractors more options and can often reduce the impact bridge construction has on its surroundings (Ralls et al., 2002).

The use of prefabricated elements also increases the overall quality of the product. By fabricating the elements off-site, work can be done ahead of time, using as much time as necessary, and often in a much more controlled environment. Plant operations are often standardized therefore ensuring quality control (Ralls et al., 2002). This results in a more durable product resulting in lower life cycle costs. Also, many times the same elements can be used for different projects and this repeatability often results in large economic benefits as well (Ralls et al., 2002).

1.3 Scanning Tour

The highway bridges of the United States are being subjected to an ever increasing volume of traffic. Many new bridges need to be built and many existing bridges are in need of replacement. Thus, new systems need to be developed that realize the many advantages

associated with prefabricated construction. The Federal Highway Administration (FHWA) and the American Association of State Highway and Transportation Officials (AASHTO) initiated a scanning tour in April of 2004 to explore the state-of-the-art technologies for rapid construction already being implemented in other industrial countries (FHWA, 2004).

A team of eleven members (three representatives from FHWA, four representatives from state departments of transportation, one representative from county engineers, one university representative, and two representatives from industry) visited Japan, the Netherlands, Belgium, Germany, and France with the overall objectives to identify international uses of prefabricated bridge elements and systems and to identify decision processes, design methodologies, construction techniques, costs, and maintenance and inspection issues associated with use of the technology (FHWA, 2004). The team was interested in all aspects of design, construction, and maintenance of bridge systems composed of multiple elements that are fabricated and assembled off-site (FHWA, 2004).

Of the many systemes observed, two of the systems had a similar methodology of handling the joint between the precast components by utilizing a joint with a liberal amount of reinforcement tied from the precast element into the joint area. Those superstructure systems also eliminated the need to place and remove formwork, thus accelerating construction and improving work-zone safety. The first system, which consisted of partial-depth concrete decks prefabricated on steel or concrete beams, was found in Germany and is shown in Figure 1.1. This system involved casting small concrete decks on steel or concrete beams prior to erection of the beams. After the beams are erected, the edges of each deck unit abut the adjacent member and there is no need to place additional formwork for the CIP concrete. This process speeds construction and reduces the potential danger of equipment falling onto the roadway below because a safe working surface is available immediately after beam erection (FHWA, 2004).

The second superstructure system, the Poutre Dalle system, was observed in France and is shown conceptually in Figure 1.2. In this system, inverted-T precast sections are placed adjacent to each other and then made composite with CIP concrete placed between the webs of the tees and over the tops of the stems to form a solid member. This system also eliminates the need to place and remove formwork and also provides a safe working surface (FHWA, 2004).

1.4 Implementation of Technology

The Minnesota Department of Transportation (Mn/DOT) developed an Inverted-T Precast Slab system based on the French Poutre Dalle system that was observed during the scanning tour. Two main features of the Poutre Dalle system were incorporated into the design of the Mn/DOT Inverted-T Precast Slab system; the section shape and the use of transverse reinforcement protruding out of the vertical sides of the precast section web. Both of these features can be seen in Figure 1.3 which shows a typical precast section used in the Poutre Dalle system in France. It was felt that both of these features could be utilized to produce a durable bridge superstructure system that was easy to construct.

The Mn/DOT Inverted-T Precast Slab system was developed by Mn/DOT engineers with input from fabricators, contractors, and faculty from the University of Minnesota. Conversations were held with local precasters to ensure constructibility by local fabricators and contractors with the idea that the inverted-T precast section would be developed for various short spans, ranging from 20 ft. to a maximum of 65 ft. After the design of the system was developed, this system was implemented in two bridge projects. Project No.1 was a bridge built over Center Lake Channel in Center City, Minnesota (Mn/DOT Bridge No. 13004), located about 40 miles

northeast of Minneapolis, Minnesota. Project No. 2 was a deck replacement for a bridge over the Tamarac River in Beltrami County in Waskish Township in northern Minnesota (Mn/DOT Bridge 04002).

1.5 Purpose of this Study

The objective of this study was to monitor the bridge built for Project No. 1 in Center City, MN (Mn/DOT Bridge No. 13004) for a period of two years to evaluate the durability and performance of the new system. The bridge was instrumented to monitor for the potential development of longitudinal reflective cracking in the CIP concrete portion of the bridge and to investigate the continuous behavior of the bridge deck for live load. This report describes the design of the Mn/DOT Inverted-T Precast Slab system and the test bridge, as well as the instrumentation and data collection system used to monitor the bridge.

1.6 Organization

Chapter Two of this report is a summary of the literature on existing prefabricated bridge superstructure systems, primarily focused on problems associated with these existing systems. Chapter Three summarizes the design of the Mn/DOT Inverted-T Precast Slab system and the implementation of this system in the test bridge (Mn/DOT Bridge No. 13004) used for this study. Chapters Four and Five present the instrumentation and the data collection system used in the test bridge, respectively. Chapter Six presents a summary and plans for future work.

Chapter 2
Literature Review

2.1 Introduction

Prefabricated concrete bridge superstructure systems have many variations. These systems are typically made of precast concrete elements oriented in either the longitudinal or transverse direction. Elements that are oriented in the transverse direction are typically decks supported by steel or prestressed concrete girders and either span from one girder to the next or the entire width of the bridge. Elements oriented in the longitudinal direction typically cross the entire span from pier cap to pier cap or abutment.

The remainder of Section 2.1 presents some typical prefabricated bridge superstructure systems found in the United States. Section 2.2 presents details on connection systems used to create continuity among the different elements of the bridge deck, including the advantages and disadvantages associated with each type of system. Section 2.3 explains the methods used for achieving continuous behavior over the piers and problems associated with achieving continuity. Sections 2.4 and 2.5 present summaries of studies performed on prefabricated bridge systems similar to the Mn/DOT Inverted-T Precast Slab System.

2.1.1 Precast Panel Systems with Transverse Joints

There are two systems commonly found in the U.S. that consist of precast panels oriented in the transverse direction The first system consists of full-depth non-prestressed concrete panels supported by either steel or prestressed concrete girders. Because of the many advantages associated with prestressed concrete, a Full-Depth Precast Prestressed Panel System has recently been developed (Yamane et al., 1998). Figure 2.1 shows a schematic of the Full-Depth Precast Prestressed Panel System. This system does not require any additional wearing course, however in many instances a non-structural bituminous pavement is used to provide a smooth driving surface (Hieber et al., 2004).

The other system commonly found in the U.S. that utilizes precast panels oriented in the transverse direction is known as a partial-depth precast panel system. This system consists of relatively thin prestressed panels that span between either steel or prestressed concrete girders and are topped with a CIP concrete topping. These panels are typically only 2.5 to 4 in. thick and span up to 6 ft. between adjacent girders. The tops of these precast panels are roughened to help achieve composite action with the CIP concrete topping. Figure 2.2 shows a cross-sectional view of a typical partial-depth precast panel system. This figure shows this type of system supported on both a steel girder and a prestressed concrete girder.

2.1.2 Prefabricated Bridge Systems with Longitudinal Joints

Prefabricated concrete bridge superstructure systems that consist of full-span precast elements exist in numerous different variations. Some of the precast elements commonly used in these systems include precast panels, box girders, T-beams, and inverted T-beams. Table 2.1 lists details of several examples of precast sections typically used in prefabricated concrete bridge superstructure systems built within the U.S. and other countries. These elements are constructed using prestressed concrete because it allows them to have longer spans along with shallower cross-sectional depths. The prestressing also provides better crack control within each element (Yamane et al., 1998). The precast elements of these full-span systems are usually

topped with a CIP concrete topping or a non-structural bituminous pavement to produce a smooth driving surface.

2.2 Prefabricated Concrete Bridge Superstructure Connection Systems

In prefabricated concrete bridge superstructures the precast sections are connected to one another in order to produce continuity within the bridge deck system and provide load sharing in each direction. The connection is typically achieved with either a longitudinal or transverse post-tensioning system, a shear key system, a CIP concrete topping, or some combination of these components. This section briefly explains each type of connection system along with associated advantages and disadvantages.

2.2.1 Post-tensioning Systems

Post-tensioning is typically added to systems to connect adjacent precast sections to achieve continuity within the deck system. Systems that utilize post-tensioning typically have post-tensioning tendons oriented perpendicular to the prestressing strands that exist within the precast elements. Figure 2.3 shows the cross section of a box-girder bridge system that utilizes transverse post-tensioning. In this system, the transverse post-tensioning allows for adequate load transfer from one element to the other in the transverse direction (El-Remaily et al., 1996). Figure 2.4 shows the elevation view of a Full-Depth Precast Prestressed Bridge Deck System. The longitudinal post-tensioning in this system allows for adequate load sharing from one element to the other in the longitudinal direction (Yamane et al., 1998). Often times cracking is a concern in full-depth panel systems, however, the two-way stressing created by the combination of prestressing and post-tensioning in this system ensures continued compression of the deck cross section during its service life providing good crack control and producing a very durable deck system (Fallaha et al., 2004).

The use of post-tensioning, however, has disadvantages. First, the large amount of post-tensioning required in these systems is typically very costly and additional time is required to install post-tensioning in the field which greatly diminishes the economic benefits otherwise associated with prefabricated construction (Badie et al., 1999). The use of post-tensioning also often requires the mobilization of a specialty contractor and increased construction monitoring to assure post-tensioning operations are performed in accordance with their special requirements which further increase the initial construction costs.

2.2.2 Shear Key Systems

Shear key systems serve two important functions. These systems effectively connect adjacent precast sections, providing adequate load transfer, while also serving to waterproof the joint. A shear key system consists of small voids between adjacent precast sections, extending along the entire length of each section. Once the precast sections are in place, the void is filled with rapid-set non-shrink grout (Yamane et al., 1998). Figures 2.5 and 2.6 show examples of different geometries used for typical shear keys found in box girder and full-depth precast panel systems, respectively.

The problem with shear key systems is that the failure of shear keys sometime during their service life is a fairly common phenomenon, especially for shear keys located in joints that are adjacent to the normal-driving-lane wheel tracks (Huckelbridge, Jr. et al., 1995). The failure of these shear keys has an effect on both the strength and serviceability of the bridge. It compromises the lateral load distribution of the bridge, which results in individual girders being

exposed to greater live loads than those for which they were designed (Huckelbridge, Jr. et al., 1995). Failure of the shear keys also results in excessive relative displacements between adjacent girders which typically leads to failure of the deck waterproofing system, resulting in the infiltration of water and waterborne contaminants through the inter-girder joints (Huckelbridge, Jr. et al., 1995). This exposure to deicing chemicals results in corrosion of the conventional reinforcement and, more importantly, of the prestressing strands adjacent to the joint. This can eventually compromise the structural integrity of the entire bridge deck system (Huckelbridge, Jr. et al., 1995).

2.2.3 Cast-in-place (CIP) Concrete Topping

CIP concrete can be placed on top of precast sections to produce a smooth riding surface. However, the use of a CIP concrete topping also serves other functions. First, the CIP concrete topping serves to connect adjacent girders creating continuity within the deck system and providing a means for transverse load sharing. In addition, this topping can be used compositely with the precast sections to improve the structural performance of the system (Hays, Jr. et al., 1980). However, in order to achieve composite action, the CIP concrete must be effectively tied to the precast sections. An effective connection is typically achieved through shear reinforcement protruding from the precast sections and/or roughened contact surfaces on the precast sections (Hays, Jr. et al., 1980).

General drawbacks to the use of a CIP concrete topping include a relatively low speed of construction, the need for strict field quality control, and the possibility of cracking due to the differential shrinkage between the CIP concrete topping and the precast sections (Fallaha et al., 1996). In addition, longitudinal reflective cracking often develops in the CIP concrete topping above the joints formed between adjacent sections (Badie et al., 1999). These cracks develop because sections that are not rigidly connected in an effective manner (i.e., no post-tensioning, ineffective shear keys or shear key failure) relegate load sharing in the transverse direction to occur through the CIP concrete. This can produce tensile stresses in the CIP concrete above the joints which can then lead to the development of longitudinal reflective cracking (Badie et al., 1999).

The development of reflective cracking is a major concern because once this cracking develops water and deicing chemicals are able to penetrate through the cracks which can then lead to concrete staining and spalling along with reinforcement corrosion (Badie et al., 1999). This can lead to the need for repair or even replacement which would create more traffic delays and increased costs, taking away from the advantages associated with using prefabricated construction.

2.3 Continuity for Live Loads over Interior Piers

Many prefabricated bridge superstructures are designed to behave continuously for live loads because continuity allows the bridge deck to consist of longer spans or fewer lines of girders, either of which result in lower overall costs compared to a simple-span design (McDonagh and Hinkley, 2003). Use of continuity in precast superstructure systems also reduces the number of longitudinal joints where durability is a concern. However, if a bridge is designed to behave continuously but the design does not provide adequate means to achieve the desired continuity, the bridge could fail at much smaller loads than it was designed to handle.

In practice, there are two different methods that are commonly used to create continuity in concrete bridge decks. The most common method involves the use of CIP concrete

diaphragms and conventional reinforcement in the CIP concrete deck. The girder ends are embedded in the diaphragms, therefore under loading, the diaphragms provide compressive resistance and the conventional reinforcement in the deck provides tensile resistance, thus combining to create negative moment resistance at this location (Saleh et al., 1995). Figure 2.7 shows a detail of an interior joint in a precast concrete girder bridge made continuous through the use of conventional deck reinforcement. The girders act as a simple-span under their own weight, the deck weight, and the construction loads, but behave continuously after the CIP concrete cures, under the effects of a relatively small superimposed dead load and live load (Saleh et al., 1995).

The other method commonly used in practice to create continuity consists of full-length post-tensioning. In this system, post-tensioning tendons are stressed after the CIP concrete deck and diaphragms have cured. Figure 2.8 shows an elevation view of a typical bridge deck with longitudinal post-tensioning. The post-tensioning provides resistance to the superimposed dead load and the live load (Saleh et al., 1995). This method for achieving continuity provides greater resistance to stresses and allows longer spans for a given girder size than the conventional deck reinforcement continuity method (Saleh et al., 1995). However, as explained in Section 2.2.1 there are some drawbacks to the use of post-tensioning systems within the bridge deck.

Regardless of the method used to achieve continuity, the amount of continuity within the system is affected by long-term effects such as creep and shrinkage. The concrete of the girder creeps as a result of the prestressing force which over time could cause the girder to camber further upwards (McDonagh and Hinkley, 2003). If there is no positive moment reinforcement over the piers, this movement can cause a gap to open at the bottom of the girder ends. Then, as loads are imposed, the girders act as simple spans until the load is large enough to close the gaps (McDonagh and Hinkley, 2003). However, if there is a positive moment connection between the girders at the piers, the upward creep will cause positive restraint moments to develop in the girders. These positive restraint moments combined with the superimposed moments of the continuous span result in a lower negative moment over the piers and a higher positive moment at the midspans (McDonagh and Hinkley, 2003). Therefore regardless of the positive moment connection at the pier, girder creep effectively reduces the amount of continuity within the system resulting in higher positive moments in the girders at the midspans (McDonagh and Hinkley, 2003).

Differential shrinkage between the CIP concrete deck and the girder concrete has the opposite effect on the amount of continuity within the system. By the time the deck concrete is poured, the girders have already had time to undergo some shrinkage. Therefore the shrinkage of the deck concrete exceeds the remaining shrinkage of the girder concrete resulting in a downward deflection of the composite bridge deck system (McDonagh and Hinkley, 2003). This results in the development of a negative restraint moment above the piers. Depending on the positive moment connection, this will either help to close the gaps at the girder ends or offset the positive restraint moments caused by the previously discussed creep effects, therefore effectively increasing the amount of continuity within the system (McDonagh and Hinkley, 2003).

The age of the girder at the time continuity is established has a large influence on the effect that creep and shrinkage have on the effective continuity within the system. The amount of creep and shrinkage remaining to develop within the girder decreases as the girder gets older. The less amount of creep remaining results in smaller gaps at the girder ends or smaller positive restraint moments, depending on the positive moment connection at the piers (McDonagh and Hinkley, 2003). The less shrinkage left to develop within the girder results in a larger shrinkage

differential between the CIP concrete deck and girder concrete which works to counter-act the effect of girder creep and shrinkage, further reducing the gaps at the girder ends or positive restraint moments. Therefore, as the girder gets older prior to the time continuity is established, it leads to smaller gaps at the girder ends or smaller positive restraint moments, which ultimately increases the amount of effective continuity within the deck system (McDonagh and Hinkley, 2003).

2.4 Case Studies Performed on Full-Span Form Panel Bridge Systems

The Mn/DOT Inverted-T Precast Slab System closely resembles a system commonly referred to as the Full-Span Form Panel Bridge System. This system consists of precast prestressed concrete form panels oriented in the longitudinal direction that cross the entire span between supporting piers, covered with a CIP concrete topping. The panels in this system are typically flat but sometimes have beveled edges adjacent to the longitudinal joints. Three studies performed on this system over the years are summarized in this section. These summaries include the objectives of the studies, testing procedures, and results and conclusions made as a result of the studies.

2.4.1 Hays, Jr. et al. Study

Hays, Jr. et al. (1980) performed a study on Full-Span Form Panel Bridge systems during the late 1970s to develop details that would reduce the development of reflective cracking that were almost always observed within the CIP concrete topping above the longitudinal joints of existing full-span form panel bridges at the time. They hoped to accomplish this through a research program that consisted of four phases: a field survey on the condition of existing bridges, analytical modeling, laboratory testing, and field testing on an existing bridge.

Field Survey

The field investigation included visits to a total of nine bridges that had been constructed using the Full-Span Form Panel System. The dimensions of the panels and CIP concrete for each bridge are provided in Table 2.2. Although there were variations in intensity and frequency, each of these bridges exhibited extensive reflective cracking in the CIP concrete topping above the longitudinal joints. Negative moment cracking was also observed above some of the piers. The longitudinal reflective cracking was observed above every longitudinal joint and extended for virtually the full length of the bridge. One bridge, the Sampson River Bridge, was visited prior to being opened to traffic and it already exhibited several major longitudinal cracks. Therefore it appeared that shrinkage had an influence on the development of the longitudinal cracking in those bridges. Note Table 2.2 includes a "comment" column that notes variations in these general observations.

In addition to the nine full-span form panel bridges visited, other bridges constructed using more conventional techniques such as a flat slab bridge with a CIP concrete deck slab or girders with either a CIP concrete deck or composite deck panels oriented in the transverse direction were visited. All of these bridges also exhibited cracking. The cracking in these bridges appeared to be less extensive and their pattern appeared to be much more random, whereas in the case of the full-span form panel bridges the excessive cracking always occurred directly above the longitudinal joints formed by the adjacent panels.

Finite Element Analyses

Two types of analytical modeling were performed. Linear elastic finite element models were used to approximate stress and displacement distributions from working loads and concrete shrinkage strains. In addition, nonlinear discrete element models were used to investigate structural behavior over a range of load levels up to ultimate strength.

Two plane stress finite element models were used to analyze stress distributions due to shrinkage throughout typical transverse bridge deck cross sections. The first model consisted of one form panel and the corresponding CIP concrete topping and the second model consisted of five form panels and the corresponding CIP concrete topping. A shrinkage strain was induced by specifying a coefficient of thermal expansion of 0.00001 in./in./°F for the finite elements of the CIP concrete topping along with a uniform decrease in temperature of 40°F. Both models were given constant values of 4000 ksi for the elastic modulus and 0.15 for the Poisson's Ratio and it was assumed that a "no-slip" condition existed between the CIP concrete topping and the form panel.

The finite element solutions obtained using these two models revealed that the top fiber stress increased towards the center of each form panel, however the maximum tensile stress occurred at the top fiber directly above the longitudinal joints where there was an abrupt increase in tension. This maximum top fiber stress exceeded the modulus of rupture. Because these models supported the observations of cracking, even within bridges that had not yet been open to traffic, it became evident that shrinkage must be considered as a major source of the stresses which cause longitudinal cracking over the longitudinal joints.

Three finite element models of the three full-span form panel laboratory specimen were used to analyze the effects of concentrated working loads. The longitudinal joint between form panels was represented in the finite element model by a decreased thickness of the specimen over an exaggerated width at the location of the longitudinal joint. The thickness of the specimen in the finite element model at this location was equal to the thickness of the CIP concrete topping. The joint width was exaggerated to approximately the size of the bridge deck thickness because preliminary finite element solutions suggested that this would provide the most accurate results from the finite element method.

Laboratory Testing combined with Finite Element Analyses

As mentioned previously, three separate specimens were constructed and tested for the laboratory phase of this project. Each specimen had two spans with two precast prestressed panels in each span for a total of four panels per specimen. An elevation view of the laboratory specimen is shown in Figure 2.9. The two cross sections considered in the test are shown in Figures 2.10 and 2.11. Specimen #1 used the standard cross section of constant thickness precast panels for both spans. Specimens #2 and #3 used the standard cross section for one span and the alternative cross section for the other span. A minimum 2.25" CIP concrete topping was added on top of the precast sections to provide a constant total thickness for the two spans of each specimen. A cold joint was constructed over the longitudinal joint of Specimen #3 to represent a worst-case condition. It was felt that this would provide a potential cracking plane. The joint was artificially roughened to increase the shear friction force transmitted through the joint.

Once the concrete of the CIP concrete deck was poured, an attempt was made to measure creep and shrinkage deflections during the curing time. However, no appreciable deflections occurred due to the short spans and relatively stable curing conditions. Also, there were no signs

of shrinkage cracking in any of the specimens. The deflection of each specimen was measured from the top of the CIP concrete topping on three lines along the length of the specimens.

Loading was applied nominally symmetric about the center support, 6 ft. from the support centerline. Hydraulic jacks were used to apply concentrated forces over the center of one of the precast panels in each span. The jacks were connected in parallel to provide an equal load in each span.

For the first two load increments near the design load either no cracking or minor hairline cracking was observed over the supports due to negative moment. Prior to failure, extensive negative moment cracking was observed over the full width of the specimen. Positive moment cracks were observed under the loaded panel and in some cases under the unloaded panel. Even after extensive cracking, the specimen had continued load capacity and exhibited good ductility. Failure occurred via a punching shear failure. No longitudinal cracking was observed except in Specimen #3, which was built with a cold joint over the longitudinal joint between form panels. No problems were found with the bond between the CIP concrete topping and the precast panels.

The data from the laboratory tests were used to obtain the chord displacement for each specimen. These chord displacements were compared to finite element solutions obtained using plate bending models of the three full-span form panel laboratory specimens and one plate bending model that did not include a longitudinal joint. This comparison showed that there was good correlation between the experimental data and the finite element solutions for the models of the three full-span form panel laboratory specimens. The comparison of the experimental data with the finite element solution for the model that did not include a longitudinal joint showed that the presence of a longitudinal joint greatly decreases the overall stiffness of the section due to the loss of two-way action. Since there was good correlation, the finite element models of the lab specimens were used to explore moment distributions. The results of these analyses showed that the presence of the longitudinal joint increased the positive and negative moment in each panel, again due to the loss of two-way action, and greatly affected the magnitude and distribution of the transverse moment. The transverse moment went from positive on the panel being loaded to negative on the unloaded panel. In addition, the presence of the longitudinal joint largely increased the torsional moment within the unloaded panel in both the positive and negative moment regions of the laboratory specimen.

The load-displacement response obtained from the experimental results was compared to the finite element solution obtained by performing a non-linear elastic analysis with a model that utilized discrete elements. This comparison showed that the non-linear analysis predicted much less ductile behavior and generally predicted failure at a smaller loading. However, the predicted failure loads from the analysis were still much higher than the design loads. The researchers concluded from these analyses that in spite of the large torsional moments, the laboratory specimens were able to transfer a sufficient amount of load across the longitudinal joint to develop more than the limit design strength based on the entire width of the specimen cross section at both the positive and negative moment sections. They felt that the major source of conservatism in the limit design values was in the approximate equation for the ultimate positive moment of the prestressed section.

Field Testing

One of the bridges visited during the field survey, the Lloyd Creek Bridge, was used for the field testing portion of this project. This bridge contained eight spans and each span had a length of 23 ft. The precast panels had a thickness of 7 in. with a CIP concrete topping thickness

of 5.5 in. The loading was applied by jacking against the bottom of a large tank trailer that had its wheels positioned over the piers. The load was applied at the midspan of Span 8 at three different transverse locations of one of the interior panels. These locations included the center of the panel and 1 ft. from each edge. The load was applied in 8 kip increments until a maximum load of 32 kips was applied which was approximately 1.5 times the design wheel load.

The load-deflection results showed that the load was indeed transferred across the longitudinal joints. Differential deflections across a longitudinal joint were in no case more than 6% of the total joint deflection under the applied load. These deflections were compared to the finite element solution obtained using a plate bending finite element model of spans 7 and 8 of the bridge. It was found these deflections showed good correlation to the finite element solution. Therefore this model was used to estimate moment distributions across the bridge. The maximum longitudinal moments from the finite element solutions compared well with computations based on the effective width formula from AASHTO (2004). Examination of the transverse moment distribution using the finite element solutions revealed that the stresses at the joint were high and indicated tension on the interface between the panels and the CIP concrete topping. Therefore the researchers concluded that steel reinforcement was needed in both the top and bottom of the CIP concrete topping.

Conclusions

After finishing the field survey, analytical modeling, and laboratory and field tests, the researchers observed that loss of bond between the CIP concrete topping and the precast panels did not occur. They attributed this to the roughness of the surface, however, they recommended that a minimum amount of shear reinforcement be used between the precast and CIP concrete to provide a factor of safety.

The researchers concluded, based on field observations and finite element testing, that stresses sufficiently high to cause shrinkage cracking in the CIP concrete can be expected. Based on laboratory and field tests, the researchers recommended a minimum amount of transverse steel reinforcement of #4 bars at 12 in. spacing and a minimum CIP concrete topping thickness of 4.5 in. They felt that this detail would provide adequate load transfer between adjacent panels and help to alleviate some of the shrinkage cracking. In addition, they felt that the panels with the alternative section design would give improved performance with regards to longitudinal cracking and load transfer. The recommended detail for this alternative section is shown in Figure 2.12.

The researchers also felt that an improved detail over the piers and end abutments with more positive transfer of shear from the panels to the supports would decrease deformations and cracking in these areas and increase the stiffness of the bridge. This could be accomplished by providing some direct bearing of the panels on the CIP concrete over the piers. They also recommended that positive moment reinforcement over the piers be provided.

2.4.2 Buckner and Turner Study

Buckner and Turner (1981) performed a study shortly after the study performed by Hays, Jr. et al. (1980) to investigate the effect of repetitive loading on the serviceability and strength of Full-Span Form Panel Bridge Systems. This study consisted of an experimental program in which six single-span simply-supported bridge decks were loaded repetitively with 2,000,000 cycles of design load followed by a test to failure. The performance was evaluated primarily based on flexural rigidity, differential deflection between panels, and the strength and ductility of

the composite system. Also considered in evaluating the specimens were visible cracks in the concrete, prestressing strand slip, and strains in the transverse steel. The objectives of this study were to develop recommendations for minimum CIP concrete topping thickness, a minimum quantity of transverse reinforcement, and a preferred type of joint (flat or beveled) between panels.

The laboratory specimens used in this experimental program had a total thickness of 13 in., overall width of 125 in., and a span length of 20 ft. Each specimen was constructed of three precast panels, with each having a width of 3 ft.-5.5 in. The thicknesses of the precast panels and CIP concrete topping were varied among different laboratory specimen while maintaining a constant overall thickness of 13 in. Three sets of specimens were cast with panel thicknesses of 5.5, 8, and 10 in. for each set. One specimen of each set with a particular panel thickness was constructed using flat precast panels and the other specimen was constructed using panels with beveled edges as shown in Figures 2.13 and 2.14, respectively. The panel thickness of 5.5 in. was chosen as the lower bound for an unshored panel form on a 20 ft. simple span, and 10 in. was chosen as the upper bound because it would minimize the CIP concrete topping thickness to 3 in. which was adequate to provide a minimum concrete cover of 2 in. It was felt that the satisfactory behavior of the lower and upper bound thicknesses would indicate satisfactory behavior for similarly designed specimens of intermediate thickness. The 8 in. panel thickness was chosen for the third set of specimens to study the effect of reflective cracking in the CIP concrete topping on the behavior of composite decks. This was done by inducing a longitudinal crack above one of the longitudinal joints and monitoring the behavior of the crack under loading.

One of the longitudinal joints between panels in each specimen had a ½ in. gap that was filled with fiberboard to minimize shear transfer by friction and to allow more freedom for transverse shrinkage. The other longitudinal joint in each specimen had no gap between adjacent panels, which was the usual construction practice. The transverse reinforcement for the specimens varied for each half of the specimen. The transverse reinforcement used in each specimen is summarized in Table 2.3.

The test specimens were designed assuming complete composite action between the precast panels and the CIP concrete topping. The design was based on normal weight concrete having specified compressive strengths of 5000 psi for the precast concrete and 4200 psi for the CIP concrete.

During construction of the test specimen, four of the specimens were cured under plastic for seven days and then exposed to air. None of these specimens developed visible shrinkage cracks on the top surface. The other two specimens, the specimens with 8 in. thick precast panels, were cured under plastic for only 48 hours and then exposed to air. This shorter curing time was intended to simulate the relatively poor curing conditions likely to occur in field bridges. As mentioned previously, a longitudinal crack was induced above the longitudinal joint that had a ½-in. fiberboard in both of the specimens with 8 in. thick precast panels to measure the behavior of the crack under loading. Six locations along the crack at approximately 3 ft. intervals were selected to monitor for crack width growth. The crack width was measured using a direct-reading measuring microscope graduated to 0.01 mm.

A single concentrated load was applied at the midspan because the primary consideration in the study was the shear transfer across the joint between panels. The load was spread into two "wheel" loads and applied to the slab through 1 in. thick neoprene bearing pads which were sized and positioned to simulate tire prints. By applying the load through the spreader beam,

approximately 1/3 of a wheel load was transferred across each longitudinal joint into the middle panel. According to the researchers, in a full-width bridge, the maximum shear transfer would occur with a wheel adjacent to a longitudinal joint, with the resultant load approximately 1 ft. from the joint. Thus, the use of a spreader beam to apply loads adjacent to the longitudinal joints yielded a reasonable approximation of the maximum shear transfer which would occur in a bridge. A cross-sectional view of the loading apparatus used in this study is provided in Figure 2.15.

The vertical deflections were measured using linear variable differential transformers (LVDTs) installed at transverse sections 2 ft. from the span centerline. Strain gages were mounted on two transverse reinforcing bars in the CIP concrete topping of each laboratory specimen. The instrumented bars were located in the proximity directly above the location of the LVDTs. Strand slip was measured using a caliper with a dial gage.

Testing started after the concrete of the CIP concrete topping had reached an age of 32 days. After 2,000,000 cycles of repetitive loading was complete the specimen was brought to failure. The load was applied in 10 kip increments and then reduced to 5 kip increments as the load neared ultimate. During this loading, the midspan deflection was measured using a dumpy level. Elevations were measured at midspan and at the supports so that rigid body movement caused by compression of the supports could be eliminated.

All six specimens exhibited satisfactory structural performance. Overall, there was no evidence of fatigue in either the CIP concrete or reinforcement, or deterioration of composite action, shear transfer strength or bond during the cyclic loading. The computed flexural rigidities of the composite specimens were from 2.06 to 3.80 times larger than for the CIP concrete topping and precast panels acting non-compositely. The deflection was essentially the same after 2,000,000 cycles of loading as it was at the beginning for each specimen. The researchers felt that this was an indication that there was no significant loss of composite action. Differential deflection was used as a measure of shear transfer across the longitudinal joint. Initially there was very little differential deflection observed between adjacent panels for all specimens and there were no significant increases after loading therefore indicating no deterioration of shear transfer.

Failure occurred in most specimens in the form of concrete crushing at midspan. These specimens showed adequate ductility and failed at loads that exceeded the ultimate design load. One of the specimens with a 3 in. CIP concrete topping failed due to sudden shear transfer failure. Inspection revealed that a vertical crack had formed over the longitudinal joint. However, the failure load for this specimen was 5.25 times the design load, thus an uncracked 3 in. CIP concrete topping would have adequate shear transfer strength.

Cracking, after the 2,000,000 cycles of the design load, other than the induced cracking, was only observed in the two specimens that were covered with plastic for only 48 hours. This transverse cracking located near the midspan was believed to be caused by shrinkage of the CIP concrete attributed to the relatively poor curing conditions of the two specimens. These cracks caused an increase in the measured service load deflection of approximately 25% compared to the uncracked specimens, but did not appear to affect the behavior near ultimate. The induced cracks in these specimens were measured periodically during the curing period and during the loading cycles. The crack widths increased about 0.002 in. during the curing period however there were no significant increases in crack widths observed during the loading cycles. These specimens failed at loads that were higher than the ultimate design load, thus indicating that

when reinforced transversely with No. 4 bars at 12-in. spacing, there was adequate shear transfer strength even across a preexisting crack.

There was no strand slip observed in any specimen at any stage of the loading indicating that bond and development of the prestressing strands within the specimens was not a problem. The strain gages on the transverse reinforcement, however, did not provide a reliable basis for evaluating the performance of the transverse reinforcement. Several of the gages were damaged during the curing period and the readings obtained varied erratically. The strain gages did, however, provide some qualitative information. The measured strains in the transverse reinforcement were relatively small during application of the live loads therefore indicating the stress range due to live load was likely to be so small that fatigue of this reinforcement should not be a problem.

As a result of this experimental program, the researchers were able to conclude that the composite section formed by the CIP concrete topping and precast panel could withstand 2,000,000 cycles of design load without any significant loss in serviceability or strength. Adequate composite action was obtained by roughening the interface surface of the precast panels. The researchers also concluded that adequate serviceability and strength could be obtained using flat precast panels rather than the more expensive beveled-edge panels. There was no indication that the relative thickness of the CIP concrete topping to the total thickness of the composite section had any effect on the fatigue strength of the section. The researchers' final recommendation was a minimum CIP concrete thickness of 5 in. with reinforcement of #4 bars spaced at 12 in. to provide adequate shear transfer strength.

2.4.3 Peterman and Ramirez Study

Peterman and Ramirez (1998) performed a study on Full-Span Form Panel Bridge Systems in the mid 90's to further investigate the strength and behavior of bridges built with this type of system. With the advent of high-performance concrete, better construction practices, and increased quality control, this type of construction had become attractive therefore requiring testing to investigate the behavior of these systems under these conditions.

This study involved a laboratory experiment during which two full-scale specimens were fabricated and subjected to 5,000,000 cycles of service loading and then tested to failure. The objectives of this study were to investigate the effects of repeated loading on the continuity at the interior piers and to evaluate the ultimate strength of multi-span bridges constructed using this system.

Each laboratory specimen consisted of two spans with two precast prestressed panels in each span. These panels were 21 ft. long, 4 ft. wide, and 6 in. thick and were topped with a 6 in. thick CIP concrete topping, as shown in Figure 2.16. The panels were supported at the center pier by a pin connection and at the ends by rollers. A raked finish was applied to the top surface of the precast form panels to attain composite action, as recommended by Buckner and Turner (1981). The differences between the two laboratory specimens were variations in prestressing steel and reinforcement in the CIP concrete topping. Specimen #1 used eight ½-in. uncoated low-relaxation strands which provided an average value of prestressing that would be expected in a precast form panel, while Specimen #2 contained only four such strands which represented a minimum expected amount of prestressing. In the CIP concrete topping, Specimen #1 had sixteen No. 4 bars over the pier while Specimen #2 had six No. 6 bars over the pier. The transverse reinforcement in the CIP concrete topping consisted of No. 4 bars spaced at 12 in. as recommended by Buckner and Turner (1981).

The instrumentation of these laboratory specimens consisted of load cells, electrical resistance strain gages, LVDTs, and dial gages. Load cells were placed underneath spreader beams at the discontinuous ends of the laboratory specimens. This enabled the researchers to determine the internal moments for this statically indeterminant structure. These cells were monitored throughout the curing period of the CIP concrete topping to monitor the combined effects of creep and shrinkage. They were also monitored throughout the cyclic loading period and during loading to failure. Electrical resistance strain gages were used to measure strains in the concrete and steel of both laboratory specimens. These gages were installed on both the prestressing steel and the mild longitudinal reinforcement of the CIP concrete topping at the center pier. Surface strain gages were installed at the midspan on the top and bottom of the precast panels prior to casting of the CIP concrete topping and also on the CIP concrete topping prior to cyclic loading. LVDTs were used to measure midspan deflections both during the cyclic loading and during loading to failure. Prestressing strand slip was also measured throughout cyclic loading and loading to failure by attaching dial gages to the strands that extended out of the panels at the discontinuous ends.

Specimen #1 was allowed to cure for 50 days and Specimen #2 was allowed to cure for 44 days. During this time the load cells at the unrestrained ends of both laboratory specimens revealed that the end reactions decreased over time in both specimens. This indicated that negative restraint moments had developed over the center piers.

After this cure time, each specimen was subjected to 5,000,000 cycles of service loading by two hydraulic actuators. This was done to evaluate the effects of repeated loading on the degree of continuity at interior piers. The actuators were centered over the precast panel joints at a distance of 8 ft.-3 in. from the center of the middle pier because this location produced the maximum negative moment over the middle pier. The load levels for cyclic loading of each bridge were chosen so that the maximum stress in the longitudinal steel over the pier ranged from 26 to 44 ksi. The upper limit of 44 ksi was equal to 120% of the maximum allowable design reinforcement stress range, according to AASHTO Specifications (2004). Thus, it was felt that this stress range was believed to represent a worst case scenario of repeated loadings in excess of the design service load.

After Specimen #1 was subjected to 2,000,000 cycles of loading, the loading was halted and the surface of the specimen near the middle pier was subjected to 48 days of southern exposure cycling. This weekly cycling consisted of 4 days of exposure to a 15% sodium chloride solution followed by a 3-day drying period. After the exposure cycling was concluded, the specimen was subjected to the remaining 3,000,000 cycles of loading. The stiffness of the specimen increased after the exposure cycling by approximately 67%. This increase in stiffness was attributed to the change in restraint moment at the pier. As a result of the exposure cycling, the restraint moment at the pier changed from -55 k-ft to +20 k-ft. The researchers believed that the re-wetting of the surface reduced the shrinkage of the CIP concrete topping therefore allowing the creep within the precast panels to develop a positive restraint moment. The positive restraint moment then closed any negative bending cracks that had developed over the middle pier providing a much stiffer section.

Specimen #2 was subjected to 5,000,000 cycles of loading continuously without any southern exposure cycling. The stiffness of the section remained unchanged throughout the loading cycle and deterioration of continuity between spans did not occur.

Each specimen was brought to failure using the same two actuators that were used in the cyclic loading. Flexural failure occurred in each specimen due to concrete crushing in the

positive moment region. These failures occurred close to the predicted capacities for each specimen using strain compatibility, however, these capacities were much higher than the AASHTO design nominal moment capacities. Strand slip was observed in these panels, but not until very high loading was reached. However, the strand slip did not prevent the section from reaching the design capacity.

The results of this study showed that the continuity between adjacent spans was not affected by 5,000,000 cycles of repeated service loading in which the calculated reinforcement stress range at the pier exceeded the AASHTO allowable design stress range by 20%. The experimentally determined positive and negative moments in both laboratory specimens at failure exceeded the AASHTO design nominal moment capacities for the composite sections by factors of 1.7 and 1.6 for Specimens #1 and #2, respectively. This was primarily due to strain hardening of the mild steel reinforcement. In addition, the researchers concluded that full composite action was attained by applying a raked finish to the surface of the precast panels and the ultimate load carrying capacity of the test bridges was not affected by time-dependent effects.

2.5 Additional Full-Span Prefabricated Bridge Systems

In this section, two recently developed prefabricated bridge systems which share similarities to the Mn/DOT Inverted-T Precast Slab System are presented. The presentation of these systems includes the objectives for developing the new system, details of the new system, details on testing that may have been performed, and any results or conclusions made as a result of the studies.

2.5.1 The Inverted Tee (IT) Shallow Bridge System for Rural Areas

Kamel and Tadros (1996) performed a study during the mid 90's to develop a new full-span precast concrete composite bridge superstructure system. The objective of this study was to develop a superstructure system that is simple to construct and takes advantage of the benefits associated with prefabricated construction while maintaining a low span-to-depth ratio. Of all the bridges built between 1950 and 1990, 95% of them had span lengths of less than 100 ft. Many of these bridges were built over railroads or waterways where clearance was limited. This new system was called the Inverted Tee (IT) System and it consisted of precast, prestressed inverted tee beams with a 6 in. CIP concrete topping. A cross section of the inverted tee beam used in the IT System is shown in Figure 2.17. This new section shape enabled the use of only one set of forms for a variety of beam depths. Also, the beams were reinforced with straight prestressing strands and welded wire fabric. Therefore these beams were simple to construct and relatively light to handle. The system had a span-to-depth ratio of 35 making it shallower than other available precast concrete products.

The IT System was developed after an extensive literature review and a national survey of fabricators and bridge designers. Initially five different shapes were considered in this survey, but the results of the survey revealed that the new IT system would be a good precast concrete system for bridges with shallow superstructure depth requirements and with spans less than 100 ft.

A full scale test was performed on the new system to validate the design of the new system, investigate the applicability of the AASHTO Specifications (2004) for its design, and determine if the AASHTO allowable concrete compressive stresses at prestress transfer and at service due to full loading could be exceeded. For the test, two 60 ft. long IT beams with a height of 15.75 in. were fabricated with 22 prestressing strands in the bottom flange. This was

the maximum number of strands that would geometrically fit in the bottom flange at a spacing of 2 in. The strands were not debonded or draped in order to investigate the impact of high compressive stresses at transfer of prestress. Two prestressing strands were added to the top of the web to keep the tensile stresses in the concrete below the AASHTO limits. Once the beams were fabricated they were positioned side by side and polystyrene foam blocks were used to fill the voids between the two beams. A CIP concrete deck was then cast on top to complete the specimen. Figure 2.18 shows a cross-sectional view of the IT System.

Once fabrication of the specimen was complete, it was tested as a 60 ft. long simple span beam subjected to two concentrated loads that were located 18.5 ft. from each end of the specimen. The testing revealed that the ultimate strength of the IT System exceeded the AASHTO Specifications (2004) for design. However, the compressive stresses in the bottom fibers of the test beams a transfer length away from the ends of the member were equal to $0.81f'_{ci}$ at prestress transfer which exceeded the limit of $0.6f'_{ci}$ in the AASHTO Specifications (2004). The compressive stress at service in the top fibers of the test specimen was calculated by standard elastic analysis to be about 33 % higher than the $0.6f'_{ci}$ AASHTO allowance. However, there was no negative impact detected during testing as a result of exceeding the allowable AASHTO concrete compressive stress either at transfer or due to service loading. Therefore the researchers felt that these limits were too conservative and increasing this allowable limit from $0.6f'_{ci}$ to $0.8f'_{ci}$ would not result in negative impact and would allow producers to reduce the amount of draped or debonded strands at the ends, or relieve compressive strength requirements.

The result of this study was a new inverted tee prestressed concrete beam system that has many advantages over other systems. This system is lightweight, simple to construct, and is cost competitive with other systems because it requires no temporary field forming, spans farther and is constructed quicker than other systems. It also has a high span-to-depth ratio making it ideal for projects where clearance is an important design factor.

2.5.2 Precast Pretensioned Trapezoidal Box Beam for Short Span Bridges

Badie et al. (1999) also performed a study in the mid 90's to develop a new precast prestressed trapezoidal box beam system. The new beam was developed in two different shapes: a closed totally precast concrete shape and an open-top shape requiring a CIP concrete topping. Figures 2.19 and 2.20 provide a cross-sectional view of closed- and open-top shapes, respectively. Box girders can span long distances and maintain a high span-to-depth ratio, eliminate the need for formwork, and produce an aesthetically pleasing superstructure. However, there were some problems associated with existing box girder systems, including longitudinal reflective cracking. Due to the large torsional stiffness of the box girders, the amount of transverse post-tensioning that would be required in this system to mitigate the reflective cracking would have significantly increased the cost of the structure. The objective of this study was to produce a new box girder that would perform better than existing box girders without the requirement of transverse post-tensioning, as well as provide additional economic benefits.

The new system was developed by first conducting a survey that was sent to bridge owners, general contractors, precast concrete fabricators, and consultants across the U.S. The results of the survey indicated that using a box beam with sloped sides was preferred because they are easy to construct and possess aesthetic appeal. A parametric study conducted on bridge girders showed that concentrating the area of the cross section in the two flanges as far apart as possible, along with having a thin web, together produced the most efficient cross section. The

sides of the flanges were shaped to create a continuous shear key that would be filled with non-shrink grout. The shape of this shear key is shown in "detail B" of Figure 2.19. Additional transverse connections were provided within blockouts of the precast concrete at an interval of approximately 23 in. These transverse connections were made of large voids that included transverse reinforcing dowels, and once they were filled with non-shrink grout would serve to form an additional connection between adjacent precast sections.

There were no laboratory or field tests conducted on this system. However, it was believed that these new beams would provide additional benefits over existing box girders. First, the large width of these new beams lowered the total number of pieces needed to complete the deck which resulted in higher construction speed and lower erection costs. Also, the design of the cross section had relatively flexible flanges and used shear keys and transverse connections to make them continuous, therefore potentially eliminating the development of longitudinal reflective cracking above the joints without the use of transverse post-tensioning. This helped to minimize maintenance costs and increase the expected life of the bridge.

2.6 Summary of Literature Review

Review of the literature on prefabricated bridge superstructure systems revealed significant information about these systems. Examination of the different types of connection systems used in prefabricated bridge superstructure systems suggested the use of a CIP concrete topping to be the most advantageous, especially in a cold climate state such as Minnesota. However, it also revealed some problems that exist with the use of a CIP concrete topping specifically the development of longitudinal reflective cracking above the longitudinal joints between adjacent precast sections. In addition, the complexity of continuous behavior revealed the importance of proper design practices and reinforcement detailing to achieve continuity.

Some conclusions made as a result of the studies performed on Full-span Form Panel Bridges were considered during the design process of the Mn/DOT Inverted-T Precast Slab System and the development of the instrumentation plan for this research project. Some of these conclusions include being able to achieve composite action through the use of raked or roughened surfaces, and the use of transverse reinforcement over the longitudinal joints as well as thinner precast section flanges near the longitudinal joints to reduce the probability for the development of longitudinal reflective cracking in the CIP concrete topping. Some aspects of the designs for the other two recently developed prefabricated bridge superstructure systems were also considered during the design process as well as the development of the instrumentation plan.

Chapter 3
Development and Implementation of the Mn/DOT Inverted-T Precast Slab System

3.1 Design Objectives of the Mn/DOT Inverted-T Precast Slab System

The objective of the design of the Mn/DOT Inverted-T Precast Slab System was to develop a durable bridge superstructure alternative to the traditional CIP slab-span bridge system that takes advantage of the benefits associated with prefabricated construction. The CIP slab-span bridge system is a superstructure of relatively short span ranges commonly used in Minnesota over streams. The construction of this system requires the use of shoring to pour the bridge deck which increases construction times and often has a negative impact on the environment adjacent to the bridge. The design of the Mn/DOT Inverted-T Precast Slab System possesses the advantages of a shallow depth slab-span, but eliminates the need for shoring by utilizing the inverted-T precast sections as stay-in-place forms that become integral with the CIP slab. The use of the new system reduces construction time at the site and ultimately reduces the impact on the traveling public.

The system concept was developed in a collaborative process between Mn/DOT engineers, the University of Minnesota, and local fabricators for spans ranging between 20 and 65 feet. The fabricator input was sought to ensure constructability and economy of the precast sections. Ultimately, Bridge No. 13004 was designed by Mn/DOT engineers using the AASHTO Load and Resistance Factor Design (LRFD) Bridge Design Specifications, Third Edition (2004). The remainder of this chapter will discuss the features of the bridge system common to all Mn/DOT inverted-T precast slab bridges and then discuss the design details for Bridge No. 13004.

3.2 Common Features of the Mn/DOT Inverted-T Precast Bridge System

This section discusses design considerations and details that are general to any bridge designed with the Mn/DOT inverted-T precast section. The common features and design assumptions of the precast section are discussed in Section 3.2.1. Section 3.2.2 discuses the general system to tie the precast sections together. Section 3.2.3 discusses the system for making the spans continuous over the piers for live load.

3.2.1 Design of the Precast Section

A cross-sectional view of an interior section of the Mn/DOT Inverted-T Precast Slab System concept is shown in Figure 3.1. This shape was based on the precast section used in the French Poutre Dalle system (Figure 1.1). The precast sections of the new system were designed to have a standard width of 6 ft. which was the maximum width that local fabricators could readily accommodate. This maximum width was chosen to minimize the number of sections required to span the width of the bridge. It was believed that this would result in economic benefits by reducing the amount of time required to fabricate the sections as well as the time required to place the sections during bridge construction. Using wider precast sections also results in fewer longitudinal joints between precast sections in the finished structure which require special reinforcement and time to construct. The exterior inverted-T precast section concept used in this system had a web, a flange on only one side, and reinforcement to

accommodate a barrier, as shown in Figure 3.2. These sections did not have a standard width. The variable width of these sections allows a bridge to have any desired width.

The inverted-T precast sections were designed with transverse hooks protruding out of the vertical sides of the web, as shown in Figure 3.1. These hooks were #6 bars spaced at 12 in. along the length of each precast section. The 12-inch spacing was chosen conservatively to ensure that an adequate amount of steel traversed the longitudinal joint. For this system, 90º hooks were used rather than 180º hooks which were used in the Poutre Dalle system because it was felt that this would simplify formwork during the precasting process as well as the placement of reinforcement in the field. Figure 3.3 shows a photograph of these transverse hooks.

Because this system is similar to slab-span bridges, the web height of the inverted-T section for each bridge project was to be determined using AASHTO LRFD Table 2.5.2.6.3-1 (2004), which specifies for slab-span bridges with continuous spans:

$$\text{Total Structure Depth} = [S+10]/30, \quad (1)$$

where S is the clear length (feet) of the longest span.

The minimum thickness of the CIP concrete above the precast section webs was set at 6 in. to provide 3 in. of cover above the longitudinal deck reinforcement, therefore the height of the precast section web would be 6 in. less than the value obtained from Eqn. (1). The longitudinal reinforcement at the top of the webs consisted of seven #8 bars spaced at 7 in. This reinforcement was used to provide resistance for tensile stresses that could develop during handling and transportation of the panels prior to placement.

The required prestressing force was a function of the span length and the dead load. The precast sections were designed to be simply supported under dead loads and continuous over the piers for live loads. The maximum span length of the precast sections was to be 65 ft.

The flanges were designed with a 1:24 slope to increase the constructibility of the section. It was felt that eliminating the flat surface on top of the flanges would simplify removal of the formwork, as well as simplify the casting of both the precast and CIP concrete by facilitating the flow of concrete. The thickness of the flanges along the exterior of each section was 5.25 in. because this was the minimum flange thickness that provided enough clearance within the flange for the #4 bar with a 180º hook around the longitudinal reinforcement and 1.5 in. of concrete cover along the bottom surface of the section. There was no concrete cover requirement at the top surface of the flanges because the flanges were covered with CIP concrete in the field, however a minimal amount of concrete was needed between the steel and the top surface of concrete in order for the steel to bond with the precast concrete. Minimizing the thickness of the flanges increased the thickness of the CIP concrete at these locations and lowered the depth of the transverse hooks that traversed the longitudinal joints, both of which increased the ability of the section to distribute loads in the transverse direction.

The web and flange corners of the precast inverted-T sections had a ¾-inch chamfer, as shown in Figure 3.1. Chamfering the corners reduced the stress concentrations at these locations to lessen the probability for the development of longitudinal reflective cracking. Caulk was used to seal the joint as well as to increase the surface area of the discontinuity and reduce the stress concentration directly above the longitudinal joints, as shown in Figure 3.4.

The contact surfaces of the precast sections (those surfaces in direct contact with the CIP concrete) were intentionally roughened to enhance the bond between the precast sections and the CIP concrete. The surfaces were roughened to have a minimum amplitude of ¼-inch. Formwork was fabricated with a form liner to create roughened surfaces, as shown in Figure 3.5.

This formwork was used to create roughened surfaces on the tops of the flanges and the vertical sides of the web. A rake was used to roughen the top of the web. The intent of these roughened surfaces was to help achieve composite action between the precast and CIP concrete and therefore help prevent the development of reflective cracking in the CIP concrete.

Transverse reinforcement was included within the precast sections to satisfy three different reinforcement requirements: horizontal shear reinforcement, anchorage zone reinforcement, and confinement reinforcement. The transverse reinforcement that was included to satisfy these requirements is highlighted in Figure 3.6. Horizontal shear reinforcement was required to ensure that composite action was achieved. The size and spacing of the horizontal shear reinforcement required for each bridge was to be a function of the surface area and roughness of the concrete interface (AASHTO LRFD 5.8.4). This reinforcement was required along the entire length of each precast section. The amount of reinforcement included for anchorage zone reinforcement and confinement reinforcement was standardized to provide a standard reinforcement detail that could be used for precast sections with a prestressing force of up to 1,000,000 lbs., which was the maximum prestressing force proposed by local fabricators. This reinforcement was only included within 18 in. of the end of each precast section. The standard anchorage zone reinforcement consisted of three #5 ties (Figure 3.6) at 2-in. spacing at the end of each section followed by two #5 ties at 6-in. spacing (AASHTO LRFD 5.10.10.1). The standard confinement reinforcement consisted of three #4 ties (Figure 3.6) at 2-in. spacing at the end of each section followed by two #4 ties at 6-in. spacing (AASHTO LRFD 5.10.10.2).

During the casting process for the inverted-T sections, styrofoam blocks were used to block out the final 10 in. of each flange at both ends of the member. After the precast sections were set in place, these block-outs formed large voids above the pier caps, as shown in Figure 3.7. These block-outs were filled with CIP concrete which served, along with reinforcement, to tie the precast sections to the pier caps.

3.2.2 Transverse Reinforcement over the Longitudinal Joints

Once the precast sections were in place, a reinforcement cage was placed over the longitudinal joint. The reinforcement detail over the joint, including the transverse hooks, is shown in Figure 3.4. The use of 90º hooks with this system enabled the reinforcement cage to be prefabricated and dropped into place above the longitudinal joints rather than tying each bar in-place individually. Figure 3.8 shows a photograph of the reinforcement cage after it was set in position above the longitudinal joints.

The transverse hooks and reinforcement cage were included in the system to provide a means for transverse load distribution. Once the sections and reinforcement were in place and the CIP concrete had cured, the transverse hooks and the reinforcement cage would serve to effectively connect adjacent sections. Thus, it was felt that this large amount of reinforcement placed in each longitudinal joint would reduce the tensile stresses that would otherwise develop within the CIP concrete topping as a result of transverse load sharing. This would therefore arrest the development of reflective cracking above the longitudinal joints.

3.2.3 Detailing for Continuous Behavior over the Piers

The Mn/DOT Inverted-T Precast Slab System was designed to behave continuously for live load by adding negative moment reinforcement at the top of the CIP concrete above the pier caps. This method for achieving continuity was much more practical than the use of longitudinal post-tensioning. Longitudinal deck reinforcement was included within the CIP concrete topping

to provide tensile resistance. This longitudinal reinforcement was designed similar to the reinforcement in the top of traditional CIP slab-span bridges.

The CIP concrete that filled the large voids created by the block-outs of the precast sections at the piers (Figure 3.3), along with the concrete between the ends of the precast sections acted similar to a concrete diaphragm, and also provided potential compressive resistance for negative continuity moments. It was felt that the combination of this compressive resistance with the tensile resistance of the longitudinal deck reinforcement would provide adequate negative moment resistance to achieve continuous behavior for live load over the piers.

As explained in Section 2.3, long-term behaviors such as creep and shrinkage can lead to the development of positive restraint moments at the pier caps. A positive moment connection must be provided to prevent the development of a gap between the CIP concrete and the precast sections above the pier caps. This positive moment connection was provided by adding additional reinforcement consisting of four #8 bars over the piers at a lower depth in the cross section. These #8 bars extended 10 ft. in each direction on each side of the pier. This reinforcement is shown in Figure 3.4. The reinforcement cages that were placed above the joints were not continuous over the piers.

3.3 Design of Mn/DOT Bridge No. 13004

The bridge instrumented for this study was Mn/DOT Bridge No. 13004, located in Center City, Minnesota. This bridge was oriented in the east-west direction on U.S. Trunk Highway 8 near the junction of Chisago County Road 9. The bridge spanned the newly created Center Lake Channel that connected North Center Lake and South Center Lake. The channel was built to enable boat travel between the two lakes. Originally a box culvert existed at this location that was not designed for boat travel. An elevation view of this bridge is shown in Figure 3.9. Complete bridge plans for this bridge are provided in Appendix A of this report.

The superstructure of the bridge was constructed using the Mn/DOT Inverted-T Precast Slab System. The thickness of the CIP concrete above the web of the precast sections was 6 in. to provide adequate concrete cover of 3 in. above the longitudinal deck steel. This produced a deck with a constant cross section thickness of 18 in. The abutments, wingwalls, and pier caps were constructed of precast concrete and were supported by CIP concrete piles (The abutments of Stage 2 were CIP rather than precast because the large weight of the precast abutments presented problems during construction). The substructure had a crown towards the center to allow for proper drainage of the bridge deck and to allow the deck to have a constant deck thickness. The wingwalls extended back from the abutments at a 90º angle. The bridge had three spans measuring 22 ft., 27 ft., and 22 ft. There was no skew between the roadway and the channel.

The general contractor for construction of the bridge was Lunda Construction. The inverted-T precast sections were fabricated by County Materials Corporation at their fabricating plant in Roberts, Wisconsin. The bridge was constructed in two stages to allow continuous flow of traffic. In Stage 1, the abutments and pier caps were precast in two separate pieces and connected using construction joints. Reinforcement dowels were placed within the construction joints and the joints were filled with grout to tie the sections together. In Stage 2, the abutments and piercaps were cast-in-place. The CIP concrete deck was also cast in two stages therefore there was a longitudinal construction joint located along the entire length of the CIP portion of the bridge deck adjacent to the centerline of U.S. Trunk Highway 8. The construction stages and construction joint within the CIP concrete deck are shown in Figure 3.10. The superstructure

was constructed integrally with the pier caps and abutments therefore there were no expansion joints installed in the bridge. There were however expansion joints installed between the approach panels and the roadway paving to allow for movement of the approach panels to accommodate the bridge expansion and contraction.

The bridge was designed to accommodate one lane in each direction, a full-width shoulder on each side, and a left-turn lane located in the center of the bridge for eastbound traffic. A bike path was located along the north side of the bridge, bordered on the north by an ornamental metal railing and on the south by a guardrail which served to separate the bike trail from the highway traffic. There was also a guardrail on the south side of the bridge.

Instrumentation was installed at several locations within the CIP portion of the deck to monitor for the development of reflective cracking and to investigate continuous behavior over the interior piers. A conduit system was constructed within the CIP portion of the deck to house the wiring for this instrumentation. The conduit traveled from the CIP concrete down through the flanges of three of the precast sections to boxes that were mounted on the pier cap. The conduit proceeded along the underside of the bridge and then underground towards a cabinet that housed the data collection system. A complete description of the conduit system is located in C*hapter 5* of this report.

3.3.1 Materials

The inverted-T precast sections were constructed using concrete with a specified minimum compressive strength of 6500 psi. The other precast elements as well as the CIP portions of the bridge were constructed using concrete with a specified minimum compressive strength of 4000 psi. The results of the compressive strength tests for both the precast and CIP concrete are provided in Tables 3.1 and 3.2, respectively.

The prestressing strands used in the precast sections were ½-inch diameter 7-wire low-relaxation strands conforming to ASTM A416 with a minimum ultimate tensile strength of 270 ksi. The mild reinforcement located in all elements of the structure was epoxy-coated rebar with a minimum tensile yield strength of 60 ksi.

The backfill material used during the construction of this bridge was a granular backfill that met Mn/DOT standard specification 3149.2D (2000). At the time of construction, this specification called for pit-run or crusher-run mineral to pass a 75 mm (3 inch) sieve, graded from coarse to fine such that the ratio of the portion passing the 75 μm (#200) sieve divided by the portion passing the 25 mm (1 inch) sieve may not exceed 20 percent by mass.

3.3.2 Design Calculations

Mn/DOT Bridge 13004 was designed according to the AASHTO LRFD Bridge Design Specifications, Third Edition (2004) and interim specifications current at the time of design (Fall 2004). An HL93 Live Load was considered for design along with an additional uniform load of 20 psf for allowance of future wearing course modifications as well as 450 plf for traffic barriers and 200 plf for a pedestrian barrier, both distributed equally to all of the precast sections. The design speed for the bridge was 45 mph. Calculations performed by engineers at the Mn/DOT Bridge Office for an interior composite section are provided in Appendix B of this report.

The precast sections acted simply-supported for their self weight but once the concrete had cured the composite section behaved continuous over the pier. Therefore the continuous composite section was designed to support the live load and superimposed dead loads. Live loads were considered to be distributed to the superstructure based on the equivalent beam

widths for slab-span type bridges (AASHTO LRFD 4.6.2.3). This distribution factor was used because once constructed the bridge most closely resembled a slab-span bridge making this live load distribution factor most appropriate.

The restraint moment was estimated using the Portland Cement Associated (PCA) Method (Freyermuth, 1969). In this method, a formula was used to calculate the moment caused by differential shrinkage in a composite concrete section. The restraint moments were then calculated using a formula that combined the shrinkage moment, the moment caused by the prestressing force about the centroid of the composite section, and the midspan moment caused by dead load to obtain the restraint moment at the piers. The restraint moments estimated using this method were combined with the dead and live load moments to check the capacity of the composite section.

The maximum total factored negative moment demand over the pier, including the estimated restraint moment and live load was conservatively calculated to be -97 ft-kips per foot of width. The longitudinal reinforcement over the piers consisted of #8 bars at 12-inch spacing and #7 bars at 4-inch spacing between the #8 bars. This detail is shown in Figure 3.3. The factored nominal negative moment capacity of this reinforcement along with the concrete above the piers was calculated to be 117 ft-kips per foot of width. Conservatism was used with these calculations because it is difficult to accurately predict restraint moments for this new system. The transverse deck reinforcement consisted of #5 bars spaced at 12 in. to satisfy shrinkage and temperature requirements (AASHTO LRFD 5.10.8.2).

3.3.3 Details of the Precast Section used for Mn/DOT Bridge No. 13004

The height of the web for the precast sections of Bridge 13004 was 12 in. This height was used to produce a deck cross section that had a constant thickness of 18 in. This bridge had initially been designed as a slab-span bridge with an 18 in. deck and by using the same thickness no changes had to be made to the grade of the roadway. Figure 3.11 shows the cross section of the interior precast sections for this bridge, including complete details of the reinforcement.

The prestressing pattern within the precast sections consisted of two layers of prestressing strands with 8 strands in each layer. The two layers had a center-to-center vertical spacing of 2 in. and each strand had a horizontal spacing of 6 in. Each of these strands were stressed to 202.5 ksi ($0.75f_{pu}$) to produce a total prestressing force per section of 496 kips. The longitudinal reinforcement within the flange tips was originally planned to consist of mild steel. However, this was changed to prestressing strands tensioned to a nominal stress of 5000 psi. The fabricators suggested this be done because it significantly simplified the placement of this reinforcement. The transverse reinforcement within the flanges consisted of #4 bars with a 180º hook around the longitudinal reinforcement within the flange, as shown in Figure 3.1. This reinforcement was used to increase the durability of the flanges during transport.

The maximum total factored positive moment demand at midspan of the center span, including the estimated restraint moment and live load, was calculated to be 393.1 ft-kips for an interior composite section. The positive design moment capacity was calculated to be 713.7 ft-kips for an interior composite section. The excess ultimate capacity was a result of satisfying serviceability requirements.

The maximum factored vertical shear demand at the critical section was calculated to be 90 kips. This was less than half of the design concrete shear capacity for the composite section therefore there was no requirement for stirrups due to vertical shear demand. The maximum factored horizontal shear demand at the interface of the precast and CIP concrete was estimated

to be 0.104 ksi near the ends of the precast sections. This slightly exceeded the 0.100 ksi maximum design horizontal shear capacity of the concrete with a roughened surface, therefore transverse reinforcement was needed near the ends of the section for horizontal shear (AASHTO LRFD 5.8.4.1). The rest of the section required only the minimum amount of reinforcement at 24-in. spacing (AASTHTO LRFD 5.8.4.1). However, due to the unique design of this system and the importance of composite action, these sections were conservatively designed with #5 ties at 12 in. along the entire length. The relatively short length of the precast sections in this bridge allowed this conservative amount of reinforcement to be used without large economical impact.

3.3.4 Details of the Bridge Deck

The entire deck of the bridge was 72 ft. 2 in. long and 76 ft. 5 in. wide. The roadway was 62 ft. 3 in. wide and the bike trail was 10 ft. wide. Holes were prefabricated into the flanges of three of the interior-end span sections to provide a means for the conduit to travel from the CIP portion of the deck to the underside of the bridge.

The approach panels extended out 20 ft. from the bridge and ran the whole width of the roadway. The thickness of the approach panels was 12 in. The approach panels were reinforced with a top and bottom mat of steel consisting of #4, #5, and #6 bars. The far end of the approach panel rested on a concrete sill and had an expansion joint between the panel and the roadway.

3.3.5 Details of the Precast Substructure

The substructure was designed to be constructed entirely out of precast concrete. However, due to problems handling the abutment sections (mostly due to weight) during Stage 1 of bridge construction, the abutments of Stage 2 were constructed using CIP concrete. In Stage 1, reinforcing dowels were used to tie adjacent precast elements together. This was done by inserting reinforcing dowels from one of the elements into prefabricated holes in another element and then filling the holes with grout. The precast sections of the superstructure were placed on elastomeric bearing pads located on top of the pier caps and/or abutments. The superstructure of the bridge was tied to the wingwalls, abutments, and pier caps by reinforcing dowels that extended out of the precast elements and into CIP portions of the bridge deck or approach panels. Figures 3.12 and 3.13 show the connection detail of the abutment to the CIP concrete of the bridge deck and approach panels and the connection detail of the pier caps to the CIP concrete of the bridge deck, respectively. The reinforcing dowels were only located within the center 50% of the bridge width to allow the outer portions of the bridge to expand and contract laterally under thermal loading.

In Stage 1, the abutments, wingwalls and pier caps were constructed of precast concrete. The abutments were 76 ft. 5 in. long, 7 ft. tall and 3 ft. thick. The wingwalls extended back approximately 10 ft. 6 in. from the face of the abutments. The reinforcement of the abutments and wingwalls consisted entirely of #5 and #6 bars. The pier caps were 76 ft. 5 in. long, 3 ft. 6 in. tall and 3 ft. 6 in. thick. The reinforcement for the pier caps consisted of #5, #7 and #9 bars.

The precast substructure was supported by CIP concrete piles. The piles consisted of steel pipes driven into the ground, closed-ended, to the depth required to reach bearing capacity. The piles used to support the abutments were 55 ft. long and had a 12 in. nominal diameter. The piles used to support the pier caps were 80 ft. long and had a 16 in. nominal diameter. Once the piles were driven to the proper depth, they were filled with high slump concrete and reinforcement was added to the top portion of the pile. This reinforcement was used in conjunction with grout to tie the CIP concrete piles to the precast substructure.

Chapter 4
Instrumentation of Mn/DOT Bridge No. 13004

4.1 Objectives of Instrumentation

The instrumentation plan for Mn/DOT Bridge No.13004 was developed with the objective of evaluating the performance of the newly developed Mn/DOT Inverted-T Precast Slab System. The behaviors to be investigated were established after an extensive literature review on other precast deck systems along with several meetings with Mn/DOT engineers. Behaviors of interest included potential development of longitudinal reflective cracking in the CIP concrete, continuity for live loading over the piers, and effectiveness of the transverse hooks in transverse load sharing.

All instrumentation for Mn/DOT Bridge 13004 was installed during Stage 1 of bridge construction, which consisted of the north half of the bridge. This Stage was selected for instrumentation for two reasons. First, after completion of Stage 1, all traffic was rerouted to that portion of the bridge while construction began on Stage 2. This subjected the north half of the bridge to potentially larger traffic volume at an early age, promoting the potential development of reflective cracking. Second, this section of the bridge was closest to the cabinet used to house the dataloggers which was stationed adjacent to the available power source. Because of symmetry, only the east half of Stage 1 was instrumented. Figure 4.1 shows a plan view of the bridge with the instrumented portion of the bridge highlighted.

The remainder of this chapter explains the behaviors that were investigated, the instrumentation that was used to investigate each behavior, and the locations of the installed instrumentation.

4.2 Longitudinal Reflective Cracking of the CIP Concrete Deck above the Precast Longitudinal Joints

The development of longitudinal reflective cracking in the CIP concrete deck was a major concern due to the implications that such cracking would have on the durability of the system, as explained in Section 2.2.3. The main area of concern for the development of cracking was the area directly above the longitudinal joints between adjacent precast sections because it was thought that this presented the most probable area for the development of cracking. Figure 4.2 shows a cross-sectional view of the deck system with the longitudinal joints highlighted. The vertical sides of the flanges on adjacent precast sections were not connected therefore the load sharing in the transverse direction across these joints had to occur within the CIP concrete. This had the potential to create tensile stresses in the CIP concrete in the transverse direction which could lead to the development of cracking. In addition, loading, such as wheel loads, could cause adjacent flanges to slightly separate from one another. The contact surfaces of the precast sections were roughened to create a bond with the CIP concrete and help to achieve composite action, however the bonding of the CIP concrete to the top of the flanges could also potentially increase the tensile stresses in the CIP concrete resulting from slight separation of the adjacent flanges due to transverse load sharing and consequently create a driving force for the development of reflective cracking.

As mentioned in Chapter 3, transverse hooks protruded out of the webs of the precast sections in addition to reinforcement cages placed between the webs to arrest the development of longitudinal reflective cracks. Figure 3.4 shows these transverse hooks along with the additional

reinforcement cages located above the longitudinal joints between the precast webs. The top corners of adjacent flanges were chamfered to reduce local stress concentrations at these locations. A single bead of caulk was applied to the top of the longitudinal joints to weather-proof the joint and to reduce stress concentrations at this location by blunting and increasing the area of the discontinuity.

4.2.1 Instrumentation for Longitudinal Reflective Cracking above the Precast Longitudinal Joints

Slight separation between adjacent flanges, which would act as a driving force for the development of reflective cracking, would most likely occur at the location of maximum downward deflection. Thus, it was felt that reflective cracking would most likely develop above the longitudinal joints of the longest span. Therefore instrumentation was installed above the longitudinal joints at the midspan of the center span at three different locations in the transverse direction. These transverse locations were chosen to be as close as possible to the nominal wheel load locations as shown in Figure 4.3.

The center span had a total of 12 longitudinal joints formed by adjacent precast sections; therefore, it would be difficult to evaluate the overall performance of these joints by instrumenting a single joint however it was not feasible to instrument every single joint. As a compromise, three joints were instrumented, to obtain a sufficient amount of information that would allow for proper evaluation of the overall performance of the longitudinal joints.

The instrumentation at each location consisted of five vibrating wire (VW) embedment strain gages oriented in the transverse direction. The VW embedment strain gages used for this instrumentation were Geokon® Model VCE-4200 VW Strain Gages as shown in Figure 4.4. Details and specifications for this strain gage are provided in Appendix C.

Once installed, each gage overlapped the adjacent gage by approximately 2 in. as shown in the instrumentation detail given in Figure 4.5. The gage length for the gages used was 6 in. Therefore each gage had approximately 2 in. where it was not overlapped by any of the adjacent gages, and 2 in. at each end that was overlapped by the adjacent gages. The gages were overlapped to ensure that the crack would not propagate around them which would allow the crack to avoid being detected. If a crack were to develop and open, it would cause any strain gage that spanned the crack to have a larger relative strain reading than adjacent strain gages. Therefore in addition to ensuring that the crack was detected, overlapping the gages would allow for determination of the crack location to within 2 in.

The five VW embedment strain gages at each transverse location were installed by tying each gage between two pieces of uncoated rebar using coated tie wire as shown in Figure 4.6. Once all the gages were tied to the rebar, this assembly was placed on top of the bottom longitudinal reinforcement steel of the reinforcement cage, positioning the gages approximately 3 in. above the top of the flanges, as shown in Figure 4.7. Once the assembly was tied in place, the final position of each gage was secured by using a zip tie to secure the gage to the coated tie wire. This prevented the gage from sliding in the transverse direction and changing position during pouring of the CIP concrete deck. The lead wire for each gage was temporarily placed in a plastic bag to protect it from the elements.

4.3 Longitudinal Reflective Cracking of the CIP Concrete Deck above the Precast Section Web Corners

A secondary area of concern for the development of longitudinal reflective cracking of the CIP concrete deck was directly above the web corners of the precast sections. Figure 4.2 shows a cross-sectional view of the deck system with the precast web corners highlighted. This area was a concern because the corner of the web of the precast section might produce high stress concentrations in the relatively thin CIP concrete. These corners were chamfered to reduce stress concentrations at this location. The contact surfaces of the precast sections were also roughened to achieve better bond with the CIP concrete to lessen the effect of the discontinuity between the precast concrete and the CIP concrete at this location.

4.3.1 Instrumentation for Longitudinal Reflective Cracking above the Precast Section Web Corners

The instrumentation above the web corners at each location consisted of ten Geokon® Model VCE-4200 VW Strain Gages oriented in the transverse direction. Details and specifications for this strain gage are provided in Appendix C. Again, these gages were placed such that each gage overlapped the adjacent gage. The gage length for the gages used was 6 in. and the overlap used for these gages was about 1.5 in. therefore each gage had approximately 3 in. where it was not overlapped by any adjacent gages. Figure 4.8 shows the plan view of the instrumentation detail for the instruments located above the web corners. This detail existed at the same locations as the instrumentation above the joints but at a higher depth in the cross section. Figure 4.9 shows a cross-sectional view that includes all the VW embedment gages located at each instrumented transverse location. This detail was used because it would provide more information in the case that cracking would develop. More specifically it would reveal if the cracking had propagated to a higher depth in the cross section and would give an approximation of the path by which the cracking had propagated.

The ten VW embedment strain gages located above the web corners were installed by tying each gage to two pieces of coated rebar using coated tie wire. In this case, epoxy-coated rebar was used due to the close proximity of these gages to the exterior surface of the CIP concrete deck. Once all the gages were tied to the rebar, the assembly was slid into position underneath the longitudinal deck steel and tied in place as shown in Figure 4.10. Again, the final position of each gage was secured by using a zip tie to secure the gage to the coated tie wire.

4.4 Continuous Behavior for Live Load over the Piers

The Mn/DOT Inverted-T Precast Slab System was designed to behave continuously over the piers for live load because continuous behavior presents many advantages, as explained in Section 2.3. Md/DOT practice for typical preacast concrete beam bridges is to design the spans as simply supported for both dead and live load; however the design of the Bridge 13004 spans included reinforcement in the CIP deck for the purpose of producing continuous behavior for live loads.

It was difficult to accurately calculate or predict the restraint moment that would develop at the piers because the methods used to predict restraint moments are based on typical bridge deck systems which have much thicker cross sections than this system. Thus, a large amount of reinforcement was chosen conservatively. The reinforcement in the negative regions of the CIP concrete deck consisted of #8 bars spaced at 12 in. with #7 bars spaced at 4 in. between the #8 bars. As mentioned in Chapter 3, additional reinforcement was added over the piers at a lower

depth in the cross section to provide a positive moment connection in case a positive restraint moment were to develop due to long-term behaviors such as creep and shrinkage. This additional reinforcement consisted of four # 8 bars above the joint as shown in Figure 3.4. Since it was difficult to calculate the size of the potential positive restraint moment, it was uncertain how effective this additional reinforcement would be. However, if this reinforcement was not added and large positive restraint moments had developed this could cause a gap to open between the precast sections and the girder ends.

Once the precast sections were placed on top of the pier caps and/or abutments, the blocked-out portions of the flanges (Figure 3.3) created large voids above the pier caps which were filled with the CIP concrete of the deck. Once the CIP concrete cured, the concrete that filled these voids along with the space between the ends of the precast sections acted as a concrete diaphragm and provided some compressive negative moment resistance. However, due to the irregular geometry of the CIP concrete and precast sections, it was difficult to analytically determine how effective this negative moment resistance would be in helping to achieve continuous behavior for live load.

4.4.1 Instrumentation for Continuous Behavior for Live Load over the Piers

The bridge superstructure for the Mn/DOT Inverted-T Precast Slab System was designed to behave continuously for live loads only. To determine the effective continuity of the bridge superstructure a live load (known test load) must be applied to the bridge. This will be done by moving a loaded sand truck to several different positions along the length of the bridge. While the sand truck is at each position, the curvature at several different locations along the length of the bridge will be determined using the installed instrumentation. The effective continuity of the bridge can be determined by comparing the curvatures obtained using instrumentation to the curvatures calculated using the known live load and assuming fully continuous behavior. The truck test had not yet been executed at the time of this report.

The instrumentation used for monitoring the continuity were Geokon® Model VK-4150 Vibrating Wire Strain Gages as shown in Figure 4.11. Details and specifications for this strain gage are provided in Appendix C. These gages were welded to the longitudinal steel reinforcement at different depths of the bridge cross section. Each gage provided a strain reading for that depth of the cross section which could be used to determine the curvature of the bridge at that location.

Due to symmetry, it was only necessary to determine the continuous behavior over one of the piers, thus six locations along only half the length of the bridge were instrumented. These locations of instrumentation are shown in Figure 4.12. At each of these locations, instrumentation was installed at several locations in the transverse direction. This was done partly to provide redundancy but also to provide information on transverse load distribution. Figure 4.13 is a plan view of Stage 1 of the bridge deck, showing the locations of all the instrumentation installed on the longitudinal steel reinforcement. In the transverse direction, instrumentation was installed at the midspan of the center span adjacent to both Joint 1 and Joint 2 and near the pier on the center span side, adjacent to Joints 1, 2, and 3. Gages were also installed on the longitudinal deck steel at several locations above Webs 1 and 2 of the precast sections on the center pier side of the east pier. These gages were used to determine if the strains in the deck steel over the pier differed between the areas above the flanges and the areas above the webs. This would provide insight on the effect that the precast section shape has on the continuous behavior of the bridge.

The ♦'s in Figure 4.13 represent locations of instrumentation where three strain gages were installed. At these locations, two strain gages were installed on the longitudinal steel of the reinforcement cage above the longitudinal joint and one strain gage was installed on the longitudinal deck steel that was closest to the other two gages, as shown in Figure 4.14. The ●'s in Figure 4.13 represent locations of instrumentation where two strain gages were installed. The instrumentation detail was different at these locations because the reinforcement cages were not continuous over the pier. At these locations, one strain gage was installed on one of the #8 bars above the pier and one strain gage was installed on the longitudinal deck steel directly above the other strain gage, as shown in Figure 4.15. The ▲'s in Figure 4.13 represent locations of instrumentation where only one strain gage was installed. At these locations the strain gage was installed on the longitudinal deck steel.

The VW spot-weldable strain gages were installed by first grinding the epoxy coating off of the longitudinal reinforcing steel at the location where the gage was to be installed. The steel was then ground flat at this location to provide a smooth surface for spot-welding the strain gage. Figure 4.16 shows a picture of a VW spot-weldable strain gage welded to longitudinal reinforcement. After the strain gage was welded to the steel, cyano-acrylate adhesive was applied to the mounting tabs to seal any gaps between the steel and the mounting tabs. The tabs were then completely covered with a water-proofing compound to protect against future corrosion. To provide mechanical protection, the entire gage was then covered with a steel cover that was secured in place using three zip ties as shown in Figure 4.17. The edges of the cover were covered with mastic tape to prevent concrete from getting inside the cover. After all of the gages were installed, the steel reinforcement that had gages attached were rotated so that the gages were located on the bottom of the steel. This was done to reduce the chances of damaging the gages during pouring of the CIP concrete deck. Figure 4.18 shows a photograph of three VW spot-weldable strain gages on the longitudinal steel near midspan and Figure 4.19 shows a photograph of two VW spot-weldable strain gages installed on the longitudinal steel above the pier.

4.5 Effectiveness of the Transverse Hooks

The transverse hooks extending out of the webs of the precast sections were intended to help with transverse load sharing and to reduce the probability for the development and propagation of longitudinal reflective cracking in the CIP concrete above the longitudinal joint. These hooks were spaced at 12 in. on center in each member. The locations of the hooks within each section were staggered slightly so that the hooks from adjacent sections would not line up directly, which would otherwise prevent proper placement of adjacent precast sections. Figure 4.20 shows a photograph of the hooks from adjacent sections lined up once the sections were in place.

The spacing of 12 in. was chosen arbitrarily because it was difficult to accurately predict the effectiveness of these hooks. Therefore to determine if this spacing was adequate to provide effective transverse load sharing, it was necessary to monitor the behavior of these hooks under applied loading. Also, if a longitudinal reflective crack were to develop in the CIP concrete it would be important to determine whether or not the steel of the transverse hooks had yielded across the crack.

4.5.1 Instrumentation to Determine Effectiveness of Transverse Hooks

The same three joints that were instrumented for longitudinal reflective cracking were also instrumented to investigate the effectiveness of the transverse hooks (Figure 4.3). At each location, two transverse hooks were instrumented above each joint directly adjacent to the VW embedment strain gages that were used to detect the development of longitudinal reflective cracking. These locations were chosen to facilitate the detection and location of reflective cracking. Also, the transverse hooks at midspan would likely experience the largest strains therefore instrumenting these hooks would likely provide the most information on their effectiveness.

Each pair of hooks that was instrumented consisted of hooks protruding from adjacent precast sections located directly adjacent to one another in the longitudinal direction. Each pair was instrumented with a total of seven Geokon® Model VK-4150 Vibrating Wire Strain Gages. Four gages were placed on one hook while three gages were placed on the adjacent hook. The gages were placed so that the gage on one hook slightly overlapped the adjacent gages on the other hook. Together, the seven gages spanned most of the distance between the webs of the adjacent precast sections. This was done to ensure that the gages would cross a crack if one were to develop. Figure 4.21 shows a plan view of the instrumentation detail for the transverse hooks.

These gages were installed in the same manner as the gages used for monitoring continuous behavior over the piers as explained in Section 4.3.2. Figure 4.22 shows a photograph of these strain gages installed on the transverse hooks.

4.6 Installation of Instrumentation

The coordinates of all the gages installed in the bridge are provided in Tables 4.1 through 4.4. These coordinates are in inches and were measured from the northeast corner of the roadway (inside the north guardrail, see Figure 4.1), using a positive coordinate system with x- being positive in the west direction along the length of the bridge, y- positive in the south direction, and z- positive in upwards direction starting from the bottom surface of the bridge superstructure. The x-direction coordinates given for the VW embedment gages is for the center of that group of gages. The gages overlap the adjacent gages, but they are not all in the same line. They have a spacing of approximately 1.5 in. between overlapping gages (see Figure 4.7). The gages were labeled according to the type of gage and the approximate location of the gage within the bridge. This labeling scheme is explained in Figure 4.23.

The installation of instrumentation took place in September of 2005. The process started on September 2 and lasted until September 28 at which point all instrumentation was connected to the data acquisition system, which is described in Chapter 5. Data was recorded intermittently throughout the installation process using a Geokon® GK-403 read-out box. A complete log of the installation process is provided in Appendix D of this report.

Chapter 5
Data Acquisition System

5.1 Design of the Data Acquisition System

A data acquisition (DAQ) system was created to facilitate long-term recording of strain and temperature readings from the VW strain gages installed within the CIP concrete portion of the bridge deck. This system consisted of two dataloggers, two VW interfaces, six multiplexers, two storage modules, and two batteries. A schematic of this system is provided in Figure 5.1. All of the components used in this system were supplied by Campbell Scientific, Inc. A general description along with some of the specifications for each component are provided in Appendix C.

The multiplexers installed in this system were AM16/32 Relay Multiplexers and were numbered 1 through 6 (from south to north). Each strain gage was connected to one of the six multiplexers used in this system. The multiplexers each had the capacity to monitor 16 differential sensors that require excitation, i.e., 16 VW strain gages, along with the differential thermistor of each gage. Thus, the use of six multiplexers enabled monitoring of 96 instruments with this DAQ system. A total of 98 instruments were installed in the bridge, however two of these instruments are not being measured. These extra gages were installed in case some of the gages were damaged during casting of the CIP concrete deck. The initial channel assignment for each strain gage is provided in Tables 5.1 though 5.6.

The signal cable from each multiplexer was connected to one of the two AVW4 VW Interfaces used in this system. The VW Interfaces are needed to convert the differential strain and temperature measurements obtained from the VW strain gage to single-ended measurements that can be read by a datalogger. Up to four multiplexers can be connected to each VW Interface. These VW interfaces were numbered 1 and 2. Multiplexers 1 through 3 were connected to VW interface 1 and Multiplexers 4 through 6 were connected to VW interface 2. Each VW interface was connected to one CR-10X datalogger. These dataloggers were programmed using the PC400 Software to measure the strain gages connected to the multiplexers. The initial programs that were downloaded into the dataloggers are provided in Appendix E of this report. The data received from the strain gages was stored in the SM16M Storage Module that was connected to each datalogger.

Each datalogger was powered by a PS100 12V Rechargeable Battery. These batteries were originally only intended to provide the dataloggers with DC power and provide a reserve power source in the case of a power outage. However, AC power was not immediately provided at the site, therefore for a period of time these batteries were the only source of power. During this time, both dataloggers were connected to one of the batteries while the other battery was charged. After a period of approximately two weeks the fully charged battery was brought to the bridge and swapped with the other battery. This process was to continue until the site was supplied with AC power at which point each battery would again be connected to one datalogger and would continually supply the datalogger with DC power, however, as of June 2006 the site had not been supplied with AC power.

5.2 Conduit System

The cables used in the DAQ system were housed within a galvanized steel conduit system that was installed by the contractor. A plan view of the conduit is provided in Figure 5.2.

Complete plans for this conduit system are shown on page 26 of the Bridge Plans provided in Appendix A. This conduit system was completely sealed prior to pouring the CIP concrete to prevent corrosive or mechanical damage to the cables or system components.

The individual wires for each of the instruments were typically spliced to a larger cable that traveled through the conduit to the multiplexers. This was less expensive and more practical than running each individual wire through the conduit. 17-pair and 6-pair shielded cables were used as necessary to accommodate the total number of instruments at each instrumented location. The cables above Joint #1 were labeled 6-#, the cables above Joint #2 were labeled 5-#, and the cables above Joint #3 were labeled 4-#. Tables 5.8 through 5.22 identify the instruments connected to each cable. Figure 5.3 shows a plan view of the cables within the bridge deck. Table 5.7 summarizes the location of each cable relative to the longitudinal joints and the multiplexer box to which each cable traveled. The spliced portions of the cables were housed within relatively large steel boxes, as shown in Figure 5.4.

The conduit traveled from the instrumented locations adjacent to the precast member joints to the eastern side of the east pier cap at which point the conduit then traveled down through the precast sections to steel boxes mounted on the eastern face of the pier cap, as shown in Figure 5.5. The portion of the conduit located within the CIP concrete had an inside diameter of 1.5 inches.

Each of the large boxes mounted on the eastern pier cap was used to house two multiplexers. These boxes were 10 in. wide, 12 in. tall, and 5 in. deep which provided adequate room for two multiplexers located side by side. The boxes were numbered 1 through 3 from south to north (from left to right in Figure 5.5). The locations of the multiplexers within these boxes are shown in Figure 5.6. The multiplexers were mounted on plywood that was secured in place against the back of the boxes using Liquid Nail® all-purpose adhesive.

A 3-inch inside diameter conduit traveled from the multiplexer boxes along the underside of the bridge to the abutment. From there the conduit originally traveled through the abutment underground to a cabinet that was intended to house the remainder of the DAQ system, however, this portion of the conduit was damaged during construction, preventing its use. A temporary cabinet was set up next to the abutment, as shown in Figure 5.7, to house the DAQ system until new conduit was installed. A new conduit was planned to travel north around the front of the abutment and underground to the cabinet that was to be used to permanently house the remainder of the DAQ system, however, as of June 2006 this new portion of the conduit had not yet been installed. The proposed new conduit is included in the plan view of the conduit provided in Figure 5.2. A photograph of the permanent DAQ cabinet is shown in Figure 5.8.

5.3 Long-term Data Collection

The dataloggers were programmed to take strain and temperature readings from all 96 VW strain gages starting at midnight of each day and again every two hours. This provided information on the influence of temperature and solar radiation, which vary throughout the day, on the behavior of the bridge. The recorded data was stored in the SM16M Storage Modules that were attached to each datalogger. For this application, it was not necessary to connect the two dataloggers to each other because there was no need for communication between them. However it was important that the clocks within each datalogger were synchronized so that both dataloggers took measurements at the same time.

The bridge was located within relatively close proximity to the U of MN campus therefore the data was downloaded about once a month. This was done by driving to the site and

swapping the two storage modules that were connected to the dataloggers with two empty storage modules. The storage modules containing the data were then brought to the U of MN where the data was downloaded onto a computer. During the period of time when the site was without power, the data was downloaded every time the batteries were swapped, which was approximately every two weeks.

Chapter 6
Summary and Future Work

6.1 Summary

The use of prefabricated bridge superstructure systems has many advantages over conventional bridge construction. These systems generally reduce the duration of construction time, which minimizes traffic disruption and increases work-zone safety. This has inspired numerous research programs to develop new superstructure systems or improve existing systems to enable them to achieve the benefits associated with prefabricated construction.

One system that has recently been developed is the Mn/DOT Inverted-T Precast Slab System. This system was inspired by the French Poutre Dalle System that was observed during a scanning tour of prefabricated technologies in foreign countries. Several features of the design for this system were incorporated into the design of the Mn/DOT Inverted-T Precast Slab System. In addition, consultation from faculty at the University of Minnesota, as well as input from fabricators and contractors, led to several modifications to the design that would enhance the durability, performance, and constructibility of this new system.

A major concern affecting the durability of precast bridge superstructure systems was the development longitudinal reflective cracking of the CIP concrete deck. The Mn/DOT Inverted-T Precast Slab System was designed to be less susceptible to the development of reflective cracking, however, additional modifications were made to further reduce the potential for the development of these cracks. The corners of the precast sections were chamfered to reduce stress concentrations within the CIP concrete. In addition, the thickness of the flanges was reduced to increase the thickness of the CIP concrete above the longitudinal joint. This increased the sections ability to share loads in the transverse direction. It was hoped that these modifications would further reduce the potential for the development of longitudinal reflective and therefore increase the durability of this system.

The Mn/DOT Inverted-T Precast Slab System was initially implemented in two bridge projects. The first project was a bridge constructed in Center City, Minnesota (Mn/DOT Bridge No. 13004), which was about 40 miles northeast of Minneapolis, Minnesota. The second project was a deck replacement for a bridge located in Beltrami County near Waskish Township in northern Minnesota (Mn/DOT Bridge No. 04002). Instrumentation was installed in the bridge located in Center City (Mn/DOT Bridge No. 13004) to monitor several behaviors that would allow the durability of the system to be evaluated. These behaviors included the development of longitudinal reflective cracking of the CIP concrete and continuous behavior over the piers for live load.

6.2 Benefits of the Mn/DOT Inverted-T Precast Slab System

The precast sections of the Mn/DOT Inverted-T Precast Slab System eliminated the need for formwork to cast the CIP concrete deck and provided a working surface for placement of the deck reinforcement and CIP concrete. During the deck replacement of the Waskish Bridge (Mn/DOT Bridge No. 04002), this improved constructibility reduced the impact of the bridge construction on the environment below the bridge. This improved constructibility also resulted in a reduction in overall construction time. The second stage of the Center City Bridge (Mn/DOT Bridge No. 13004) was completed in 18 working days (23 total days). The first stage took longer because of delays caused by the installation of instrumentation in this portion of the

bridge. If the second stage of the bridge had been constructed using a traditional CIP slab-span type bridge system, it would have taken 20 working days (28 total days). Thus, if there were not delays caused by the installation of instrumentation, the Mn/DOT Inverted-T Precast Slab System would have shortened the construction time by 4 working days and 10 total days. This shorter construction time reduced traffic disruption and improved work-zone safety by shortening the amount of time that construction workers were exposed to this dangerous environment.

It was hoped that the Mn/DOT Inverted-T Precast Slab System would provide a faster bridge construction process for a small premium over conventional bridge superstructure systems. The estimated costs for the two bridges built using the new superstructure system were compared to those of a traditional slab-span bridge to determine if the economic impact of this new system. This comparison is provided in Table 6.1. This table shows that the costs of the Waskish Bridge (Mn/DOT Bridge No. 04002) and Center City Bridge (Mn/DOT Bridge No. 13004) compared well with the cost of a traditional CIP slab-span bridge. There was an expectation that the "rapid construction" associated with this system, as well as the start-up costs for the precaster , would cause this system to be more expensive than a traditional slab-span bridge; however, the start-up costs should not recur as additional bridges of this type are built and future comparisons between costs should be made.

6.3 Preliminary Conclusions

The Center City Bridge (Mn/DOT Bridge No. 13004) was built during September of 2005. As of June 2006, analysis of the collected data and visual inspection of the bridge deck had indicated that no cracking had developed within the CIP concrete topping. No significant information about the continuous behavior of the bridge had been obtained during this period. It was expected that the majority of the information about the continuous behavior of the bridge would be obtained after the truck load test was performed.

6.4 Future Work

The instrumentation in Mn/DOT Bridge No. 13004 was to be monitored for a period of two years. A truck load test was planned to be performed on the bridge during this time period to obtain more information on the continuous behavior of the bridge. In addition to the field testing, a laboratory test and finite element analysis were to be conducted. The objective of the laboratory test was to investigate the effect of several design modifications on the behavior of the bridge. The modifications were made to further increase the durability and constructibility of the system. In addition, the test provided a means to investigate behaviors that could not be investigated with the instrumented bridge in the field such as composite action and loss of prestressing force. The laboratory experiment was to include a full-scale specimen with two spans and two precast sections in each span. Reinforcement details and other aspects of the design were to be varied within each precast section and each span to allow for a more thorough investigation of variations of several parameters including precast section flange thickness, roughened surfaces, continuity steel, horizontal shear reinforcement, and anchorage zone and confinement reinforcement. It was hoped that after complete analysis of the field data, along with completion of the laboratory tests and finite element analysis, final design recommendations could be made for the Mn/DOT Inverted-T Precast Slab System to be implemented in future projects to enhance the performance, constructibility, and durability of this bridge superstructure system.

References

American Association of State Highway Transportation Officials (AASHTO). *AASHTO LRFD Bridge Design Specifications, Third Edition.* Washington, D.C.: 2004.

Badie, Sameh S., Mounir R. Kamel, and Maher K. Tadros. "Precast Pretensioned Trapezoidal Box Beam for Short Span Bridges." *PCI Journal,* vol. 44, no.1 (January-February 1999): 48-59.

Buckner, C. Dale, and H. T. Turner. *Performance Tests of Full Span Panel Form Bridges (Final Report 80-1c).* (Baton Rouge, LA: Louisiana State University, Research and Development Section Louisiana Department of Transportation and Development, 1981).

El-Remaily, Ahmed, et al. "Transverse Design of Adjacent Precast Prestressed Concrete Box Girder Bridges." *PCI Journal,* vol. 41, no.4 (July-August 1996): 96-113.

Fallaha, Sam, et al. "High Performance Precast Concrete NUDECK Panel System for Nebraska's Skyline Bridge." *PCI Journal,* vol. 49, no. 5, (September-October 2004): 40-50.

Freyermuth, C. "Design of Continuous Highway Bridges with Precast, Prestressed Concrete Girders." *PCI Journal*, vol. 14, no. 2 (March-April 1969): 14-39.

Hagen, Kevin, et al. "Development and Construction of a Precast Inverted T System for Expediting Minnesota Slab Span Bridge Projects." *2005 Concrete Bridge Conference.*

Hagen, Kevin. "Development of Mn/DOT Precast Slab System". Presentation ed. Mn/DOT & FHWA Precast Slab System Workshop, September 8, 2005.

Hays, C. O. Jr., R. L. Cox, Jr., and G. O. Obranic, Jr. *Full Span Form Panels for Short Span Highway Bridges (Final Report U17F).* (Gainesville, FL: Department of Civil Engineering, University of Florida, 1980)

Hieber, David G., et al. *State-of-the-Art Report on Precast Concrete Systems for Rapid Construction of Bridges (Draft Interim Report).* (Seattle, WA: Department of Civil Engineering and Environmental Engineering, University of Washington, August 2004.)

Huckelbridge, Arthur A. Jr., Hassan El-Esnawi, and Fred Moses. "Shear Key Performance in Multibeam Box Girder Bridges." *Journal of Performance of Constructed Facilities,* vol. 9, no. 4 (April 1995): 271-85.

Kamel, Mounir R., and Maher K. Tadros. "The Inverted Tee Shallow Bridge System for Rural Areas." PCI *Journal,* vol. 41, no. 5 (September-October 1996): 28-43.

McDonagh, Michael D., and Kevin B. Hinkley. "Resolving Restraint Moments: Designing for Continuity in Precast Prestressed Concrete Girder Bridges." *PCI Journal*, vol. 48, no. 4 (April 2003): 104-19.

Minnesota Department of Transportation. *Standard Specifications for Construction,* 2000 Edition.

Peterman, Robert J., and Julio A. Ramirez. "Behavior and Strength of Bridges with Full-Span Prestressed Concrete Form Panels." *PCI Journal*, vol. 43, no. 2 (March- April 1998): 80-91.

Peterman, Robert J., and Julio A. Ramirez. "Restraint Moments in Bridges with Full-Span Prestressed Concrete Form Panels." *PCI Journal*, vol. 43, no.1 (January-February 1998): 54-73.

"Prefabricated Bridge Elements and Systems in Japan and Europe- Summary Report." FHWA International Technology Exchange Programs. May 2004.

Ralls, Mary Lou, Ronald D. Medlock and Sharon Slagle. "Prefabricated Bridge National Implementation Initiative." *2002 Concrete Bridge Conference.*

Saleh, Mohsen A., Amin Einea, and Maher K. Tadros. "Creating Continuity in Precast Girder Bridges." *Concrete International*, vol. 17, no. 8 (August 1995): 27-32.

Tadros, M.K. and Baishya, M.C., "Rapid Replacement for Bridge Decks," *NCHRP Report 407*, National Cooperative Highway Research Program, Washington D.C., 1998.

Yamane, Takashi, et al. "Full Depth Precast, Prestressed Concrete Bridge Deck System." *PCI Journal*, vol. 43, no. 3 (May-June 1998): 50-66.

Tables

Table 2.1 Cross sections of different precast sections (Kamel and Tadros, 1996)

Typical Section	Width (in.)	Depth (in.)	Span range (ft.)
Solid Slab	36 to 96	10 to 18	up to 30
Voided Slab	36 to 48	15 to 23	20 to 60
Multi-stem	48	16 to 23	20 to 60
Double Stem	60 to 96	16 to 23	20 to 60
Single Stem	48 to 72	24 to 48	35 to 80
Box Girder	36 to 48	27 to 42	60 to 100
Deck Bulb Tee	48 to 84	29 to 41	60 to 110
I-Girder	18 to 26	36 to 45	40 to 80

Table 2.2 Dimensions of form panels and CIP concrete for the bridges visited in Florida during the study performed by Hays, Jr. et al. (1980) (variables t_1, t_2, and t_3 are shown in Figures 2.10 and 2.11)

Bridge	Span (ft.)	Thickness (in.) t_1	t_2	t_3	Panel Width (in.)	Year/Comments
Lloyd Creek Bridge SR 59, Jefferson County	23	7	--	5.5	48	1977/ Neg. Mom Cracks Less extensive
Hurricane Creek Bridge SR2A, Holmes County	30	6	5	5	79	1977
Sanders Creek Bridge SR 20, Okalossa County	30	10	--	4	48	1977/ Long. Cracks Less extensive
Fort Gasden Creek SR 65, Liberty County	26	4	5	4	80	1977
Black Creek Bridge SR 65, Liberty County	26	4	5	4	80	1976
Sampson River Bridge SR 18, Bradford County	32	7	5	4.5	80	1979/ Neg. Mom. Cracks less extensive
Harney Canal Bridge - C136 US 301, Hillsborough County	27	5	5	5	80	1977/ Exstensive random surface cracking Widest longitudinal cracks
Cypress Creek Bridge Kings Point Boulevard Hillsborough County	28	5	5	5	60	1978/ Extensive random cracking No longitudinal cracking Very light traffic
Shingle Creek Bridge SR 528A, Orange County	27	6	5	4.5	51	1978/ Less long. cracking when joint near center of traffic lane

Table 2.3 Reinforcement details and dimensions of the laboratory specimen used in the study performed by Buckner and Turner (1981) ("S" = flat panel, "B" = beveled panel) (variables t_d and t_p are shown in Figures 2.13 and 2.14)

Specimen Mark	t_d (in.)	t_p (in.)	Transverse Reinforcement		No. of Strands Per Panel
			Left Half	Right Half	
S - 5.5 – 10	7.5	5.5	#4 @ 15" o.c.	#4 @ 12" o.c.	10
B - 5.5 -10	7.5	5.5	#4 @ 15" o.c.	#4 @ 12" o.c.	10
S - 8 – 8	5	8	#3 @ 12" o.c.	#4 @ 12" o.c.	8
B - 8 – 8	5	8	#3 @ 12" o.c.	#4 @ 12" o.c.	8
S -10 – 8	3	10	#3 @ 15" o.c.	#4 @ 12" o.c.	8
B -10 -8	3	10	#3 @ 15" o.c.	#4 @ 12" o.c.	8

Table 3.1 Compressive concrete strength of concrete used for precast sections in the superstructure of Stage 1 of Mn/DOT Bridge No. 13004

Date Poured	Release Strength (psi)	28 Day Strength (psi)
8/18/2005	7650 6780	9880
8/19/2005	6760 6380	9870
8/22/2005	7340 6990	9850
8/24/2005	6760 8080	9840
8/25/2005	6680 7040	9850
8/29/2005	6900 7370	9850

Table 3.2 Compressive concrete strength of CIP concrete used in Stage 1 of the superstructure for Mn/DOT Bridge No. 13004

Date Poured	7 Day Strength (psi)	10 Day Strength (psi)	28 Day Strength (psi)
9/19/2005	3875	3613	3979

Table 4.1 Coordinates of the VW embedment strain gages installed directly above the precast longitudinal joints (see Figure 4.1 for coordinate system, "Z" is depth within cross section from bottom of bridge)

	Instrument No.	X (in.)	Y (in.)	Z (in.)
Joint #1	CJ1-51-1	438.0	280.5	8.5
	CJ1-51-2	438.0	276.5	8.5
	CJ1-51-3	438.0	272.5	8.5
	CJ1-51-4	438.0	268.5	8.5
	CJ1-51-5	438.0	264.5	8.5
Joint #2	CJ2-51-1	438.0	208.5	8.5
	CJ2-51-2	438.0	204.5	8.5
	CJ2-51-3	438.0	200.5	8.5
	CJ2-51-4	438.0	196.5	8.5
	CJ2-51-5	438.0	192.5	8.5
Joint #3	CJ3-51-1	438.0	136.5	8.5
	CJ3-51-2	438.0	132.5	8.5
	CJ3-51-3	438.0	128.5	8.5
	CJ3-51-4	438.0	124.5	8.5
	CJ3-53-5	438.0	120.5	8.5

Table 4.2 Coordinates of the VW embedment strain gages installed directly above the precast section web corners (see Figure 4.1 for coordinate system, "Z" is depth within cross section from bottom of bridge)

	Instrument No.	X (in.)	Y (in.)	Z (in.)
Joint #1	CJ1-53-1	438.0	293.0	13.5
	CJ1-53-2	438.0	288.5	13.5
	CJ1-53-3	438.0	284.0	13.5
	CJ1-53-4	438.0	279.5	13.5
	CJ1-53-5	438.0	275.0	13.5
	CJ1-53-6	438.0	270.5	13.5
	CJ1-53-7	438.0	266.0	13.5
	CJ1-53-8	438.0	261.5	13.5
	CJ1-53-9	438.0	257.0	13.5
	CJ1-53-10	438.0	252.5	13.5
Joint #2	CJ2-53-1	438.0	221.0	13.5
	CJ2-53-2	438.0	216.5	13.5
	CJ2-53-3	438.0	212.0	13.5
	CJ2-53-4	438.0	207.5	13.5
	CJ2-53-5	438.0	203.0	13.5
	CJ2-53-6	438.0	198.5	13.5
	CJ2-53-7	438.0	194.0	13.5
	CJ2-53-8	438.0	189.5	13.5
	CJ2-53-9	438.0	185.0	13.5
	CJ2-53-10	438.0	180.5	13.5
Joint #3	CJ3-53-1	438.0	149.0	13.5
	CJ3-53-2	438.0	144.5	13.5
	CJ3-53-3	438.0	140.0	13.5
	CJ3-53-4	438.0	135.5	13.5
	CJ3-53-5	438.0	131.0	13.5
	CJ3-53-6	438.0	126.5	13.5
	CJ3-53-7	438.0	122.0	13.5
	CJ3-53-8	438.0	117.5	13.5
	CJ3-53-9	438.0	113.0	13.5
	CJ3-53-10	438.0	108.5	13.5

Table 4.3 Coordinates of the VW spot-weldable strain gages installed on longitudinal reinforcement (see Figure 4.1 for coordinate system, "Z" is depth within cross section from bottom of bridge)

	Instrument No.	X (in.)	Y (in.)	Z (in.)
Joint #1	SJ1-51-1	429.0	264.0	9.0
	SJ1-52-1	429.0	264.0	12.5
	SJ1-53-1	427.5	276.5	15.5
	SJ1-53-2	427.5	263.5	15.5
	SJ1-41-1	290.0	268.5	9.0
	SJ1-43-1	290.0	280.0	15.5
	SJ1-43-2	290.0	268.5	15.5
	SJ1-C1-1	271.0	268.5	9.0
	SJ1-C3-1	271.0	268.5	15.5
	SJ1-C3-2	271.0	296.0	15.5
	SJ1-31-1	252.0	268.5	9.0
	SJ1-33-1	251.0	280.0	15.5
	SJ1-33-2	250.0	269.5	15.5
	SJ1-21-1	128.5	264.0	9.0
	SJ1-22-1	128.5	264.0	12.5
	SJ1-23-1	130.0	261.5	15.5
	SJ1-11-1	22.0	264.0	9.0
	SJ1-12-1	22.0	264.0	12.5
	SJ1-13-1	21.0	261.5	15.5
Joint #2	SJ2-51-1	427.5	192.0	9.0
	SJ2-52-1	427.5	192.0	12.5
	SJ2-53-1	426.5	193.5	15.5
	SJ2-41-1	289.5	198.0	9.0
	SJ2-43-1	291.5	197.0	15.5
Joint #3	SJ3-41-1	287.0	124.5	9.0
	SJ3-43-1	286.0	124.0	15.5
Web #1	SW1-43-1	292.5	249.5	15.5
	SW1-43-2	292.5	236.0	15.5
	SW1-43-3	292.5	225.0	15.5
Web #2	SW2-43-1	291.0	177.5	15.5
	SW2-43-2	291.0	165.5	15.5
	SW2-43-3	291.0	154.5	15.5

Table 4.4 Coordinates of the VW spot-weldable strain gages installed on the transverse hooks of the precast sections (see Figure 4.1 for coordinate system, "Z" is depth within cross section from bottom of bridge)

	Instrument No.	X (in.)	Y (in.)	Z (in.)
Joint #1	SJ1-5T-1	434.0	278.5	7.0
	SJ1-5T-2	432.5	276.5	7.0
	SJ1-5T-3	434.0	274.5	7.0
	SJ1-5T-4	432.5	272.5	7.0
	SJ1-5T-5	434.0	270.5	7.0
	SJ1-5T-6	432.5	268.5	7.0
	SJ1-5T-7	434.0	266.5	7.0
Joint #2	SJ2-5T-1	434.0	206.5	7.0
	SJ2-5T-2	432.5	204.5	7.0
	SJ2-5T-3	434.0	202.5	7.0
	SJ2-5T-4	432.5	200.5	7.0
	SJ2-5T-5	434.0	198.5	7.0
	SJ2-5T-6	432.5	196.5	7.0
	SJ2-5T-7	434.0	194.5	7.0
Joint #3	SJ3-5T-1	434.0	134.5	7.0
	SJ3-5T-2	432.5	132.5	7.0
	SJ3-5T-3	434.0	130.5	7.0
	SJ3-5T-4	432.5	128.5	7.0
	SJ3-5T-5	434.0	126.5	7.0
	SJ3-5T-6	432.5	124.5	7.0
	SJ3-5T-7	434.0	122.5	7.0

Table 5.1 Channel assignments for Multiplexer #1

Multiplexer #1	
Ch.	Gage #
1.1-	CJ1-53-5
1.2-	CJ1-53-6
1.3-	CJ1-53-7
1.4-	CJ1-53-8
1.5-	CJ1-53-9
1.6-	CJ1-53-10
1.7-	SJ1-51-1
1.8-	SJ1-52-1
1.9-	SJ1-53-2
1.10-	SJ1-53-1
1.11-	SJ1-21-1
1.12-	SJ1-22-1
1.13-	SJ1-23-1
1.14-	SJ1-11-1
1.15-	SJ1-12-1
1.16-	SJ1-13-1

Table 5.2 Channel assignments for Multiplexer #2

Multiplexer #2	
Ch.	Gage #
2.1-	SJ1-5T-1
2.2-	SJ1-5T-2
2.3-	SJ1-5T-3
2.4-	SJ1-5T-4
2.5-	SJ1-5T-5
2.6-	SJ1-5T-6
2.7-	SJ1-5T-7
2.8-	CJ1-51-1
2.9-	CJ1-51-2
2.10-	CJ1-51-3
2.11-	CJ1-51-4
2.12-	CJ1-51-5
2.13-	CJ1-53-1
2.14-	CJ1-53-2
2.15-	CJ1-53-3
2.16-	CJ1-53-4

Table 5.3 Channel assignments for Multiplexer #3

Multiplexer #3	
Ch.	Gage #
3.1-	CJ2-53-5
3.2-	CJ2-53-6
3.3-	CJ2-53-7
3.4-	CJ2-53-8
3.5-	CJ2-53-9
3.6-	CJ2-53-10
3.7-	SJ2-51-1
3.8-	SJ2-52-1
3.9-	SJ2-53-1
3.10-	SJ1-41-1
3.11-	SJ1-43-2
3.12-	SJ1-43-1
3.13-	SJ1-C1-1
3.14-	SJ1-31-1
3.15-	SJ1-33-2
3.16-	SJ1-33-1

Table 5.4 Channel assignments for Multiplexer #4

Multiplexer #4	
Ch.	Gage #
4.1-	SJ2-5T-1
4.2-	SJ2-5T-2
4.3-	SJ2-5T-3
4.4-	SJ2-5T-4
4.5-	SJ2-5T-5
4.6-	SJ2-5T-6
4.7-	SJ2-5T-7
4.8-	CJ2-51-1
4.9-	CJ2-51-2
4.10-	CJ2-51-3
4.11-	CJ2-51-4
4.12-	CJ2-51-5
4.13-	CJ2-53-1
4.14-	CJ2-53-2
4.15-	CJ2-53-3
4.16-	CJ2-53-4

Table 5.5 Channel assignments for Multiplexer #5

Multiplexer #5	
Ch.	Gage #
5.1-	CJ3-53-5
5.2-	CJ3-53-6
5.3-	CJ3-53-7
5.4-	CJ3-53-8
5.5-	CJ3-53-9
5.6-	CJ3-53-10
5.7-	SJ3-41-1
5.8-	SJ3-43-1
5.9-	SW2-43-1
5.10-	SW2-43-2
5.11-	SW2-43-3
5.12-	SJ2-41-1
5.13-	SJ2-43-1
5.14-	SW1-43-1
5.15-	SW1-43-2
5.16-	SW1-43-3

Table 5.6 Channel assignments for Multiplexer #6

Multiplexer #6	
Ch.	Gage #
6.1-	SJ3-5T-1
6.2-	SJ3-5T-2
6.3-	SJ3-5T-3
6.4-	SJ3-5T-4
6.5-	SJ3-5T-5
6.6-	SJ3-5T-6
6.7-	SJ3-5T-7
6.8-	CJ3-51-1
6.9-	CJ3-51-2
6.10-	CJ3-51-3
6.11-	CJ3-51-4
6.12-	CJ3-51-5
6.13-	CJ3-53-1
6.14-	CJ3-53-2
6.15-	CJ3-53-3
6.16-	CJ3-53-4

Table 5.7 Locations of the cables in the conduit relative to the precast longitudinal joints (see Figure 5.3 for plan view of cables)

Joint #	Span	Cable #	Multiplexer Box #
Joint #1	Center Span	**Cable 6-1**	Box #1
		Cable 6-2	
		Cable 6-3	
		Cable 6-4	
Joint #1	East Span	**Cable 6-5**	
		Cable 6-6	
Joint #2	Center Span	**Cable 5-1**	Box #2
		Cable 5-2	
		Cable 5-3	
		Cable 5-4	
		Cable 5-5	Box #3
Joint #3	Center Span	**Cable 4-1**	
		Cable 4-2	
		Cable 4-3	
		Cable 4-4	

Table 5.8 Instrumentation connected to Cable 6-1

Cable 6-1	
	Instrument-Cable
SJ1-5T-1	red-green black-white
	green-green white-blue
SJ1-5T-2	red-red black-orange
	green-red white-brown
SJ1-5T-3	red-green black-yellow
	green-green white-brown
SJ1-5T-7	red-red black-black
	green-black white-yellow
SJ1-5T-5	red-red black-yellow
	green-blue white-black
SJ1-5T-6	red-black black-green
	green-red white-white
SJ1-5T-4	red-black black-orange
	green-blue white-red
CJ1-51-1	red-red black-green
	green-brown white-black

Table 5.9 Instrumentation connected to Cable 6-2

Cable 6-2	
	Instrument-Cable
CJ1-51-3	red-green black-blue
	green-red white-orange
CJ1-51-4	red-red black-brown
	green-green white-yellow
CJ1-51-5	red-green black-brown
	green-red white-black
CJ1-53-1	red-black black-yellow
	green-red white-yellow
CJ1-53-2	red-blue black-black
	green-black white-green
CJ1-53-3	red-red black-white
	green-black white-green
CJ1-53-4	red-red black-white
	green-black white-orange
CJ1-53-5	red-blue black-red
	green-red white-green

Table 5.10 Instrumentation connected to Cable 6-3

Cable 6-3	
	Instrument-Cable
CJ1-53-6	red-green black-white
	green-green white-blue
CJ1-53-7	red-red black-orange
	green-red white-brown
CJ1-53-8	red-green black-yellow
	green-green white-brown
CJ1-53-9	red-red black-black
	green-black white-yellow
CJ1-53-10	red-red black-yellow
	green-blue white-black
SJ1-53-1	red-black black-green
	green-red white-white
CJ1-51-2	red-black black-orange
	green-blue white-red

Table 5.11 Instrumentation connected to Cable 6-4

Cable 6-4	
	Instrument-Cable
SJ1-51-1	red-black black-green
	green-green white-white
SJ1-52-1	red-red black-black
	green-green white-white
SJ1-53-2	red-red black-black
	green-green white-white

Table 5.12 Instrumentation connected to Cable 6-5

Cable 6-5	
	Instrument-Cable
SJ1-11-1	red-black black-green
	green-brown white-black
SJ1-12-1	red-black black-blue
	green-black white-yellow
SJ1-13-1	red-red black-black
	green-black white-white

Table 5.13 Instrumentation connected to Cable 6-6

Cable 6-6	
	Instrument-Cable
SJ1-21-1	red-black black-green
	green-brown white-black
SJ1-22-1	red-black black-blue
	green-black white-yellow
SJ1-23-1	red-red black-black
	green-black white-white

Table 5.14 Instrumentation connected to Cable 5-1

Cable 5-1	
	Instrument-Cable
SJ2-5T-1	red-green black-white
	green-green white-blue
SJ2-5T-2	red-red black-orange
	green-red white-brown
SJ2-5T-3	red-green black-yellow
	green-green white-brown
SJ2-5T-7	red-red black-black
	green-black white-yellow
SJ2-5T-5	red-red black-yellow
	green-blue white-black
SJ2-5T-6	red-black black-green
	green-red white-white
SJ2-5T-4	red-black black-orange
	green-blue white-red
CJ2-51-1	red-red black-green
	green-brown white-black

Table 5.15 Instrumentation connected to Cable 5-2

Cable 5-2	
	Instrument-Cable
CJ2-51-3	red-green black-blue
	green-red white-orange
CJ2-51-4	red-red black-brown
	green-green white-yellow
CJ2-51-5	red-green black-brown
	green-red white-black
CJ2-53-1	red-black black-yellow
	green-red white-yellow
CJ2-53-2	red-blue black-black
	green-black white-green
CJ2-53-3	red-red black-white
	green-black white-orange
CJ2-53-4	red-blue black-red
	green-red white-green
CJ2-53-5	red-brown black-black
	green-black white-white

Table 5.16 Instrumentation connected to Cable 5-3

Cable 5-3	
	Instrument-Cable
CJ2-53-6	red-green black-white
	green-green white-blue
CJ2-53-7	red-red black-orange
	green-red white-brown
CJ2-53-8	red-green black-yellow
	green-green white-brown
CJ2-53-9	red-red black-black
	green-black white-yellow
CJ2-53-10	red-red black-yellow
	green-blue white-black
CJ2-51-2	red-black black-green
	green-red white-white

Table 5.17 Instrumentation connected to Cable 5-4

Cable 5-4	
	Instrument-Cable
SJ2-51-1	red-black black-green
	green-brown white-black
SJ2-52-1	red-black black-blue
	green-black white-yellow
SJ2-53-1	red-red black-black
	green-black white-white

Table 5.18 Instrumentation connected to Cable 5-5

Cable 5-5	
	Instrument-Cable
SJ2-41-1	red-black
	black-green
	green-brown
	white-black
SJ2-43-1	red-black
	black-blue
	green-black
	white-yellow
SW1-43-1	red-red
	black-black
	green-black
	white-white
SW1-43-2	red-red
	black-yellow
	green-black
	white-orange
SW1-43-3	red-red
	black-brown
	green-green
	white-red

Table 5.19 Instrumentation connected to Cable 4-1

Cable 4-1	
	Instrument-Cable
SJ3-5T-1	red-green black-white
	green-green white-blue
SJ3-5T-2	red-red black-orange
	green-red white-brown
SJ3-5T-3	red-green black-yellow
	green-green white-brown
SJ3-5T-7	red-red black-black
	green-black white-yellow
SJ3-5T-5	red-red black-yellow
	green-blue white-black
SJ3-5T-6	red-black black-green
	green-red white-white
SJ3-5T-4	red-black black-orange
	green-blue white-red
CJ3-51-1	red-red black-green
	green-brown white-black

Table 5.20 Instrumentation connected to Cable 4-2

Cable 4-2	
	Instrument-Cable
CJ3-51-3	red-green black-blue
	green-red white-orange
CJ3-51-4	red-red black-brown
	green-green white-yellow
CJ3-51-5	red-green black-brown
	green-red white-black
CJ3-53-1	red-black black-yellow
	green-red white-yellow
CJ3-53-2	red-blue black-black
	green-black white-green
CJ3-53-3	red-red black-white
	green-black white-orange
CJ3-53-4	red-blue black-red
	green-red white-green
CJ3-53-5	red-brown black-black
	green-black white-white

Table 5.21 Instrumentation connected to Cable 4-3

Cable 4-3	
	Instrument-Cable
CJ3-53-6	red-green black-white
	green-green white-blue
CJ3-53-7	red-red black-orange
	green-red white-brown
CJ3-53-8	red-green black-yellow
	green-green white-brown
CJ3-53-9	red-red black-black
	green-black white-yellow
CJ3-53-10	red-red black-yellow
	green-blue white-black
CJ3-51-2	red-black black-green
	green-red white-white

Table 5.22 Instrumentation connected to Cable 4-4

Cable 4-4	
	Instrument-Cable
SW2-43-1	red-black black-green
	green-brown white-black
SW2-43-2	red-black black-blue
	green-black white-yellow
SW2-43-3	red-red black-black
	green-black white-white

Table 6.1 Superstructure cost comparison of bridges built with the Mn/DOT Inverted-T Precast Slab System to traditional slab-span bridges

Waskish Bridge (Mn/DOT Bridge No. 04002)	**$64/S.F.**
Center City Bridge (Mn/DOT Bridge No. 13004)	**$64/S.F.**
Traditional Slab-span Bridge	**$60-$65/S.F.**

Figures

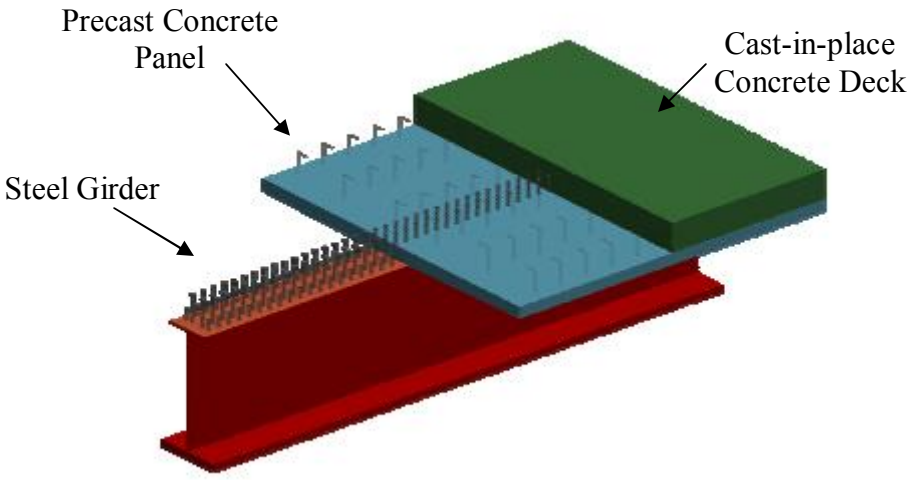

Figure 1.1 Partial-depth concrete decks prefabricated on steel or concrete beams (FHWA, 2004)

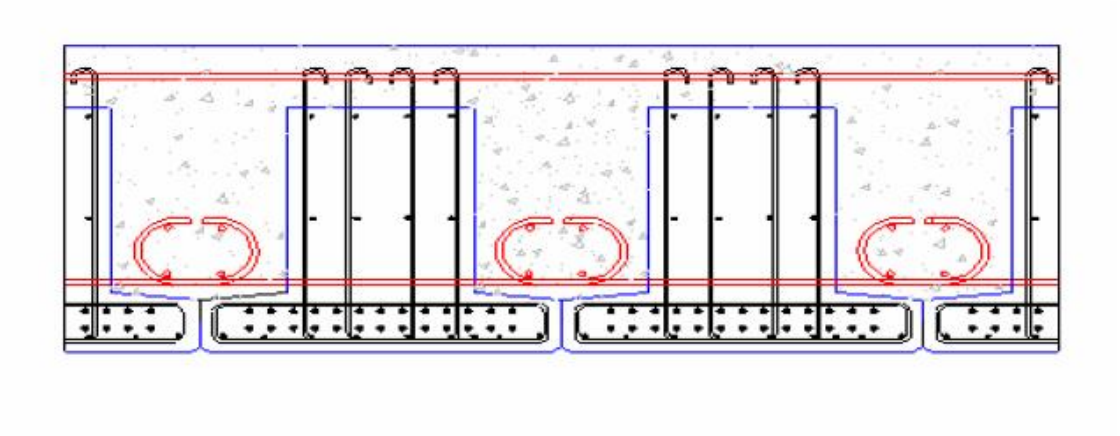

Figure 1.2 Cross section of Poutre Dalle System (Hagen, 2005)

Figure 1.3 Photograph of precast section used in Poutre Dalle System (Hagen, 2005)

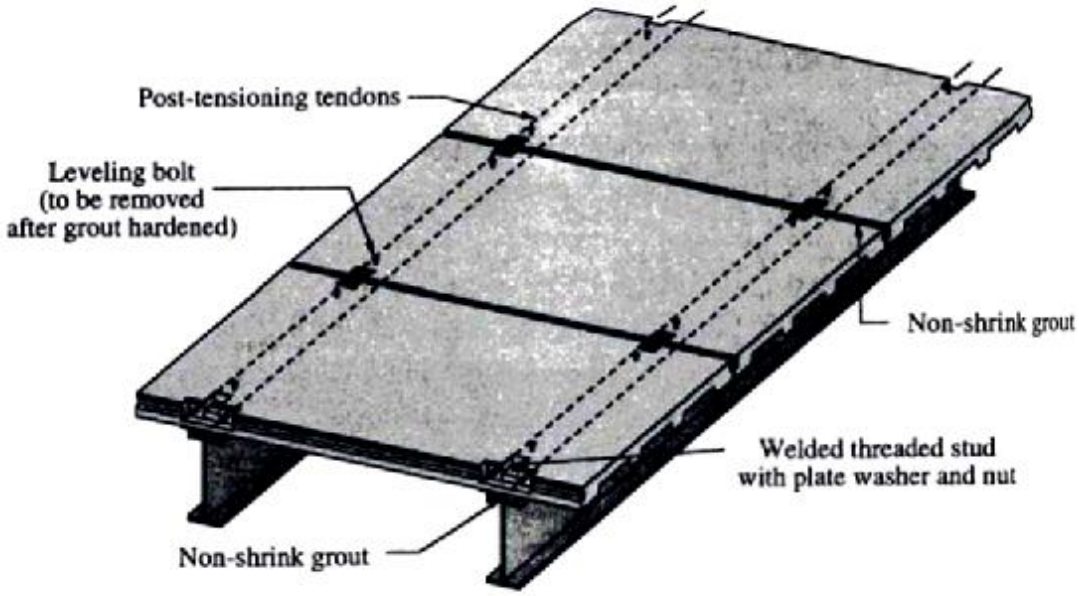

Figure 2.1 Full-Depth Precast Prestressed Bridge Deck System (Yamane et al., 1998)

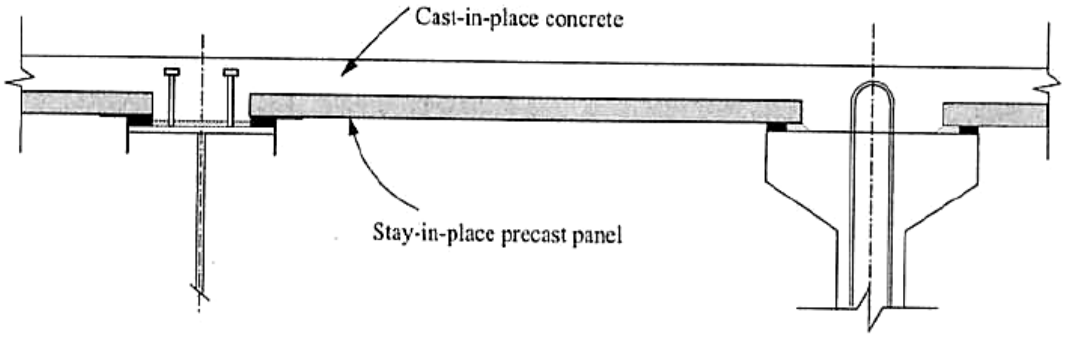

Figure 2.2 Cross section of a partial-depth precast concrete panel system (Tadros and Baishya, 1998)

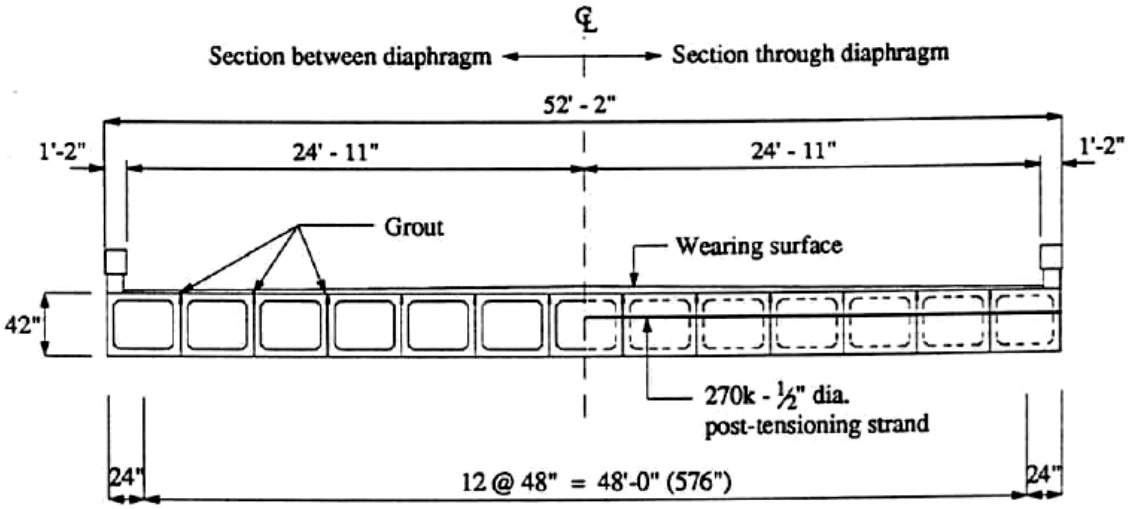

Figure 2.3 Cross section of a box girder bridge system with transverse post-tensioning (El-Remaily et al., 1996)

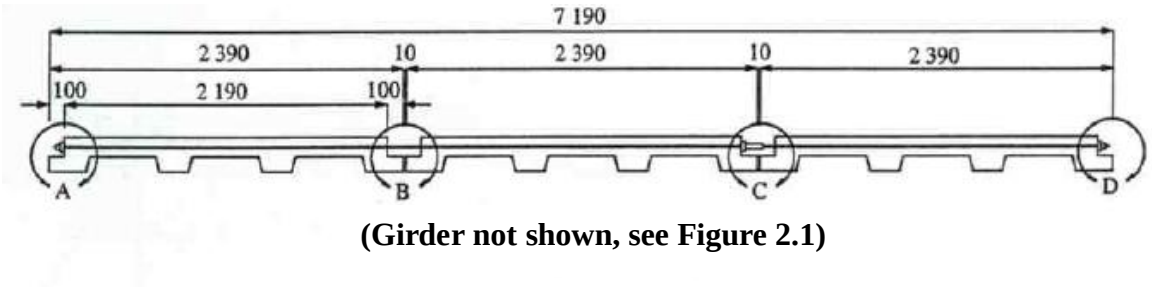

(Girder not shown, see Figure 2.1)

Figure 2.4 Elevation view of longitudinal post-tensioning in a Full-Depth Precast Prestressed Bridge Deck System (dimensions are in mm) (Yamane et al., 1998)

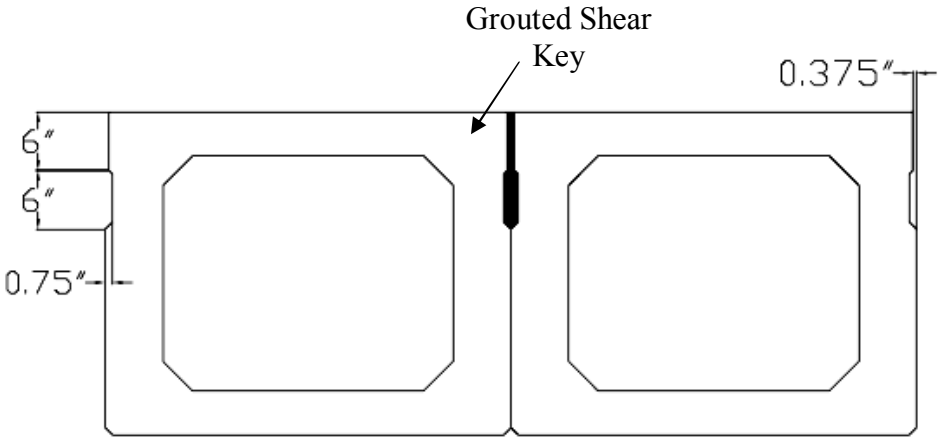

Figure 2.5 Typical geometry of a shear key used in a box girder system (Huckelbridge, Jr. et al., 1995)

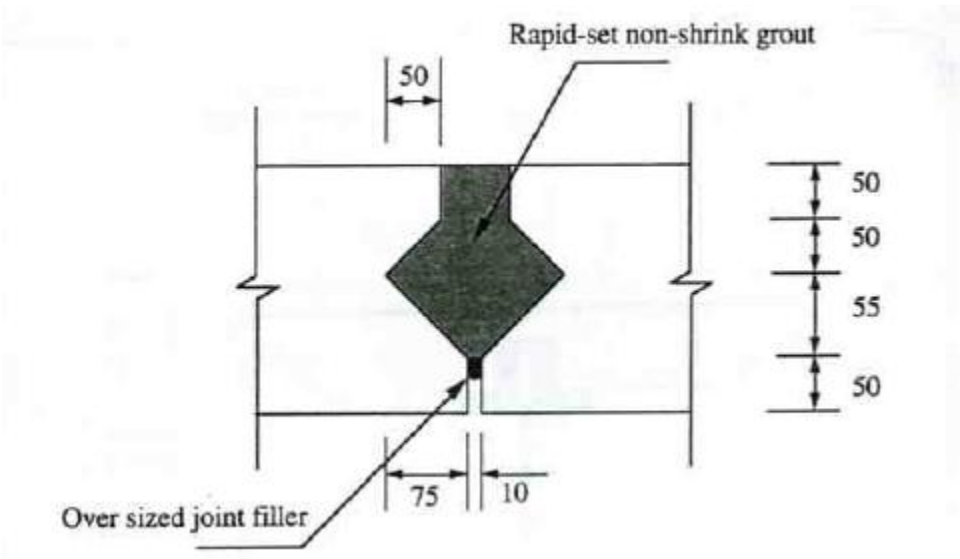

Figure 2.6 Typical geometry of a shear key used in a Full-Depth Precast Prestressed Panel System (dimensions are in mm) (Yamane et al., 1998)

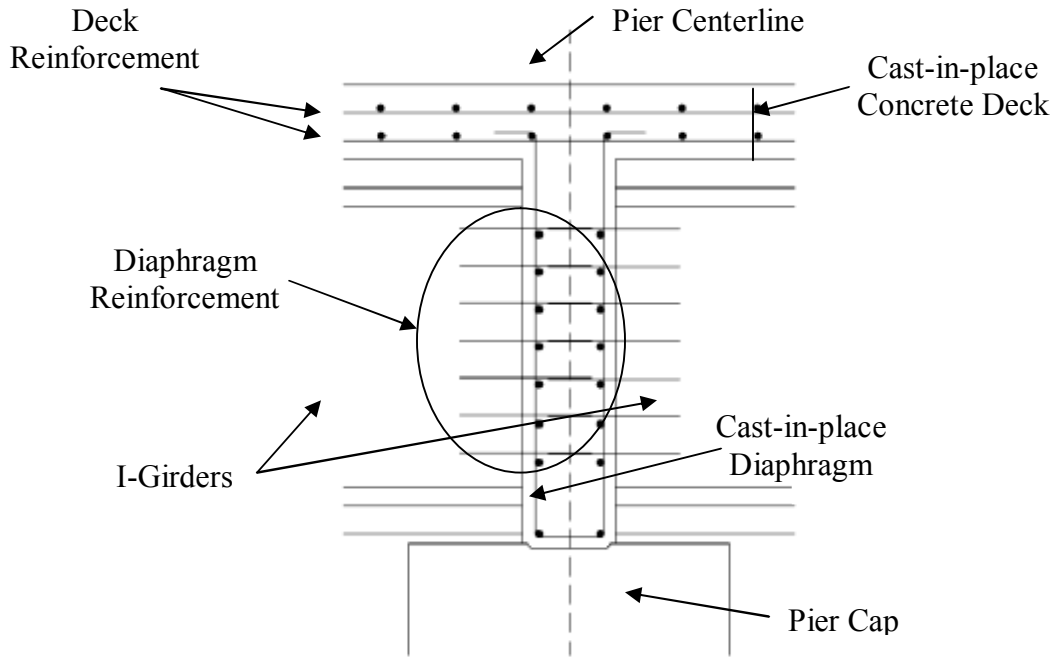

Figure 2.7 Interior joint detail of a precast concrete bridge girder made continuous using the Conventional Reinforcement Method (Saleh et al., 1995)

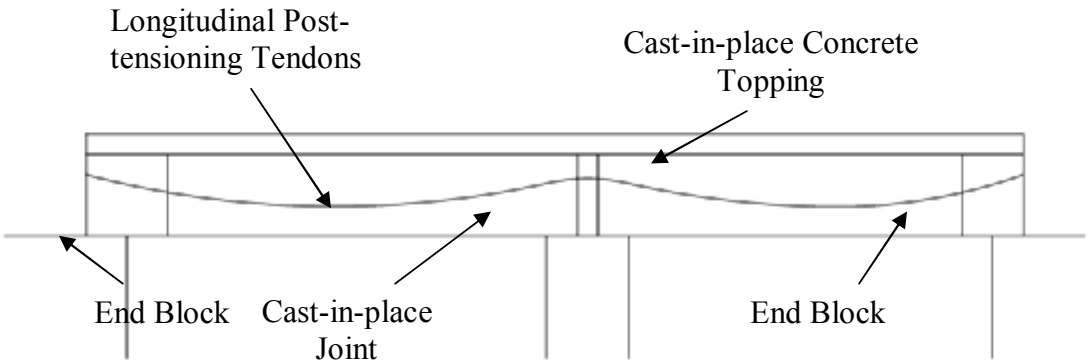

Figure 2.8 Elevation view of a bridge made continuous over the pier through the use of longitudinal post-tensioning (Saleh et al., 1995)

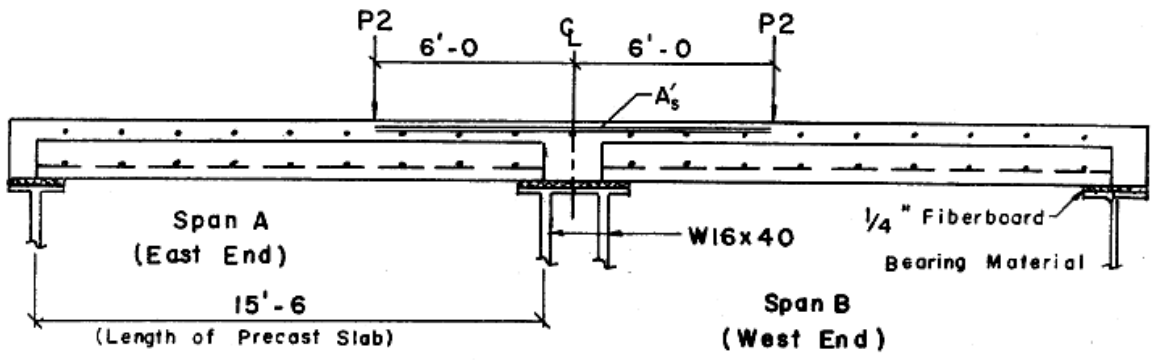

Figure 2.9 Elevation view of the lab specimen used in the study performed by Hays, Jr. et al. (1980)

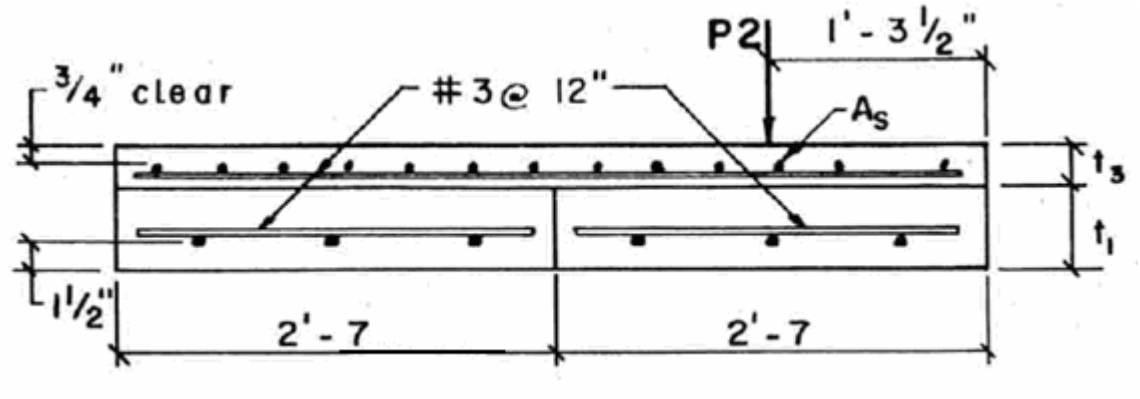

Figure 2.10 Cross-sectional view of the standard span of the lab specimen used in the study performed by Hays, Jr. et al. (1980)

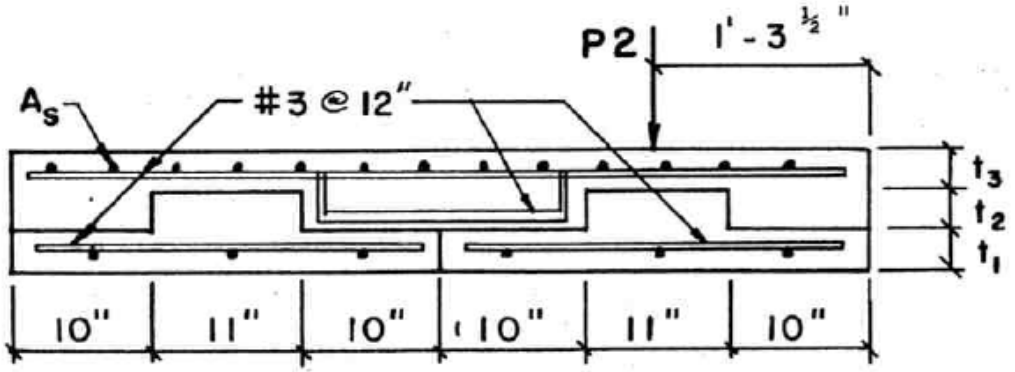

Figure 2.11 Cross-sectional view of the alternative span of the lab specimen used in the study performed by Hays, Jr. et al. (1980)

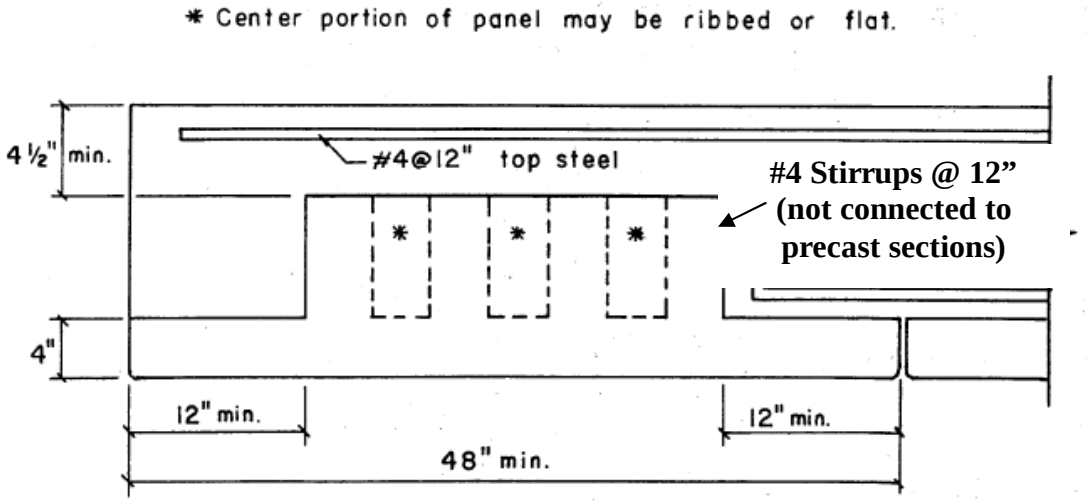

Figure 2.12 Cross section of the panel detail recommended by Hays, Jr. et al. (1980)

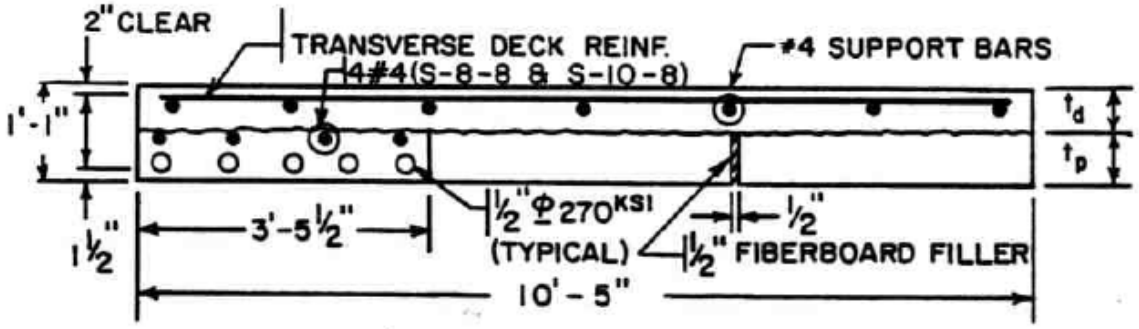

Figure 2.13 Cross section of the flat panel laboratory specimen used in study performed by Buckner and Turner (1981) (see Table 2.3 for notation)

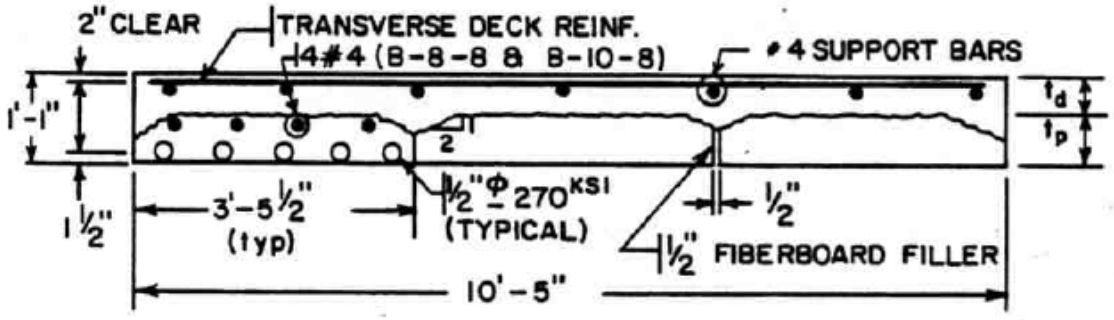

Figure 2.14 Cross section of the beveled-edge laboratory specimen used in study performed by Buckner and Turner (1981) (see Table 2.3 for notation)

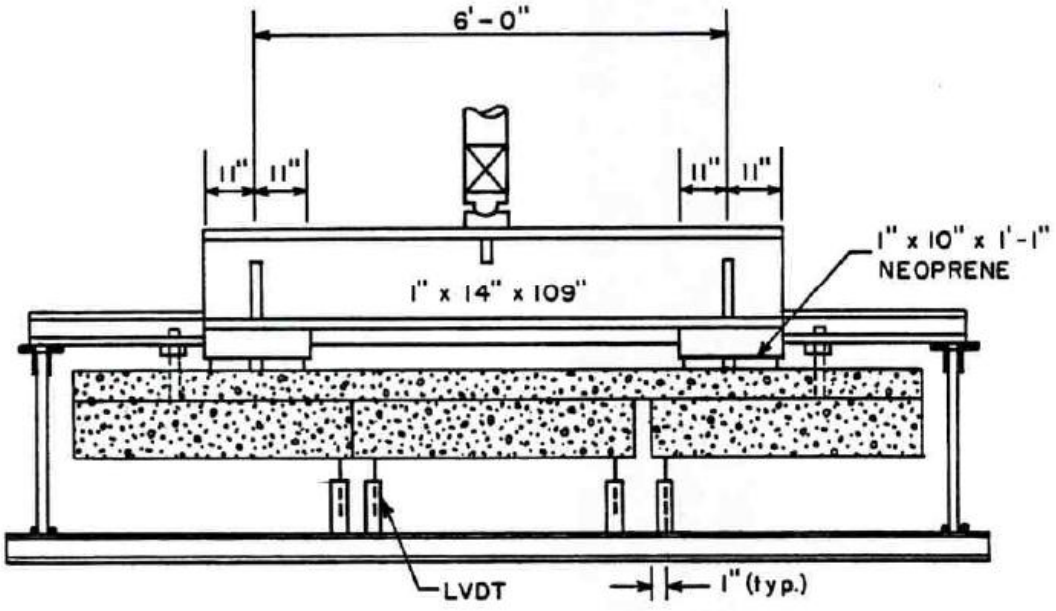

Figure 2.15 Cross-sectional view of the loading apparatus used in the study performed by Buckner and Turner (1981)

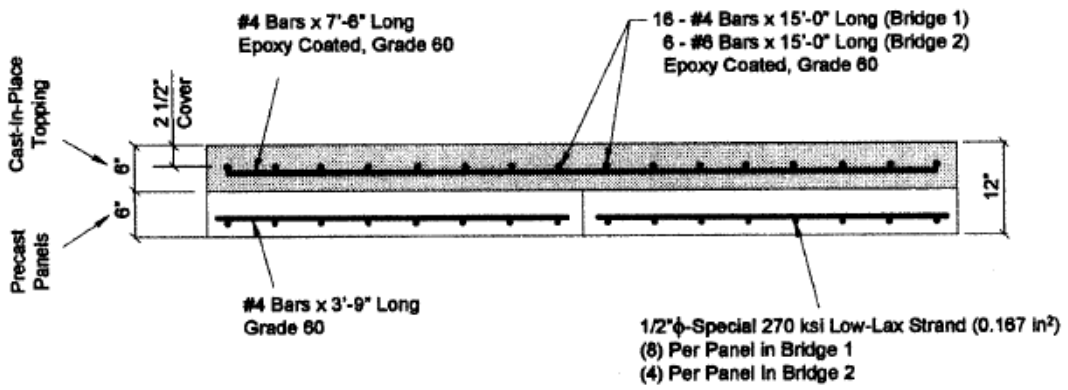

(Panels are 4 ft. wide and 21 ft. long)

Figure 2.16 Cross section of the laboratory specimen used in study performed by Peterman and Ramirez (1998a, 1998b)

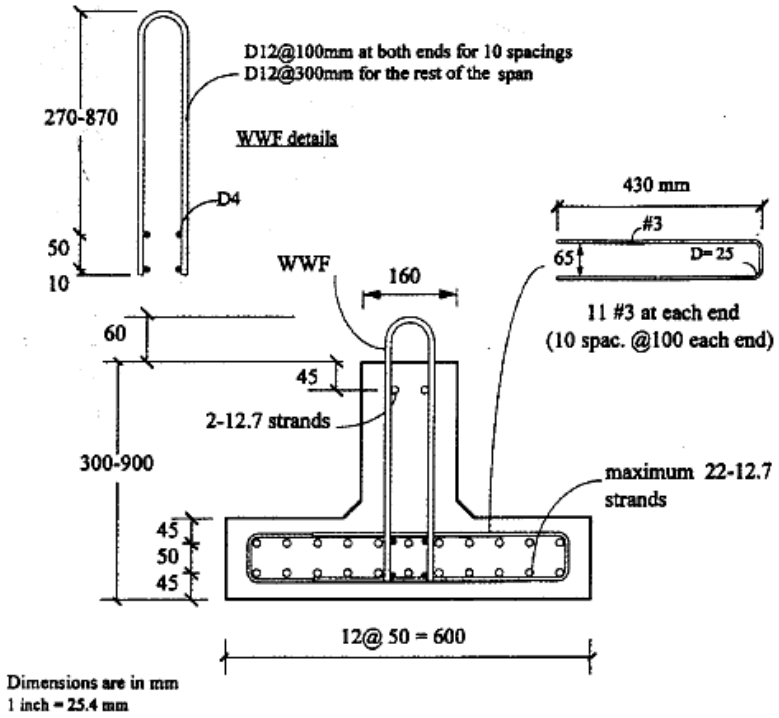

Figure 2.17 Cross section and reinforcement details for a tee beam used in the IT System (Kamel and Tadros, 1996)

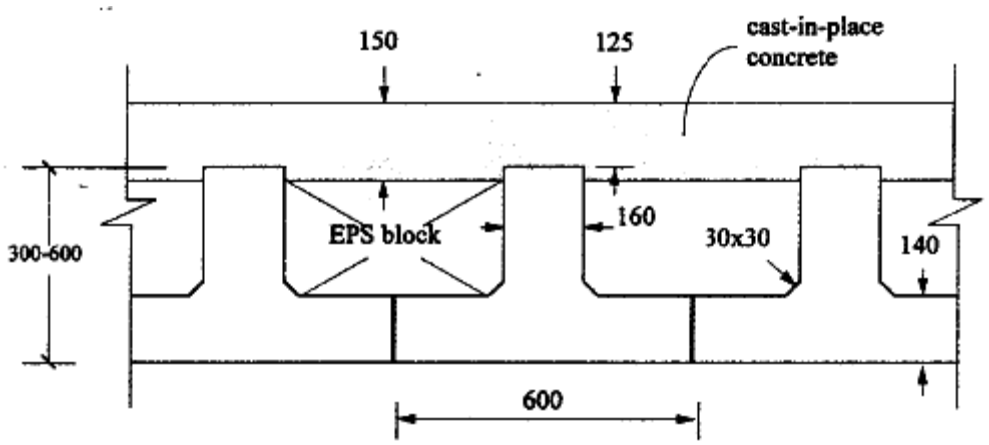

Figure 2.18 Cross section of the IT System (dimensions are in mm) (Kamel and Tadros, 1996)

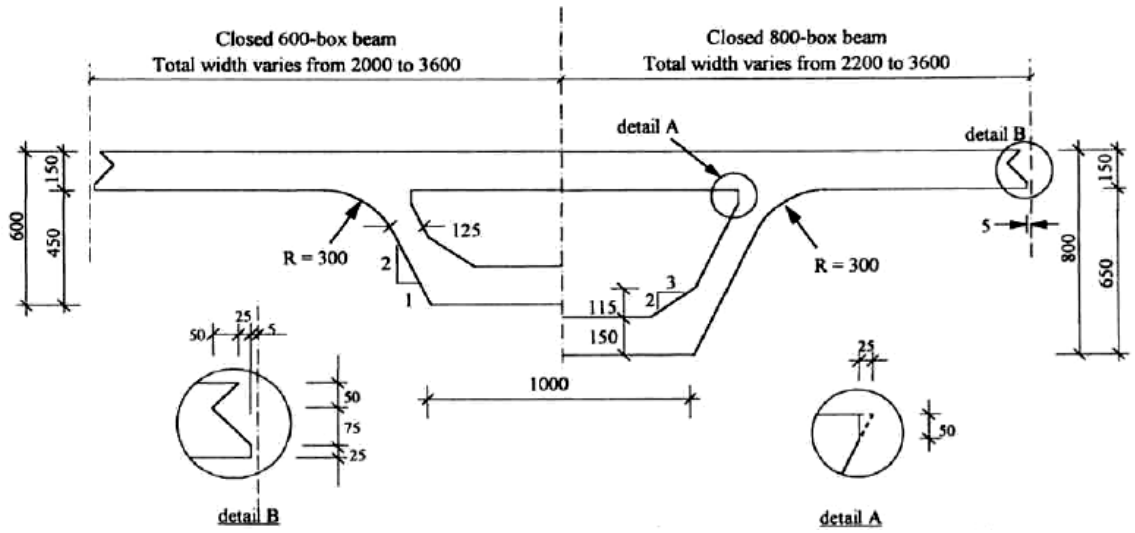

Figure 2.19 Cross section of the closed trapezoidal box beam (dimensions are in mm) (Badie et al., 1999)

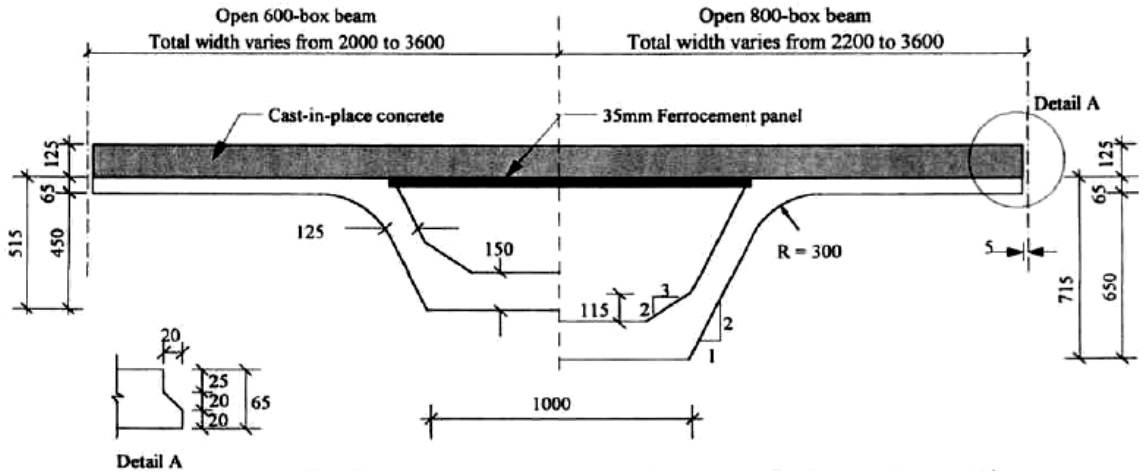

Figure 2.20 Cross section of the open trapezoidal box beam (dimensions are in mm) (Badie et al., 1999)

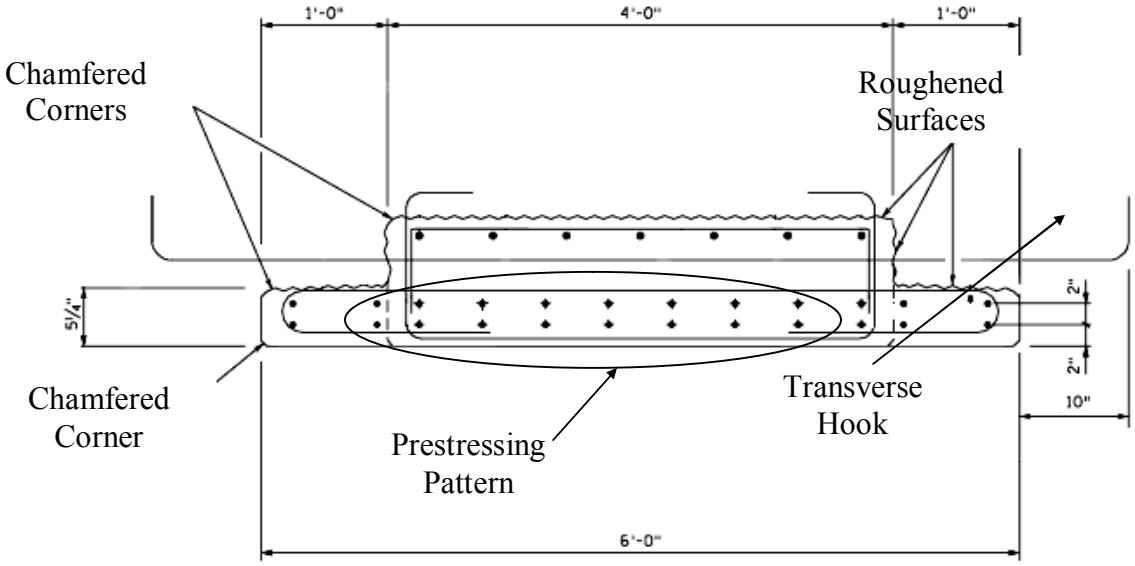

Figure 3.1 Cross-sectional view of interior inverted-T precast section concept

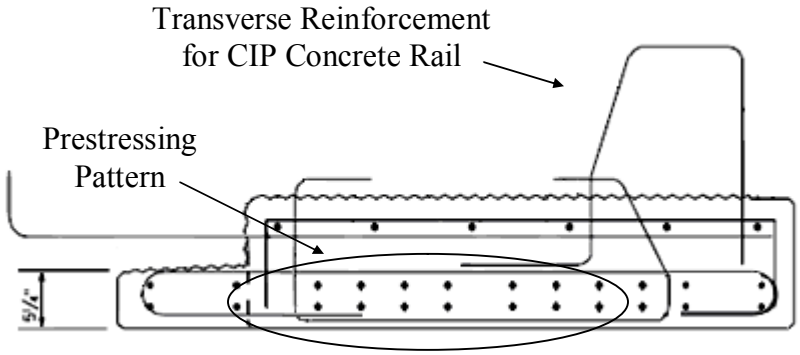

Figure 3.2 Cross-sectional view of exterior inverted-T precast section concept

Figure 3.3 Photograph of the transverse hooks of the precast sections

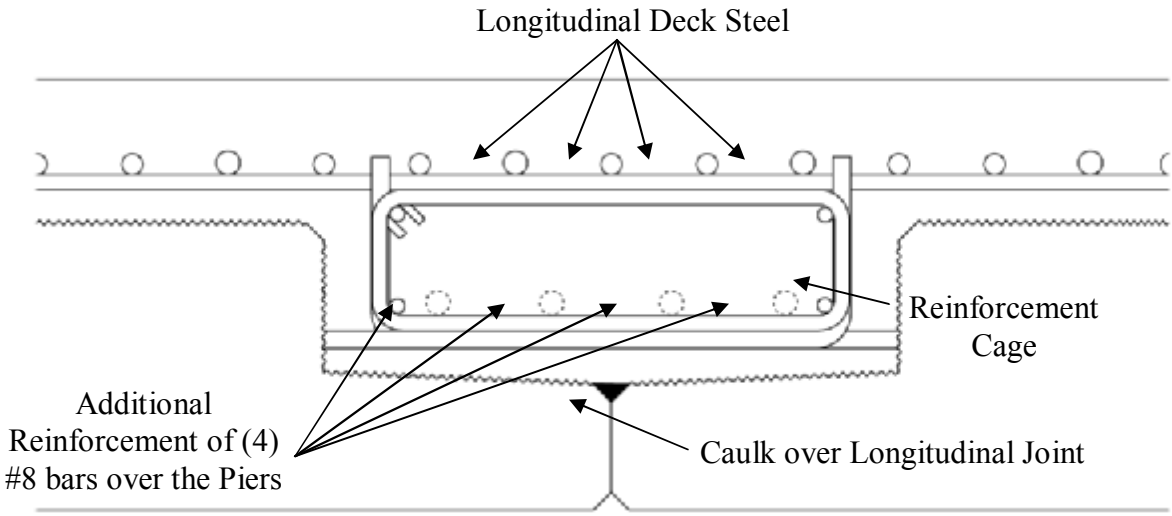

Figure 3.4 Cross-sectional view of the precast longitudinal joint detail

Figure 3.5 Photograph of formwork with indented inner surface

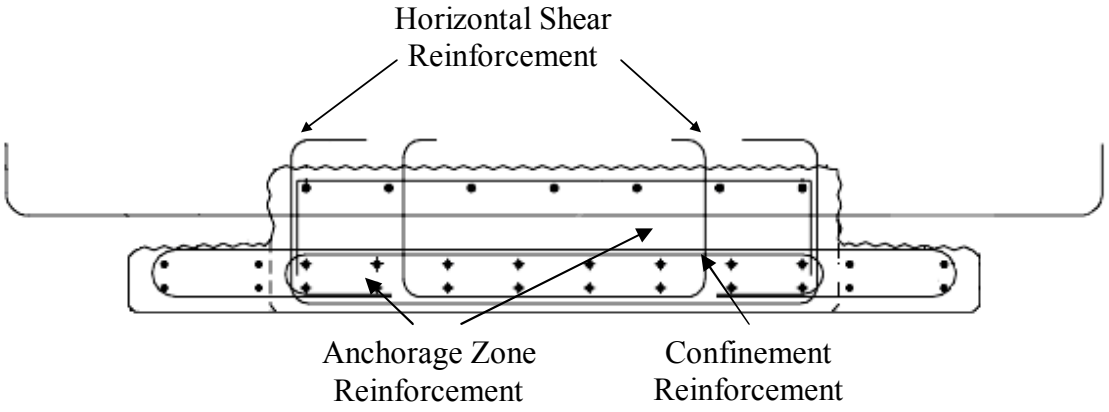

Figure 3.6 Cross-sectional view of an interior inverted-T precast section detailing transverse reinforcement within the precast sections

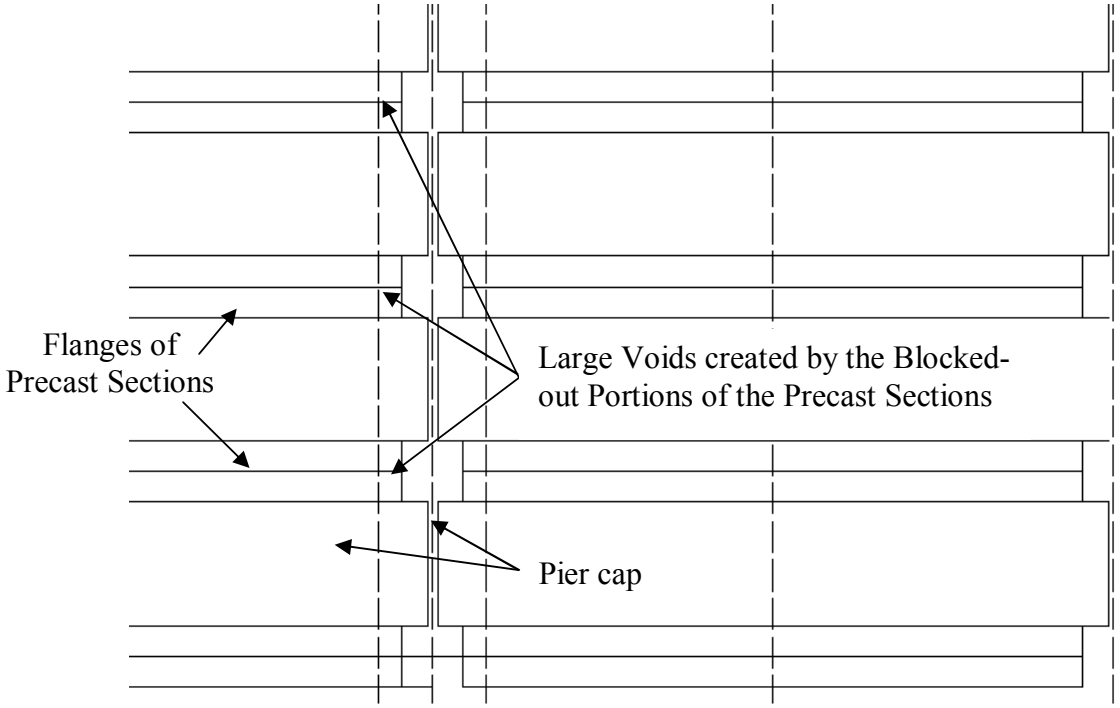

Figure 3.7 Plan view of precast section layout showing blocked-out portions of the precast section flanges

Figure 3.8 Photograph of the reinforcement cage installed above the precast longitudinal joint

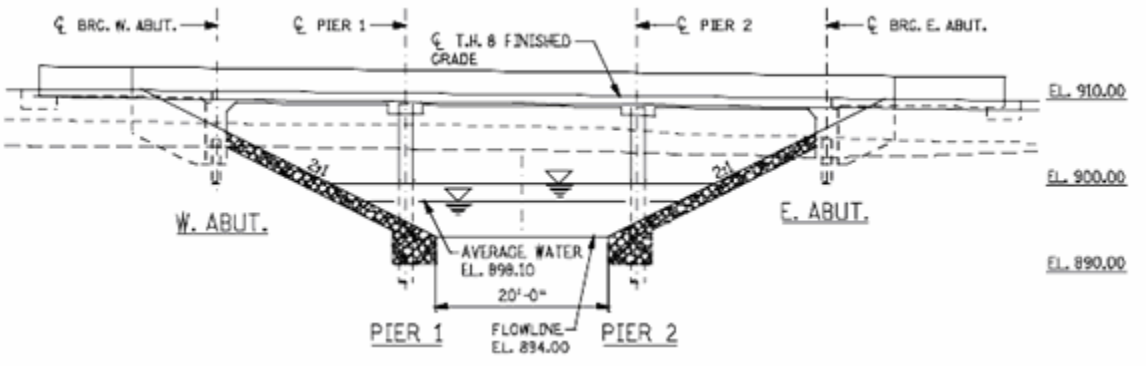

Figure 3.9 Elevation view of Mn/DOT Bridge No. 13004 (Hagen, 2005)

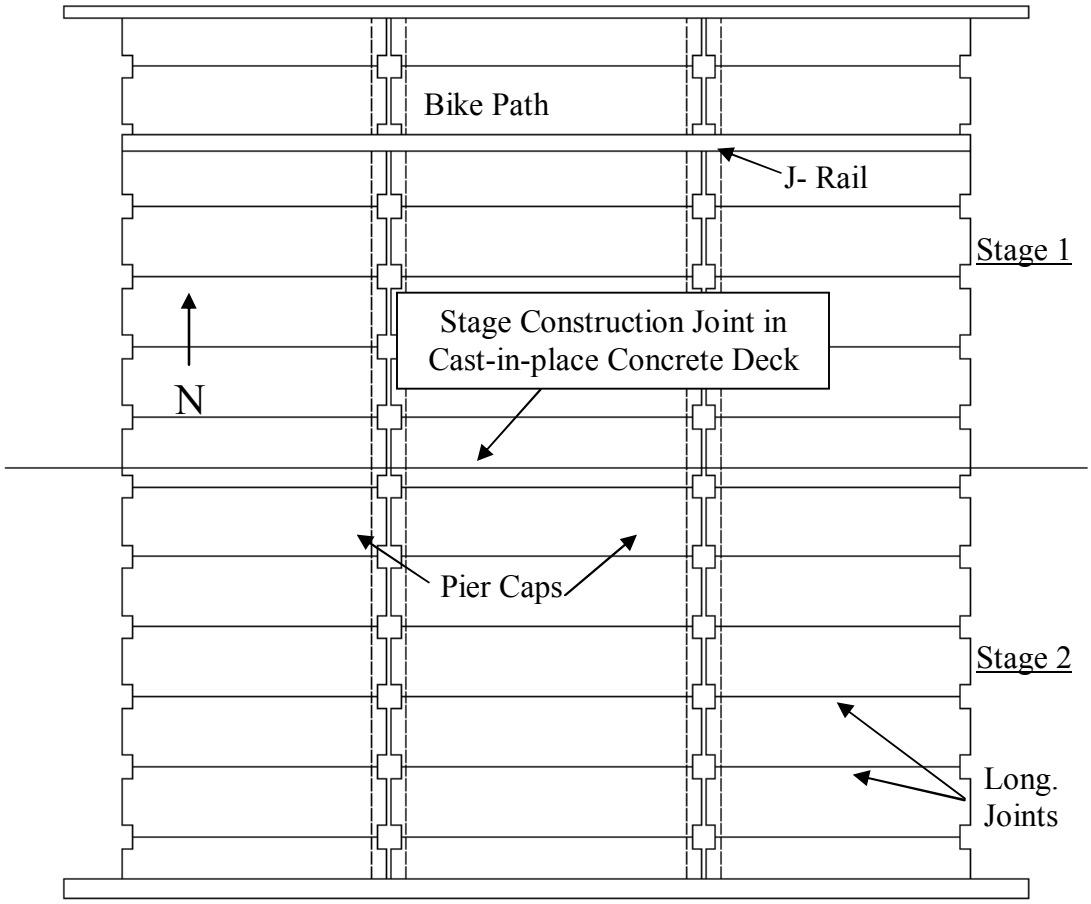

Figure 3.10 Plan view of Mn/DOT Bridge No. 13004 with construction stages and construction joint highlighted

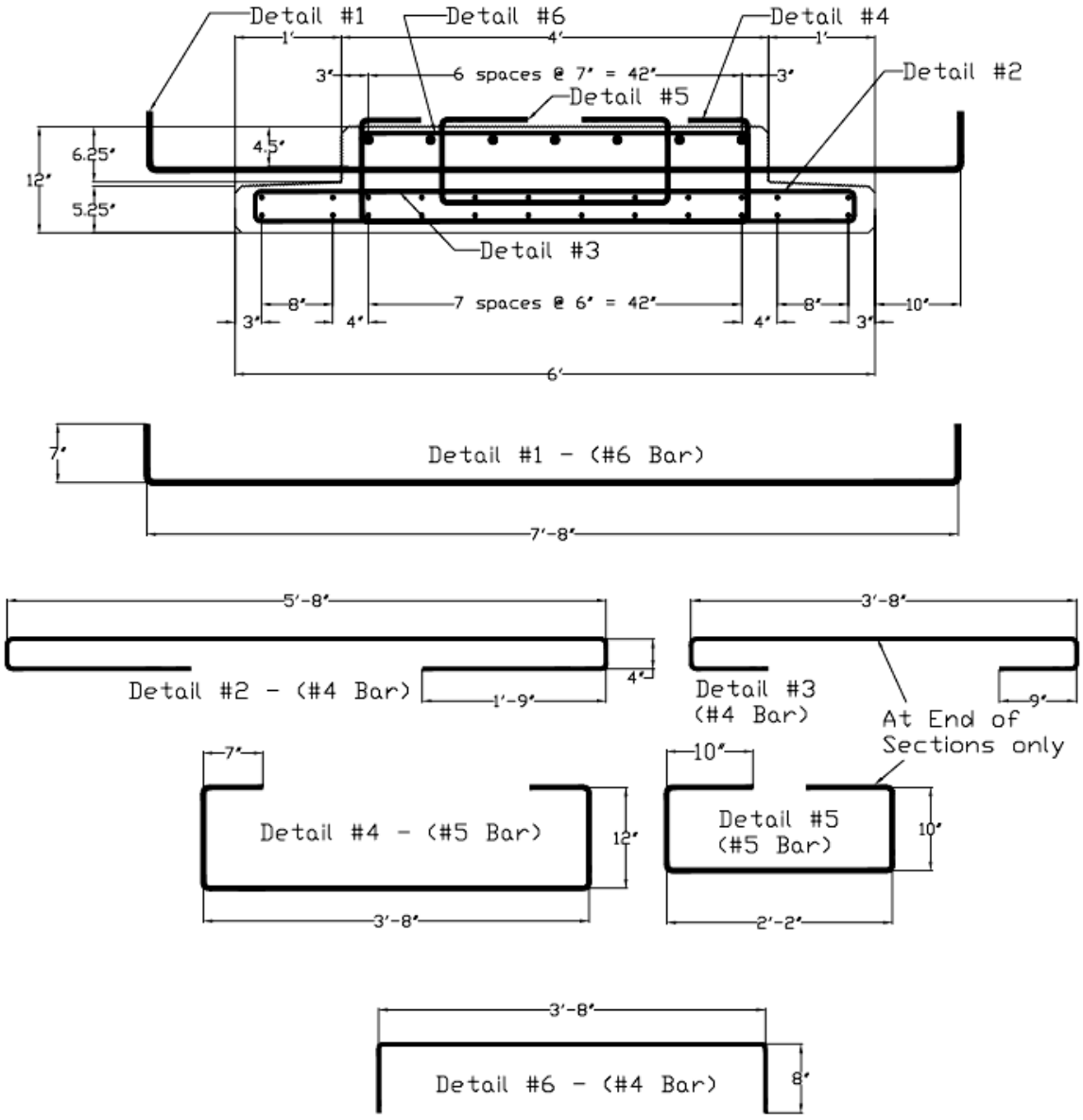

Figure 3.11 Cross-sectional view and reinforcement details for an interior inverted-T precast section used in Mn/DOT Bridge No. 13004 (the dimensions of the reinforcement are taken from the outside of the bar)

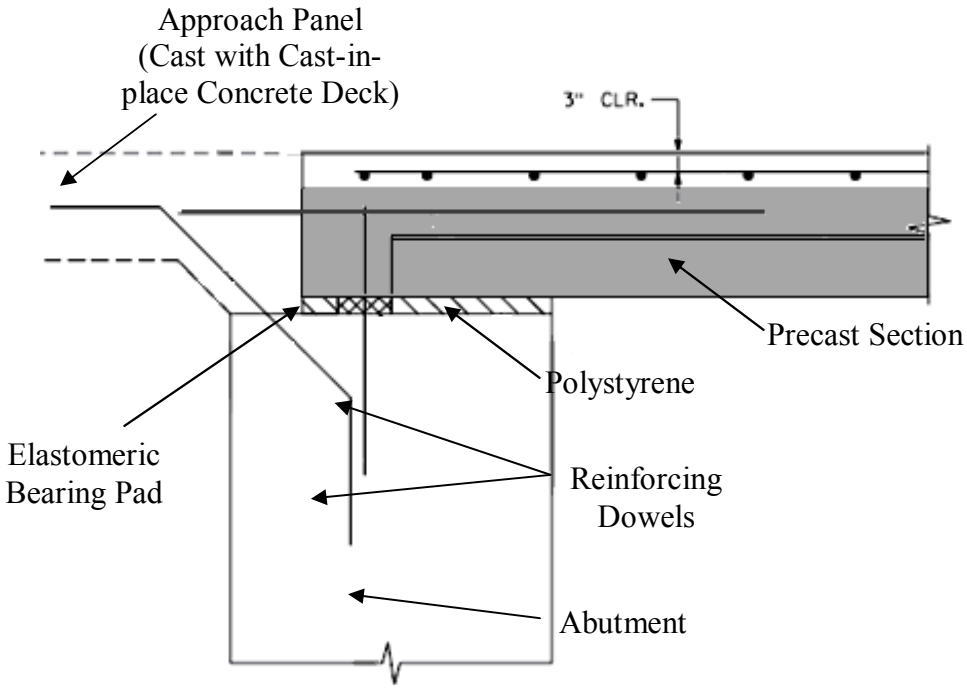

Figure 3.12 Connection detail at abutment, bridge deck, and approach panel

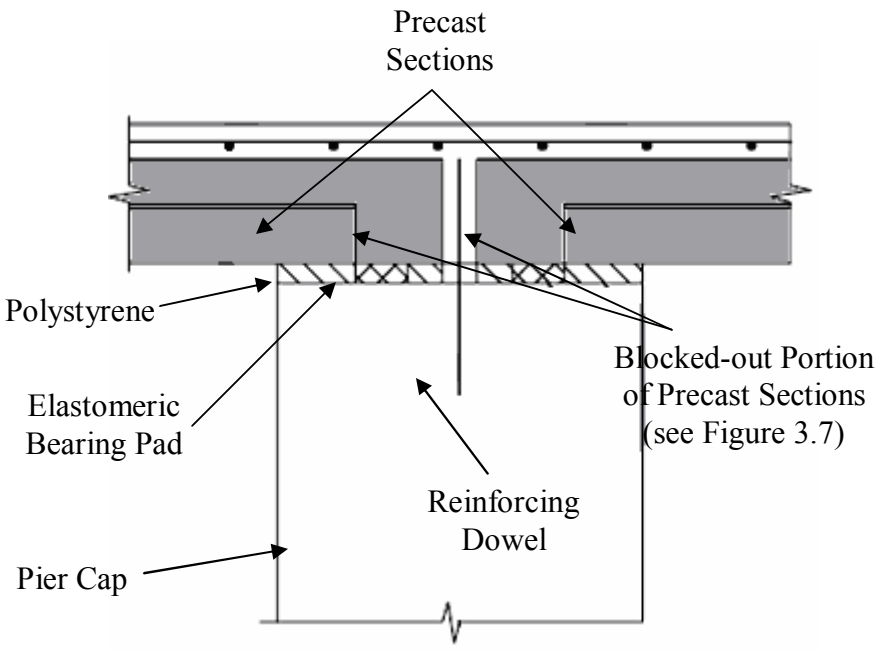

Figure 3.13 Connection detail at pier cap

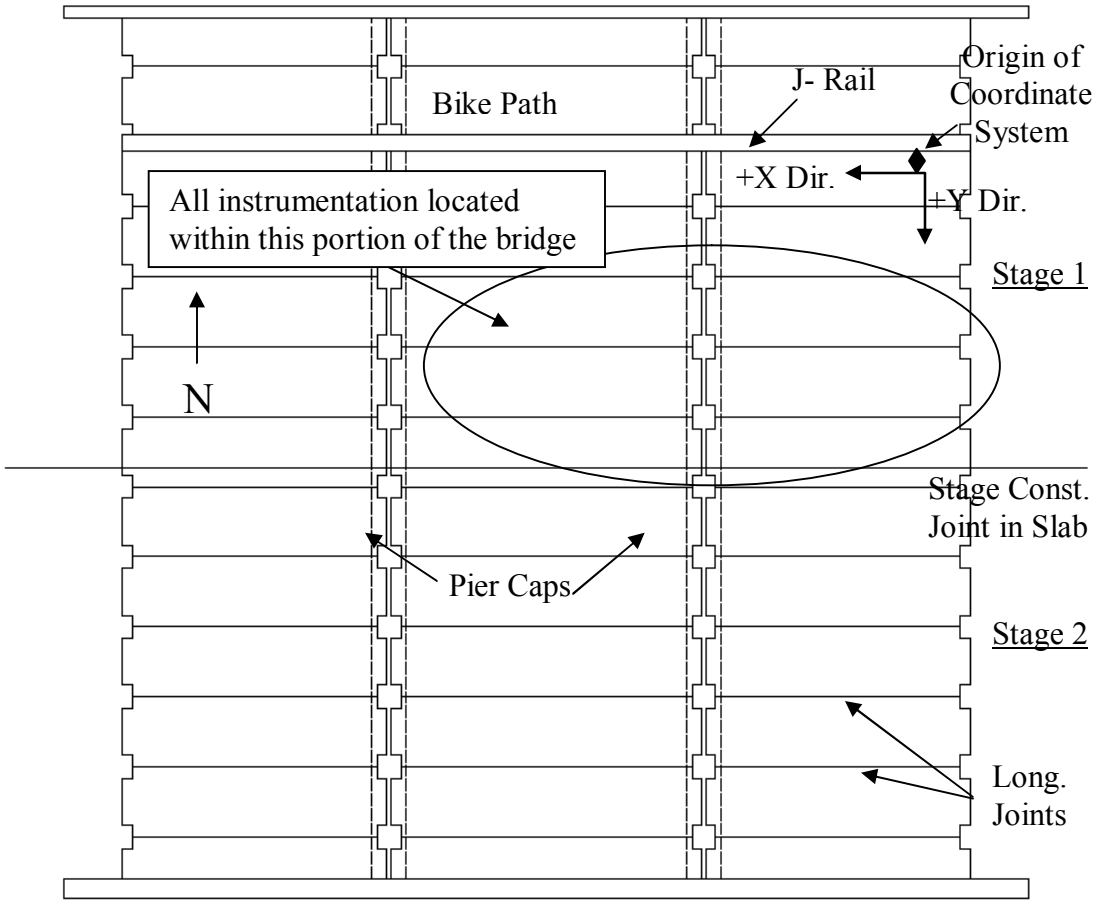

Figure 4.1 Plan view of Mn/DOT Bridge No. 13004 with instrumented portion highlighted

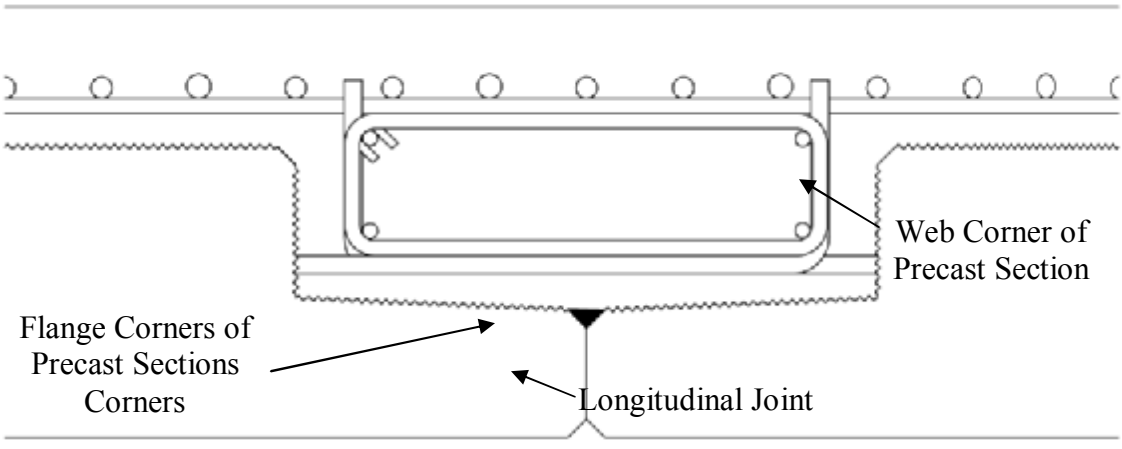

Figure 4.2 Cross-sectional view of precast longitudinal joint

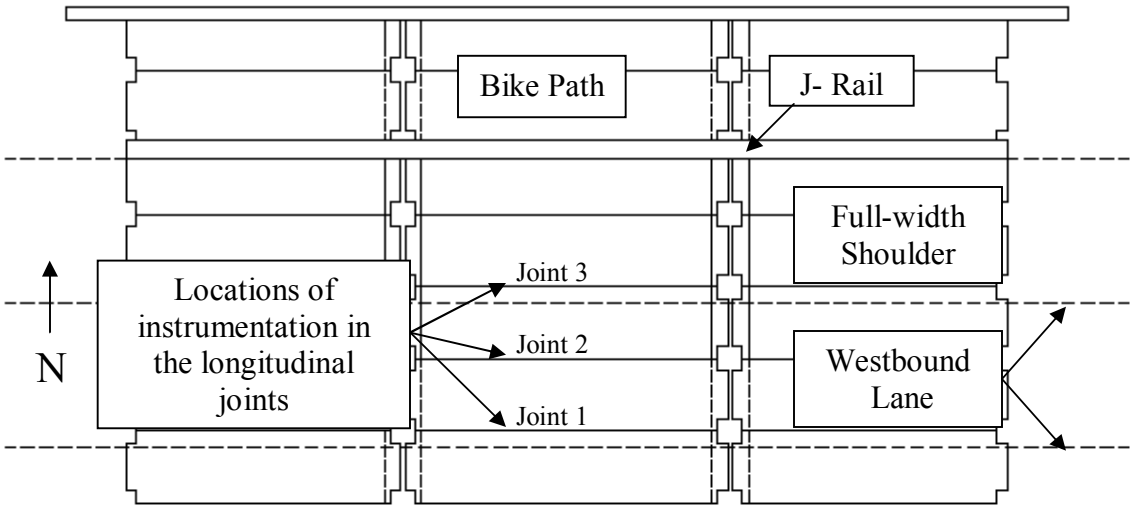

Figure 4.3 Plan view of Stage 1 of the bridge construction for Mn/DOT Bridge No. 13004 highlighting the instrumented joints

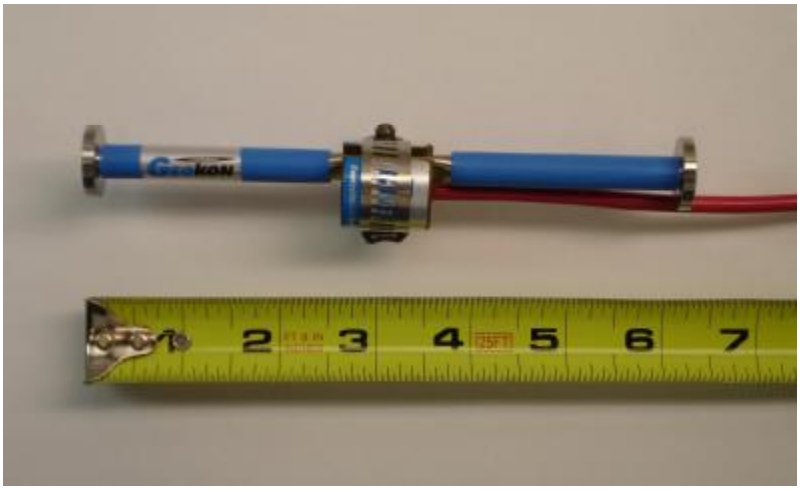

Figure 4.4 Photograph of Geokon® Model VCE-4200 VW Embedment Strain Gage

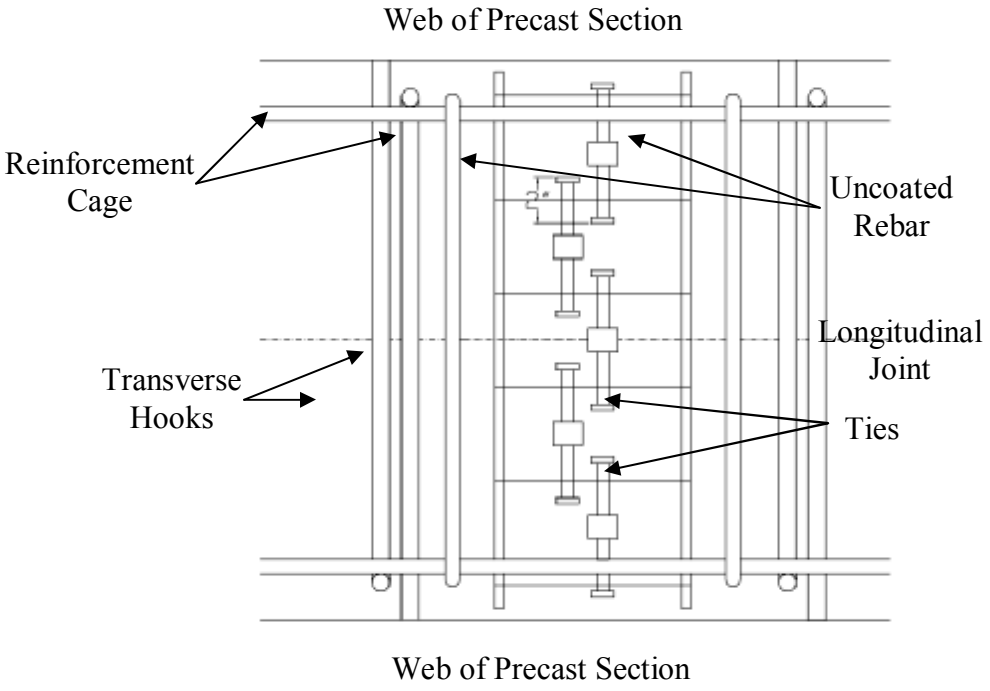

Figure 4.5 Plan view of instrumentation detail for VW embedment strain gages located directly above precast longitudinal joints

Figure 4.6 Photograph of VW embedment strain gage tied to uncoated rebar

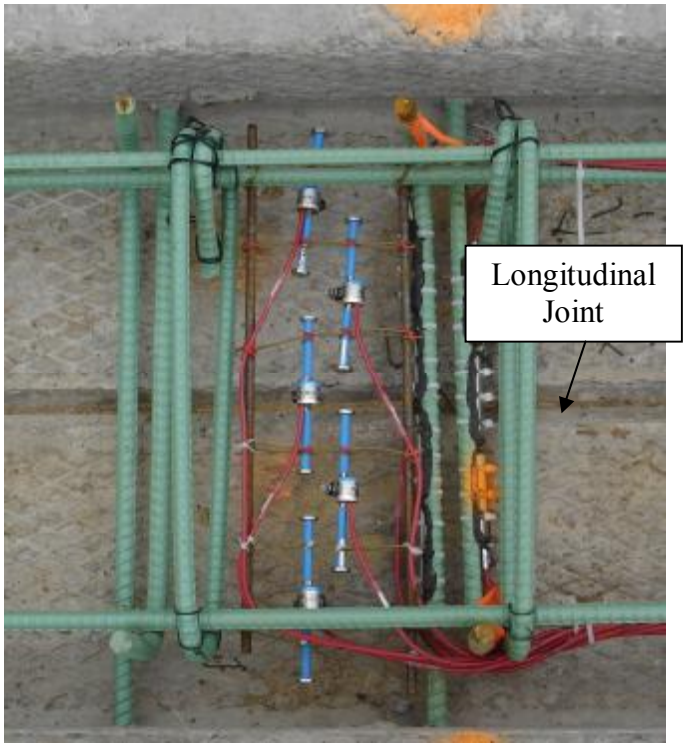

Figure 4.7 Photograph of VW embedment strain gages installed above precast longitudinal joints

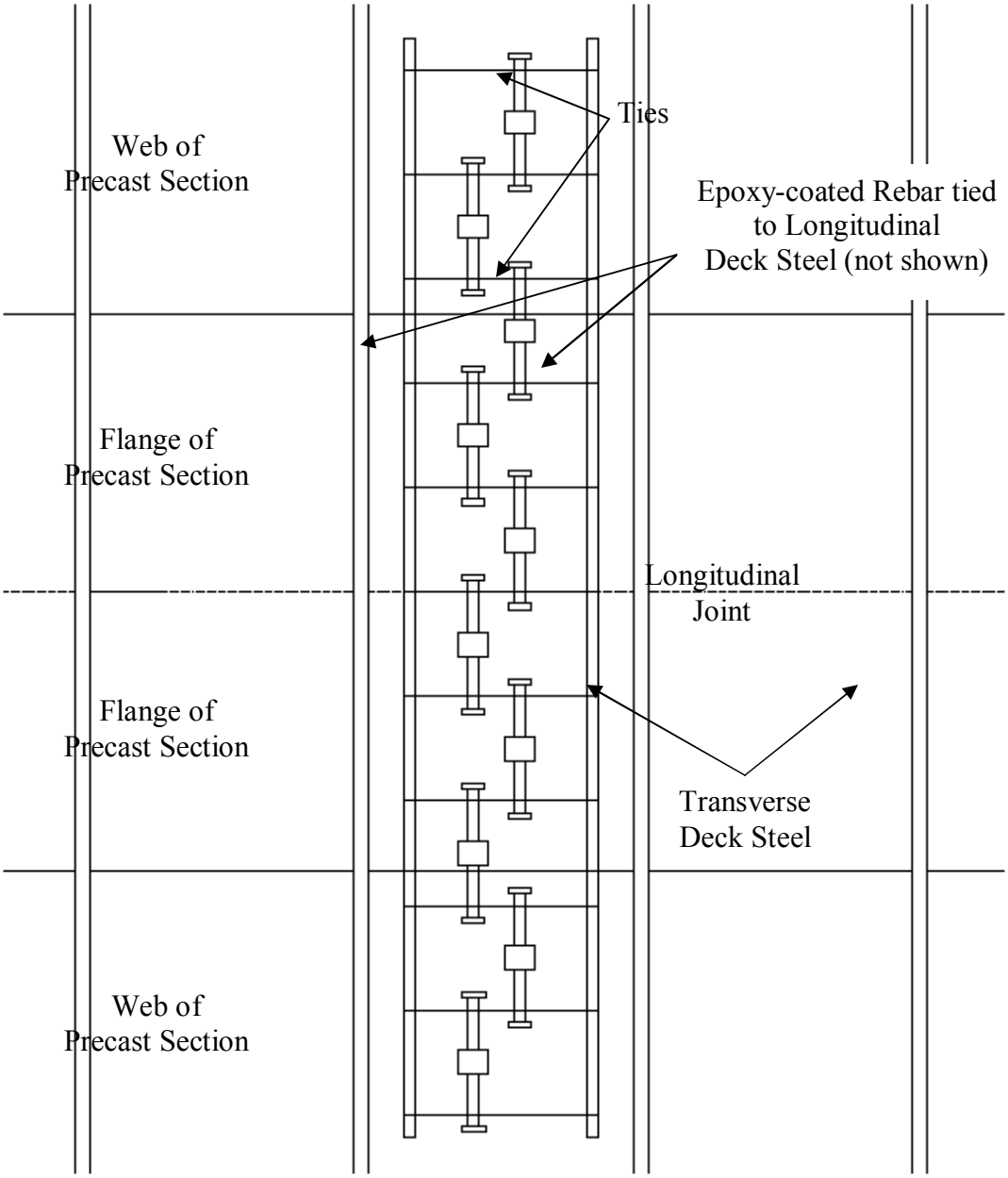

Figure 4.8 Plan view of instrumentation detail for VW embedment strain gages located directly above the precast section web corners

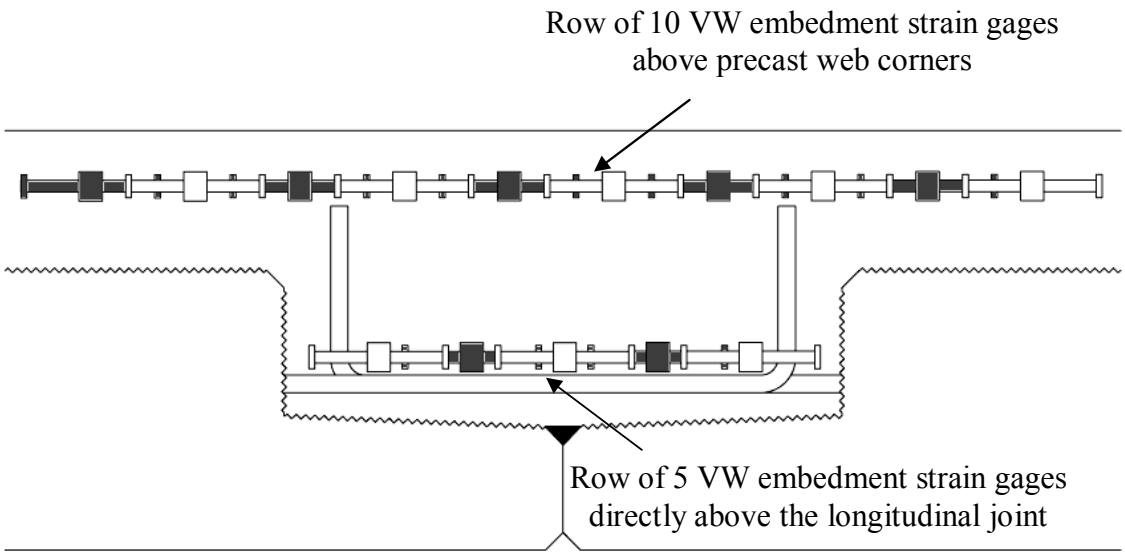

Figure 4.9 Cross-sectional view of instrumentation detail for VW embedment strain gages at each instrumented joint

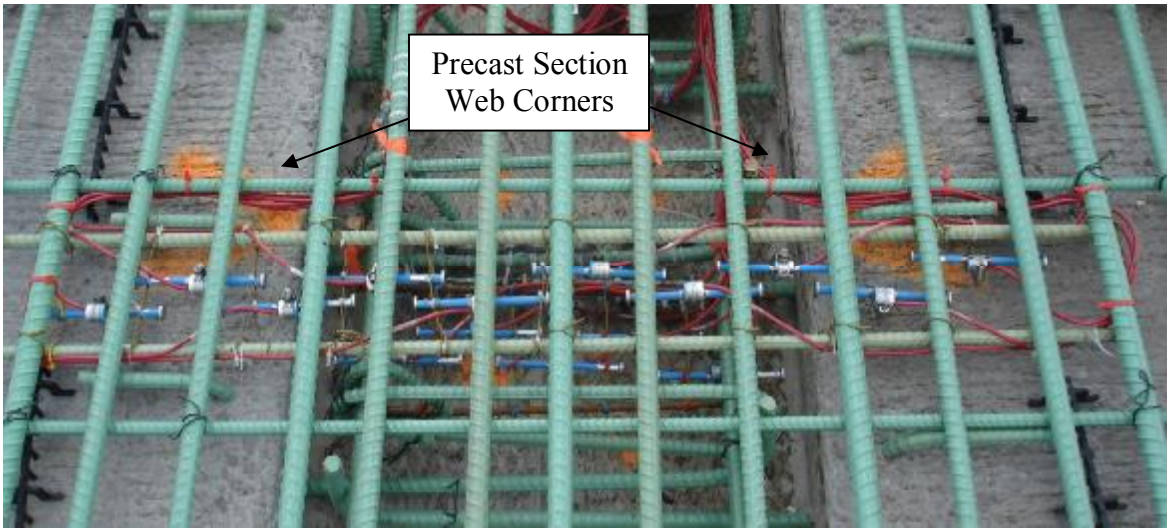

Figure 4.10 Photograph of VW embedment strain gages installed above precast section web corners and above precast longitudinal joint

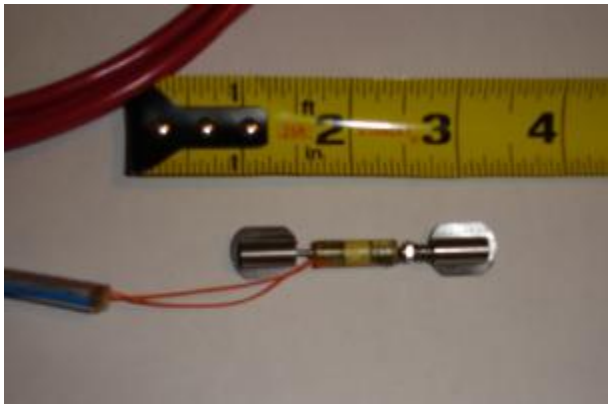

Figure 4.11 Photograph of Geokon® Model VK-4150 VW Spot-weldable Strain Gage

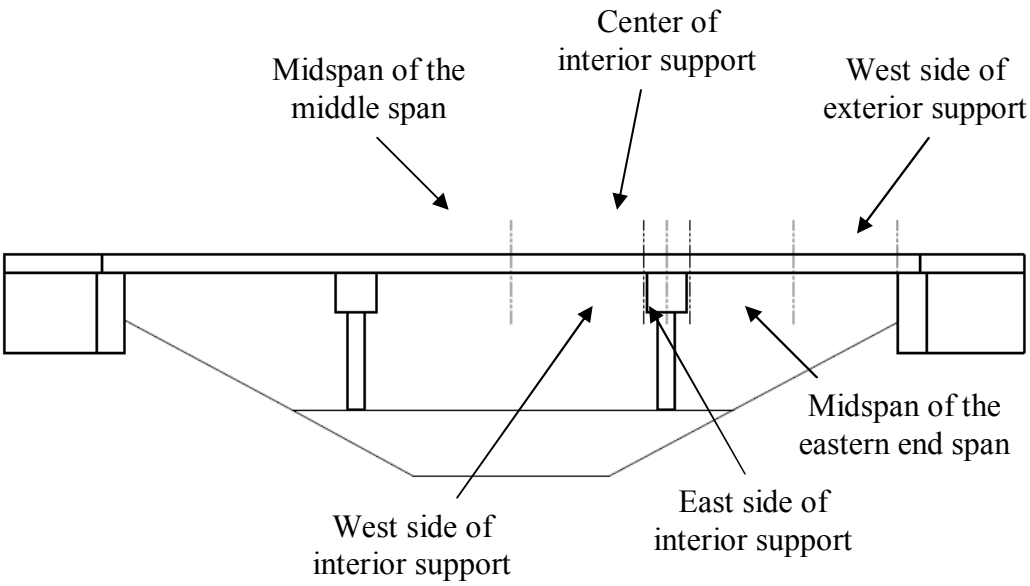

Figure 4.12 Elevation view of Mn/DOT Bridge No. 13004 showing locations of instrumentation along the length of the bridge for continuous behavior over the piers

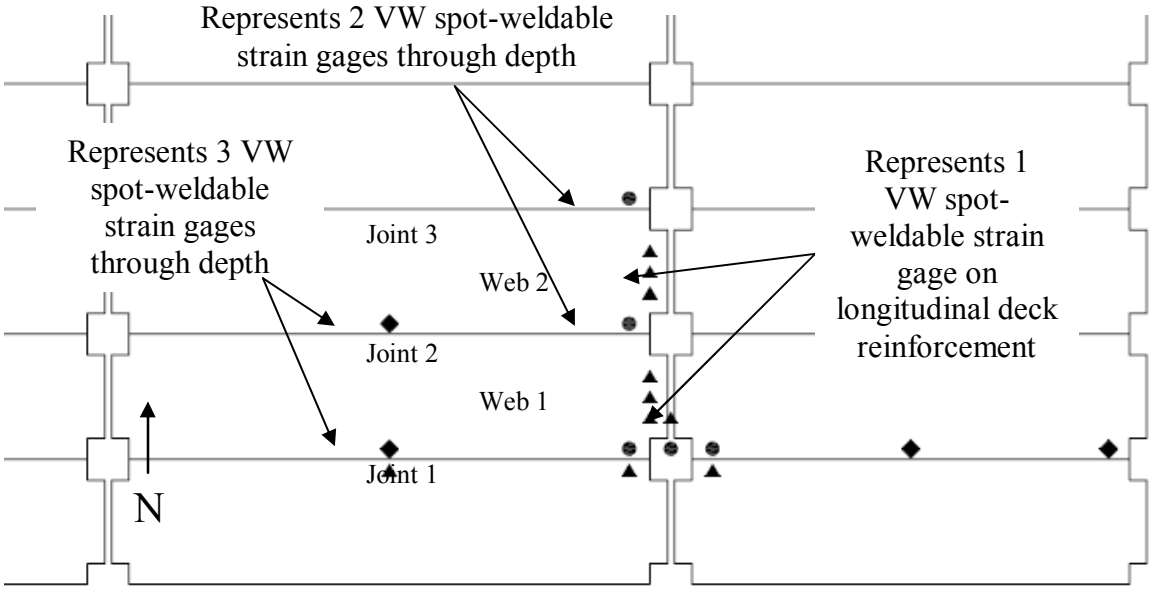

Figure 4.13 Plan view of Stage 1 of the bridge construction of Mn/DOT Bridge No. 13004 showing locations of instrumentation for continuous behavior over the piers

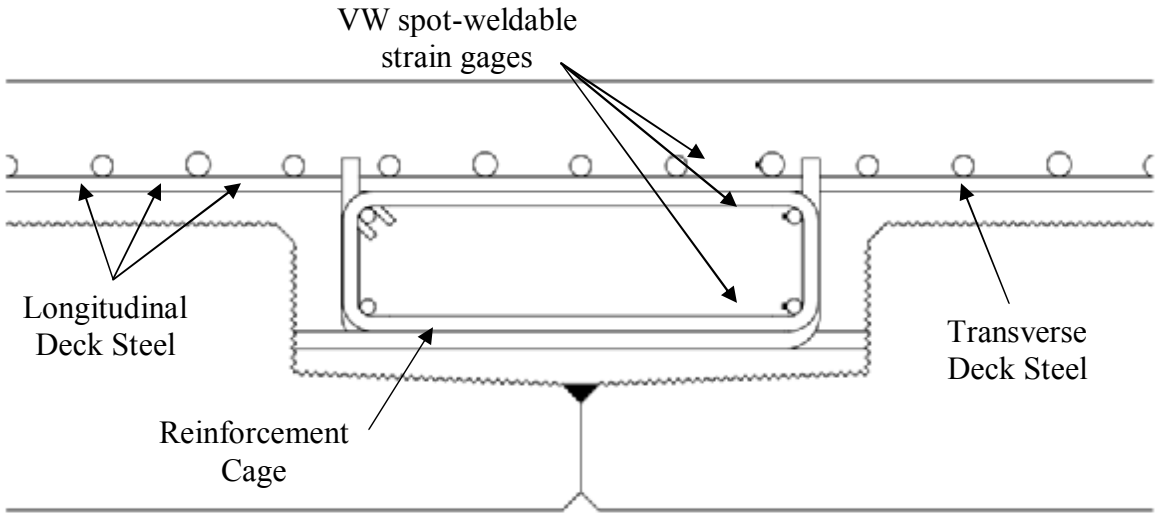

Figure 4.14 Cross-sectional view of instrumentation detail for locations with 3 VW spot-weldable strain gages ("♦" in Figure 4.13)

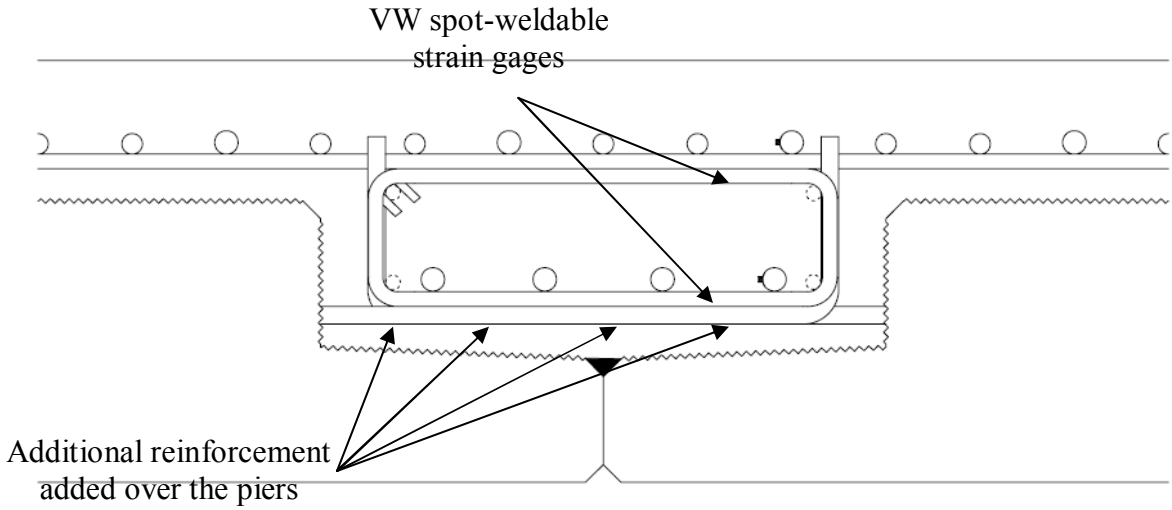

Figure 4.15 Cross-sectional view of instrumentation detail for locations with 2 VW spot-weldable strain gages ("●" in Figure 4.13)

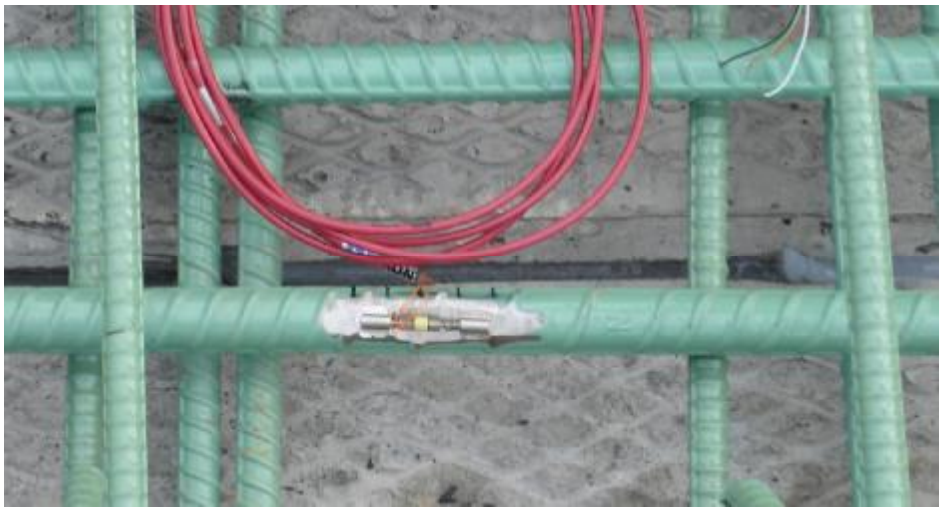

Figure 4.16 Photograph of VW spot-weldable strain gage welded to longitudinal reinforcement

Figure 4.17 Photograph of VW spot-weldable strain gage with waterproofing and steel cover

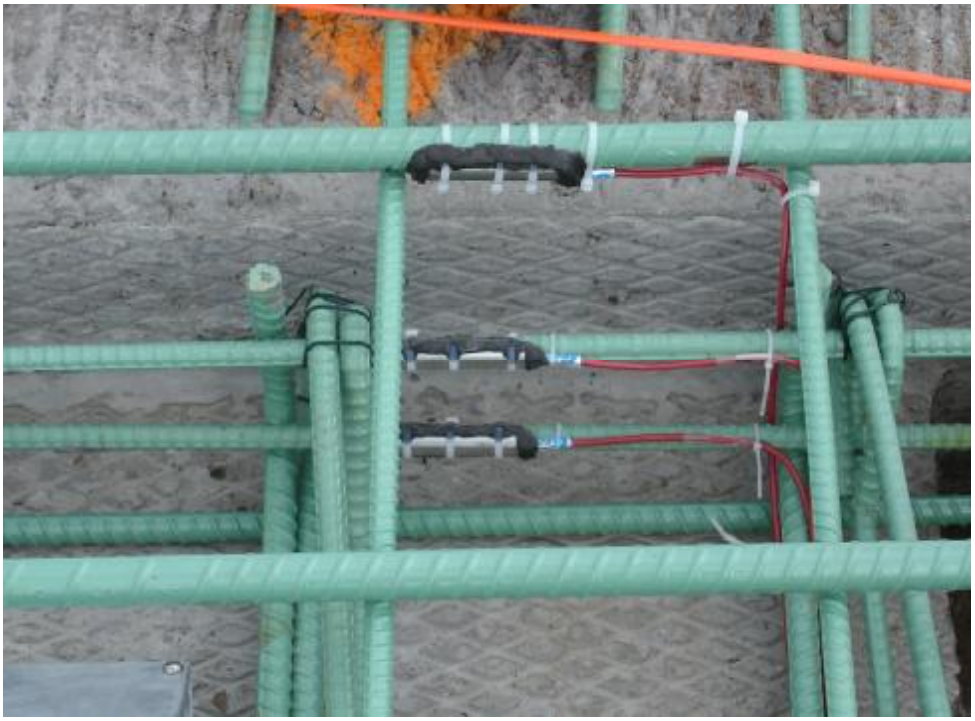

Figure 4.18 Photograph of 3 VW spot-weldable stain gages installed on the longitudinal reinforcement at east end of east span

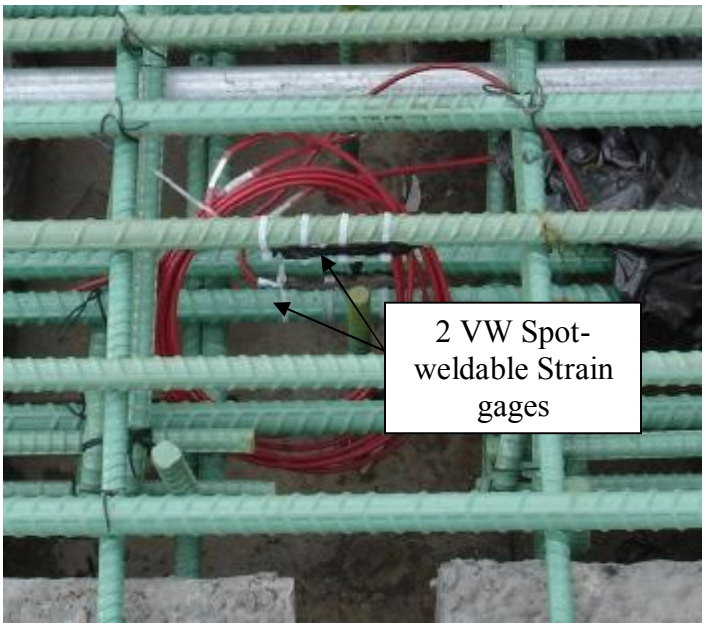

Figure 4.19 Photograph of 2 VW spot-weldable strain gages on longitudinal reinforcement located at the centerline of the pier cap

Figure 4.20 Photograph of transverse hooks of adjacent precast sections

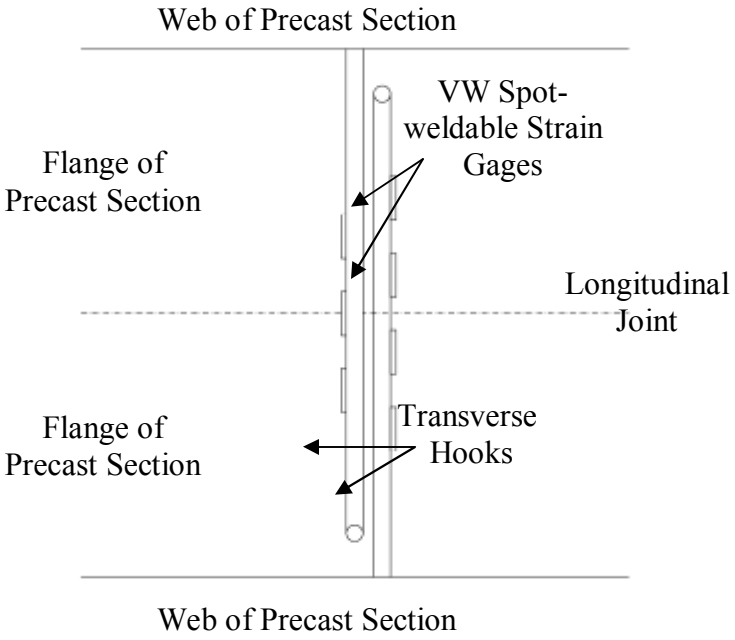

Figure 4.21 Plan view of instrumentation detail for VW spot-weldable strain gages on transverse hooks

Figure 4.22 Photograph of VW spot-weldable strain gages on transverse hooks

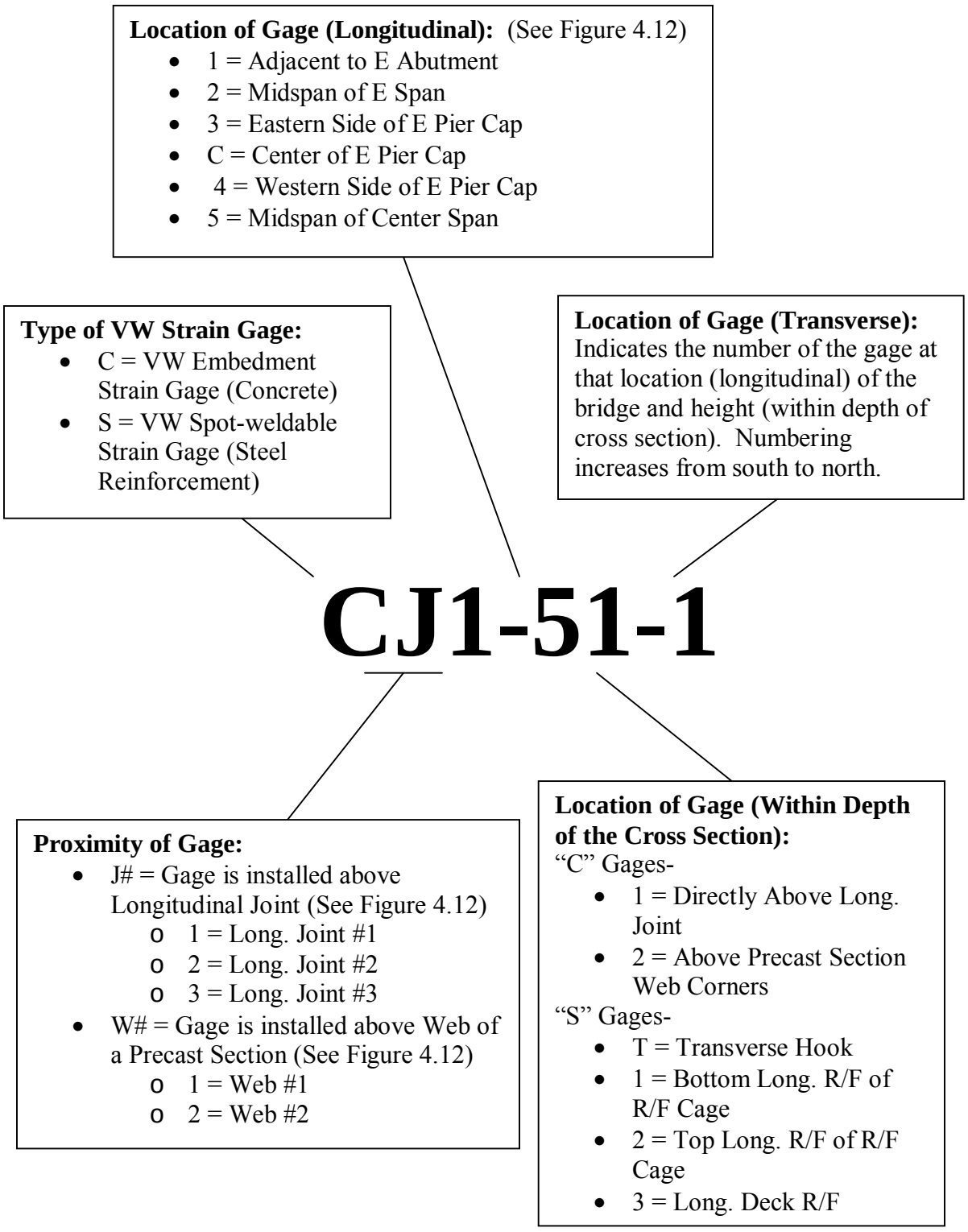

Figure 4.23 Labeling scheme used for gages installed in Mn/DOT Bridge No. 13004

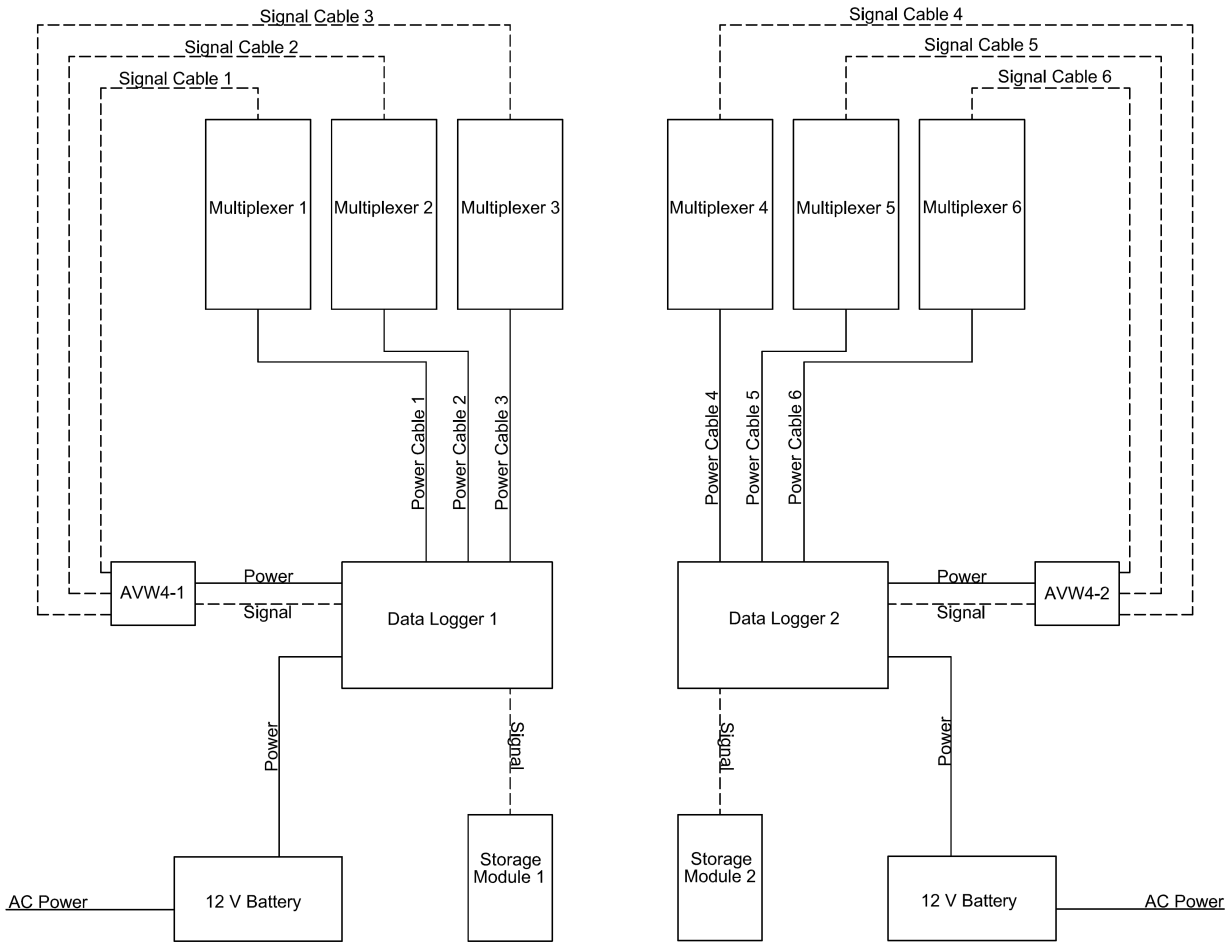

Figure 5.1 Schematic of the data acquisition system used to monitor instrumentation installed in Mn/DOT Bridge No. 13004

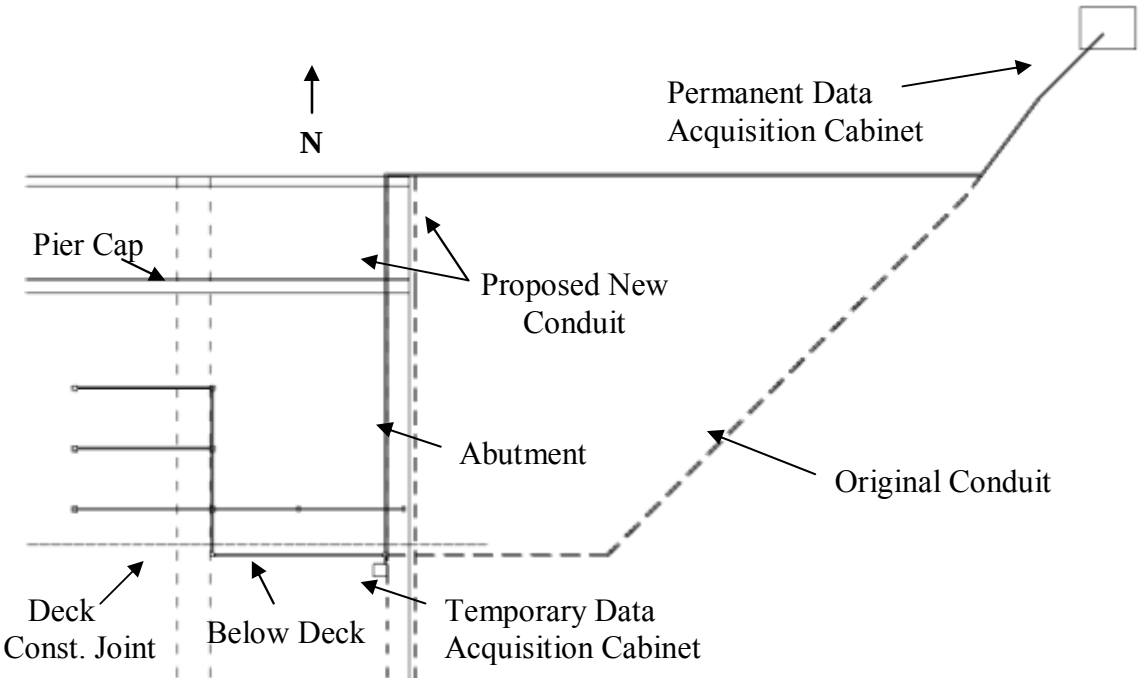

Figure 5.2 Plan view of the conduit system

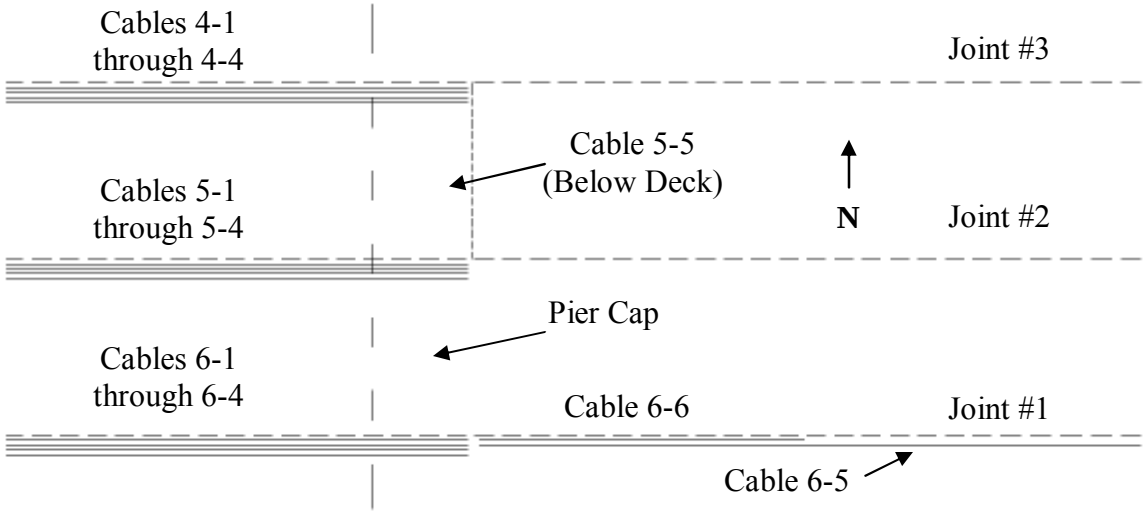

Figure 5.3 Plan view of cables within conduit system

Figure 5.4 Photograph of embedded wiring junction box located above precast longitudinal joint

Figure 5.5 Photograph of multiplexer boxes located on the east face of the east pier cap (north is to the right)

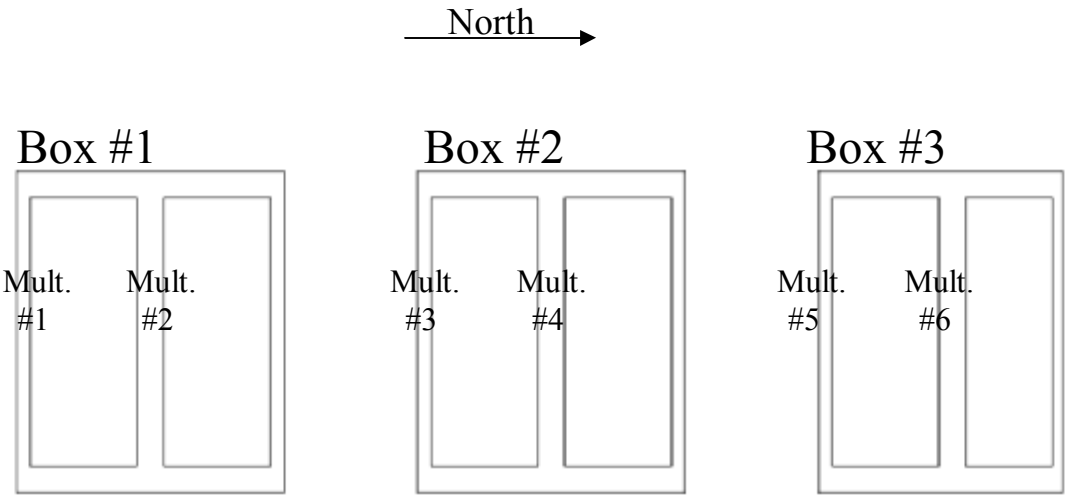

Figure 5.6 Locations of the multiplexers within the boxes on the east face of the east pier cap

Figure 5.7 Photograph of temporary data acquisition system cabinet

Figure 5.8 Photograph of permanent data acquisition system cabinet

Appendix A

Bridge Plans

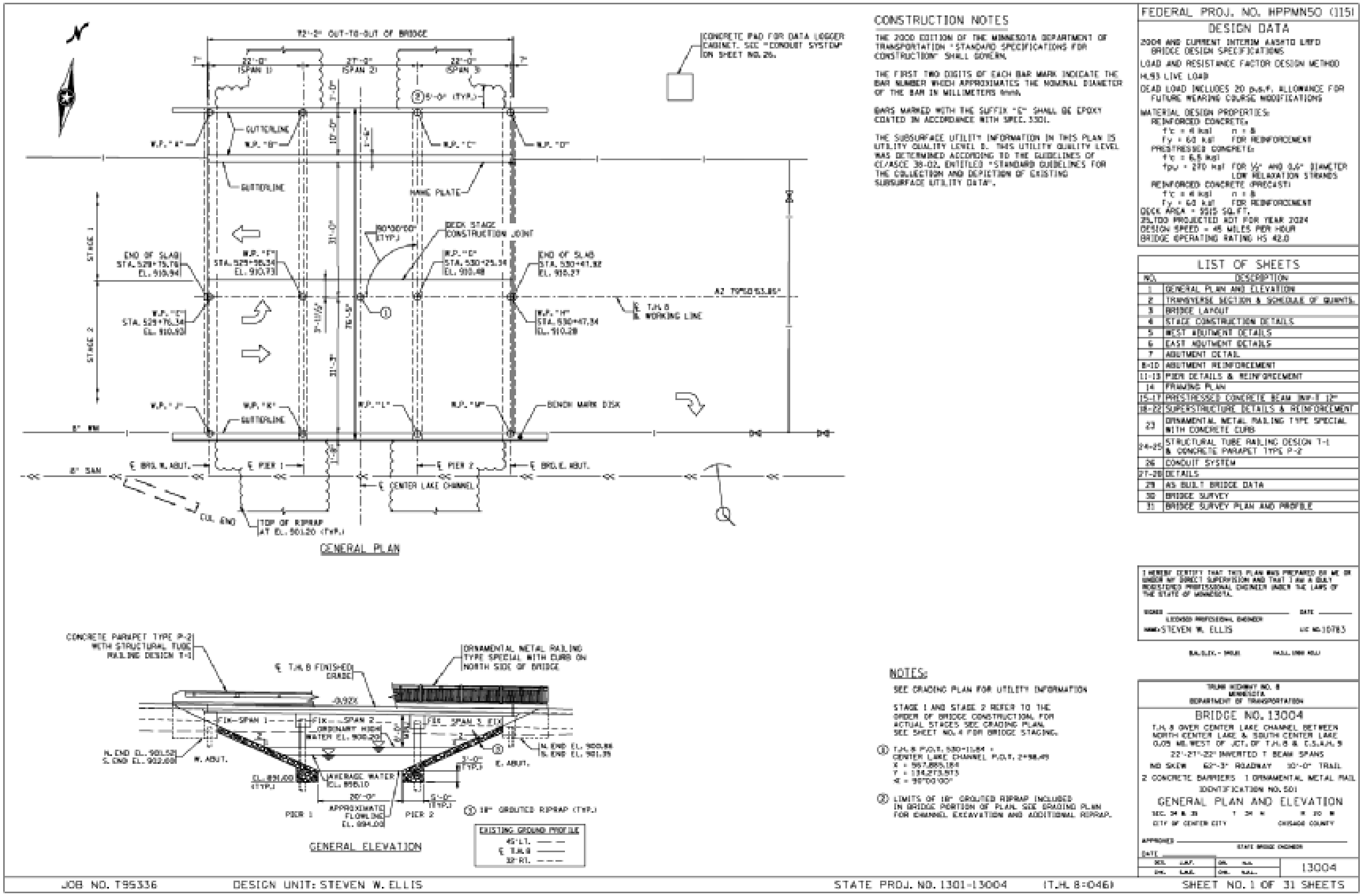

92'-2" OUT-TO-OUT OF BRIDGE
22'-0" (SPAN 1)
27'-2" (SPAN 2)
22'-0" (SPAN 3)
GUTTERLINE
W.P. "A"
W.P. "B"
W.P. "C"
W.P. "D"
NAME PLATE
DECK STAGE CONSTRUCTION JOINT
STAGE 1
STAGE 2
END OF SLAB STA. 529+75.76 EL. 910.94
W.P. "E" STA. 529+98.34 EL. 910.73
W.P. "G" STA. 530+25.34 EL. 910.48
END OF SLAB STA. 530+41.92 EL. 910.27
W.P. "I" STA. 529+76.34 EL. 910.93
W.P. "H" STA. 530+47.34 EL. 910.28
T.H. 8 WORKING LINE
W.P. "J"
W.P. "K"
W.P. "L"
W.P. "M"
BENCH MARK DISK
BRG. W. ABUT.
PIER 1
PIER 2
BRG. E. ABUT.
CENTER LAKE CHANNEL
CUL END
TOP OF RIPRAP AT EL. 901.20 (TYP.)
GENERAL PLAN
CONCRETE PAD FOR DATA LOGGER CABINET. SEE "CONDUIT SYSTEM" ON SHEET NO. 26.
CONCRETE PARAPET TYPE P-2 WITH STRUCTURAL TUBE RAILING DESIGN T-1
T.H. 8 FINISHED GRADE
ORNAMENTAL METAL RAILING TYPE SPECIAL WITH CURB ON NORTH SIDE OF BRIDGE
FIX—SPAN 1
FIX — SPAN 2
FIX SPAN 3 EXP
ORDINARY HIGH WATER EL. 906.20
N. END EL. 901.52 S. END EL. 902.60
W. ABUT.
E. ABUT.
N. END EL. 900.86 S. END EL. 901.35
AVERAGE WATER EL. 898.10
APPROXIMATE FLOWLINE EL. 894.00
PIER 1
PIER 2
18" GROUTED RIPRAP (TYP.)
EXISTING GROUND PROFILE
GENERAL ELEVATION
CONSTRUCTION NOTES
THE 2000 EDITION OF THE MINNESOTA DEPARTMENT OF TRANSPORTATION "STANDARD SPECIFICATIONS FOR CONSTRUCTION" SHALL GOVERN.
THE FIRST TWO DIGITS OF EACH BAR MARK INDICATE THE BAR NUMBER WHICH APPROXIMATES THE NOMINAL DIAMETER OF THE BAR IN MILLIMETERS (mm).
BARS MARKED WITH THE SUFFIX "E" SHALL BE EPOXY COATED IN ACCORDANCE WITH SPEC. 3301.
THE SUBSURFACE UTILITY INFORMATION IN THIS PLAN IS UTILITY QUALITY LEVEL D. THIS UTILITY QUALITY LEVEL WAS DETERMINED ACCORDING TO THE GUIDELINES OF CI/ASCE 38-02, ENTITLED "STANDARD GUIDELINES FOR THE COLLECTION AND DEPICTION OF EXISTING SUBSURFACE UTILITY DATA".
NOTES:
SEE GRADING PLAN FOR UTILITY INFORMATION
STAGE 1 AND STAGE 2 REFER TO THE ORDER OF BRIDGE CONSTRUCTION. FOR ACTUAL STAGES SEE GRADING PLAN. SEE SHEET NO. 4 FOR BRIDGE STAGING.
(1) T.H. 8 P.O.T. 530+11.84 = CENTER LAKE CHANNEL P.O.T. 2+98.49
(2) LIMITS OF 18" GROUTED RIPRAP INCLUDED IN BRIDGE PORTION OF PLAN. SEE GRADING PLAN FOR CHANNEL EXCAVATION AND ADDITIONAL RIPRAP.
FEDERAL PROJ. NO. HPPMN50 (115)
DESIGN DATA
2004 AND CURRENT INTERIM AASHTO LRFD BRIDGE DESIGN SPECIFICATIONS
LOAD AND RESISTANCE FACTOR DESIGN METHOD
HL93 LIVE LOAD
DEAD LOAD INCLUDES 20 p.s.f. ALLOWANCE FOR FUTURE WEARING COURSE MODIFICATIONS
MATERIAL DESIGN PROPERTIES:
REINFORCED CONCRETE:
PRESTRESSED CONCRETE:
REINFORCED CONCRETE (PRECAST):
DECK AREA = 2515 SQ.FT.
25,700 PROJECTED ADT FOR YEAR 2024
DESIGN SPEED = 45 MILES PER HOUR
BRIDGE OPERATING RATING HS 42.0
LIST OF SHEETS
NO. DESCRIPTION
1 GENERAL PLAN AND ELEVATION
2 TRANSVERSE SECTION & SCHEDULE OF QUANTS.
3 BRIDGE LAYOUT
4 STAGE CONSTRUCTION DETAILS
5 WEST ABUTMENT DETAILS
6 EAST ABUTMENT DETAILS
7 ABUTMENT DETAIL
8-10 ABUTMENT REINFORCEMENT
11-13 PIER DETAILS & REINFORCEMENT
14 FRAMING PLAN
15-17 PRESTRESSED CONCRETE BEAM
18-22 SUPERSTRUCTURE DETAILS & REINFORCEMENT
23 ORNAMENTAL METAL RAILING TYPE SPECIAL WITH CONCRETE CURB
24-25 STRUCTURAL TUBE RAILING DESIGN T-1 & CONCRETE PARAPET TYPE P-2
26 CONDUIT SYSTEM
27-28 DETAILS
29 AS BUILT BRIDGE DATA
30 BRIDGE SURVEY
31 BRIDGE SURVEY PLAN AND PROFILE
STEVEN W. ELLIS
BRIDGE NO. 13004
T.H. 8 OVER CENTER LAKE CHANNEL BETWEEN NORTH CENTER LAKE & SOUTH CENTER LAKE
22'-27'-22' INVERTED T BEAM SPANS
2 CONCRETE BARRIERS 1 ORNAMENTAL METAL RAIL
GENERAL PLAN AND ELEVATION
13004
JOB NO. T95336
DESIGN UNIT: STEVEN W. ELLIS
STATE PROJ. NO. 1301-13004 (T.H. 8=046)
SHEET NO. 1 OF 31 SHEETS

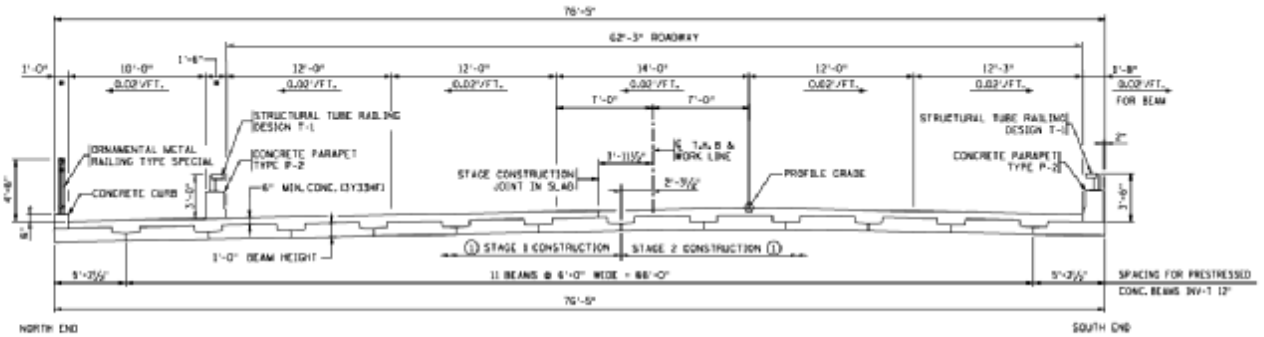

TRANSVERSE SECTION

① SEE SHEET NO. 4 FOR STAGE CONSTRUCTION DETAILS

* SLOPE IS 0.02"/FT.

SCHEDULE OF QUANTITIES FOR ENTIRE BRIDGE

	ITEM NO.	ITEM	UNIT	QUANTITY
	2401.512	BRIDGE SLAB CONCRETE (SY339#1)	SQ. FT.	5815 (P)
	2401.513	TYPE CURB RAILING CONCRETE (3746)	LIN. FT.	88 (P)
	2401.513	TYPE P-2 RAILING CONCRETE (3746)	LIN. FT.	351 (P)
	2401.541	REINFORCEMENT BARS (EPOXY COATED)	POUND	53810 (P)
	2401.601	STRUCTURE EXCAVATION	LUMP SUM	1
②	2401.618	BRIDGE DECK PLANING	SQ. FT.	6610 (P)
	2402.583	ORNAMENTAL METAL RAILING TYPE SPECIAL	LIN. FT.	88 (P)
	2402.583	STRUCTURAL TUBE RAILING DESIGN T-1	LIN. FT.	155 (P)
	2402.590	ELASTOMERIC BEARING PAD TYPE 1	EACH	78
	2405.602	PRECAST CONC. BRIDGE SUBSTRUCTURE (PIER CAP)	EACH	2
	2405.602	PRECAST CONC. BRIDGE SUBSTRUCTURE (ABUT.)	EACH	2
	2405.603	PRESTRESSED BEAM INV-1 12" TYPE 1	LIN. FT.	787 (P)
	2405.603	PRESTRESSED BEAM INV-1 12" TYPE 2	LIN. FT.	143 (P)
	2452.507	C.I.P. PILING DELIVERED 12"	LIN. FT.	540
	2452.507	C.I.P. PILING DELIVERED 16"	LIN. FT.	990
	2452.508	C.I.P. PILING DRIVEN 12"	LIN. FT.	540
	2452.508	C.I.P. PILING DRIVEN 16"	LIN. FT.	560
	2457.519	C.I.P. CONCRETE TEST PILE 55 FT. LONG 12"	EACH	6
	2457.519	C.I.P. CONCRETE TEST PILE 80 FT. LONG 16"	EACH	6
③	2452.602	PILE REDRIVING	EACH	6
	2511.507	GROUTED RIPRAP	CU.YD.	340
	2545.509	CONDUIT SYSTEM	LUMP SUM	1
④	2405.603	PRESTRESSED BEAM INV-1 12" (RESEARCH)	LIN. FT.	90

② INCLUDES 2357 SQ. FT. FOR APPROACH PANELS.

③ ITEM INCLUDES ALL TEST PILES FOR PIERS 1 AND 2.

④ THESE BEAMS ARE FOR RESEARCH ONLY AND ARE NOT TO BE USED ON THE BRIDGE. SEE THE SPECIAL PROVISIONS.

CERTIFIED BY Steven W. Ellis JAN. 31, 2008 (LICENSED PROFESSIONAL ENGINEER) (DATE)
NAME: STEVEN W. ELLIS LIC. NO. 10783

TITLE: TRANSVERSE SECTION & SCHEDULE OF QUANTITIES

DES. J.M.F. | DR. N.A. | APPROVED:
CHK. S.W.E. | CHK. N.K.L.

SHEET NO. 2 OF 31 SHEETS

BRIDGE NO. 13004

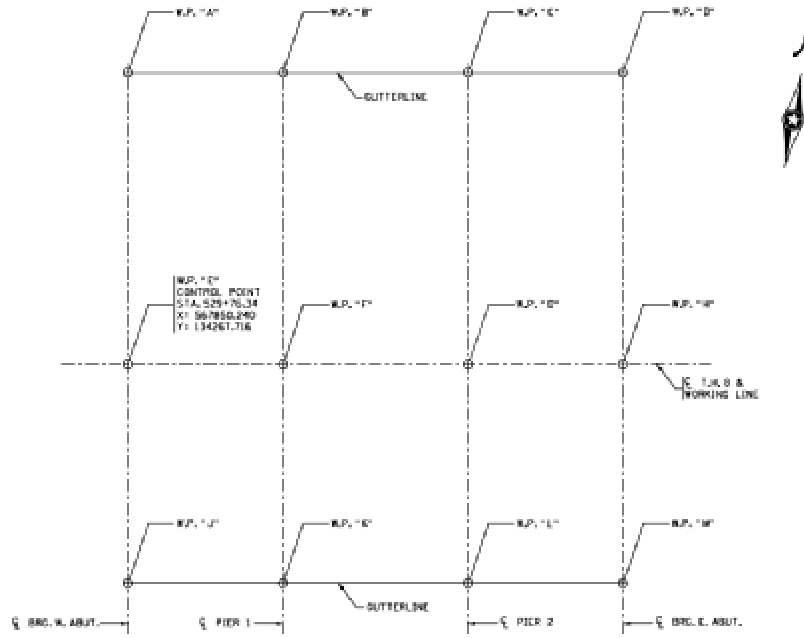

WORKING POINT LAYOUT

	DIMENSIONS BETWEEN WORKING POINTS															ELEVATIONS			
POINT	STATION	X-COORDIN	Y-COORDIN	A	B	C	D	E	F	G	H	J	K	L	M	TOP OF ROADWAY	TOP OF RDWY TO BR. SEAT	BRIDGE SEAT	POINT
A	529+76.34	567842.749	134309.551		22.00			42.50	47.86				76.96	88.54		910.08	1.54	908.54	A
B	529+98.34	567864.405	134313.428			27.00			42.50	50.35		76.96		78.54	88.54	909.88	1.54	908.34	B
C	530+25.34	567890.982	134318.187				22.00			42.50	41.86	88.54	78.54		76.96	909.63	1.54	908.09	C
D	530+47.34	567912.837	134322.065								42.50		88.54	76.96		909.43	1.54	907.89	D
E	529+76.34	567850.240	134267.716						22.00			31.25	38.22						E
F	529+98.34	567871.895	134271.594							27.00			31.25	41.30					F
G	530+25.34	567898.473	134276.352								22.00			31.25	38.22				G
H	530+47.34	567920.128	134280.230												31.25				H
J	529+76.34	567855.748	134236.555										22.00			910.59	1.55	909.04	J
K	529+98.34	567877.403	134240.833											27.00		910.38	1.55	908.83	K
L	530+25.34	567903.981	134245.592												22.00	910.14	1.55	908.59	L
M	530+47.34	567925.636	134249.469													909.93	1.55	908.38	M

TOP OF ROADWAY TO BRIDGE SEAT					
	DECK THICKNESS	BEAM HEIGHT	BEARING PAD. HEIGHT	TOTAL INCHES	TOTAL FEET
NORTH GUTTER	6"	12"	1/2"	18 1/2"	1.54
SOUTH GUTTER	6 5/8"	12"	1/2"	18 5/8"	1.55

NOTE:
SEE SUBSTRUCTURE DETAIL SHEETS FOR ELEVATIONS NEEDED FOR CONSTRUCTION.

CERTIFIED BY: Steven W. Ellis (signature), LICENSED PROFESSIONAL ENGINEER, JAN. 31, 2005 (DATE); NAME: STEVEN W. ELLIS, LIC. NO. 10783	TITLE: BRIDGE LAYOUT	DES: J.M.F. / CK: N.A. / DRN: S.M.E. / CKD: S.M.E. / APPROVED: — SHEET NO. 3 OF 31 SHEETS	BRIDGE NO. 13004

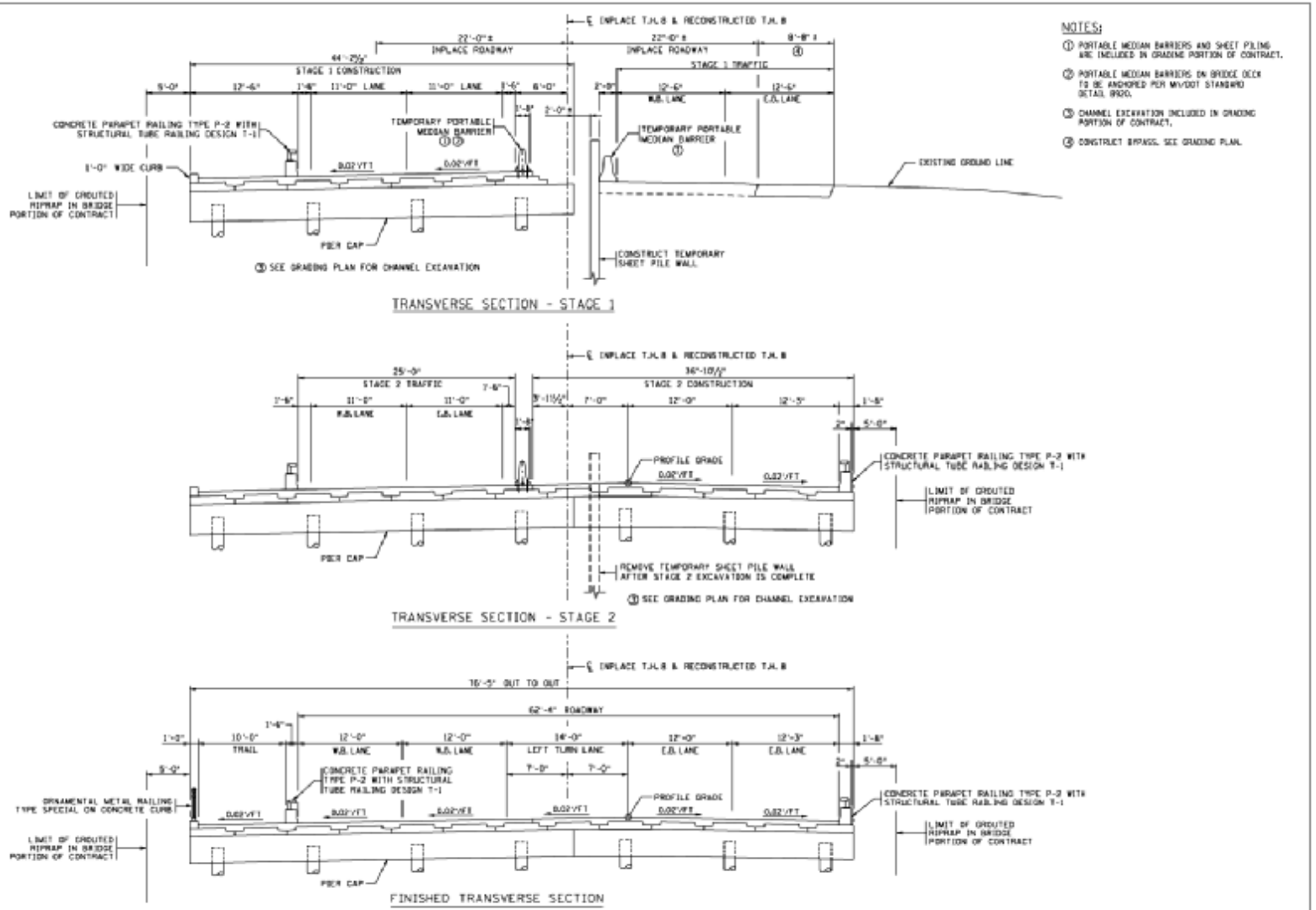
NOTES:
① PORTABLE MEDIAN BARRIERS AND SHEET PILING ARE INCLUDED IN GRADING PORTION OF CONTRACT.
② PORTABLE MEDIAN BARRIERS ON BRIDGE DECK TO BE ANCHORED PER MnDOT STANDARD DETAIL 8820.
③ CHANNEL EXCAVATION INCLUDED IN GRADING PORTION OF CONTRACT.
④ CONSTRUCT BYPASS. SEE GRADING PLAN.
℄ INPLACE T.H. 8 & RECONSTRUCTED T.H. 8
22'-0"± INPLACE ROADWAY
44'-2½" STAGE 1 CONSTRUCTION
22'-0" ± INPLACE ROADWAY
8'-8" ±
STAGE 1 TRAFFIC
5'-0"
12'-6"
1'-8"
11'-0" LANE
11'-0" LANE
1'-6"
6'-0"
2'-8"
12'-6" W.B. LANE
12'-6" E.B. LANE
1'-8"
2'-0" ±
CONCRETE PARAPET RAILING TYPE P-2 WITH STRUCTURAL TUBE RAILING DESIGN T-1
TEMPORARY PORTABLE MEDIAN BARRIER ①②
TEMPORARY PORTABLE MEDIAN BARRIER ①
EXISTING GROUND LINE
1'-0" WIDE CURB
0.02'/FT
0.02'/FT
LIMIT OF GROUTED RIPRAP IN BRIDGE PORTION OF CONTRACT
PIER CAP
CONSTRUCT TEMPORARY SHEET PILE WALL
③ SEE GRADING PLAN FOR CHANNEL EXCAVATION
TRANSVERSE SECTION - STAGE 1
℄ INPLACE T.H. 8 & RECONSTRUCTED T.H. 8
25'-0" STAGE 2 TRAFFIC
36'-10½" STAGE 2 CONSTRUCTION
1'-6"
11'-0" W.B. LANE
11'-0" E.B. LANE
7'-6"
5'-11½"
7'-0"
12'-0"
12'-5"
1'-6"
1'-8"
2"
5'-0"
PROFILE GRADE
0.02'/FT
0.02'/FT
CONCRETE PARAPET RAILING TYPE P-2 WITH STRUCTURAL TUBE RAILING DESIGN T-1
LIMIT OF GROUTED RIPRAP IN BRIDGE PORTION OF CONTRACT
PIER CAP
REMOVE TEMPORARY SHEET PILE WALL AFTER STAGE 2 EXCAVATION IS COMPLETE
③ SEE GRADING PLAN FOR CHANNEL EXCAVATION
TRANSVERSE SECTION - STAGE 2
℄ INPLACE T.H. 8 & RECONSTRUCTED T.H. 8
76'-5" OUT TO OUT
62'-4" ROADWAY
1'-8"
1'-0"
10'-0" TRAIL
12'-0" W.B. LANE
12'-0" W.B. LANE
14'-0" LEFT TURN LANE
12'-0" E.B. LANE
12'-3" E.B. LANE
1'-8"
5'-0"
CONCRETE PARAPET RAILING TYPE P-2 WITH STRUCTURAL TUBE RAILING DESIGN T-1
7'-0"
7'-0"
2"
5'-0"
ORNAMENTAL METAL RAILING TYPE SPECIAL ON CONCRETE CURB
0.02'/FT
0.02'/FT
0.02'/FT
PROFILE GRADE
0.02'/FT
0.02'/FT
CONCRETE PARAPET RAILING TYPE P-2 WITH STRUCTURAL TUBE RAILING DESIGN T-1
LIMIT OF GROUTED RIPRAP IN BRIDGE PORTION OF CONTRACT
PIER CAP
FINISHED TRANSVERSE SECTION
CERTIFIED BY Steven W. Ellis JAN. 18, 2005
LICENSED PROFESSIONAL ENGINEER
DATE
NAME: STEVEN W. ELLIS
LIC. NO. 10783
TITLE: STAGE CONSTRUCTION DETAILS
DES. JMF
CHK. TJE
DR. NKL
CHK. SWE
APPROVED:
SHEET NO. 4 OF 31 SHEETS
BRIDGE NO. 13004

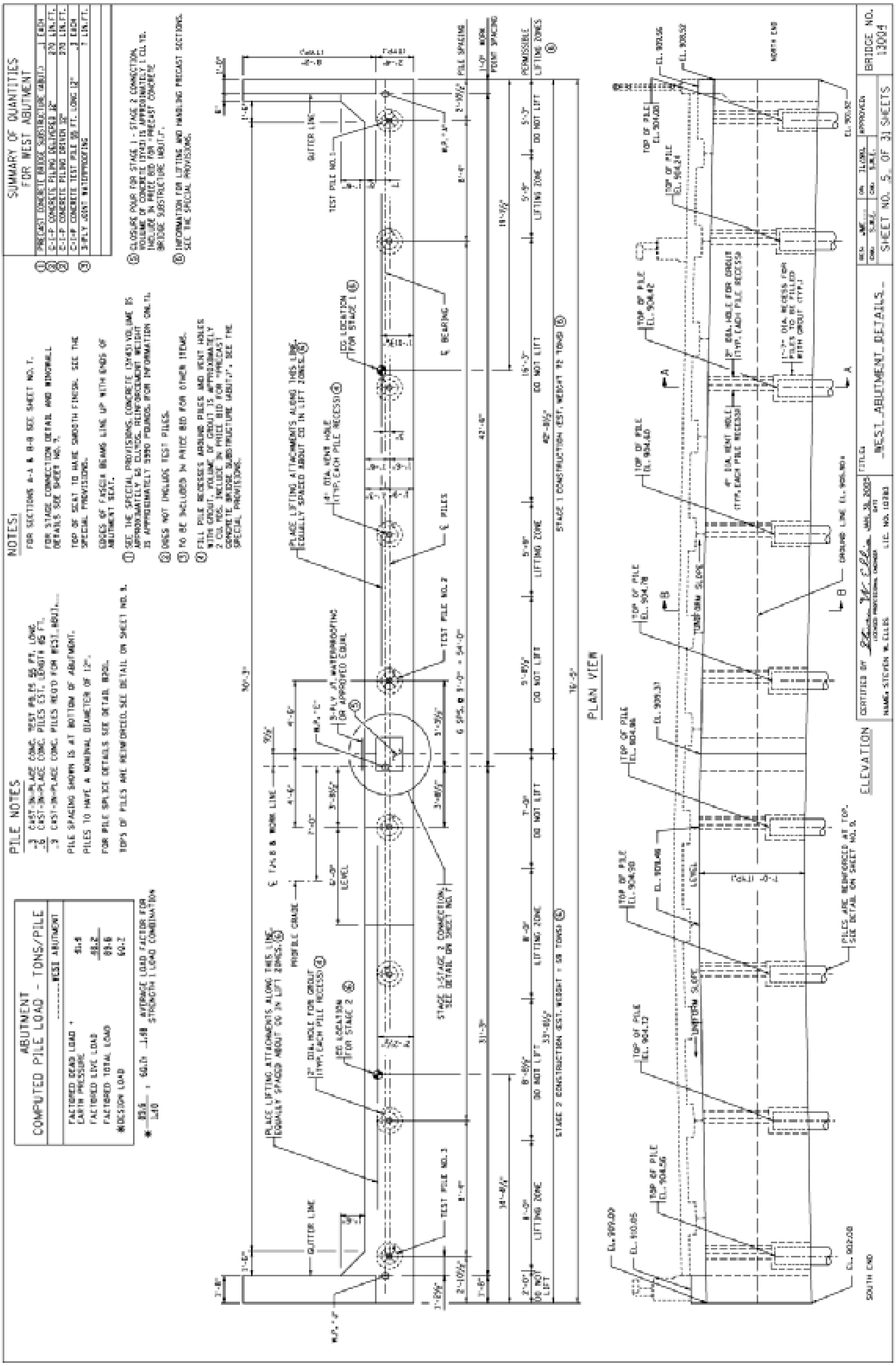
SUMMARY OF QUANTITIES FOR WEST ABUTMENT
COMPUTED PILE LOAD - TONS/PILE
PILE NOTES
NOTES:
PLAN VIEW
ELEVATION
WEST ABUTMENT DETAILS
BRIDGE NO. 13004

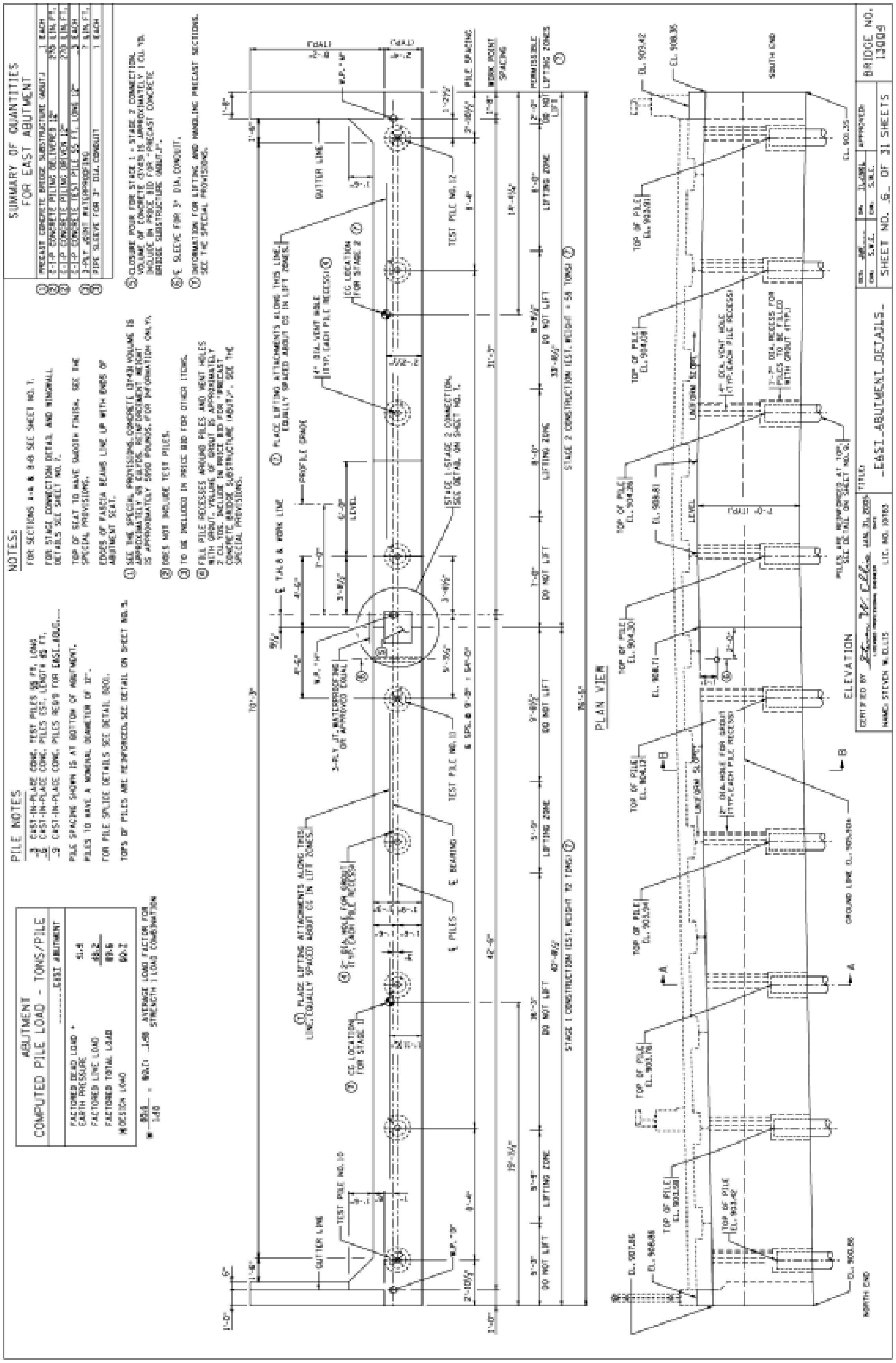
SUMMARY OF QUANTITIES
FOR EAST ABUTMENT
NOTES:
PILE NOTES
ABUTMENT
COMPUTED PILE LOAD - TONS/PILE
PLAN VIEW
ELEVATION
EAST ABUTMENT DETAILS
BRIDGE NO. 13004
SHEET NO. 6 OF 31 SHEETS
NORTH END
SOUTH END

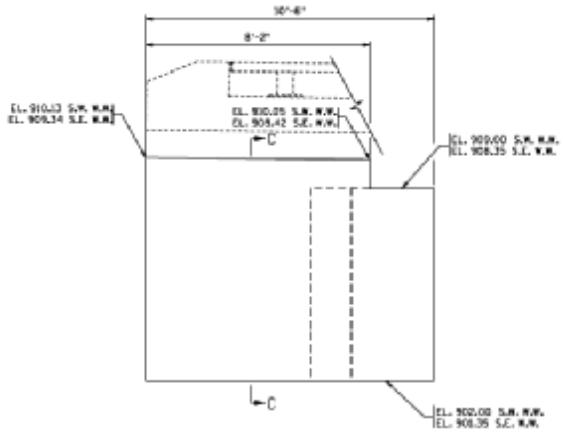

SOUTHWEST & SOUTHEAST
WINGWALL ELEVATION
(WEST ABUTMENT SHOWN, EAST ABUTMENT SIMILAR BY MIRROR IMAGE)

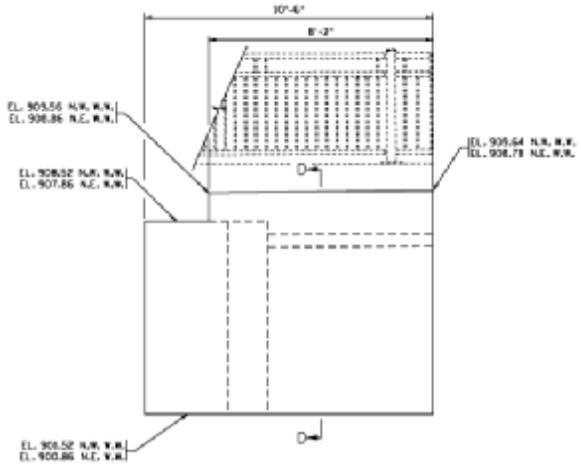

NORTHWEST & NORTHEAST
WINGWALL ELEVATION
(WEST ABUTMENT SHOWN, EAST ABUTMENT SIMILAR BY MIRROR IMAGE)

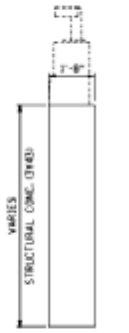

SECTION C-C

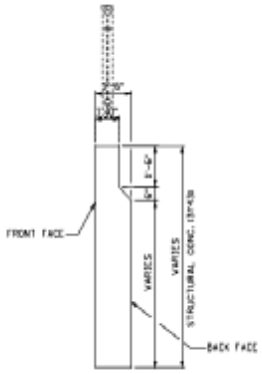

SECTION D-D

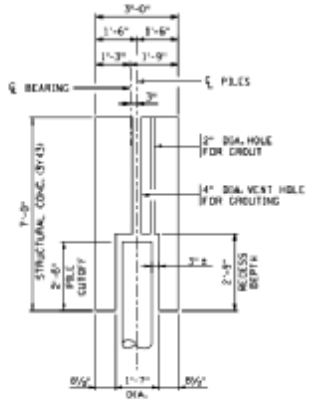

SECTION A-A

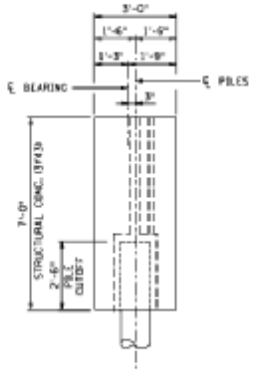

SECTION B-B

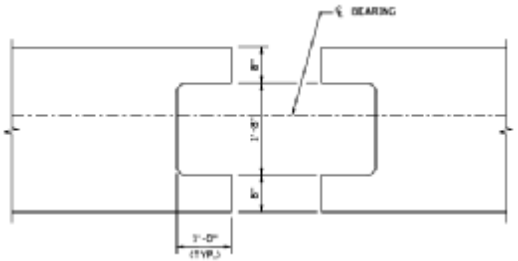

STAGE 1 - STAGE 2 CONNECTION PLAN VIEW

CERTIFIED BY Steven W. Ellis JAN. 31, 2008 (DATE) LICENSED PROFESSIONAL ENGINEER NAME: STEVEN W. ELLIS LIC. NO. 10783	TITLE: ABUTMENT DETAILS	DES: JMLF. DR: M.R.J./M.R. APPROVED: CHK: S.W.E. DW: S.W.E.	BRIDGE NO. 13004
		SHEET NO. 7 OF 31 SHEETS	

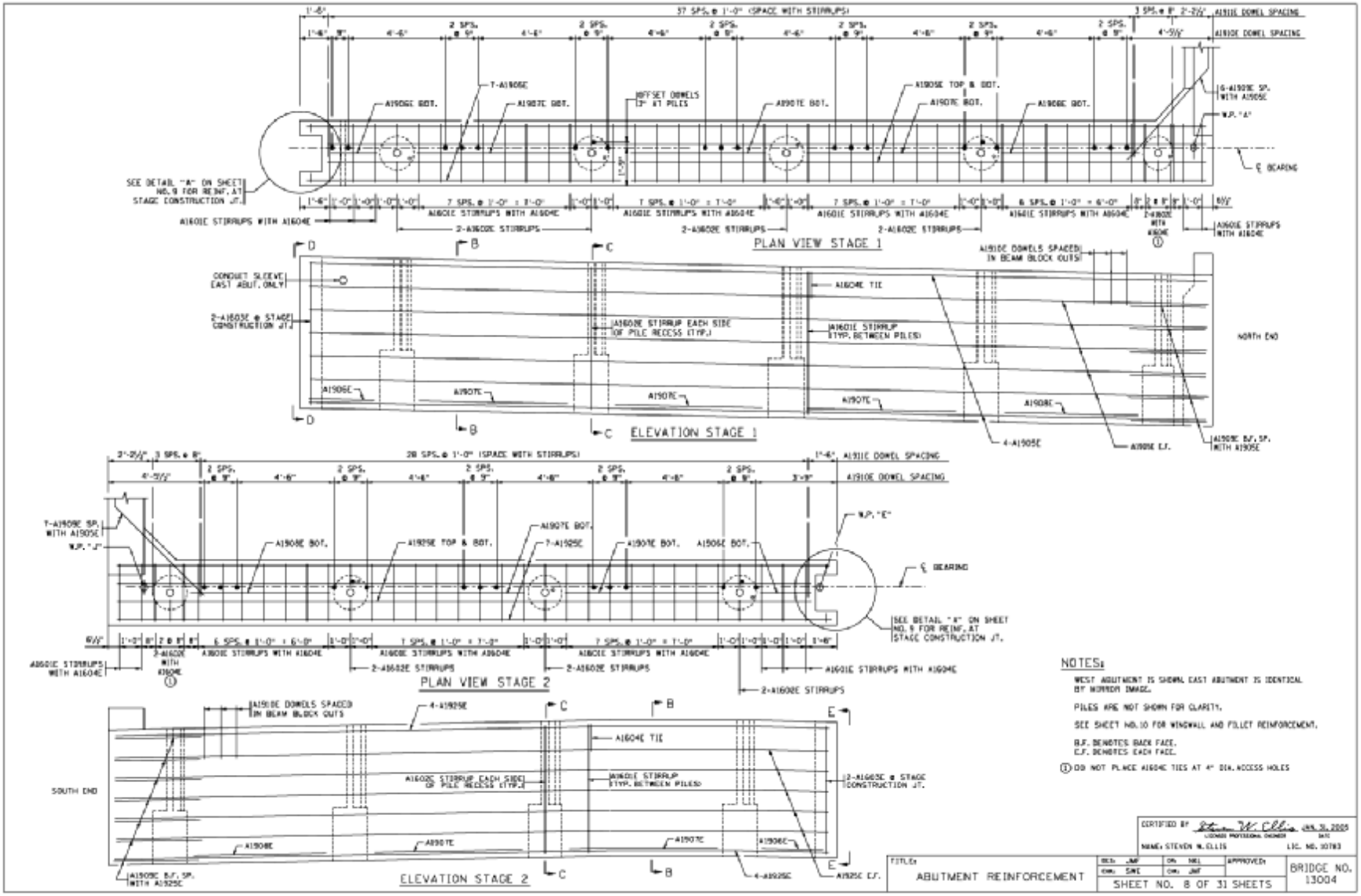

NOTES:

WEST ABUTMENT IS SHOWN, EAST ABUTMENT IS IDENTICAL BY MIRROR IMAGE.

PILES ARE NOT SHOWN FOR CLARITY.

SEE SHEET NO. 10 FOR WINGWALL AND FILLET REINFORCEMENT.

B.F. DENOTES BACK FACE.
E.F. DENOTES EACH FACE.

① DO NOT PLACE A1604E TIES AT 4" DIA. ACCESS HOLES

CERTIFIED BY Steven W. Ellis JAN. 31, 2005
NAME: STEVEN W. ELLIS LIC. NO. 10783

DES. JMF DW. NEL APPROVED
CHK. SWE CHK. JMF

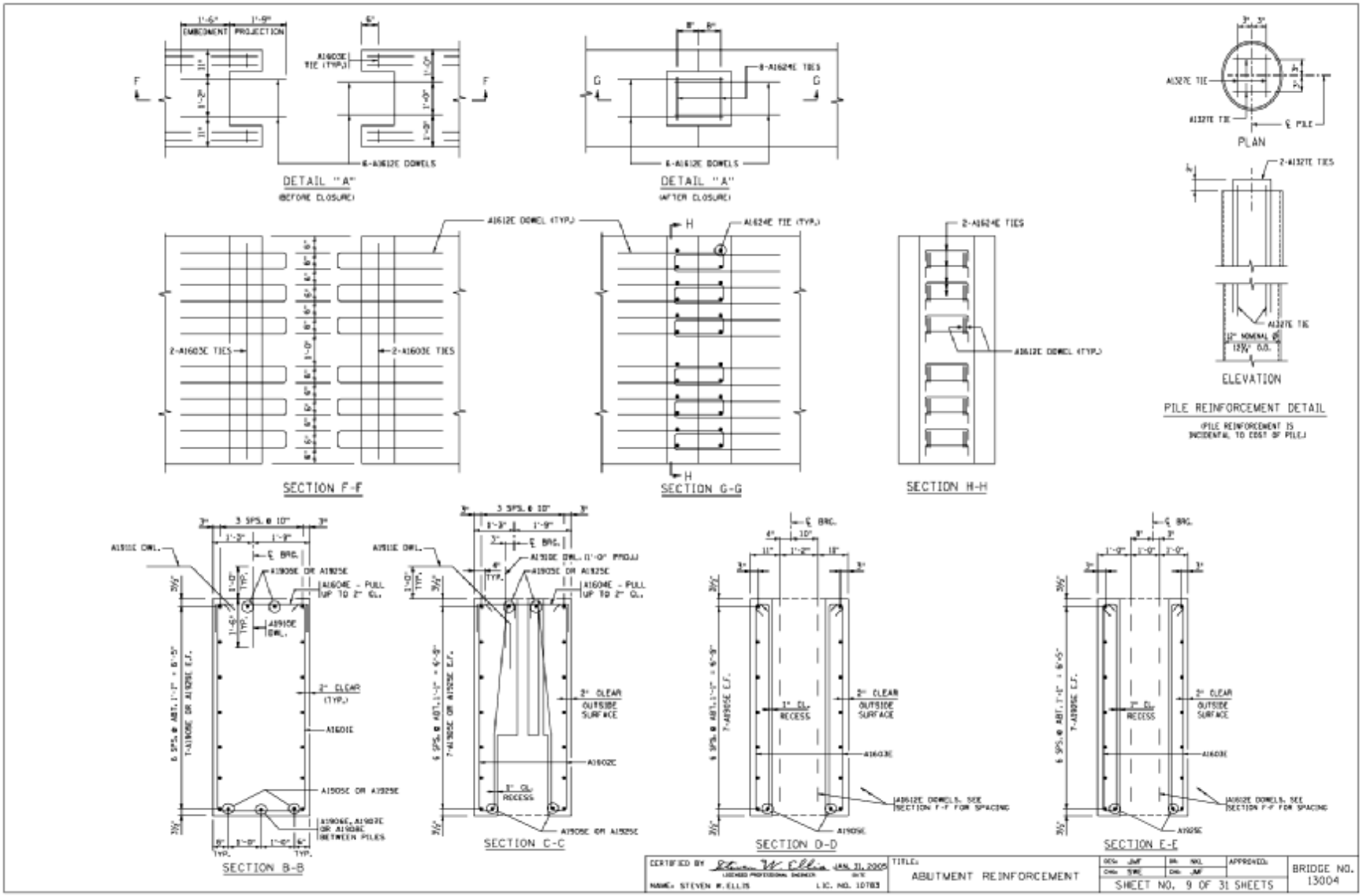

CERTIFIED BY Steven W. Ellis JAN. 31, 2005
LICENSED PROFESSIONAL ENGINEER
NAME: STEVEN W. ELLIS LIC. NO. 10783

TITLE: ABUTMENT REINFORCEMENT

DES. JMF DR. WKL APPROVED:
CHK. TWE DW. JMF

SHEET NO. 9 OF 31 SHEETS

BRIDGE NO. 13004

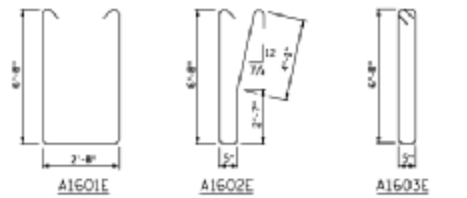

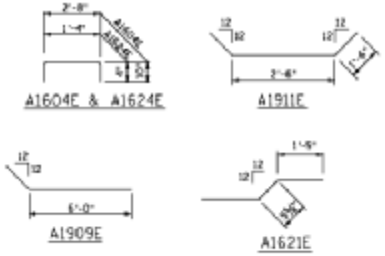

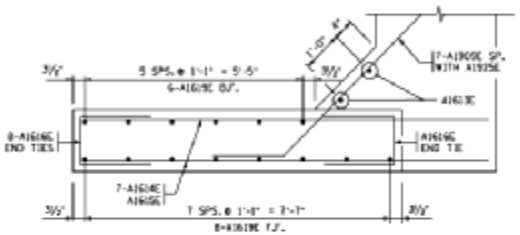

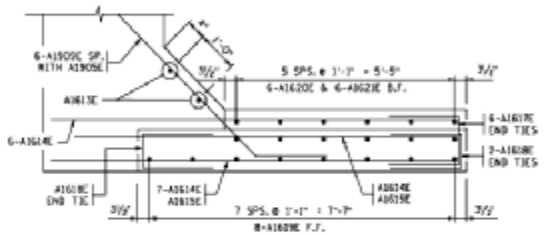

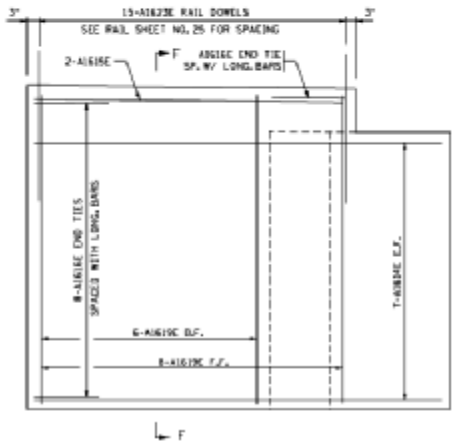

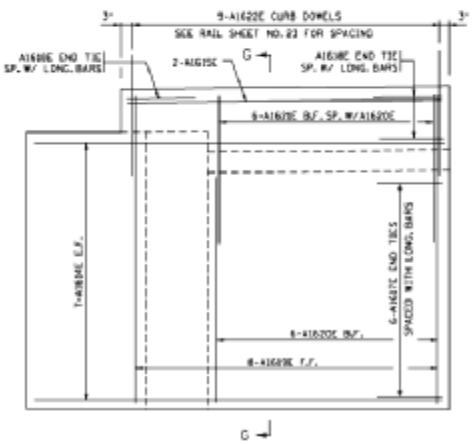

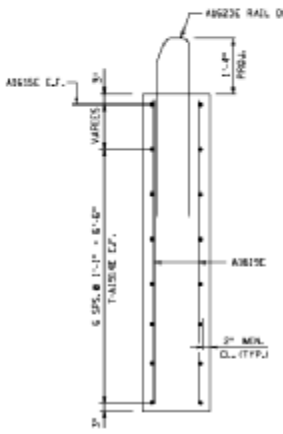

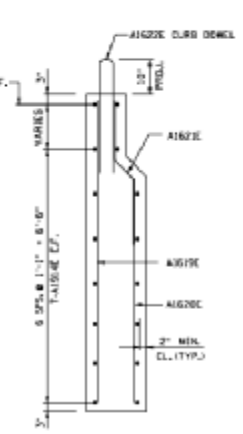

① BILL OF REINFORCEMENT FOR TWO ABUTMENTS

	BAR	NO.	LENGTH	SHAPE	LOCATION
	A1601E	628	8'-8"		STIRRUP
	A1602E	52	14'-1.5"		STIRRUP
	A1603E	8	15'-1"		VERTICAL TIE
	A1604E	136	4'-4"		SEAT TIE
	A1605E	36	42'-4"		LONGITUDINAL
	A1606E	4	2'-4"		LONGITUDINAL BOTTOM
	A1607E	10	7'-1"		LONGITUDINAL BOTTOM
	A1608E	4	6'-3"		LONGITUDINAL BOTTOM
	A1609E	76	1'-6"		FILLET TIE
	A1610E	70	2'-6"		DECK DOWEL
	A1611E	146	5'-6"		APPROACH PANEL DOWEL
	A1612E	48	1'-0"		CLOSURE POUR DOWEL
	A1613E	8	5'-9"		FILLET VERTICAL
	A1614E	56	10'-2"		WINGWALL LONGITUDINAL
	A1615E	8	7'-9"		WINGWALL LONGITUDINAL
	A1616E	18	4'-4"		WINGWALL END TIE
	A1617E	12	4'-2"		WINGWALL END TIE
	A1618E	8	3'-8"		WINGWALL END TIE
	A1619E	44	7'-7"		WINGWALL VERTICAL
	A1620E	12	5'-9"		WINGWALL VERTICAL
	A1621E	12	4'-0"		WINGWALL VERTICAL
	A1622E	18	5'-1"		CURB DOWEL
	A1623E	30	8'-8"		RAIL DOWEL
	A1624E	48	3'-0"		CLOSURE POUR TIE
	A1625E	36	33'-4"		LONGITUDINAL
②	A1327E	12	9'-0"		PILE REINFORCEMENT TIE

NOTES:

F.F. DENOTES FRONT FACE.
B.F. DENOTES BACK FACE.
E.F. DENOTES EACH FACE.

① BILL OF REINFORCEMENT IS FOR INFORMATION ONLY. WEIGHT OF REINFORCEMENT IS APPROXIMATELY 107.0 POUNDS. REINFORCEMENT IS INCLUDED IN PRICE BID FOR "PRECAST CONCRETE BRIDGE SUBSTRUCTURE (ABUT.)".

② PILE REINFORCEMENT IS INCIDENTAL TO COST OF PILES.

CERTIFIED BY Steven W. Ellis JAN. 31, 2005
LICENSED PROFESSIONAL ENGINEER DATE
NAME: STEVEN W. ELLIS LIC. NO. 10763

TITLE: ABUTMENT REINFORCEMENT

DES. JMF | DR. NKL | CK. SWE | CK. JMF | APPROVED:

SHEET NO. 10 OF 31 SHEETS

BRIDGE NO. 13004

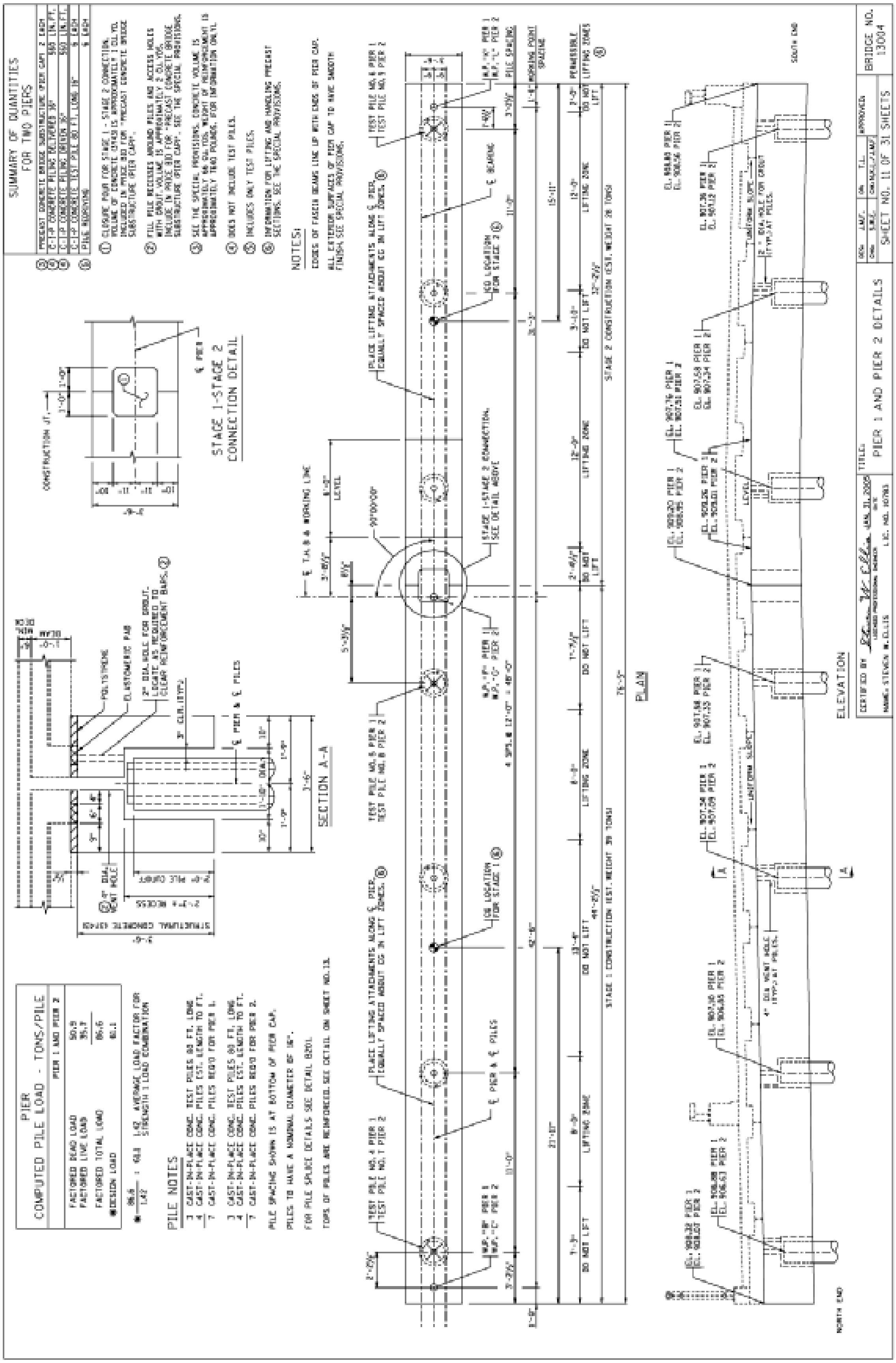
SUMMARY OF QUANTITIES FOR TWO PIERS
PIER COMPUTED PILE LOAD - TONS/PILE
PILE NOTES
NOTES:
SECTION A-A
STAGE 1-STAGE 2 CONNECTION DETAIL
PLAN
ELEVATION
PIER 1 AND PIER 2 DETAILS
BRIDGE NO. 13004
SHEET NO. 11 OF 31 SHEETS

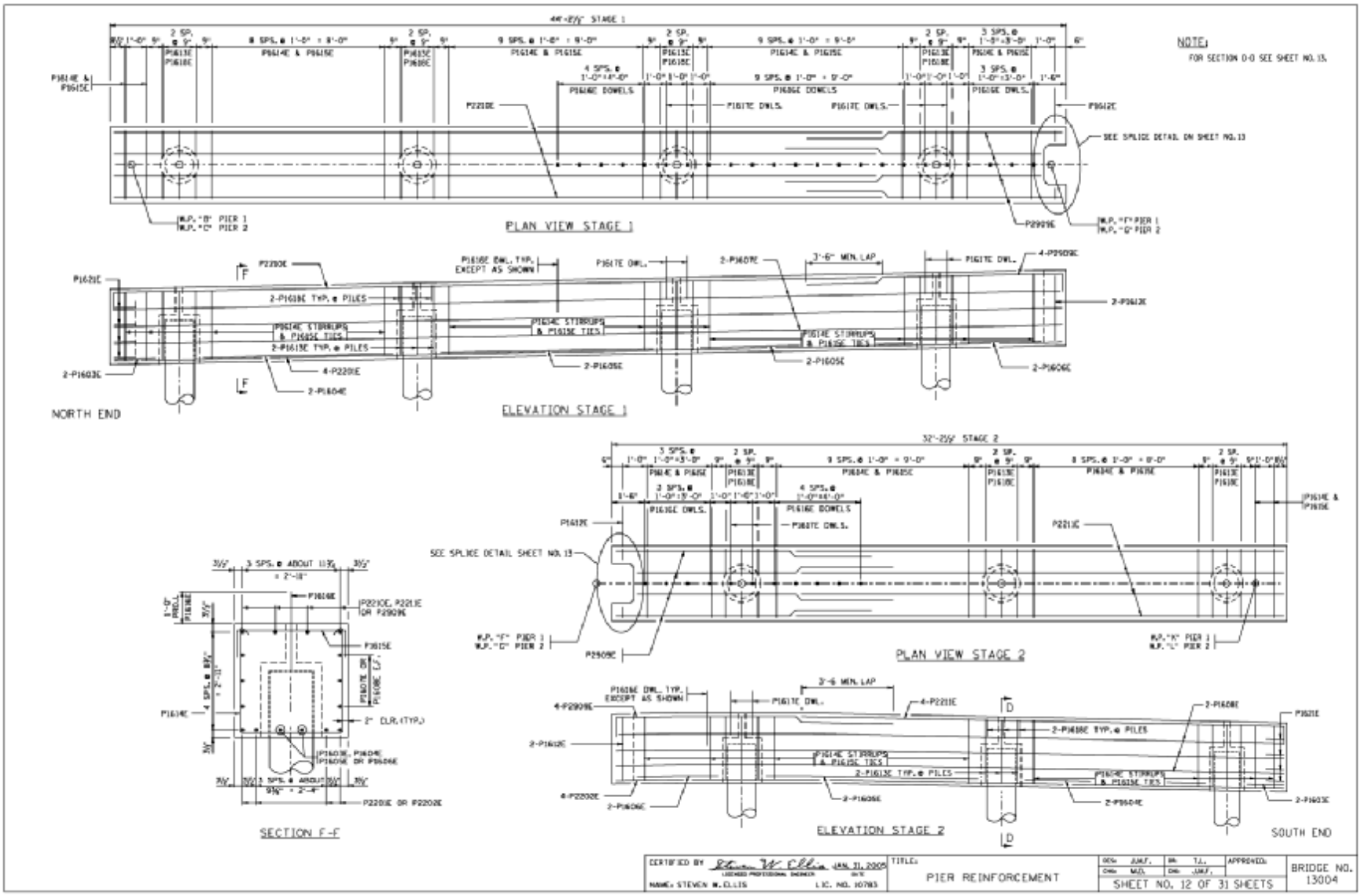
NOTE:
FOR SECTION D-D SEE SHEET NO. 15.
PLAN VIEW STAGE 1
ELEVATION STAGE 1
NORTH END
SECTION F-F
PLAN VIEW STAGE 2
ELEVATION STAGE 2
SOUTH END
SEE SPLICE DETAIL ON SHEET NO. 13
SEE SPLICE DETAIL SHEET NO. 13
P1612E
P1613E
P1614E & P1615E
P2210E
P2909E
P1616E DWLS.
P1617E DWLS.
2-P1618E TYP. @ PILES
2-P1613E TYP. @ PILES
4-P2210E
2-P1604E
2-P1605E
2-P1606E
2-P1603E
P2211E
P1615E
P1614E
P2210E, P2211E OR P2909E
P2202E OR P2203E
2" CLR. (TYP.)
CERTIFIED BY
NAME: STEVEN W. ELLIS
LIC. NO. 10783
TITLE:
PIER REINFORCEMENT
SHEET NO. 12 OF 31 SHEETS
APPROVED:
BRIDGE NO. 13004

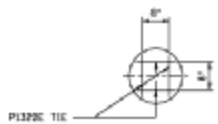

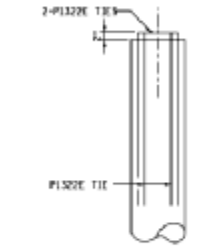

DETAIL OF PILE REINFORCEMENT

(PILE REINFORCEMENT IS INCIDENTAL TO COST OF PILE.)

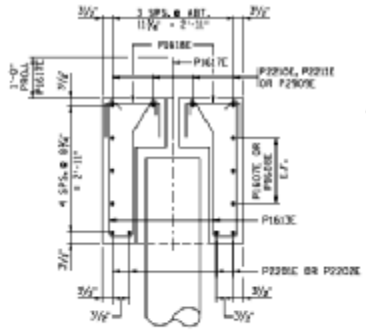

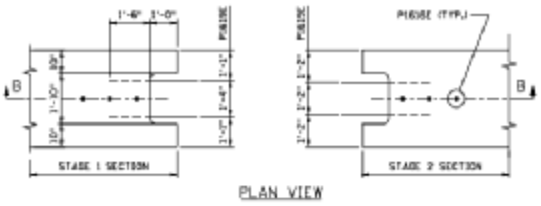

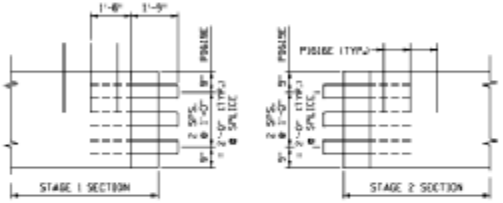

① BILL OF REINFORCEMENT FOR TWO PIER

	BAR	NO.	LENGTH	SHAPE	LOCATION
	P2290E	8	45'-10"		BOTTOM LONGITUDINALS
	P2202E	8	51'-10"		BOTTOM LONGITUDINALS
	P1603E	8	1'-11"		BOTTOM LONGITUDINALS
	P1604E	8	8'-10"		BOTTOM LONGITUDINALS
	P1605E	12	9'-10"		BOTTOM LONGITUDINALS
	P1606E	8	3'-8"		BOTTOM LONGITUDINALS
	P1607E	12	45'-10"		MIDDLE LONGITUDINALS
	P1608E	12	51'-10"		MIDDLE LONGITUDINALS
	P2909E	16	13'- 5"		TOP LONG. AT SPLICE
	P2210E	8	38'-11"		TOP LONGITUDINALS
	P2211E	8	24'- 11"		TOP LONGITUDINALS
	P1612E	8	8'-3"		STIRRUPS AT SPLICE
	P1613E	68	7'- 11"		STIRRUPS AT PILES
	P1614E	120	10'- 5"		BOTTOM STIRRUPS
	P1615E	102	5'- 2"		TOP TIES
	P1616E	56	2'- 6"		DOWELS
	P1617E	12	2'- 0"		DOWELS
	P1618E	68	3'- 4"		TOP TIES AT PILES
	P1619E	24	1'- 0"		TIES IN SPLICE
	P1620E	24	2'- 0"		TIES IN SPLICE
	P1621E	16	6'- 2"		PIER CAP END TIES
②	P1322E	56	9'-8"		PILE REINFORCEMENT TIE

NOTES:

E.F. DENOTES EACH FACE.

① BILL OF REINFORCEMENT IS FOR INFORMATION ONLY. REINFORCEMENT IS INCLUDED IN PRICE BID FOR "PRECAST CONCRETE BRIDGE SUBSTRUCTURE (PIER CAP)".

② PILE REINFORCEMENT IS INCIDENTAL TO COST OF PILES.

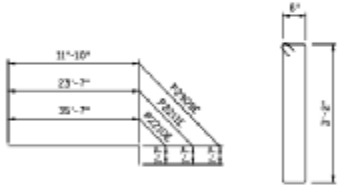

P2909E, P2210E, P2211E

P1612E

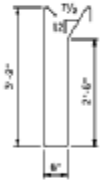

P1613E

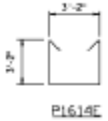

P1614E

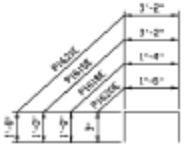

P1615E, P1618E, P1620E, P1621E

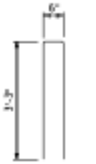

P1619E

P1322E

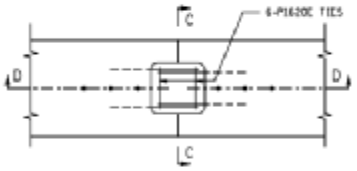

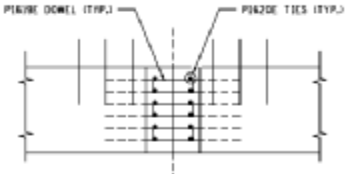

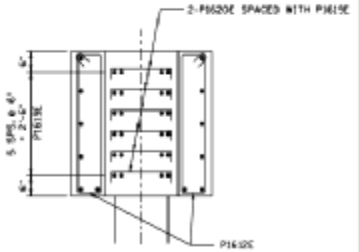

CERTIFIED BY Steven W. Ellis (JAN. 31, 2005) PROFESSIONAL ENGINEER

NAME: STEVEN W. ELLIS LIC. NO. 19183

TITLE: PIER REINFORCEMENT

DES. J.M.F. DR. T.J. APPROVED:

CHK. M.D. CHK. J.M.F.

SHEET NO. 13 OF 31 SHEETS

BRIDGE NO. 13004

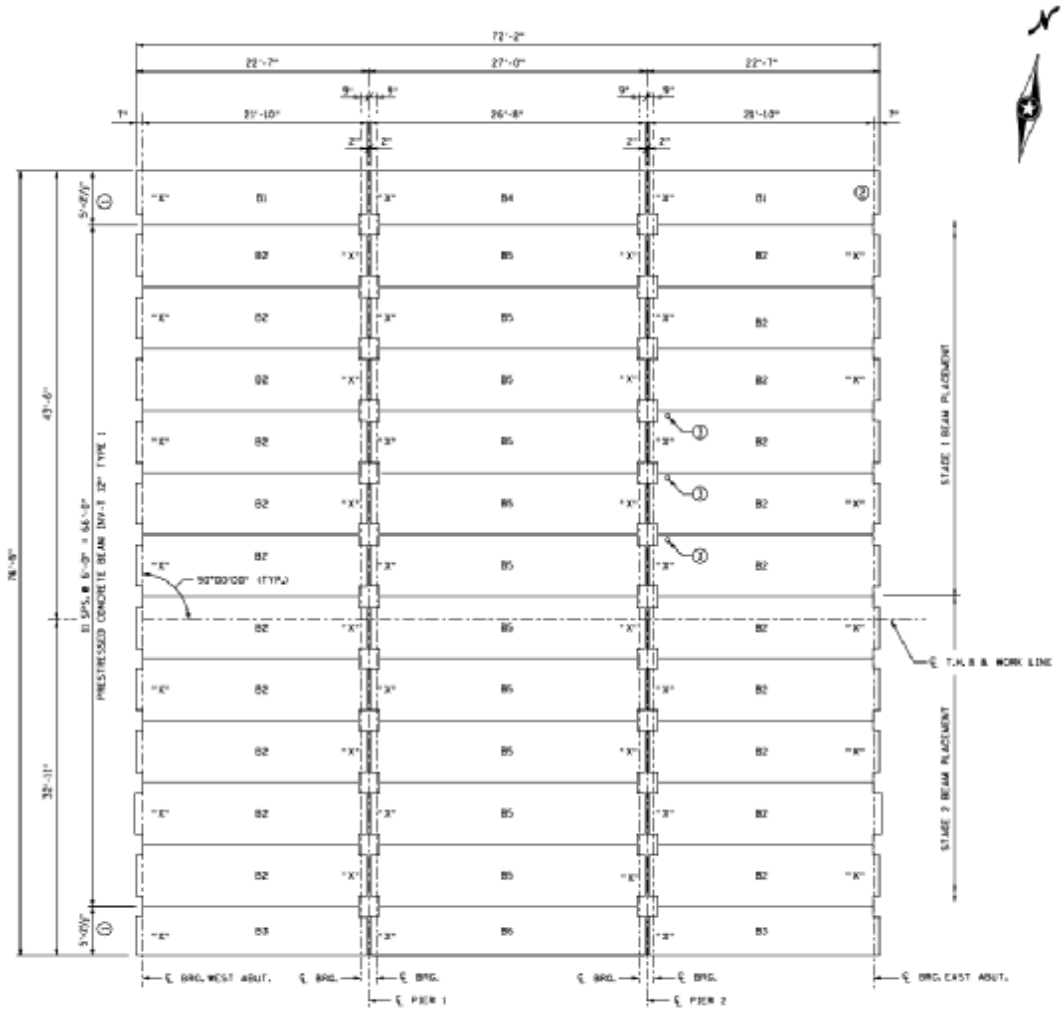

FRAMING PLAN

NOTES:

"X" DENOTES X END OF BEAM.

① PRESTRESSED CONCRETE BEAM INV-1 12" TYPE I.

② "ELASTOMERIC BEARING PAD TYPE 1" TYPICAL AT BOTH ENDS OF ALL BEAMS. SEE DETAILS ON SHEET NO. 15.

③ HOLE THROUGH BEAM FLANGE FOR 3" DIAMETER CONDUIT. SEE SHEET NO. 35.

CERTIFIED BY Steven W. Ellis JAN. 16 2026
LICENSED PROFESSIONAL ENGINEER DATE
NAME: STEVEN W. ELLIS LIC. NO. 10783

TITLE: FRAMING PLAN

DES: JMF DR: LKL APPROVED:
CHK: SWE CHK: NKL

SHEET NO. 14 OF 31 SHEETS

BRIDGE NO. 13004

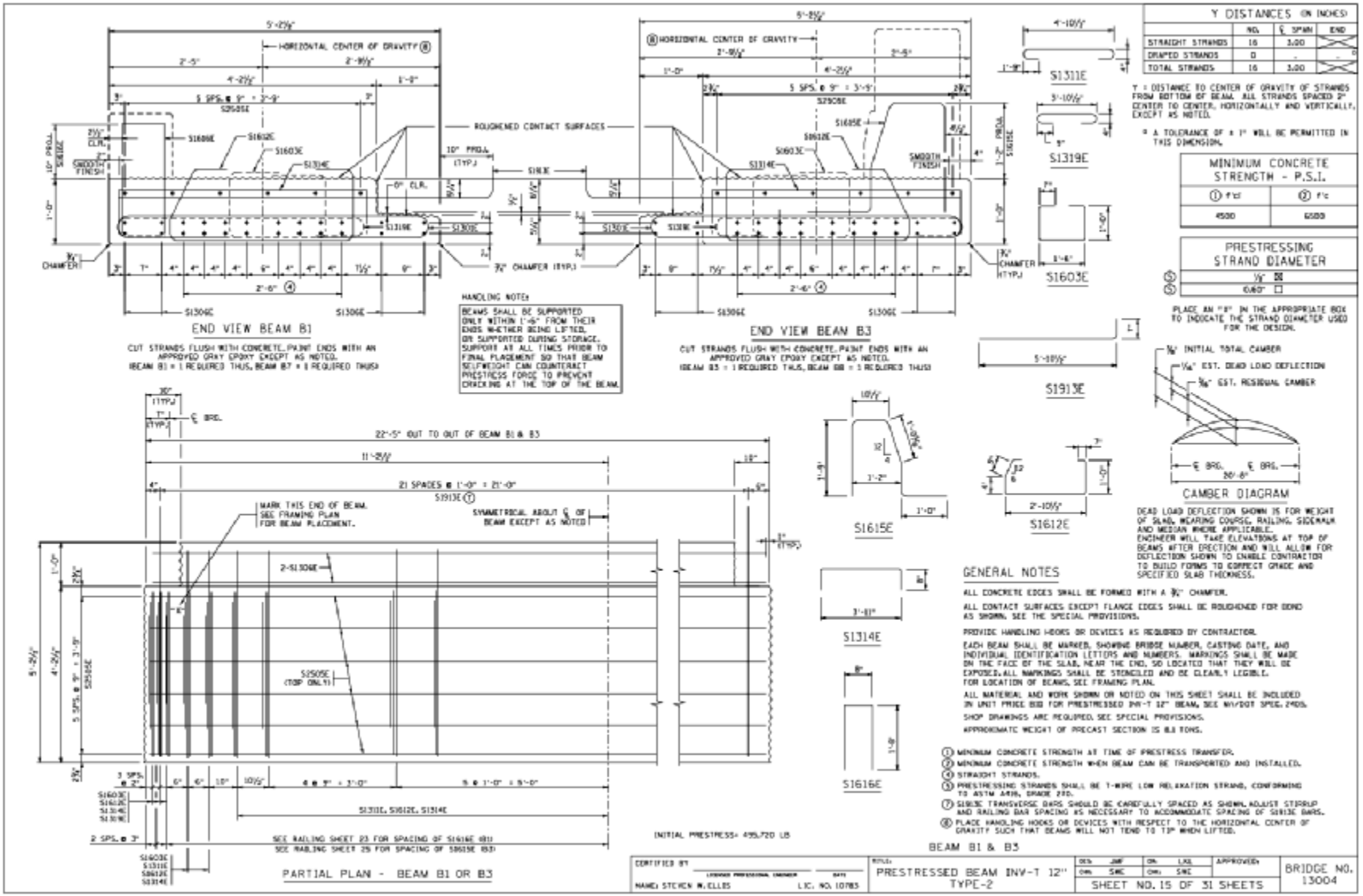
END VIEW BEAM B1
CUT STRANDS FLUSH WITH CONCRETE. PAINT ENDS WITH AN APPROVED GRAY EPOXY EXCEPT AS NOTED.
(BEAM B1 = 1 REQUIRED THUS, BEAM B7 = 8 REQUIRED THUS)
HANDLING NOTE:
BEAMS SHALL BE SUPPORTED ONLY WITHIN 1'-6" FROM THEIR ENDS WHETHER BEING LIFTED, OR SUPPORTED DURING STORAGE. SUPPORT AT ALL TIMES PRIOR TO FINAL PLACEMENT SO THAT BEAM SELF WEIGHT CAN COUNTERACT PRESTRESS FORCE TO PREVENT CRACKING AT THE TOP OF THE BEAM.
END VIEW BEAM B3
CUT STRANDS FLUSH WITH CONCRETE. PAINT ENDS WITH AN APPROVED GRAY EPOXY EXCEPT AS NOTED.
(BEAM B3 = 1 REQUIRED THUS, BEAM B8 = 5 REQUIRED THUS)
ROUGHENED CONTACT SURFACES
¾" CHAMFER (TYP.)
PARTIAL PLAN - BEAM B1 OR B3
22'-5" OUT TO OUT OF BEAM B1 & B3
21 SPACES @ 1'-0" = 21'-0"
MARK THIS END OF BEAM. SEE FRAMING PLAN FOR BEAM PLACEMENT.
SYMMETRICAL ABOUT ℄ OF BEAM EXCEPT AS NOTED
SEE RAILING SHEET 23 FOR SPACING OF S1616E (B1)
SEE RAILING SHEET 25 FOR SPACING OF S1615E (B3)
INITIAL PRESTRESS= 495,720 LB
S1311E
S1319E
S1603E
S1913E
S1615E
S1612E
S1314E
S1616E
Y DISTANCES (IN INCHES)
NO. ℄ SPMN END
STRAIGHT STRANDS 16 3.00
DRAPED STRANDS 0 - -
TOTAL STRANDS 16 3.00
Y = DISTANCE TO CENTER OF GRAVITY OF STRANDS FROM BOTTOM OF BEAM. ALL STRANDS SPACED 2" CENTER TO CENTER, HORIZONTALLY AND VERTICALLY, EXCEPT AS NOTED.
* A TOLERANCE OF ± 1" WILL BE PERMITTED IN THIS DIMENSION.
MINIMUM CONCRETE STRENGTH - P.S.I.
① f'ci ② f'c
4500 6000
PRESTRESSING STRAND DIAMETER
½" ☒
0.60" ☐
PLACE AN "X" IN THE APPROPRIATE BOX TO INDICATE THE STRAND DIAMETER USED FOR THE DESIGN.
½" INITIAL TOTAL CAMBER
1¼" EST. DEAD LOAD DEFLECTION
⅜" EST. RESIDUAL CAMBER
℄ BRG. ℄ BRG.
CAMBER DIAGRAM
DEAD LOAD DEFLECTION SHOWN IS FOR WEIGHT OF SLAB, WEARING COURSE, RAILING, SIDEWALK AND MEDIAN WHERE APPLICABLE. ENGINEER WILL TAKE ELEVATIONS AT TOP OF BEAMS AFTER ERECTION AND WILL ALLOW FOR DEFLECTION SHOWN TO ENABLE CONTRACTOR TO BUILD FORMS TO CORRECT GRADE AND SPECIFIED SLAB THICKNESS.
GENERAL NOTES
ALL CONCRETE EDGES SHALL BE FORMED WITH A ¾" CHAMFER.
ALL CONTACT SURFACES EXCEPT FLANGE EDGES SHALL BE ROUGHENED FOR BOND AS SHOWN. SEE THE SPECIAL PROVISIONS.
PROVIDE HANDLING HOOKS OR DEVICES AS REQUIRED BY CONTRACTOR.
EACH BEAM SHALL BE MARKED, SHOWING BRIDGE NUMBER, CASTING DATE, AND INDIVIDUAL IDENTIFICATION LETTERS AND NUMBERS. MARKINGS SHALL BE MADE ON THE FACE OF THE SLAB, NEAR THE END, SO LOCATED THAT THEY WILL BE EXPOSED. ALL MARKINGS SHALL BE STENCILED AND BE CLEARLY LEGIBLE. FOR LOCATION OF BEAMS, SEE FRAMING PLAN.
ALL MATERIAL AND WORK SHOWN OR NOTED ON THIS SHEET SHALL BE INCLUDED IN UNIT PRICE BID FOR PRESTRESSED INV-T 12" BEAM, SEE NVDOT SPEC. 2405.
SHOP DRAWINGS ARE REQUIRED. SEE SPECIAL PROVISIONS.
APPROXIMATE WEIGHT OF PRECAST SECTION IS 83 TONS.
① MINIMUM CONCRETE STRENGTH AT TIME OF PRESTRESS TRANSFER.
② MINIMUM CONCRETE STRENGTH WHEN BEAM CAN BE TRANSPORTED AND INSTALLED.
④ STRAIGHT STRANDS.
⑤ PRESTRESSING STRANDS SHALL BE 7-WIRE LOW RELAXATION STRAND, CONFORMING TO ASTM A416, GRADE 270.
⑦ S1913E TRANSVERSE BARS SHOULD BE CAREFULLY SPACED AS SHOWN. ADJUST STIRRUP AND RAILING BAR SPACING AS NECESSARY TO ACCOMMODATE SPACING OF S1913E BARS.
⑧ PLACE HANDLING HOOKS OR DEVICES WITH RESPECT TO THE HORIZONTAL CENTER OF GRAVITY SUCH THAT BEAMS WILL NOT TEND TO TIP WHEN LIFTED.
BEAM B1 & B3
CERTIFIED BY
NAME: STEVEN W. ELLIS
LIC. NO. 10785
TITLE: PRESTRESSED BEAM INV-T 12" TYPE-2
DES. JMF DR. LKL CHK. SWE APPROVED: SWE
SHEET NO. 15 OF 31 SHEETS
BRIDGE NO. 13004

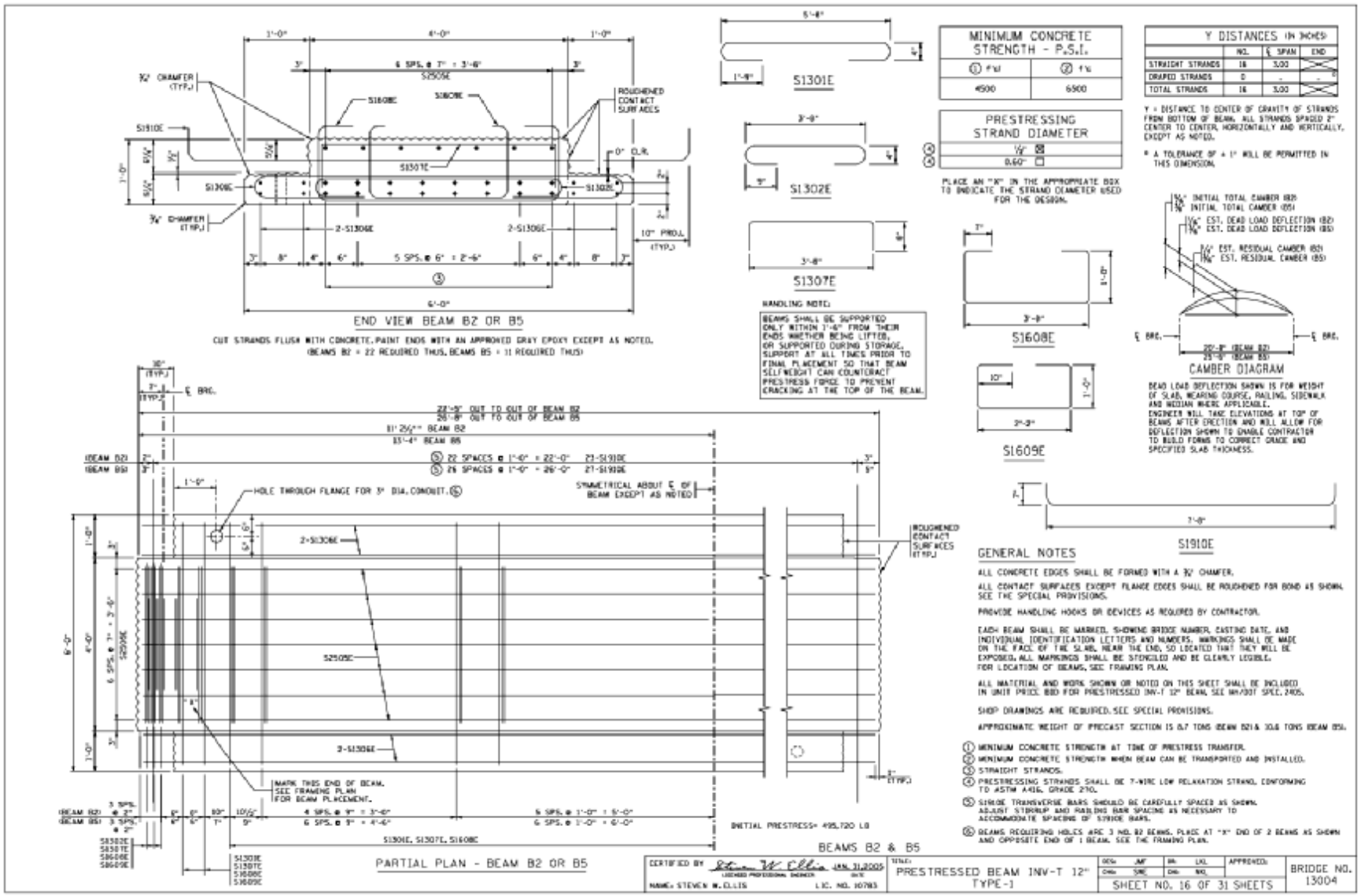
END VIEW BEAM B2 OR B5
CUT STRANDS FLUSH WITH CONCRETE, PAINT ENDS WITH AN APPROVED GRAY EPOXY EXCEPT AS NOTED.
(BEAMS B2 = 22 REQUIRED THUS, BEAMS B5 = 11 REQUIRED THUS)
S1301E
S1302E
S1307E
S1608E
S1609E
S1910E
MINIMUM CONCRETE STRENGTH - P.S.I.
PRESTRESSING STRAND DIAMETER
Y DISTANCES (IN INCHES)
HANDLING NOTE:
BEAMS SHALL BE SUPPORTED ONLY WITHIN 1'-6" FROM THEIR ENDS WHETHER BEING LIFTED, OR SUPPORTED DURING STORAGE. SUPPORT AT ALL TIMES PRIOR TO FINAL PLACEMENT SO THAT BEAM SELFWEIGHT CAN COUNTERACT PRESTRESS FORCE TO PREVENT CRACKING AT THE TOP OF THE BEAM.
CAMBER DIAGRAM
PARTIAL PLAN - BEAM B2 OR B5
BEAMS B2 & B5
GENERAL NOTES
ALL CONCRETE EDGES SHALL BE FORMED WITH A ¾" CHAMFER.
ALL CONTACT SURFACES EXCEPT FLANGE EDGES SHALL BE ROUGHENED FOR BOND AS SHOWN. SEE THE SPECIAL PROVISIONS.
PROVIDE HANDLING HOOKS OR DEVICES AS REQUIRED BY CONTRACTOR.
EACH BEAM SHALL BE MARKED, SHOWING BRIDGE NUMBER, CASTING DATE, AND INDIVIDUAL IDENTIFICATION LETTERS AND NUMBERS. MARKINGS SHALL BE MADE ON THE FACE OF THE SLAB, NEAR THE END, SO LOCATED THAT THEY WILL BE EXPOSED. ALL MARKINGS SHALL BE STENCILED AND BE CLEARLY LEGIBLE. FOR LOCATION OF BEAMS, SEE FRAMING PLAN.
ALL MATERIAL AND WORK SHOWN OR NOTED ON THIS SHEET SHALL BE INCLUDED IN UNIT PRICE BID FOR PRESTRESSED INV-T 12" BEAM, SEE MHDOT SPEC. 2405.
SHOP DRAWINGS ARE REQUIRED. SEE SPECIAL PROVISIONS.
APPROXIMATE WEIGHT OF PRECAST SECTION IS 6.7 TONS (BEAM B2) & 10.6 TONS (BEAM B5).
① MINIMUM CONCRETE STRENGTH AT TIME OF PRESTRESS TRANSFER.
② MINIMUM CONCRETE STRENGTH WHEN BEAM CAN BE TRANSPORTED AND INSTALLED.
③ STRAIGHT STRANDS.
④ PRESTRESSING STRANDS SHALL BE 7-WIRE LOW RELAXATION STRAND, CONFORMING TO ASTM A416, GRADE 270.
⑤ STIRRUP TRANSVERSE BARS SHOULD BE CAREFULLY SPACED AS SHOWN. ADJUST STIRRUP AND RAILING BAR SPACING AS NECESSARY TO ACCOMMODATE SPACING OF STIRRUP BARS.
⑥ BEAMS REQUIRING HOLES ARE 3 NO. B2 BEAMS. PLACE AT "X" END OF 2 BEAMS AS SHOWN AND OPPOSITE END OF 1 BEAM. SEE THE FRAMING PLAN.
CERTIFIED BY Steven W. Ellis JAN. 31, 2005
NAME: STEVEN W. ELLIS LIC. NO. 10783
PRESTRESSED BEAM INV-T 12" TYPE-1
SHEET NO. 16 OF 31 SHEETS
BRIDGE NO. 13004

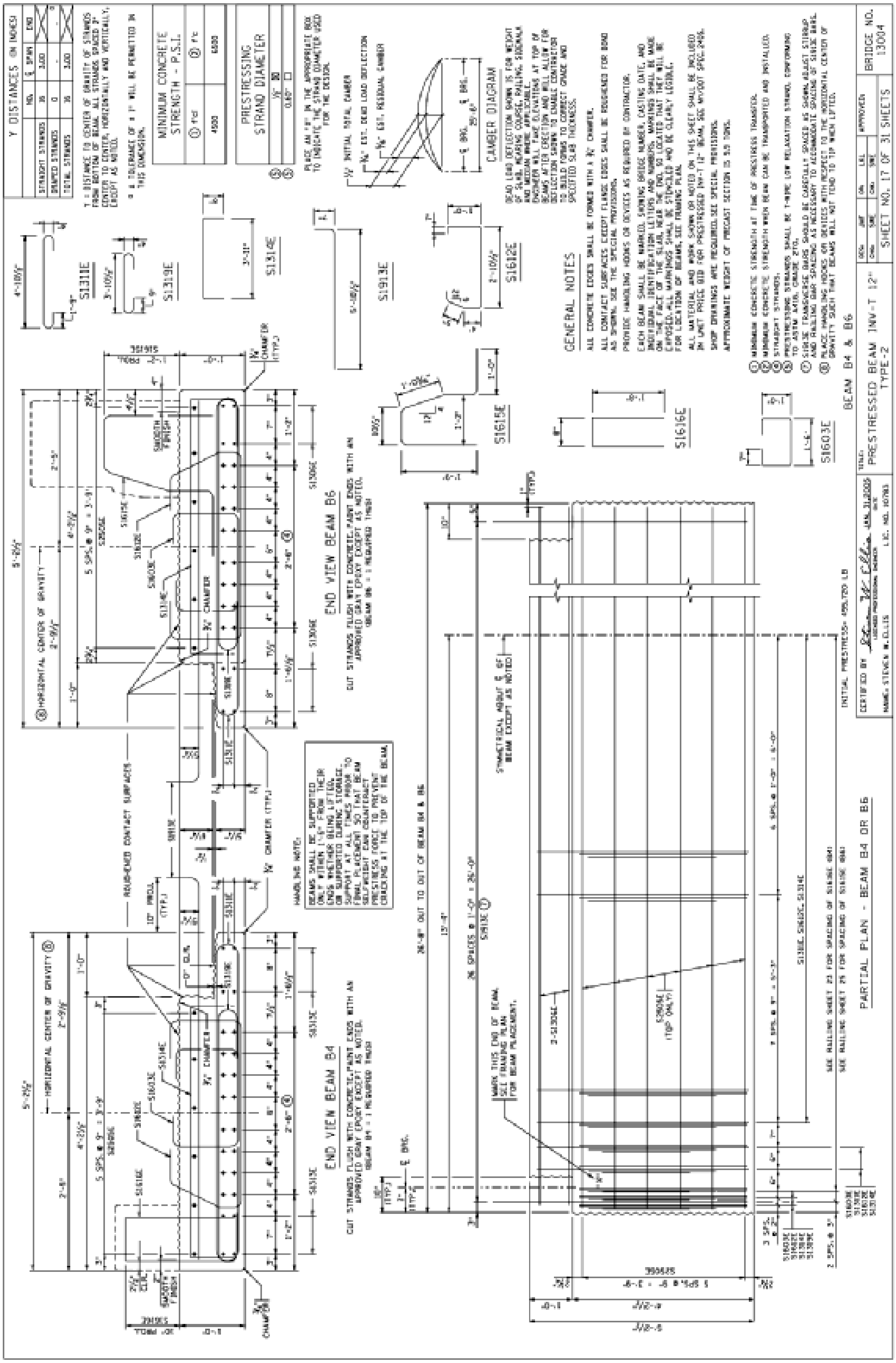

Y DISTANCES (IN INCHES)
MINIMUM CONCRETE STRENGTH - P.S.I.
PRESTRESSING STRAND DIAMETER
CAMBER DIAGRAM
GENERAL NOTES
END VIEW BEAM B6
END VIEW BEAM B4
HANDLING NOTE:
PARTIAL PLAN - BEAM B4 OR B6
BEAM B4 & B6
PRESTRESSED BEAM INV-T 12" TYPE-2
BRIDGE NO. 13004
SHEET NO. 17 OF 31 SHEETS

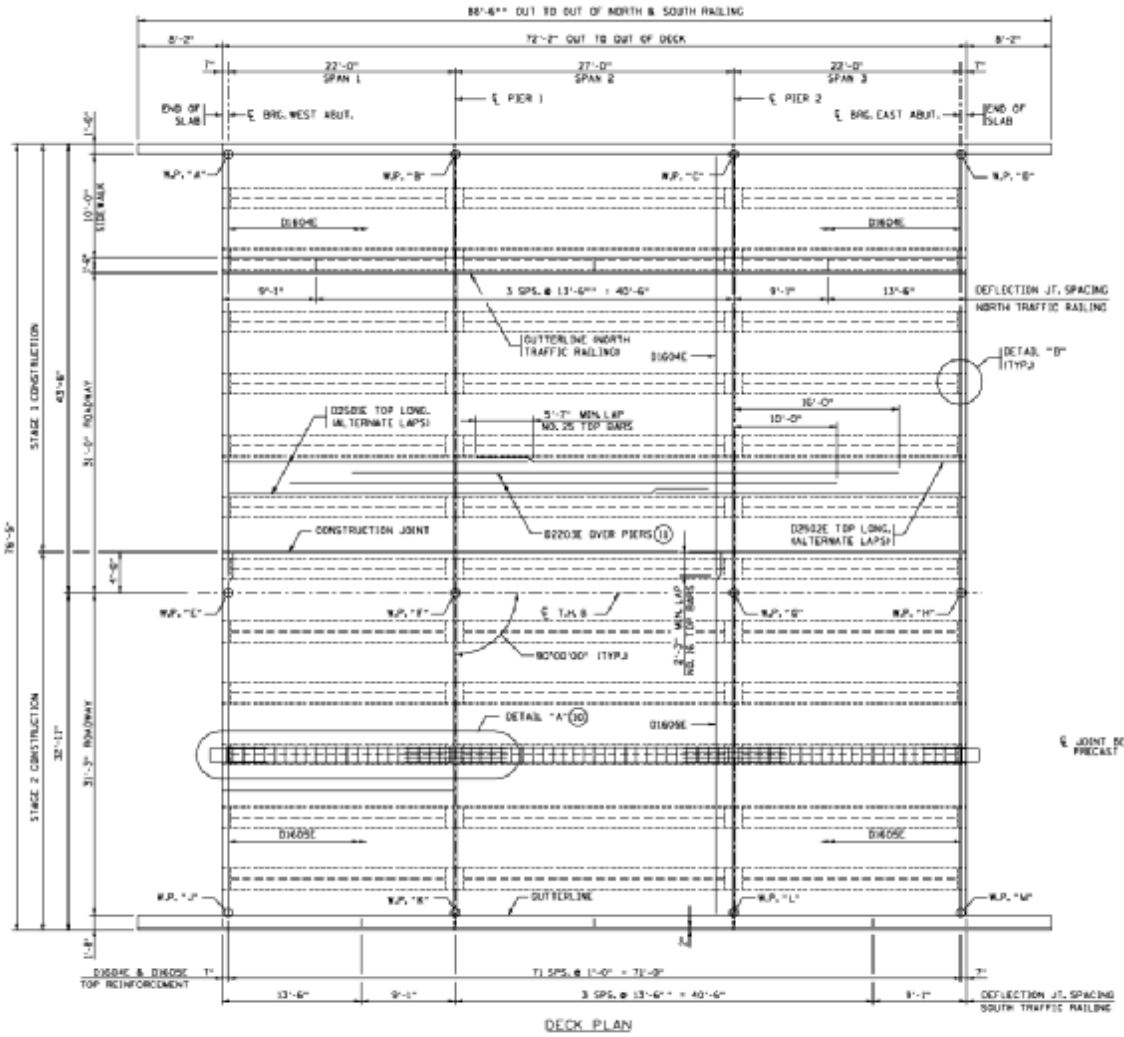

DECK PLAN

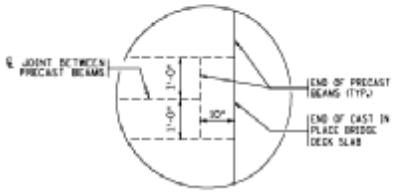

DETAIL "B"

SUMMARY OF QUANTITIES FOR SUPERSTRUCTURE

①	BRIDGE SLAB (CONCRETE (3)(3)4F)	5515 SQ.FT.
②	TYPE P-2 RAILING CONCRETE (3)4G)	361 LIN.FT.
③	TYPE CURB RAILING CONCRETE (3)4G)	88 LIN.FT.
④	REINFORCEMENT BARS (EPOXY COATED)	51190 POUND
	STRUCTURAL TUBE RAILING, DESIGN T-1	155 LIN.FT.
	ORNAMENTAL METAL RAILING TYPE SPECIAL	89 LIN.FT.
	ELASTOMERIC BEARING PAD TYPE 1	18 EACH
⑦	PRESTRESSED BEAM (NU-T 12" TYPE 1	787 LIN.FT.
⑧	PRESTRESSED BEAM (NU-T 12" TYPE 2	143 LIN.FT.
⑨	BRIDGE DECK PLANING	6615 SQ.FT.
⑤	BENCH MARK DISK	1 UNIT
	1" THICK CORK	25 SQ.FT.
⑥	BRIDGE NAME PLATE	1 UNIT
⑥	1/2" THICK POLYSTYRENE	600 SQ.FT.

① "BRIDGE SLAB CONCRETE (3)(3)4F" VOLUME IS APPROXIMATELY 106 CU. YDS. FOR STAGE 1 CONSTRUCTION & 109 CU. YDS. FOR STAGE 2 CONSTRUCTION.

② "TYPE P-2 RAILING CONCRETE (3)4G" VOLUME IS APPROXIMATELY 22 CU. YDS.

③ "TYPE CURB RAILING CONCRETE (3)4G" VOLUME IS APPROXIMATELY 4 CU. YDS.

④ INCLUDES SLAB AND RAILING REINFORCEMENT.

⑤ STATE WILL FURNISH DISK. BEND PRONGS OUTWARD TO ANCHOR DISK IN CONCRETE. BOTTOM OF DESK TOP TO BE PLACED FLUSH WITH CONCRETE. PAYMENT FOR PLACING TO BE INCLUDED IN PRICE BID FOR OTHER ITEMS.

⑥ TO BE INCLUDED IN PRICE BID FOR OTHER ITEMS.

⑦ "PRESTRESSED BEAM (NU-T 12" TYPE 1" INCLUDES BEAMS DESIGNATED AS B2 & B5.

⑧ "PRESTRESSED BEAM (NU-T 12" TYPE 2" INCLUDES BEAMS DESIGNATED AS B1, B3, B4 & B6.

⑨ INCLUDES 2357 SQ.FT. FOR APPROACH PANELS.

⑩ FOR DETAIL "A" SEE SHEET NO. 21.

⑪ ALTERNATE STAGGER D22G3E AT ABOUT 4' CENTERS BETWEEN D25G3E, D25G2E, TOP LONGITUDINAL REINFORCEMENT. PLACE FULL WIDTH OF DECK.

CERTIFIED BY Steven W. Ellis JAN. 31, 2005
NAME: STEVEN W. ELLIS LIC. NO. 30783

TITLE: SUPERSTRUCTURE DETAILS AND REINFORCEMENT

DES. JMF | DR. LEL | APPROVED
CHK. SWE | CHK. JMF

SHEET NO. 18 OF 31 SHEETS

BRIDGE NO. 13004

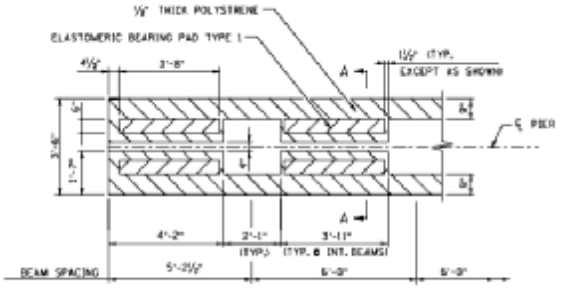

ELASTOMERIC BEARING PAD TYPE 1 AT PIER

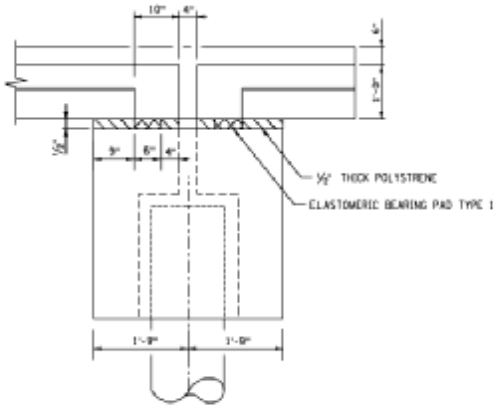

SECTION A-A

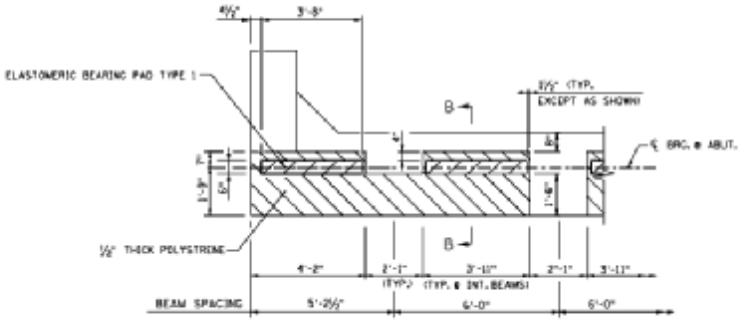

ELASTOMERIC BEARING PAD TYPE 1 AT ABUTMENT

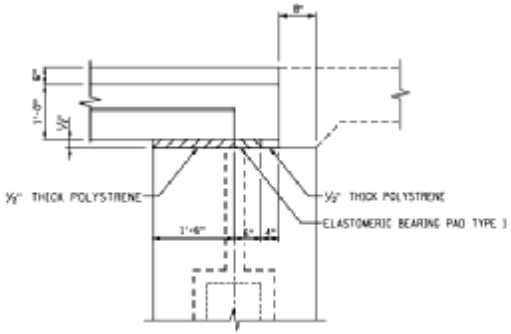

SECTION B-B

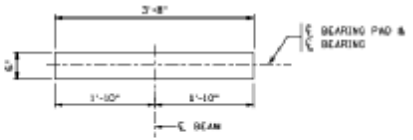

ELASTOMERIC BEARING PAD TYPE 1 PLAN VIEW

(PAD IS ½" THICK PLAIN PAD)

CERTIFIED BY Steven W. Ellis JAN. 31,2005 LICENSED PROFESSIONAL ENGINEER

NAME: STEVEN W. ELLIS LIC. NO. 10783

TITLE: SUPERSTRUCTURE DETAILS

DESIGN JMF DRAWN RJS APPROVED

CHK'D SWE CHK'D MEL

SHEET NO. 19 OF 31 SHEETS

BRIDGE NO. 13004

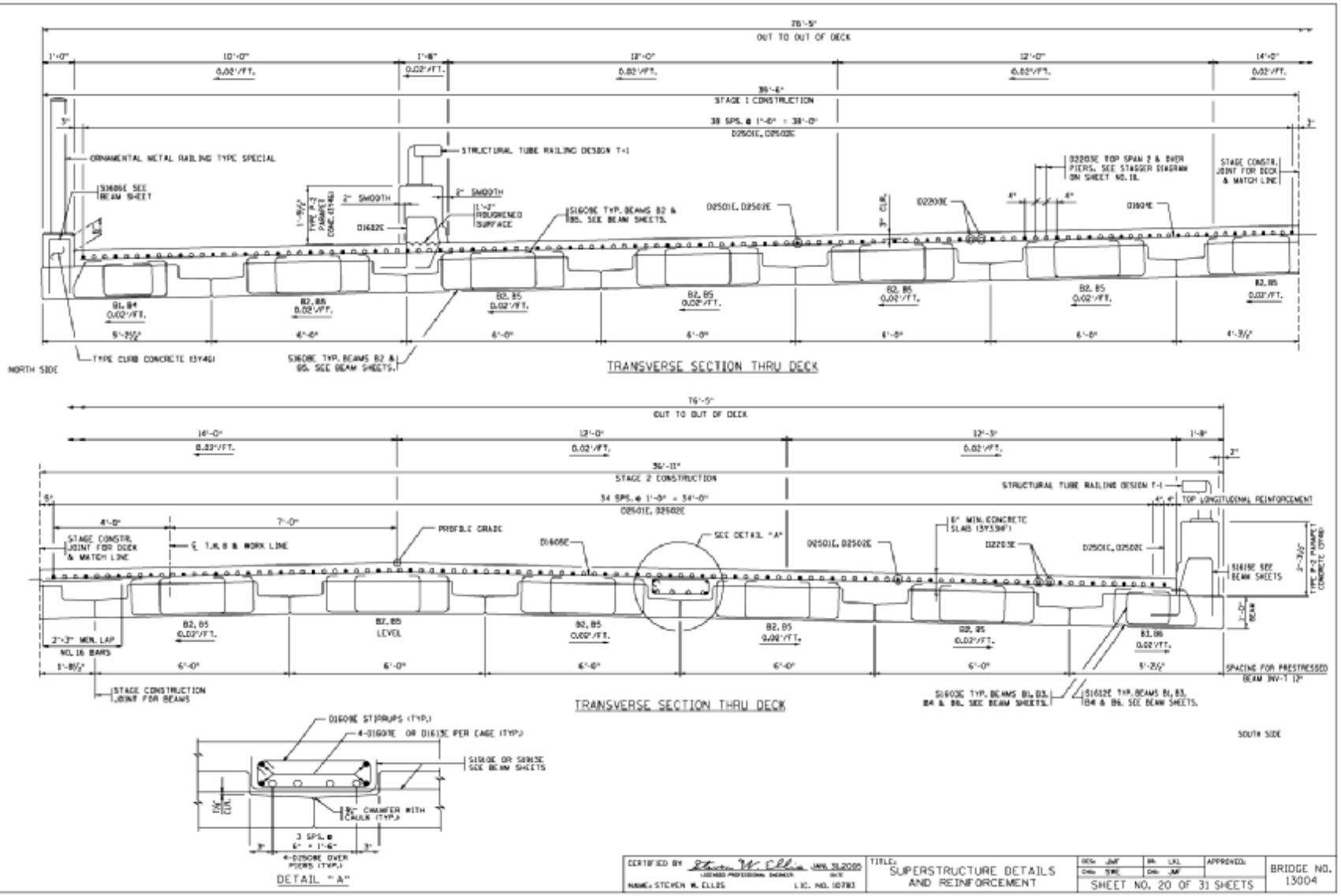

CERTIFIED BY Steven W. Ellis JAN. 15,2015 LICENSED PROFESSIONAL ENGINEER NAME: STEVEN W. ELLIS LIC. NO. 16783	TITLE: SUPERSTRUCTURE DETAILS AND REINFORCEMENT	DES: JMF DWN: TWE CHK: TWE DW: JMF	APPROVED:	BRIDGE NO. 13004
		SHEET NO. 20 OF 31 SHEETS		

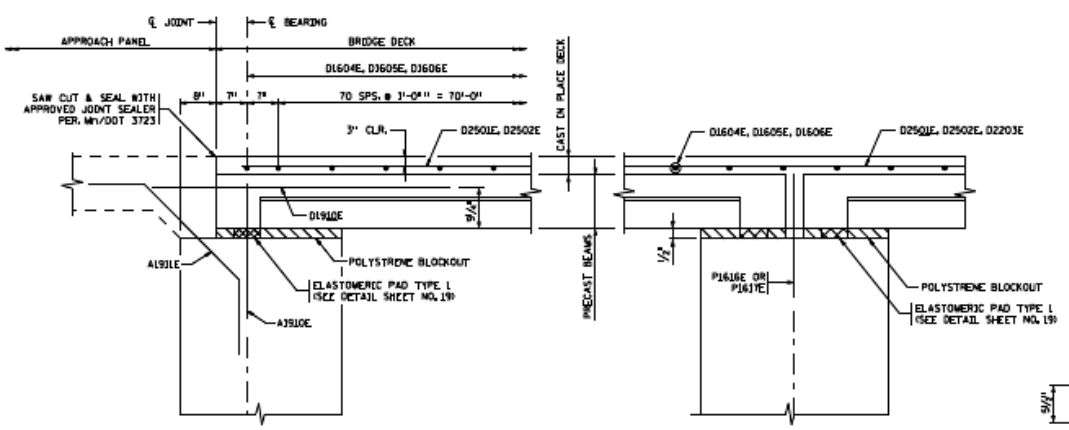

TYP. LONG. SECTION @ ABUTS.

TYP. LONG. SECTION @ PIERS

BILL OF REINFORCEMENT FOR SUPERSTRUCTURE

BAR	NO. FOR STAGE 1 CONSTRUCTION	NO. FOR STAGE 2 CONSTRUCTION	LENGTH	SHAPE	LOCATION
D2501E	39	36	30'-0"	——	DECK TOP LONGITUDINAL
D2502E	39	36	47'-5"	——	DECK TOP LONGITUDINAL
D2203E	74	66	53'-0"	——	DECK TOP LONGIT. OVER PIERS
D1604E	-	72	40'-8"	——	DECK TOP TRANSVERSE
D1605E	72	-	35'-0"	——	DECK TOP TRANSVERSE
D1607E	48	48	21'-11"	——	DECK LONGITUDINAL
D2508E	48	48	20'-0"	——	DECK BOTTOM LONGITUDINAL
D1609E	438	438	5'-2"	▭	DECK TIES
D1910E	12	12	12'-3"	▭	DECK END TIES
D1612E	83	-	4'-6"	⊓	RAIL TIE
D1613E	24	24	26'-9"	——	DECK LONGITUDINAL

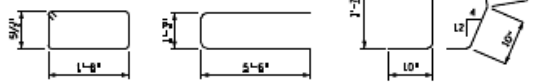

D1609E D1910E D1612E

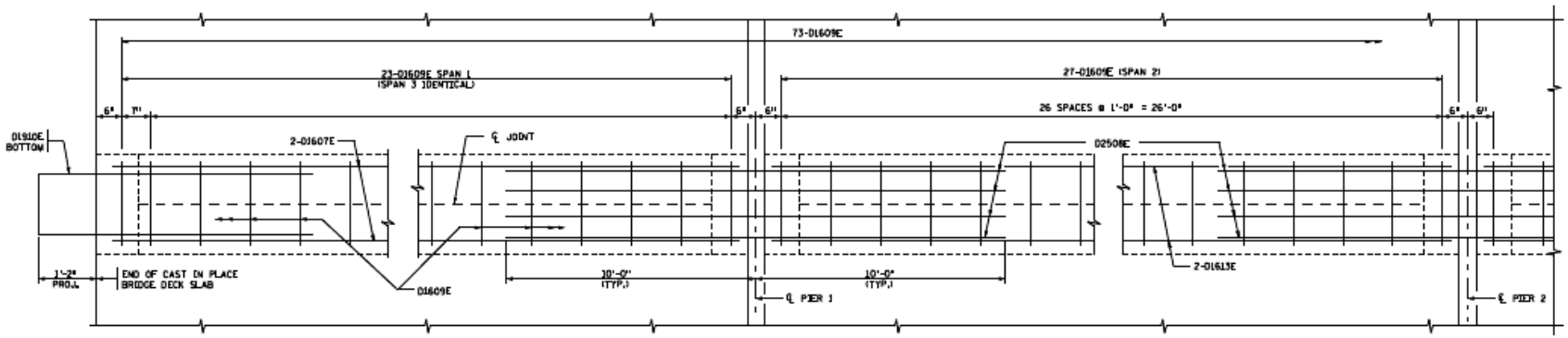

DETAIL "A"

(TYPICAL AT JOINTS BETWEEN BEAMS)

REVISION				
DATE	DESCRIPTION	DR. BY	CHK. BY	APPROVED BY
5-19-05	DIMENSIONS OF BAR D1609E CHANGED	MKL	SWE	SWE

CERTIFIED BY Steven W. Ellis MAY 19, 2005 (LICENSED PROFESSIONAL ENGINEER) (DATE)

NAME: STEVEN W. ELLIS LIC. NO. 30783

TITLE: SUPERSTRUCTURE DETAILS

DES. JWF DR. MA/LKL APPROVED:

CHK. SWE CHK. JWF

SHEET NO. 21B OF 31 SHEETS

BRIDGE NO. 13009

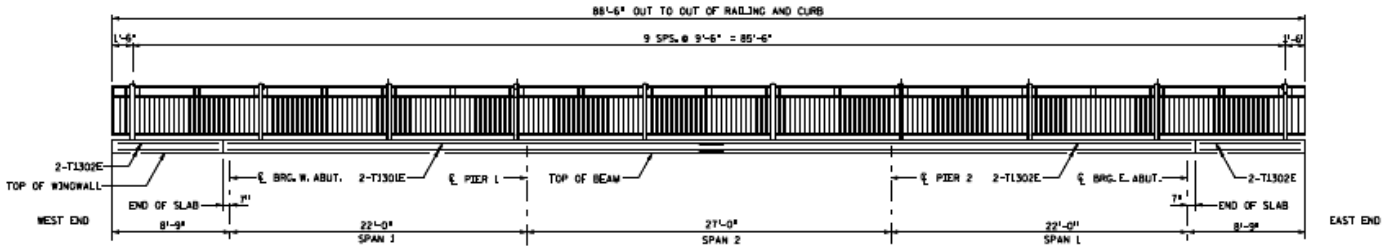

PEDESTRIAN RAILING INSIDE ELEVATION

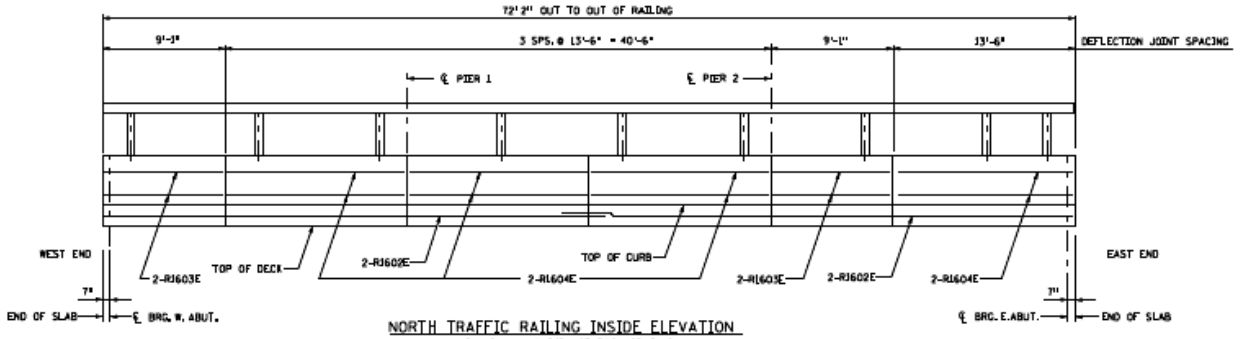

NORTH TRAFFIC RAILING INSIDE ELEVATION
(SEE SHEET NO. 24R FOR POST SPACING.)

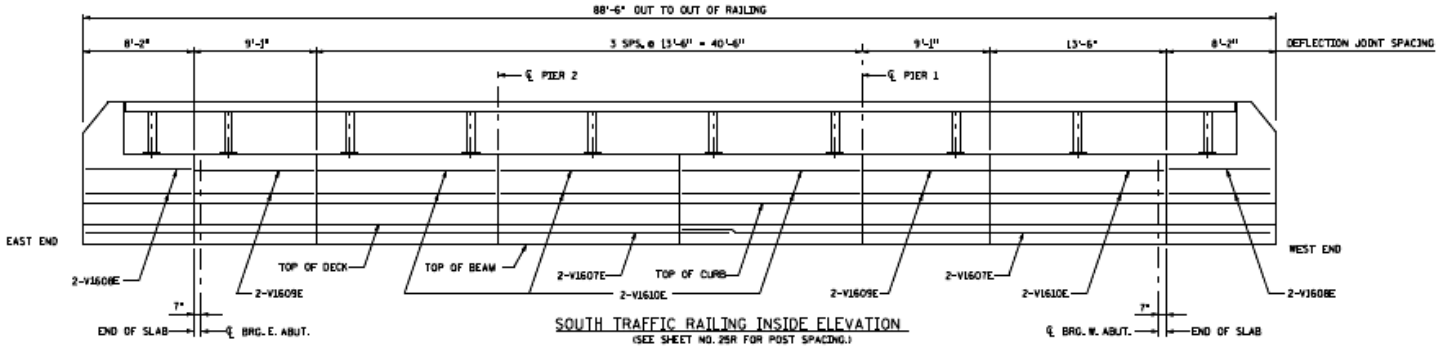

SOUTH TRAFFIC RAILING INSIDE ELEVATION
(SEE SHEET NO. 25R FOR POST SPACING.)

REVISION				
DATE	DESCRIPTION	DR. BY	CHK. BY	APPROVED BY
5-19-05	POST SPACING FOR NORTH & SOUTH RAILINGS REMOVED.	NKL	SWE	SWE

CERTIFIED BY Steven W. Ellis MAY 19, 2005
LICENSED PROFESSIONAL ENGINEER — DATE
NAME: STEVEN W. ELLIS — LIC. NO. 10783

TITLE: SUPERSTRUCTURE DETAILS ---AND REINFORCEMENT---

DES. JWF | DR. LRL/NKL | APPROVED:
CHK. SWE | CHK. NRL/JWF

SHEET NO. 22B OF 31 SHEETS

BRIDGE NO. 13009

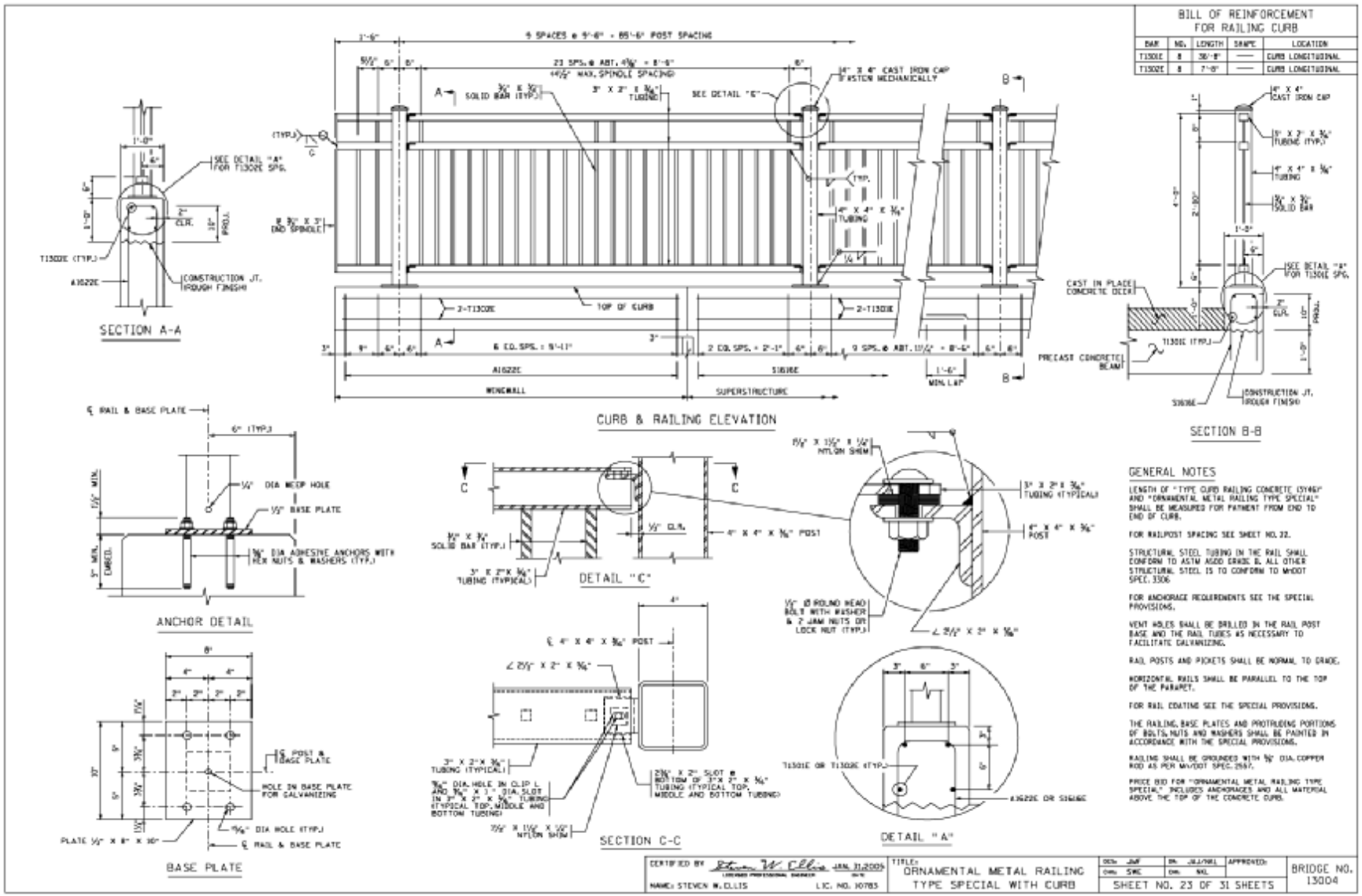
BILL OF REINFORCEMENT FOR RAILING CURB
BAR | NO. | LENGTH | SHAPE | LOCATION
T1301E | 8 | 30'-8" | — | CURB LONGITUDINAL
T1302E | 8 | 7'-8" | — | CURB LONGITUDINAL
5 SPACES @ 9'-6" = 85'-6" POST SPACING
23 SPS. @ ABT. 4'-0" = 8'-6" 44½" MAX. SPINDLE SPACING
SEE DETAIL "B"
SEE DETAIL "A" FOR T1302E SPS.
SECTION A-A
CURB & RAILING ELEVATION
SECTION B-B
SEE DETAIL "B" FOR T1301E SPS.
CAST IN PLACE CONCRETE DECK
PRECAST CONCRETE BEAM
CONSTRUCTION JT. BROOM FINISH
ANCHOR DETAIL
BASE PLATE
DETAIL "C"
SECTION C-C
DETAIL "A"
GENERAL NOTES
LENGTH OF "TYPE CURB RAILING CONCRETE (SY46)" AND "ORNAMENTAL METAL RAILING TYPE SPECIAL" SHALL BE MEASURED FOR PAYMENT FROM END TO END OF CURB.
FOR RAILPOST SPACING SEE SHEET NO. 22.
STRUCTURAL STEEL TUBING IN THE RAIL SHALL CONFORM TO ASTM A500 GRADE B. ALL OTHER STRUCTURAL STEEL IS TO CONFORM TO MDOT SPEC. 3306.
FOR ANCHORAGE REQUIREMENTS SEE THE SPECIAL PROVISIONS.
VENT HOLES SHALL BE DRILLED IN THE RAIL POST BASE AND THE RAIL TUBES AS NECESSARY TO FACILITATE GALVANIZING.
RAIL POSTS AND PICKETS SHALL BE NORMAL TO GRADE.
HORIZONTAL RAILS SHALL BE PARALLEL TO THE TOP OF THE PARAPET.
FOR RAIL COATING SEE THE SPECIAL PROVISIONS.
THE RAILING, BASE PLATES AND PROTRUDING PORTIONS OF BOLTS, NUTS AND WASHERS SHALL BE PAINTED IN ACCORDANCE WITH THE SPECIAL PROVISIONS.
RAILING SHALL BE GROUNDED WITH ⅝" DIA. COPPER ROD AS PER MDOT SPEC. 2557.
PRICE BID FOR "ORNAMENTAL METAL RAILING TYPE SPECIAL" INCLUDES ANCHORAGES AND ALL MATERIAL ABOVE THE TOP OF THE CONCRETE CURB.
CERTIFIED BY Steven W. Ellis JAN. 31 2005
NAME: STEVEN W. ELLIS LIC. NO. 10783
TITLE: ORNAMENTAL METAL RAILING TYPE SPECIAL WITH CURB
DES: JMF DR: JBJ/WEL APPROVED:
CHK: SWE CHK: WEL
SHEET NO. 23 OF 31 SHEETS
BRIDGE NO. 13004

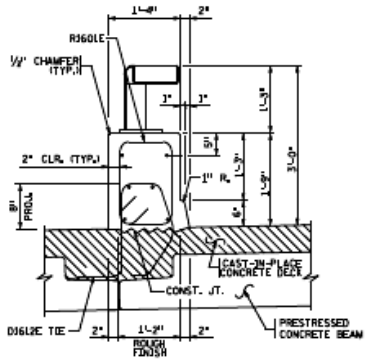

SECTION A-A

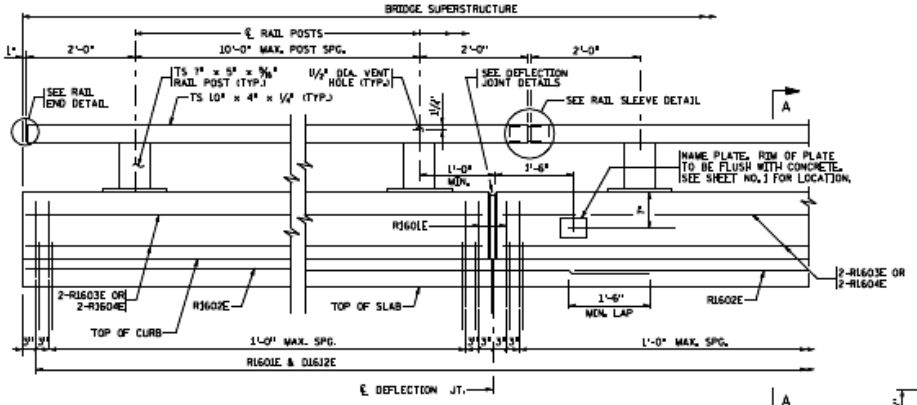

INSIDE ELEVATION OF RAILING

CAST-IN-PLACE CONCRETE DECK NOT SHOWN

RAIL MEETS TEST LEVEL 4 REQUIREMENTS OF NCHRP REPORT 350.

R1601E

BILL OF REINFORCEMENT FOR PARAPET				
BAR	NO.	LENGTH	SHAPE	LOCATION
R1601E	92	5'-8"		VERTICAL TIE
R1602E	4	36'-8"		LONGITUDINAL
R1603E	8	8'-8"		LONGITUDINAL
R1604E	16	13'-1"		LONGITUDINAL

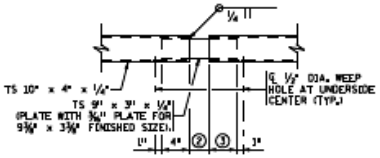

RAIL SLEEVE DETAIL

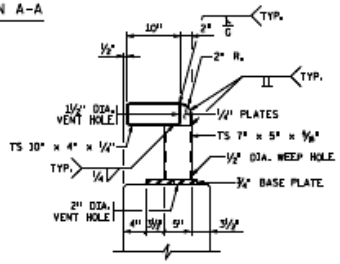

STRUCTURAL TUBE RAIL DETAIL

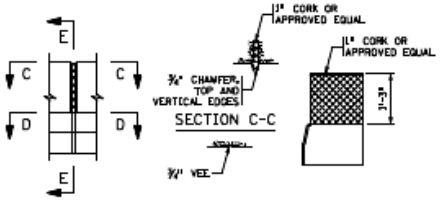

ELEVATION SECTION D-D SECTION E-E

DEFLECTION JOINT DETAILS

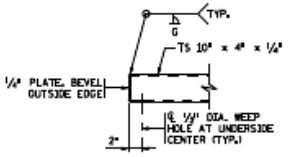

RAIL END DETAIL

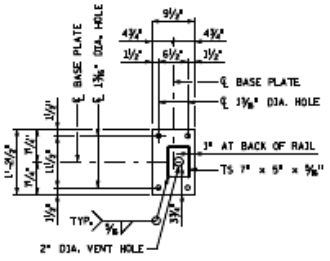

BASE PLATE

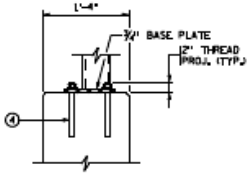

ANCHOR DETAIL

GENERAL NOTES

LENGTH OF "TYPE P-2 RAILING CONCRETE (3Y46)" FOR PAYMENT SHALL BE MEASURED BETWEEN THE OUTSIDE FACES OF THE CONCRETE PARAPET.

LENGTH OF "STRUCTURAL TUBE RAILING, DESIGN T-1" FOR PAYMENT SHALL BE MEASURED FROM END TO END OF TUBING WITH NO DEDUCTION FOR JOINTS.

CONCRETE PARAPET = 359 LBS./FT. 10.09 CU YDS./FT.)

FINISH ALL EDGES OF RAIL WITH 1/2" VEE, EXCEPT WHERE OTHERWISE NOTED.

MAX. SPACING OF CONCRETE DEFLECTION JOINTS SHALL BE 20 FT.

SEE SUPERSTRUCTURE SHEET FOR JOINT SPACING.

ANCHORAGES SHALL BE ACCURATELY PLACED AND SUPPORTED TO PROVIDE CORRECT ALIGNMENT OF RAILING NORMAL TO GRADE.

STRUCTURAL STEEL PER Wm/DOT SPEC. 3309. STRUCTURAL TUBES ARE A.S.T.M. A500, GRADE B PER Wm/DOT SPEC. 3362.

GALVANIZE BOLTS, NUTS, AND WASHERS PER Wm/DOT SPEC. 3392.

GALVANIZE ALL OTHER STRUCTURAL STEEL PER Wm/DOT SPEC. 3394 AFTER FABRICATION.

PRICE BID FOR "STRUCTURAL TUBE RAILING, DESIGN T-1" INCLUDES ANCHORAGES AND ALL MATERIAL ABOVE TOP OF CONCRETE PARAPET.

ALL MATERIAL IN THE CONCRETE PARAPET IS INCLUDED IN SUMMARY OF QUANTITIES FOR SUPERSTRUCTURE.

SEE SPECIAL PROVISIONS FOR PAINT REQUIREMENTS.

(2) 1" AT DEFLECTION JOINTS.

(3) 4" AT DEFLECTION JOINTS.

(4) 3/4" DIA. CHEMICAL ANCHOR RODS, Wm/DOT SPEC. 3385, TYPE C, WITH HEX NUTS AND WASHERS. MINIMUM ULTIMATE BOND STRENGTH SHALL BE 46,600 POUNDS, WITH A MINIMUM 9" EMBEDMENT LENGTH. SEE SPECIAL PROVISIONS.

NORTH TRAFFIC RAIL

(MODIFIED)

FIG. 5-397.157

REVISED: _

APPROVED: DECEMBER 18, 2003

STATE BRIDGE ENGINEER

REVISION				
DATE	DESCRIPTION	DR. BY	CHK. BY	APPROVED BY
5-19-05	POST SPACING AT SLEEVES ALTERED.	NBL	SWE	SWE

CERTIFIED BY Steven W. Ellis LICENSED PROFESSIONAL ENGINEER MAY 19, 2005 DATE

NAME: STEVEN W. ELLIS LIC. NO. 10783

TITLE: STRUCTURAL TUBE RAILING (DESIGN T-1) AND CONCRETE PARAPET (TYPE P-2)

DES. JWF CK. LKL

DR. SWE CH. NBL

APPROVED:

SHEET NO. 248 OF 31 SHEETS

BRIDGE NO. 13009

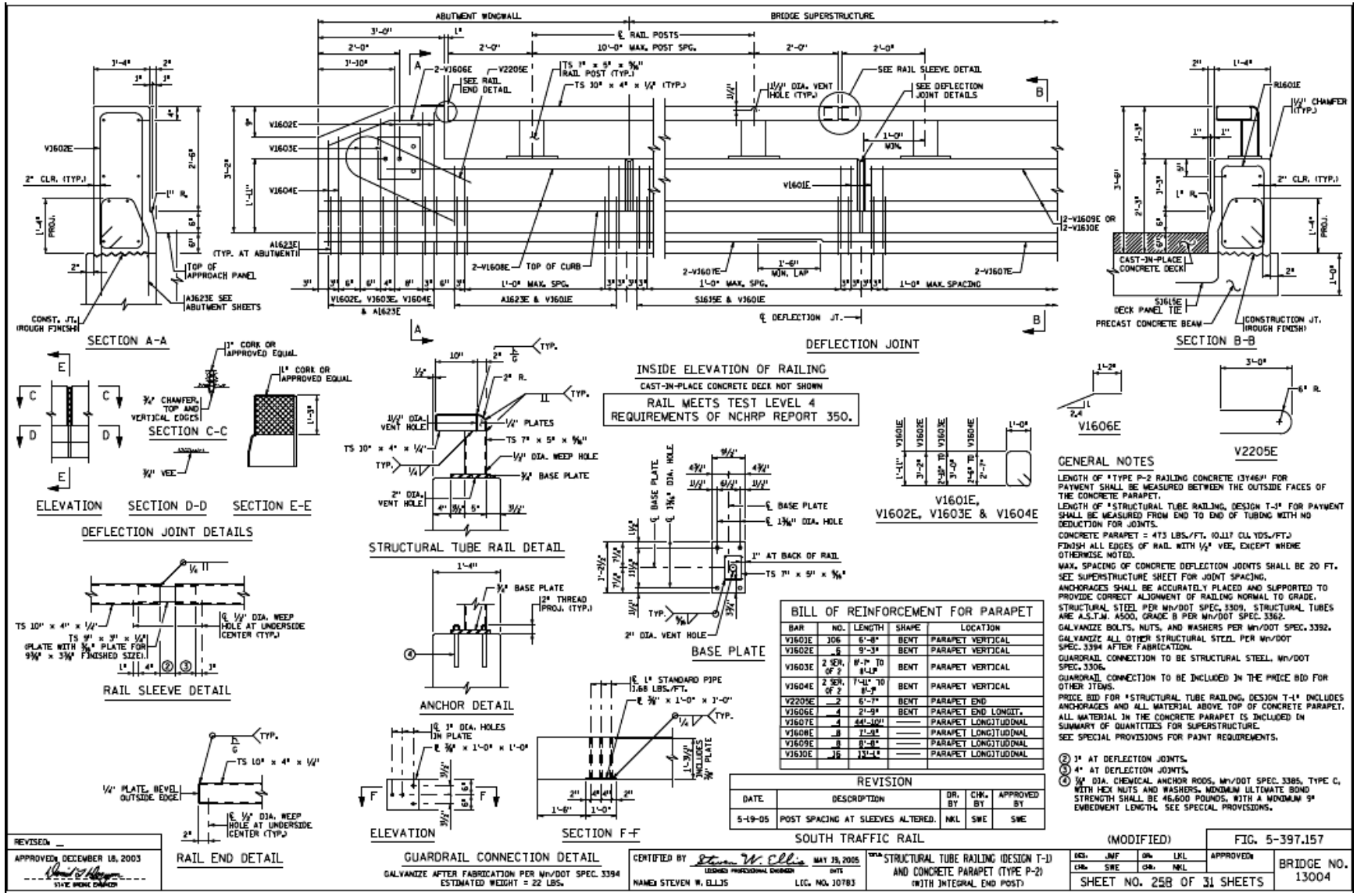

GENERAL NOTES

LENGTH OF "TYPE P-2 RAILING CONCRETE (3Y46)" FOR PAYMENT SHALL BE MEASURED BETWEEN THE OUTSIDE FACES OF THE CONCRETE PARAPET.

LENGTH OF "STRUCTURAL TUBE RAILING, DESIGN T-1" FOR PAYMENT SHALL BE MEASURED FROM END TO END OF TUBING WITH NO DEDUCTION FOR JOINTS.

CONCRETE PARAPET = 473 LBS./FT. (0.117 CU. YDS./FT.)

FINISH ALL EDGES OF RAIL WITH ½" VEE, EXCEPT WHERE OTHERWISE NOTED.

MAX. SPACING OF CONCRETE DEFLECTION JOINTS SHALL BE 20 FT.

SEE SUPERSTRUCTURE SHEET FOR JOINT SPACING.

ANCHORAGES SHALL BE ACCURATELY PLACED AND SUPPORTED TO PROVIDE CORRECT ALIGNMENT OF RAILING NORMAL TO GRADE.

STRUCTURAL STEEL PER Wn/DOT SPEC. 9309. STRUCTURAL TUBES ARE A.S.T.M. A500, GRADE B PER Wn/DOT SPEC. 9362.

GALVANIZE BOLTS, NUTS, AND WASHERS PER Wn/DOT SPEC. 9392.

GALVANIZE ALL OTHER STRUCTURAL STEEL PER Wn/DOT SPEC. 3394 AFTER FABRICATION.

GUARDRAIL CONNECTION TO BE STRUCTURAL STEEL, Wn/DOT SPEC. 3306.

GUARDRAIL CONNECTION TO BE INCLUDED IN THE PRICE BID FOR OTHER ITEMS.

PRICE BID FOR "STRUCTURAL TUBE RAILING, DESIGN T-1" INCLUDES ANCHORAGES AND ALL MATERIAL ABOVE TOP OF CONCRETE PARAPET. ALL MATERIAL IN THE CONCRETE PARAPET IS INCLUDED IN SUMMARY OF QUANTITIES FOR SUPERSTRUCTURE.

SEE SPECIAL PROVISIONS FOR PAINT REQUIREMENTS.

② 1" AT DEFLECTION JOINTS.
③ 4" AT DEFLECTION JOINTS.
④ ⅝" DIA. CHEMICAL ANCHOR RODS, Wn/DOT SPEC. 9385, TYPE C, WITH HEX NUTS AND WASHERS. MINIMUM ULTIMATE BOND STRENGTH SHALL BE 46,600 POUNDS, WITH A MINIMUM 9" EMBEDMENT LENGTH. SEE SPECIAL PROVISIONS.

BILL OF REINFORCEMENT FOR PARAPET

BAR	NO.	LENGTH	SHAPE	LOCATION
V1601E	106	6'-8"	BENT	PARAPET VERTICAL
V1602E	6	9'-3"	BENT	PARAPET VERTICAL
V1603E	2 SER. OF 7	8'-7" TO 8'-11"	BENT	PARAPET VERTICAL
V1604E	2 SER. OF 7	7'-11" TO 8'-3"	BENT	PARAPET VERTICAL
V2205E	2	6'-7"	BENT	PARAPET END
V1606E	4	2'-9"	BENT	PARAPET END LONGIT.
V1607E	4	44'-10½"	——	PARAPET LONGITUDINAL
V1608E	8	7'-0"	——	PARAPET LONGITUDINAL
V1609E	8	8'-8"	——	PARAPET LONGITUDINAL
V1610E	16	13'-1"	——	PARAPET LONGITUDINAL

REVISION

DATE	DESCRIPTION	DR. BY	CHK. BY	APPROVED BY
5-19-05	POST SPACING AT SLEEVES ALTERED.	NKL	SWE	SWE

SOUTH TRAFFIC RAIL

REVISED: —

APPROVED: DECEMBER 18, 2003

STATE BRIDGE ENGINEER

CERTIFIED BY Steven W. Ellis MAY 19, 2005
LICENSED PROFESSIONAL ENGINEER — DATE

NAME: STEVEN W. ELLIS LIC. NO. 10783

TITLE: STRUCTURAL TUBE RAILING (DESIGN T-1) AND CONCRETE PARAPET (TYPE P-2) (WITH INTEGRAL END POST) (MODIFIED)

FIG. 5-397.157

DES. JWF CK. SWE DR. LKL CHK. NKL

APPROVED:

BRIDGE NO. 13004

SHEET NO. 258 OF 31 SHEETS

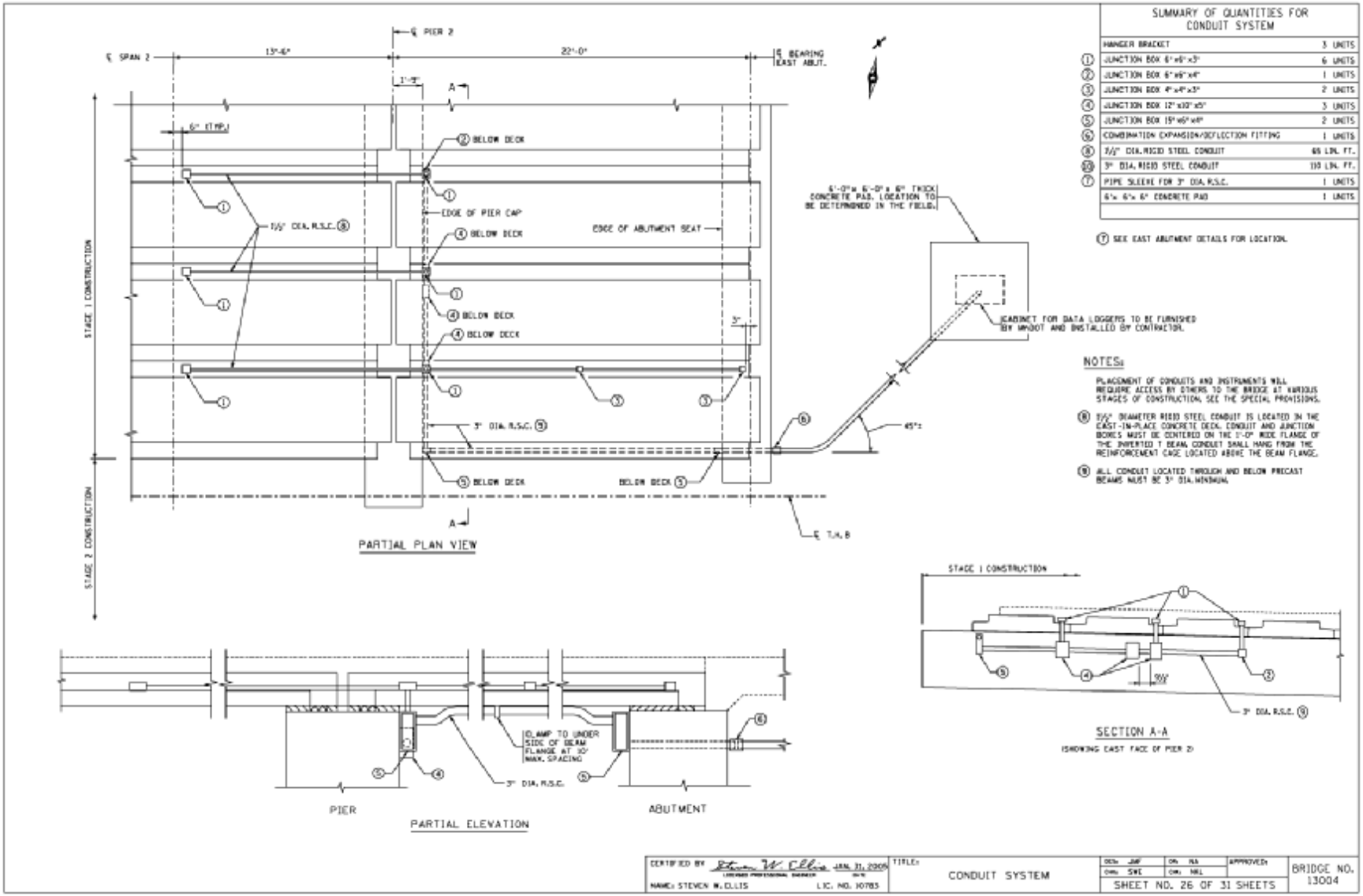

SUMMARY OF QUANTITIES FOR CONDUIT SYSTEM	
HANGER BRACKET	3 UNITS
① JUNCTION BOX 6"x6"x3"	6 UNITS
② JUNCTION BOX 6"x6"x4"	1 UNITS
③ JUNCTION BOX 4"x4"x3"	2 UNITS
④ JUNCTION BOX 12"x10"x5"	3 UNITS
⑤ JUNCTION BOX 15"x6"x4"	2 UNITS
⑥ COMBINATION EXPANSION/DEFLECTION FITTING	1 UNITS
⑧ 1½" DIA. RIGID STEEL CONDUIT	65 LIN. FT.
⑨ 3" DIA. RIGID STEEL CONDUIT	110 LIN. FT.
⑦ PIPE SLEEVE FOR 3" DIA. R.S.C.	1 UNITS
6'-6"x 6'-6" x 6" CONCRETE PAD	1 UNITS

⑦ SEE EAST ABUTMENT DETAILS FOR LOCATION.

CERTIFIED BY Steven W. Ellis JAN. 31, 2005
NAME: STEVEN W. ELLIS LIC. NO. 10785

TITLE: CONDUIT SYSTEM

DES: JMF DR: WA CHK: SWE CHK: NEL APPROVED:

SHEET NO. 26 OF 31 SHEETS

BRIDGE NO. 13004

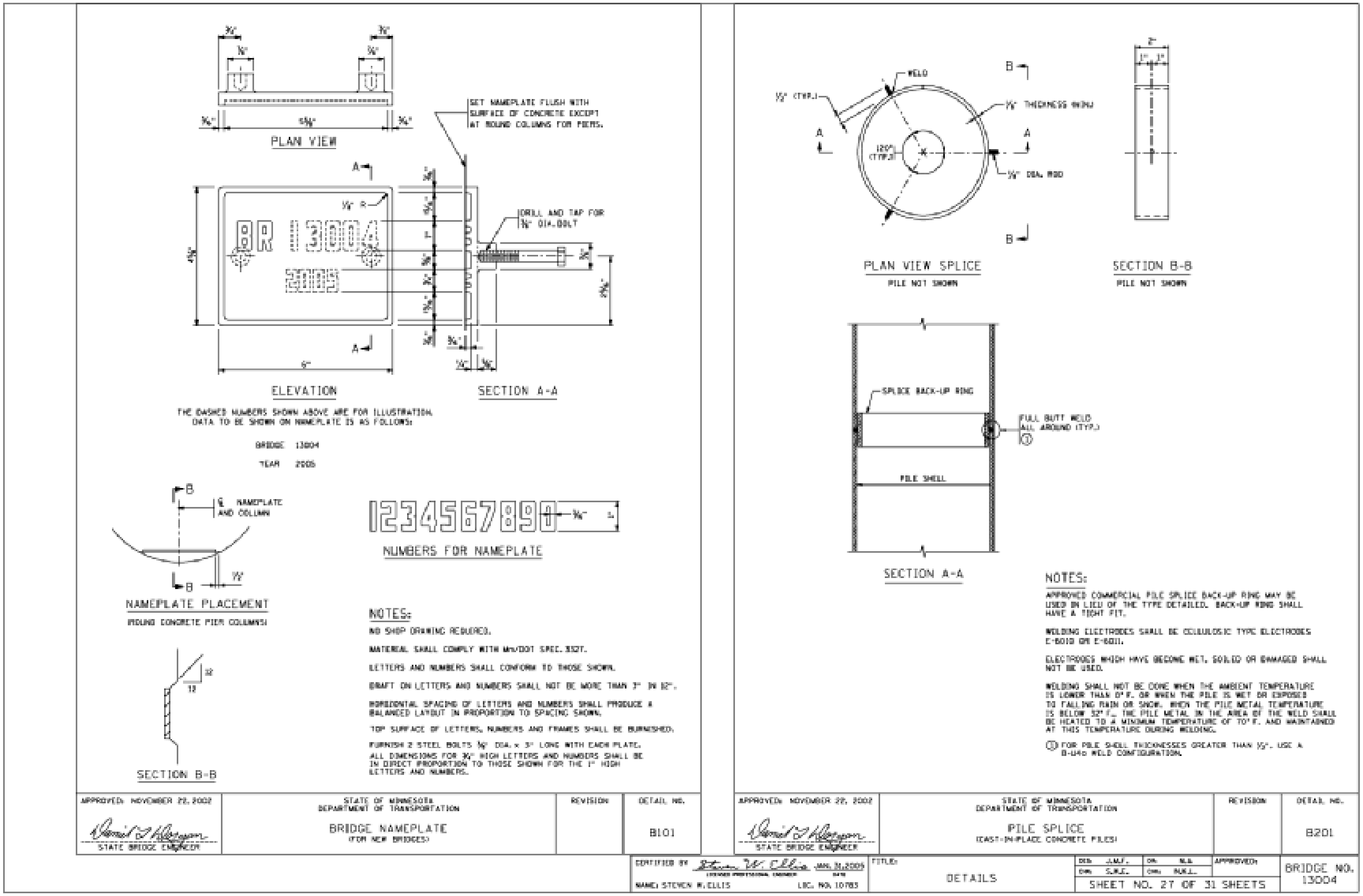
PLAN VIEW
SET NAMEPLATE FLUSH WITH SURFACE OF CONCRETE EXCEPT AT ROUND COLUMNS FOR PIERS.
DRILL AND TAP FOR DIA. BOLT
BR 13004
2005
ELEVATION
SECTION A-A
THE DASHED NUMBERS SHOWN ABOVE ARE FOR ILLUSTRATION. DATA TO BE SHOWN ON NAMEPLATE IS AS FOLLOWS:
BRIDGE 13004
YEAR 2005
NAMEPLATE AND COLUMN
NAMEPLATE PLACEMENT
(ROUND CONCRETE PIER COLUMNS)
1234567890
NUMBERS FOR NAMEPLATE
SECTION B-B
NOTES:
NO SHOP DRAWING REQUIRED.
MATERIAL SHALL COMPLY WITH Mn/DOT SPEC. 3327.
LETTERS AND NUMBERS SHALL CONFORM TO THOSE SHOWN.
DRAFT ON LETTERS AND NUMBERS SHALL NOT BE MORE THAN 1" IN 12".
HORIZONTAL SPACING OF LETTERS AND NUMBERS SHALL PRODUCE A BALANCED LAYOUT IN PROPORTION TO SPACING SHOWN.
TOP SURFACE OF LETTERS, NUMBERS AND FRAMES SHALL BE BURNISHED.
FURNISH 2 STEEL BOLTS DIA. x 3" LONG WITH EACH PLATE.
ALL DIMENSIONS FOR HIGH LETTERS AND NUMBERS SHALL BE IN DIRECT PROPORTION TO THOSE SHOWN FOR THE 1" HIGH LETTERS AND NUMBERS.
APPROVED: NOVEMBER 22, 2002
STATE BRIDGE ENGINEER
STATE OF MINNESOTA
DEPARTMENT OF TRANSPORTATION
BRIDGE NAMEPLATE
(FOR NEW BRIDGES)
REVISION
DETAIL NO.
B101
WELD
(TYP.)
THICKNESS (MIN.)
120° (TYP.)
DIA. ROD
PLAN VIEW SPLICE
PILE NOT SHOWN
SECTION B-B
PILE NOT SHOWN
SPLICE BACK-UP RING
FULL BUTT WELD ALL AROUND (TYP.)
PILE SHELL
SECTION A-A
NOTES:
APPROVED COMMERCIAL PILE SPLICE BACK-UP RING MAY BE USED IN LIEU OF THE TYPE DETAILED. BACK-UP RING SHALL HAVE A TIGHT FIT.
WELDING ELECTRODES SHALL BE CELLULOSIC TYPE ELECTRODES E-6010 OR E-6011.
ELECTRODES WHICH HAVE BECOME WET, SOILED OR DAMAGED SHALL NOT BE USED.
WELDING SHALL NOT BE DONE WHEN THE AMBIENT TEMPERATURE IS LOWER THAN 0° F. OR WHEN THE PILE IS WET OR EXPOSED TO FALLING RAIN OR SNOW. WHEN THE PILE METAL TEMPERATURE IS BELOW 32° F., THE PILE METAL IN THE AREA OF THE WELD SHALL BE HEATED TO A MINIMUM TEMPERATURE OF 70° F. AND MAINTAINED AT THIS TEMPERATURE DURING WELDING.
(1) FOR PILE SHELL THICKNESSES GREATER THAN , USE A B-U4b WELD CONFIGURATION.
APPROVED: NOVEMBER 22, 2002
STATE BRIDGE ENGINEER
STATE OF MINNESOTA
DEPARTMENT OF TRANSPORTATION
PILE SPLICE
(CAST-IN-PLACE CONCRETE PILES)
REVISION
DETAIL NO.
B201
CERTIFIED BY Steven W. Ellis JAN. 31, 2005
LICENSED PROFESSIONAL ENGINEER DATE
NAME: STEVEN W. ELLIS LIC. NO. 10783
TITLE:
DETAILS
APPROVED:
SHEET NO. 27 OF 31 SHEETS
BRIDGE NO. 13004

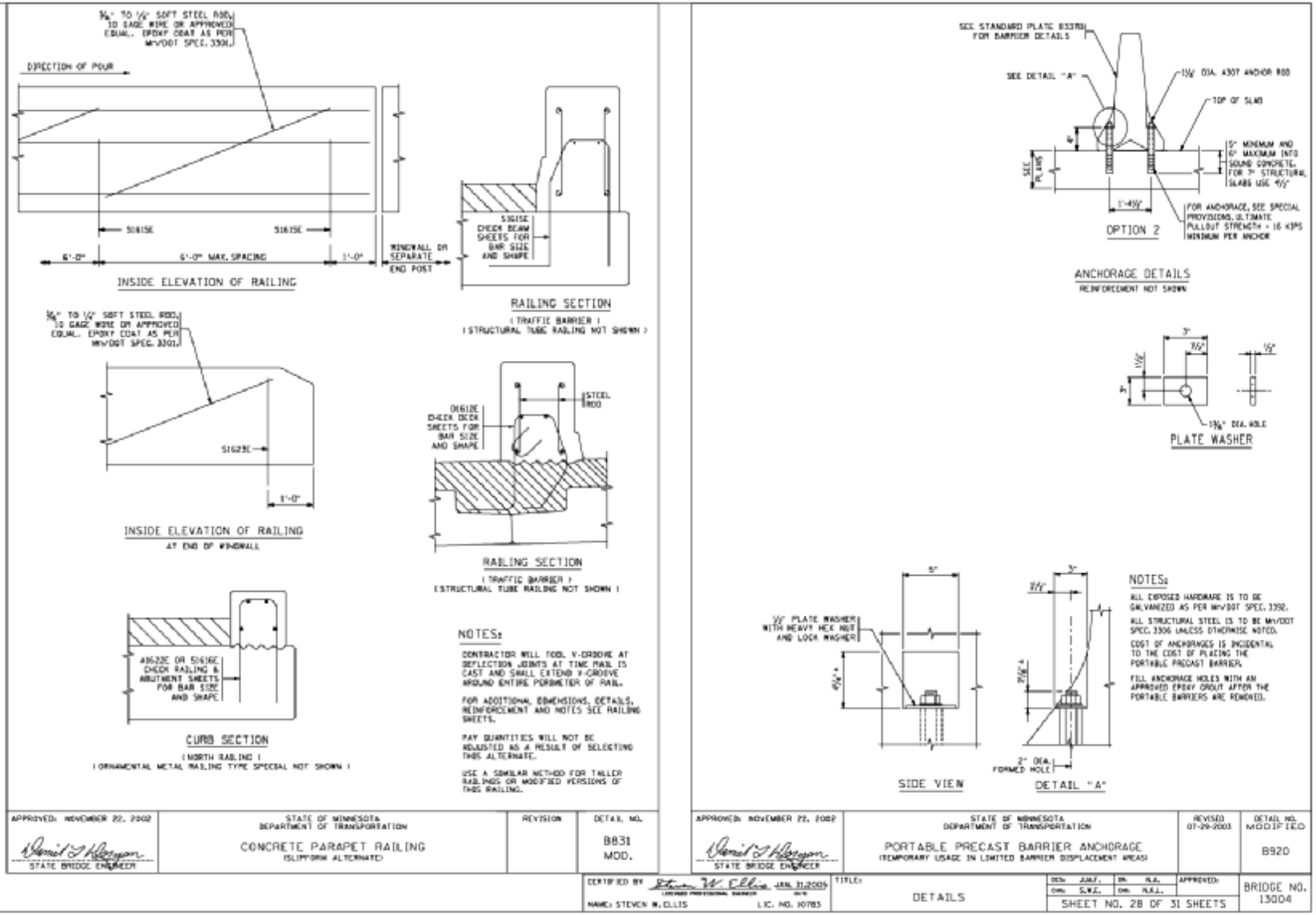
3/8" TO 1/2" SOFT STEEL ROD, 10 GAGE WIRE OR APPROVED EQUAL. EPOXY COAT AS PER MnDOT SPEC. 3301.
DIRECTION OF POUR
S1615E
S1615E
6'-0"
6'-0" MAX. SPACING
1'-0"
WINGWALL OR SEPARATE END POST
INSIDE ELEVATION OF RAILING
S1615E CHECK BEAM SHEETS FOR BAR SIZE AND SHAPE
RAILING SECTION
(TRAFFIC BARRIER)
(STRUCTURAL TUBE RAILING NOT SHOWN)
3/8" TO 1/2" SOFT STEEL ROD, 10 GAGE WIRE OR APPROVED EQUAL. EPOXY COAT AS PER MnDOT SPEC. 3301.
S1629E
1'-0"
INSIDE ELEVATION OF RAILING
AT END OF WINGWALL
STEEL ROD
D1612E CHECK DECK SHEETS FOR BAR SIZE AND SHAPE
RAILING SECTION
(TRAFFIC BARRIER)
(STRUCTURAL TUBE RAILING NOT SHOWN)
A1622E OR S1616E CHECK RAILING & ABUTMENT SHEETS FOR BAR SIZE AND SHAPE
CURB SECTION
(NORTH RAILING)
(ORNAMENTAL METAL RAILING TYPE SPECIAL NOT SHOWN)
NOTES:
CONTRACTOR WILL TOOL V-GROOVE AT DEFLECTION JOINTS AT TIME RAIL IS CAST AND SHALL EXTEND V-GROOVE AROUND ENTIRE PERIMETER OF RAIL.
FOR ADDITIONAL DIMENSIONS, DETAILS, REINFORCEMENT AND NOTES SEE RAILING SHEETS.
PAY QUANTITIES WILL NOT BE ADJUSTED AS A RESULT OF SELECTING THIS ALTERNATE.
USE A SIMILAR METHOD FOR TALLER RAILINGS OR MODIFIED VERSIONS OF THIS RAILING.
APPROVED: NOVEMBER 22, 2002
STATE BRIDGE ENGINEER
STATE OF MINNESOTA
DEPARTMENT OF TRANSPORTATION
CONCRETE PARAPET RAILING
(SLIPFORM ALTERNATE)
REVISION
DETAIL NO.
B831
MOD.
SEE STANDARD PLATE B337(1) FOR BARRIER DETAILS
SEE DETAIL "A"
1½" DIA. A307 ANCHOR ROD
TOP OF SLAB
4"
SEE PLANS
5" MINIMUM AND 6" MAXIMUM INTO SOUND CONCRETE. FOR 7" STRUCTURAL SLABS USE 4½"
1'-4½"
FOR ANCHORAGE, SEE SPECIAL PROVISIONS. ULTIMATE PULLOUT STRENGTH = 16 KIPS MINIMUM PER ANCHOR
OPTION 2
ANCHORAGE DETAILS
REINFORCEMENT NOT SHOWN
3"
3½"
1½"
3"
½"
1⅜" DIA. HOLE
PLATE WASHER
5"
¾" PLATE WASHER WITH HEAVY HEX NUT AND LOCK WASHER
4½"
3"
3½"
3½"
2" DIA. FORMED HOLE
SIDE VIEW
DETAIL "A"
NOTES:
ALL EXPOSED HARDWARE IS TO BE GALVANIZED AS PER MnDOT SPEC. 3392.
ALL STRUCTURAL STEEL IS TO BE MnDOT SPEC. 3306 UNLESS OTHERWISE NOTED.
COST OF ANCHORAGES IS INCIDENTAL TO THE COST OF PLACING THE PORTABLE PRECAST BARRIER.
FILL ANCHORAGE HOLES WITH AN APPROVED EPOXY GROUT AFTER THE PORTABLE BARRIERS ARE REMOVED.
APPROVED: NOVEMBER 22, 2002
STATE BRIDGE ENGINEER
STATE OF MINNESOTA
DEPARTMENT OF TRANSPORTATION
PORTABLE PRECAST BARRIER ANCHORAGE
(TEMPORARY USAGE IN LIMITED BARRIER DISPLACEMENT AREAS)
REVISED 07-29-2003
DETAIL NO. MODIFIED
B920
CERTIFIED BY Steven W. Ellis JAN. 31, 2005
NAME: STEVEN W. ELLIS
LIC. NO. 10783
TITLE:
DETAILS
DES: JJM/. DR: R.L.L.
CHK: S.W.E. CHK: R.L.L.
APPROVED:
SHEET NO. 28 OF 31 SHEETS
BRIDGE NO. 13004

CONCRETE OVERLAY

☐ LOW SLUMP

☐ OTHER _____
TYPE OR MANUFACTURER

EXPANSION JOINTS

JOINT MANUFACTURER _____
NAME AND ADDRESS (CITY, STATE)

MANUFACTURER'S IDENTIFICATION _____
MFR'S No. AND/OR LETTER DESIGNATION FOR JOINT USED

GLAND MANUFACTURER _____
NAME AND ADDRESS (CITY, STATE)

SIZE OF GLAND _____

MANUFACTURER'S IDENTIFICATION _____
MFR'S No. AND/OR LETTER DESIGNATION FOR GLAND USED

BEARING PADS

NEOPRENE PAD MANUFACTURER _____
NAME AND ADDRESS (CITY, STATE)

SPECIAL SURFACE TREATMENT

TYPE: _____ COLOR: _____

FINISHING ROADWAY FACES OF BARRIER RAILING

TYPE: _____ COLOR: _____

ANTI-GRAFFITI COATING

MANUFACTURER _____
NAME AND ADDRESS (CITY, STATE)

PRODUCT NAME: _____ LOCATION: _____

PAINT SYSTEM

Mn/DOT CONSTRUCTION SPECIFICATION NUMBER _____
2478 OR 2478 OR 2479

MANUFACTURER _____
NAME AND ADDRESS (CITY, STATE)

PRIME COAT _____
Mn/DOT MATERIAL SPECIFICATION NUMBER

INTERMEDIATE COAT _____
Mn/DOT MATERIAL SPECIFICATION NUMBER

FINISH COAT _____ _____
Mn/DOT MATERIAL SPECIFICATION NUMBER COLOR

PLAN QUALITY

RATE 1 (AGREE), 2 (NEUTRAL), OR 3 (DISAGREE). PLEASE COMMENT BELOW)

DIMENSIONING AND DETAILING ADEQUATELY DESCRIBED REQUIRED CONSTRUCTION. _____

BAR LISTS AND QUANTITIES WERE TYPICALLY COMPLETE AND FREE OF ERRORS. _____

SCALE OF DRAWINGS AND OVERALL LEGIBILITY OF LINES AND TEXT WAS GOOD. _____

(SB) SPECIAL PROVISIONS ADEQUATELY DESCRIBED SPECIAL WORK AND PAYMENT. _____

COMMENTS: _____

NUMBER OF BRIDGE SUPPLEMENTAL AGREEMENTS: _____ COST: $ _____

LIST SIGNIFICANT ERRORS OR OMISSIONS IN PLAN DETAILS OR PAY QUANTITIES IN THE SPACE PROVIDED AT RIGHT.

OTHER ITEMS ①

① UTILITIES ADDED DURING CONSTRUCTION AND SPECIALTY ITEMS.

FINAL QUANTITIES ENTERED ON SCHEDULE OF QUANTITIES: YES ☐ NO ☐

SUMMARY OF SIGNIFICANT AS-BUILT CHANGES

THE AS-BUILT INFORMATION WAS ADDED TO THE PLAN BY:

_____ _____
INSPECTOR(S) DATE

CHECKED BY: _____ _____
PROJECT ENGINEER / SUPERVISOR DATE

SUBMIT THIS FORM WITH THE PROJECT FINAL, AND SUBMIT A COPY TO THE OFFICE OF BRIDGES AND STRUCTURES - ATTN: REGIONAL CONSTRUCTION ENGINEER (MS660).

REVISION:
APPROVED, SEPTEMBER 26, 2003
Edward D. Morgan
STATE BRIDGE ENGINEER

AS-BUILT DETAILS
(AS NEEDED)

FIG. 5-397.900

TITLE: AS-BUILT BRIDGE DATA

DES: DR: CHK: CHK:

APPROVED:

SHEET NO. 29 OF 31 SHEETS

BRIDGE NO. 13004

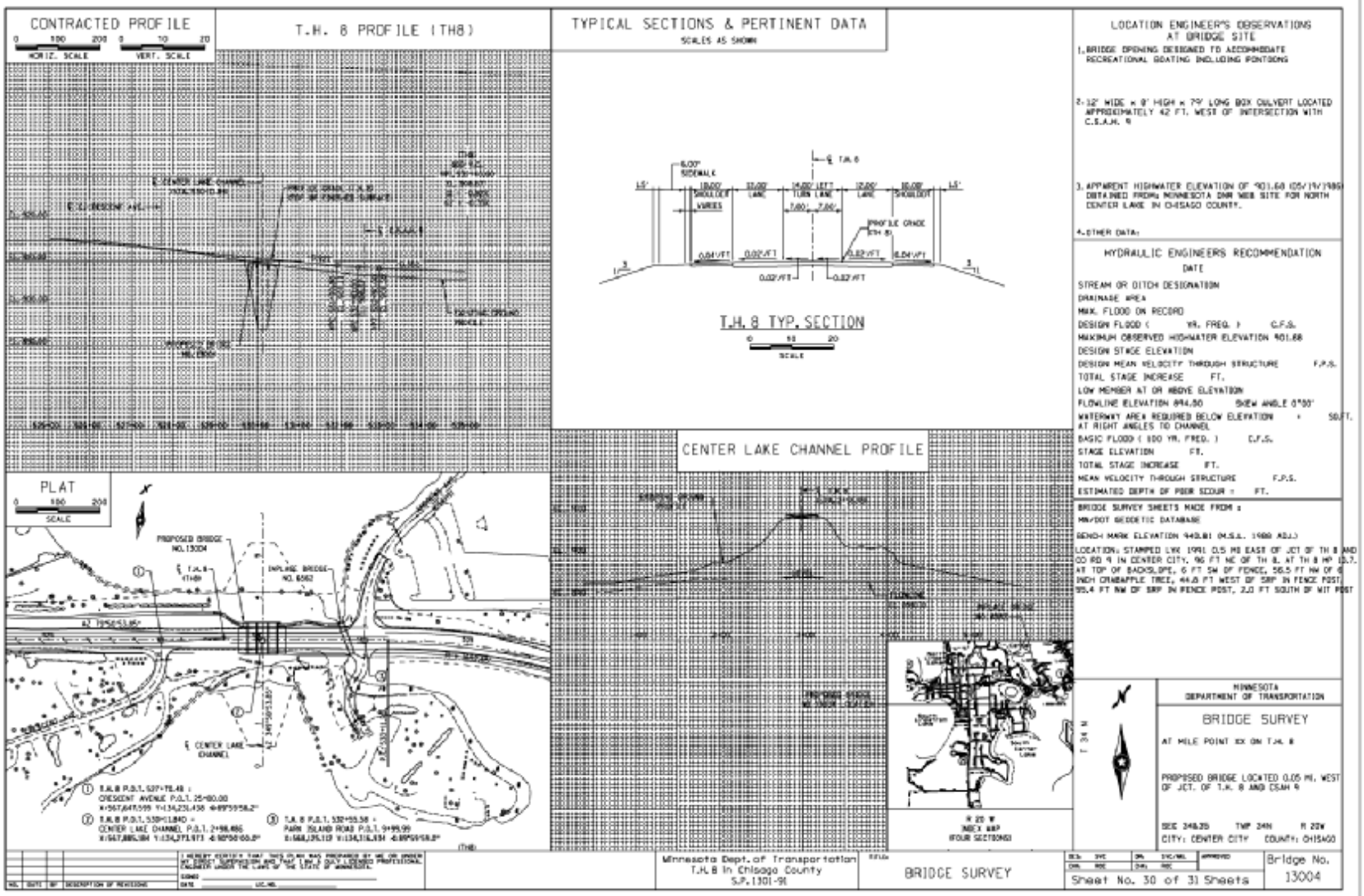
CONTRACTED PROFILE
T.H. 8 PROFILE (TH8)
TYPICAL SECTIONS & PERTINENT DATA
SCALES AS SHOWN
T.H. 8 TYP. SECTION
CENTER LAKE CHANNEL PROFILE
PLAT
PROPOSED BRIDGE NO.13004
EXPLORE BRIDGE NO. 8562
CENTER LAKE CHANNEL
LOCATION ENGINEER'S OBSERVATIONS AT BRIDGE SITE
1. BRIDGE OPENING DESIGNED TO ACCOMMODATE RECREATIONAL BOATING INCLUDING PONTOONS
2- 12' WIDE x 9' HIGH x 79' LONG BOX CULVERT LOCATED APPROXIMATELY 42 FT. WEST OF INTERSECTION WITH C.S.A.H. 9
3. APPARENT HIGHWATER ELEVATION OF 901.68 (05/19/1986) OBTAINED FROM: MINNESOTA DNR WEB SITE FOR NORTH CENTER LAKE IN CHISAGO COUNTY.
4- OTHER DATA:
HYDRAULIC ENGINEERS RECOMMENDATION
DATE
STREAM OR DITCH DESIGNATION
DRAINAGE AREA
MAX. FLOOD ON RECORD
DESIGN FLOOD (YR. FREQ.) C.F.S.
MAXIMUM OBSERVED HIGHWATER ELEVATION 901.68
DESIGN STAGE ELEVATION
DESIGN MEAN VELOCITY THROUGH STRUCTURE F.P.S.
TOTAL STAGE INCREASE FT.
LOW MEMBER AT OR ABOVE ELEVATION
FLOWLINE ELEVATION 894.50 SKEW ANGLE 0°00'
WATERWAY AREA REQUIRED BELOW ELEVATION + SQ.FT. AT RIGHT ANGLES TO CHANNEL
BASIC FLOOD (100 YR. FREQ.) C.F.S.
STAGE ELEVATION FT.
TOTAL STAGE INCREASE FT.
MEAN VELOCITY THROUGH STRUCTURE F.P.S.
ESTIMATED DEPTH OF POOR SCOUR = FT.
BRIDGE SURVEY SHEETS MADE FROM :
MN/DOT GEODETIC DATABASE
BENCH MARK ELEVATION 940.81 (M.S.L. 1988 ADJ.)
LOCATION: STAMPED LYK 1991 0.15 MI EASE OF JCT OF TH 8 AND CO RD 9 IN CENTER CITY, 96 FT NE OF TH 8, AT TH 8 MP 13.7, AT TOP OF BACKSLOPE, 6 FT SW OF FENCE, 56.5 FT NW OF 6 INCH CRABAPPLE TREE, 44.8 FT WEST OF SRF IN FENCE POST, 55.4 FT NW OF SRF IN FENCE POST, 2.0 FT SOUTH OF WIT POST
MINNESOTA DEPARTMENT OF TRANSPORTATION
BRIDGE SURVEY
AT MILE POINT XX ON T.H. 8
PROPOSED BRIDGE LOCATED 0.05 MI. WEST OF JCT. OF T.H. 8 AND CSAH 9
SEC 34&35 TWP 34N R 20W
CITY: CENTER CITY COUNTY: CHISAGO
Minnesota Dept. of Transportation
T.H. 8 In Chisago County
S.P. 1301-91
BRIDGE SURVEY
Sheet No. 30 of 31 Sheets
Bridge No. 13004

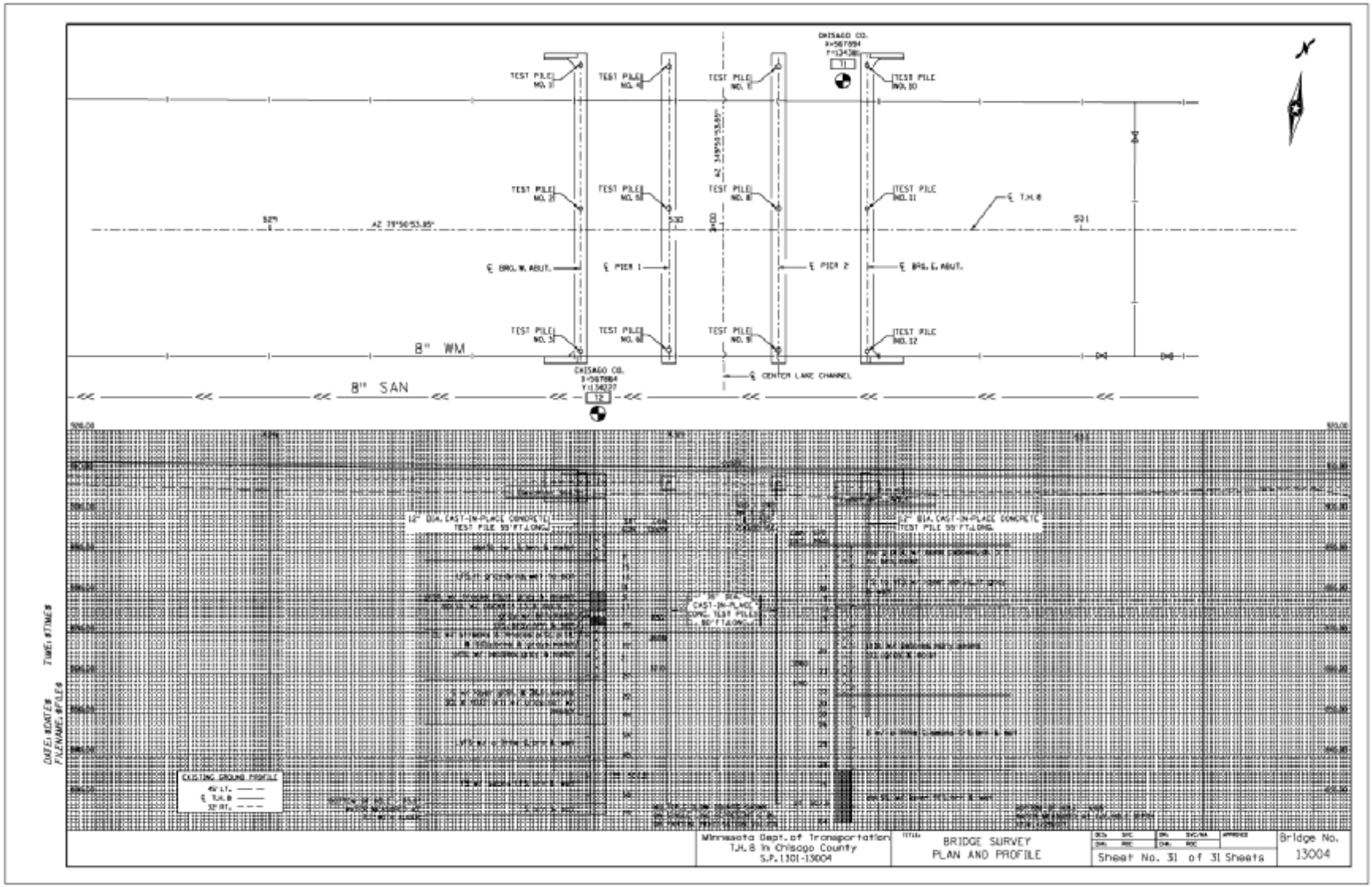
TEST PILE NO. 7
TEST PILE NO. 6
TEST PILE NO. 5
TEST PILE NO. 10
TEST PILE NO. 4
TEST PILE NO. 3
TEST PILE NO. 8
TEST PILE NO. 11
TEST PILE NO. 2
TEST PILE NO. 9
TEST PILE NO. 12
℄ BRG. W. ABUT.
℄ PIER 1
℄ PIER 2
℄ BRG. E. ABUT.
℄ T.H. 8
℄ CENTER LAKE CHANNEL
8" WM
8" SAN
AZ 79°56'53.85"
AZ 349°03'55.85"
EXISTING GROUND PROFILE
℄ T.H. 8
Minnesota Dept. of Transportation
T.H. 8 In Chisago County
S.P. 1301-13004
BRIDGE SURVEY
PLAN AND PROFILE
Sheet No. 31 of 31 Sheets
Bridge No.
13004

Appendix B

Design Calculations

B.1 Design of Interior Composite Section

The inverted-T sections of the Mn/DOT Inverted-T Precast Slab System were designed to behave as a simple span under self weight and the weight of the CIP concrete deck. After the CIP concrete of the deck had cured, the deck then behaved continuously for live loads over the interior piers.

The design of the inverted-T precast sections for Mn/DOT Bridge No. 13004 was performed using a MathCAD® Worksheet. This program allows the user to make iterative calculations rather easily. If one variable is changed, the program changes all of the calculations within the worksheet. This worksheet was originally written to be used for the design of I-girders, but it was modified to be applicable to the design of inverted-T sections. The remainder of Section B.1 presents the calculations for the design of an interior inverted-T precast section of the center span of Mn/DOT Bridge No. 13004.

B.1.1 Program Defaults and Inputs (B-2 through B-5)

The first page of the calculations provided program defaults that allowed a user to select a beam size and strand size then provided them with the dimensions for the selected beam and strand. The rest of this section allowed the user to input material properties, additional geometry requirements (i.e., span length, etc.), loads, load factors, and the strand pattern design, all of which would be used later in the calculations.

Simple-Span Interior Pretensioned I-Girder Design - v 1.0

****** *US CUSTOMARY UNITS* ******

Limitations: Design of a simple-span composite precast/pretensioned concrete I-beam in accordance with AASHTO LRFD. Strand patterns are assumed to be 2-pt. depressed patterns, although straight patterns can be used, but without debonding. The template checks all pertinent limit states. Flexural checks for service, strength, and fatigue limit states are performed. Live load generation is good for spans of 12.9 meters or greater.

References: *AASHTO LRFD Bridge Design Specifications*, Second Edition

Author: Roy L. Eriksson, P.E., modified for MN/DOT by DJD

Last Update: 11-25-2003

These calculations consider the effect of Restraint Moments.

INPUT ===> **Filename:** Filename := "INT SECT SPAN2 MR.mcd"

Bridge Number: Bridge_no := "13004"

Description: Description := "Special PS Section for Center Span w/Restraining Moments"

Units:

k := 1000·lbf ksi := 1000·psi

Beam Data:

Prestressed Concrete Beam Properties: y := 1 .. 8

$Section_y$:=	y =	H_y :=	$Apcb_y$:=	y_{cgb_y} :=	$Ipcb_y$:=	A_{c_y} :=	bf_y :=	bw_y :=	tf_y :=
"27M"	1	27	516	13.59	43075	294.5	30	6	6
"36M"	2	36	570	17.96	93528	321.5	30	6	6
"MAIN"	3	12	738	5.424	8399	594.0	48	48	3
"FASC"	4	12	687	5.691	8072	535.5	50.5	50.5	3
"54M"	5	54	678	26.75	265828	375.5	30	6	6
"63M"	6	63	732	31.17	392056	402.5	30	6	6
"72M"	7	72	786	35.60	547922	429.5	30	6	6
"81M"	8	81	840	40.04	735615	456.5	30	6	6

Note: A_c for "SPEC" section is the bottom half (of final section depth) of precast section only.

Strand size & area x := 1 .. 3

$Strand_x$:=	x =	dia_x :=	$Area_x$:=
"0.5 in"	1	0.5	0.153
"0.5 in special"	2	0.5	0.174
"0.6 in"	3	0.6	0.217

PROGRAM INPUT

Select Beam Size: $yy := 3$ $\quad Section := Section_{yy}$ $\quad Section = \text{"MAIN"}$

PCB	yy DESIGNATION
27M	1
36M	2
SPEC	3
45M	4
54M	5
63M	6
72M	7
81M	8

$h := H_{yy} \cdot in$ $\quad h = 12\,in$ $\quad b_f := bf_{yy} \cdot in$ $\quad b_f = 48\,in$

$A := Apcb_{yy} \cdot in^2$ $\quad A = 738\,in^2$ $\quad t_f := tf_{yy} \cdot in$ $\quad t_f = 3\,in$

$I := Ipcb_{yy} \cdot in^4$ $\quad I = 8399\,in^4$ $\quad b_v := bw_{yy} \cdot in$ $\quad b_v = 48\,in$

$y_b := y_{cgb_{yy}} \cdot in$ $\quad y_b = 5.42\,in$ $\quad A_c := A_{c_{yy}} \cdot in^2$ $\quad A_c = 594.0\,in^2$

Select Strand Size: $xx := 1$ $\quad Strand_{xx} = \text{"0.5 in"}$

STRAND	xx DESIGNATION
0.5 in	1
0.5 in special	2
0.6 in	3

$A_{strand} := Area_{xx} \cdot in^2$ $\quad A_{strand} = 0.153\,in^2$

$d_{str} := dia_{xx} \cdot in$ $\quad d_{str} = 0.5\,in$

Materials: Beam Concrete: $f_c := 6.5 \cdot ksi$ $\quad f_{ci} := 4.5 \cdot ksi$ $\quad w_c := 0.155 \cdot \frac{k}{ft^3}$

Deck Concrete: $f_{ct} := 4.0 \cdot ksi$ $\quad w_{ct} := 0.150 \cdot \frac{k}{ft^3}$ $\quad$ Strand: $E_p := 28500 \cdot ksi$ $\quad f_{pu} := 270 \cdot ksi$

Rebar: $f_y := 60 \cdot ksi$ $\quad E_s := 29000 \cdot ksi$ $\quad$ Relative Humidity: $H := 73$

Geometry: Span: $L_{ovr} := 26.6667 \cdot ft$ $\quad L_{brng} := 14 \cdot in$ $\quad L_{des} := L_{ovr} - L_{brng}$ $\quad L_{des} = 25.5\,ft$ $\quad$ Skew: $\theta := 0.00$

Bridge: $N_g := 13$ $\quad S := 6.0 \cdot ft$ $\quad d_e := .744 \cdot ft$ $\quad$ "interior" or "exterior" beam?: $beam := \text{"interior"}$

Deck: slab thickness for section properties, comp for DC2 & DW $t_{sDC2} := 6.00 \cdot in$ $\quad h_{stprop} := 0.0 \cdot in$

comp for LL & FWC $t_{sLL} := 6.00 \cdot in$

slab thickness for load calculations, $t_{sload} := 7.75 \cdot in$ $\quad t_{wc} := 0.0 \cdot in$ $\quad h_{stload} := 0.0 \cdot in$

width from gutterline to gutterline, $Width_{gtg} := 73.75 \cdot ft$ $\quad$ overhang from centerline of beam, $Width_{oh} := 2.41 \cdot ft$

Loads: Uniform Dead: $w_{barrier_1} := 0.396 \cdot \frac{k}{ft}$ $\quad w_{barrier_2} := 0.0 \cdot \frac{k}{ft}$ $\quad$ Live: HL-93 $\quad w_{lane} := 0.64 \cdot \frac{k}{ft}$

$w_{fws} := 0.020 \cdot \frac{k}{ft^2}$ $\quad w_{barrier_3} := 0.539 \cdot \frac{k}{ft}$ $\quad w_{barrier_4} := 0.190 \cdot \frac{k}{ft}$

Diaphragms (maximum of 2 symmetrical interior diaphragms): $N_{dia} := 0$ $\quad P_{diaph} := 0.00 \cdot k$ $\quad$ at location $x_{diaph} := 0 \cdot ft$

Factors: Flexure: $\phi_f := 1.00$ $\quad$ Shear: $\phi_v := 0.90$ $\quad DLA := 0.33$ $\quad$ (LRFD 3.6.2.1-1)

Strand Pattern Design:

Initial Pull Fraction: Pull := 0.75

Hold Down Point Fraction of Design Span: Dep_Frac := 0

Number of Draped Strands: No_Draped := 0

Draped c.g. from bottom at end: $dr\_cg_{end} := 0 \cdot in$

Draped c.g. from bottom at midspan: $dr\_cg_{mid} := 0 \cdot in$

$$EPat\_n := \begin{pmatrix} 0 \\ 0 \\ 0 \\ 0 \\ 0 \\ 0 \\ 0 \\ 0 \\ 0 \\ 8 \\ 8 \end{pmatrix} \quad EPat\_h := \begin{pmatrix} 0 \\ 0 \\ 0 \\ 0 \\ 0 \\ 0 \\ 0 \\ 0 \\ 0 \\ 4.0 \\ 2.0 \end{pmatrix} \cdot in \qquad MPat\_n := \begin{pmatrix} 0 \\ 0 \\ 0 \\ 0 \\ 0 \\ 0 \\ 0 \\ 0 \\ 0 \\ 8 \\ 8 \end{pmatrix} \quad MPat\_h := \begin{pmatrix} 0 \\ 0 \\ 0 \\ 0 \\ 0 \\ 0 \\ 0 \\ 0 \\ 0 \\ 4.0 \\ 2.0 \end{pmatrix} \cdot in$$

End Pattern

$No\_StrandsE := \sum EPat\_n$

No_StrandsE = 16

Mid Pattern

$No\_StrandsM := \sum MPat\_n$

No_StrandsM = 16

No_Strands_Check := if(No_StrandsE = No_StrandsM, "OK" , "NG")

No_Strands_Check = "OK"

Shear Design:

Input of estimated θ values for iteration is found on page 24.

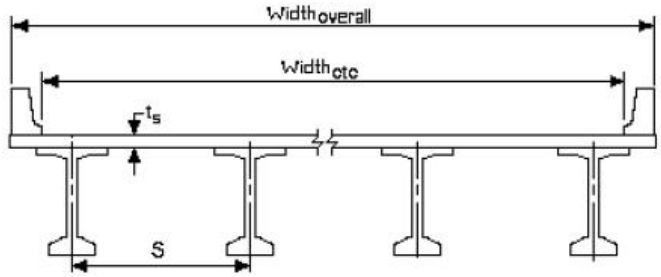

Figure 1: Cross section of bridge with input variable definitions.

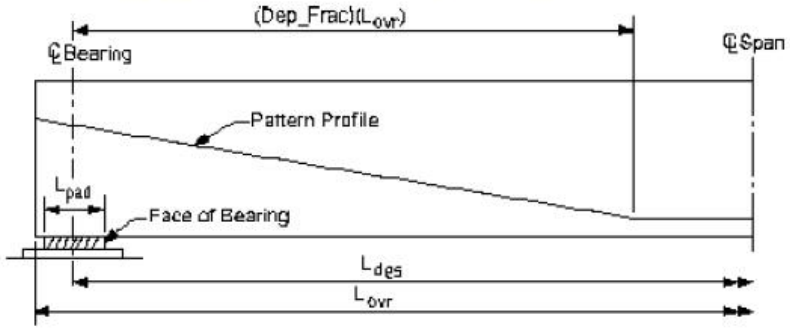

Figure 2: Half beam elevation.

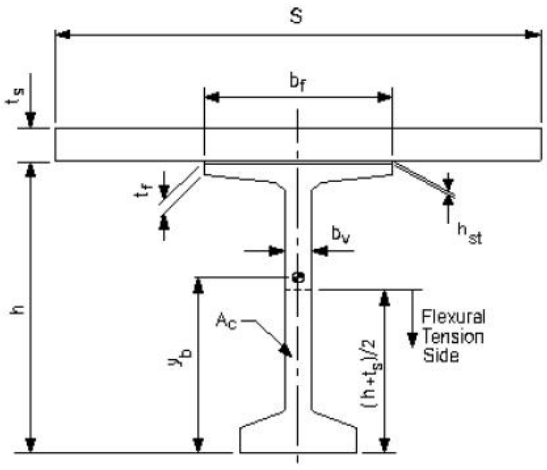

Input values for the dimensions and section properties of the beam itself and for the dimensions of the slab are entered on page 1 and defined as shown in Figure 3.

Note that the parameter 'A_c' is specifically defined in LRFD as the area of concrete on the flexural tension side of the member as shown in Figure 3 (LRFD Article 5.8.3.4.2 and LRFD Fig. 5.8.3.4.2-3). A_c is used in the shear calculations.

Figure 3: Cross section of one girder with associated slab with input variable definitions.

B.1.2 Calculation of Section Properties (B-6 through B-9)

This section of the calculations used the program defaults and user inputs from the first section to calculate the properties of the composite section. The properties that were calculated in this section included the area, moment of interia, and section moduli.

CALCULATIONS

Section Properties

Non-Composite Section Properties:

$S_b := \frac{I}{y_b}$ $S_b = 1548\,in^3$ $y_t := h - y_b$ $S_t := \frac{I}{y_t}$ $S_t = 1277\,in^3$

Composite Section Properties for DC2 and DW :

Effective Flange Width:

The effective width of the composite section is the least of: (LRFD 4.6.2.6.1)

for int beam, $b_{eff\_int_1} := \frac{L_{des}}{4}$ for ext beam, $b_{eff\_ext_1} := \frac{b_{eff\_int_1}}{2} + if\left(Width_{oh} < \frac{L_{des}}{8}, Width_{oh}, \frac{L_{des}}{8}\right)$

$b_{eff\_int_2} := \frac{b_f}{2} + 12 \cdot t_{sDC2}$ $b_{eff\_ext_2} := \frac{b_{eff\_int_2}}{2} + if\left(Width_{oh} < \frac{b_{eff\_int_2}}{2}, Width_{oh}, \frac{b_{eff\_int_2}}{2}\right)$

$b_{eff\_int_3} := S$ $b_{eff\_ext_3} := \frac{b_{eff\_int_3}}{2} + Width_{oh}$

$b_{effDC2} := if\left(beam = "interior", min\left(b_{eff\_int}\right), min\left(b_{eff\_ext}\right)\right)$ $b_{effDC2} = 72.00\,in$

$E_{cdeck} := \left[33000 \cdot \left(w_{ct} \cdot \frac{ft^3}{k} - 0.005\right)^{1.5} \cdot \sqrt{f_{ct}}\right] \cdot ksi^{0.5}$ $E_{cdeck} = 3644\,ksi$

$E_{cbeamf} := \left(1265 \cdot \sqrt{f_c} + 1000 \cdot \frac{k^{0.5}}{in}\right) \cdot ksi^{0.5}$ $E_{cbeamf} = 4225.1\,ksi$

$n_{db} := \frac{E_{cdeck}}{E_{cbeamf}}$ $n_{db} = 0.8625$ $b_{tranDC2} := n_{db} \cdot b_{effDC2}$ $b_{tranDC2} = 62.10\,in$

$h_{comp1} := 5.0in$ thickness of CIP concrete between webs above top of flange slopes

$b_{comp1} := 24.0in$ total width of CIP concrete between from edge of web to edge of flange

Properties:

$A_{slabDC2} := b_{tranDC2} \cdot t_{sDC2}$ $A_{slabDC2} = 372.6\,in^2$ $A_{stool} := b_f \cdot h_{stprop} \cdot n_{db}$ $A_{stool} = 0\,in^2$

$A_{comp1} := b_{comp1} \cdot h_{comp1} \cdot n_{db}$ $A_{comp1} = 103.5\,in^2$

$A_{compDC2} := A + A_{slabDC2} + A_{stool} + A_{comp1}$ $A_{compDC2} = 1214.1\,in^2$

$$y_{bcDC2} := \frac{A \cdot y_b + A_{slabDC2} \cdot \left(h + h_{stprop} + \frac{t_{sDC2}}{2}\right) + A_{stool} \cdot \left(h + \frac{h_{stprop}}{2}\right) + A_{comp1} \cdot \left(h - \frac{h_{comp1}}{2}\right)}{A_{compDC2}}$$

$y_{bcDC2} = 8.71\,in$

$h_{cDC2} := h + h_{stprop} + t_{sDC2}$

$y_{tcDC2} := h_{cDC2} - y_{bcDC2}$ $y_{tcDC2} = 9.29\,in$

$$I_{slabDC2} := \frac{b_{tranDC2} \cdot t_{sDC2}^3}{12}$$ $I_{slabDC2} = 1118\,in^4$ $$I_{stool} := \frac{n_{db} \cdot b_f \cdot h_{stprop}^3}{12}$$

$$I_{comp1} := \frac{(b_{comp1} \cdot n_{db}) \cdot h_{comp1}^3}{12}$$ $I_{comp1} = 215.6\,in^4$

$$I_{cDC2} := I + A \cdot (y_b - y_{bcDC2})^2 + I_{slabDC2} + A_{slabDC2} \cdot \left(h + h_{stprop} + \frac{t_{sDC2}}{2} - y_{bcDC2}\right)^2 \ldots$$
$$+ I_{stool} + A_{stool} \cdot \left(h + \frac{h_{stprop}}{2} - y_{bcDC2}\right)^2 + I_{comp1} + A_{comp1} \cdot \left(h - \frac{h_{comp1}}{2} - y_{bcDC2}\right)^2$$

$I_{cDC2} = 32507\,in^4$

$$S_{bcDC2} := \frac{I_{cDC2}}{y_{bcDC2}}$$ $S_{bcDC2} = 3732\,in^3$ $$S_{tcDC2} := \frac{I_{cDC2}}{y_{tcDC2} \cdot n_{db}}$$ $S_{tcDC2} = 4057\,in^3$

Composite section modulus at the top of the prestressed beam:

$y_{tcbDC2} := h - y_{bcDC2}$ $$S_{tcbDC2} := \frac{I_{cDC2}}{y_{tcbDC2}}$$ $S_{tcbDC2} = 9881\,in^3$

Composite Section Properties for LL :

Effective Flange Width: (LRFD 4.6.2.6.1)

The effective width of the composite section is the least of:

for int beam, $b_{eff\_int_1} := \frac{L_{des}}{4}$ for ext beam, $b_{eff\_ext_1} := \frac{b_{eff\_int_1}}{2} + if\left(Width_{oh} < \frac{L_{des}}{8}, Width_{oh}, \frac{L_{des}}{8}\right)$

$b_{eff\_int_2} := \frac{b_f}{2} + 12 \cdot t_{sLL}$ $b_{eff\_ext_2} := \frac{b_{eff\_int_2}}{2} + if\left(Width_{oh} < \frac{b_{eff\_int_2}}{2}, Width_{oh}, \frac{b_{eff\_int_2}}{2}\right)$

$b_{eff\_int_3} := S$ $b_{eff\_ext_3} := \frac{b_{eff\_int_3}}{2} + Width_{oh}$

$b_{effLL} := if\left(beam = "interior", min\left(b_{eff\_int}\right), min\left(b_{eff\_ext}\right)\right)$ $b_{effLL} = 72.00\,in$

$n_{db} = 0.8625$ $b_{tranLL} := n_{db} \cdot b_{effLL}$ $b_{tranLL} = 62.10\,in$

Properties:

$A_{slabLL} := b_{tranLL} \cdot t_{sLL}$ $A_{slabLL} = 372.6\,in^2$ $A_{stool} := b_f \cdot h_{stprop} \cdot n_{db}$ $A_{stool} = 0.0\,in^2$

$A_{compLL} := A + A_{slabLL} + A_{stool} + A_{comp1}$ $A_{compLL} = 1214.1\,in^2$

$$y_{bcLL} := \frac{A \cdot y_b + A_{slabLL} \cdot \left(h + h_{stprop} + \frac{t_{sLL}}{2}\right) + A_{stool} \cdot \left(h + \frac{h_{stprop}}{2}\right) + A_{comp1} \cdot \left(h - \frac{h_{comp1}}{2}\right)}{A_{compLL}} \qquad y_{bcLL} = 8.71\,in$$

$h_{cLL} := h + h_{stprop} + t_{sLL}$ $h_{cLL} = 18.00\,in$

$y_{tcLL} := h_{cLL} - y_{bcLL}$ $y_{tcLL} = 9.29\,in$

$I_{slabLL} := \frac{b_{tranLL} \cdot t_{sLL}^3}{12}$ $I_{slabLL} = 1118\,in^4$ $I_{stool} := \frac{n_{db} \cdot b_f \cdot h_{stprop}^3}{12}$ $I_{stool} = 0\,in^4$

$$I_{cLL} := \left[I + A \cdot \left(y_b - y_{bcLL}\right)^2 + I_{slabLL} + A_{slabLL} \cdot \left(h + h_{stprop} + \frac{t_{sLL}}{2} - y_{bcLL}\right)^2\right] \ldots \qquad I_{cLL} = 32507\,in^4$$
$$+ I_{stool} + A_{stool} \cdot \left(h + \frac{h_{stprop}}{2} - y_{bcLL}\right)^2 + I_{comp1} + A_{comp1} \cdot \left(h - \frac{h_{comp1}}{2} - y_{bcLL}\right)^2$$

$S_{bcLL} := \frac{I_{cLL}}{y_{bcLL}}$ $S_{bcLL} = 3732\,in^3$ $S_{tcLL} := \frac{I_{cLL}}{y_{tcLL} \cdot n_{db}}$ $S_{tcLL} = 4057\,in^3$

Composite section modulus at the top of the prestressed beam:

$y_{tcbLL} := h - y_{bcLL}$ $y_{tcbLL} = 3.29\,in$ $S_{tcbLL} := \frac{I_{cLL}}{y_{tcbLL}}$ $S_{tcbLL} = 9881\,in^3$

Section Properties Summary

Input hand calculated section properties considering transformed mild reinforcement.

Noncomposite -

$A = 738\,in^2$ $S_t = 1277\,in^3$

$I = 8399\,in^4$ $S_b = 1548\,in^3$

$y_b = 5.42\,in$ $S_t := 1407in^3$ $S_b := 1620in^3$

Composite for DC2 and DW - $A_{compDC2} = 1214\,in^2$ $S_{tcDC2} = 4057\,in^3$

$I_{cDC2} = 32507\,in^4$ $S_{tcbDC2} = 9881\,in^3$

$y_{bcDC2} = 8.71\,in$ $S_{bcDC2} = 3732\,in^3$

$b_{tranDC2} = 62.10\,in$ $S_{tcbDC2} := 11844in^3$ $S_{bcDC2} := 3923in^3$

Composite for LL - $A_{compLL} = 1214\,in^2$ $S_{tcLL} = 4057\,in^3$

$I_{cLL} = 32507\,in^4$ $S_{tcbLL} = 9881\,in^3$

$y_{bcLL} = 8.71\,in$ $S_{bcLL} = 3732\,in^3$

$b_{tranLL} = 62.10\,in$ $S_{tcbLL} := 11844in^3$ $S_{bcLL} := 3923in^3$

B.1.3 Calculations of Moments and Shear Forces (B-10 through B-20)

This section of the calculations used the section properties and user inputs to calculate the maximum moments and shear forces of which the composite section would be subjected. Moments and shear forces were calculated due to the self weight of the precast section, weight of the CIP concrete deck, weight of the barrier, and weight of the future wearing surface. In addition, the live load distribution factors were calculated and used to determine the maximum live load moments and shear forces. However, since the composite section was designed to behave continuously for live load, the live load moments and shears were also calculated based on continuous behavior using the BTBEAM program and then input into this worksheet. These live load moments and shears were used for the remainder of the calculations. The restraint moments were calculated by hand using the PCA Method and input into the worksheet at the end of this section.

Moments and Shears

Dead Loads:

Girder self-weight at release: (end-to-end length of beam is used)

For moment and shear, these are the locations along the girder of interest:

1. CL Bearing: $x_{r_1} := 0.0 \cdot L_{des} + \frac{L_{ovr} - L_{des}}{2}$

2. Transfer point of strands: $x_{r_2} := 60 \cdot d_{str}$

3. Tenth points

$$x_{r_3} := 0.1 \cdot L_{des} + \frac{L_{ovr} - L_{des}}{2}$$

$$x_{r_4} := 0.2 \cdot L_{des} + \frac{L_{ovr} - L_{des}}{2}$$

$$x_{r_5} := 0.3 \cdot L_{des} + \frac{L_{ovr} - L_{des}}{2}$$

$$x_{r_6} := 0.4 \cdot L_{des} + \frac{L_{ovr} - L_{des}}{2}$$

4. Midspan of beam: $x_{r_7} := 0.5 \cdot L_{ovr}$

$$x_{r_8} := 0.6 \cdot L_{des} + \frac{L_{ovr} - L_{des}}{2}$$

$$x_{r_9} := 0.7 \cdot L_{des} + \frac{L_{ovr} - L_{des}}{2}$$

$$x_{r_{10}} := 0.8 \cdot L_{des} + \frac{L_{ovr} - L_{des}}{2}$$

$$x_{r_{11}} := 0.9 \cdot L_{des} + \frac{L_{ovr} - L_{des}}{2}$$

5. Transfer point of strands: $x_{r_{12}} := L_{ovr} - 60 \cdot d_{str}$

6. CL Bearing $x_{r_{13}} := 1.0 \cdot L_{des} + \frac{L_{ovr} - L_{des}}{2}$

Moment Due to Beam Self-Weight:

$w_{sw} := w_c \cdot A$ $\quad w_{sw} = 0.794 \frac{k}{ft}$

$i := 1 .. 13$

$$M_{swr_i} := \frac{w_{sw} \cdot x_{r_i}}{2} \cdot \left(L_{ovr} - x_{r_i}\right)$$

Girder self-weight, final : (center to center of bearing length is used)

$M_{swr} =$

	1
1	6.0
2	24.0
3	29.3
4	47.4
5	60.3
6	68.0
7	70.6
8	68.0
9	60.3
10	47.4
11	29.3
12	24.0
13	6.0

k·ft

$x_r =$

	1	
1	0.6	CL Bearing
2	2.5	Transfer
3	3.1	0.1L
4	5.7	0.2L
5	8.2	0.3L
6	10.8	0.4L
7	13.3	0.5L
8	15.9	0.6L
9	18.4	0.7L
10	21.0	0.8L
11	23.5	0.9L
12	24.2	Transfer
13	26.1	CL Bearing

ft

For moment and shear, these are the points of interest:

1. CL Bearing $x_{f_1} := 0.0 \cdot L_{des}$

2. The critical section for shear is d_v from the face of the support. At this point in the calculations d_v is not known, so a reasonable value must be assumed. Assume d_v equals 75% of the composite height of the section. Thus, from the centerline of bearing, the critical point for she

$$x_{f_2} := 0.75 \cdot h_{cLL} + \frac{L_{bmg}}{2} \qquad x_{f_2} = 20.5\,in$$

3. Tenth points

$x_{f_3} := 0.1 \cdot L_{des}$

$x_{f_4} := 0.2 \cdot L_{des}$

$x_{f_5} := 0.3 \cdot L_{des}$

$x_{f_6} := 0.4 \cdot L_{des}$

4. Midspan of beam: $x_{f_7} := 0.5 \cdot L_{des}$

$x_{f_8} := 0.6 \cdot L_{des}$

$x_{f_9} := 0.7 \cdot L_{des}$

$x_{f_{10}} := 0.8 \cdot L_{des}$

$x_{f_{11}} := 0.9 L_{des}$

INPUT actual location of critical section for shear from later calculation on page 24:

$x_{f_2} := 20.7 \cdot in$

5. Critical Section $x_{f_{12}} := L_{des} - \left(x_{f_2}\right)$

6. CL Bearing $x_{f_{13}} := 1.0 \cdot L_{des}$

$j := 1 .. 13$

$w_{sw} := w_c \cdot A$ $\quad w_{sw} = 0.794 \frac{k}{ft}$ $\quad Beam\_wt := \frac{w_{sw} \cdot L_{ovr}}{2.0 \cdot \frac{k}{ton}}$ $\quad Beam\_wt = 10.6\,ton$

$M_{swf_j} := \frac{w_{sw} \cdot x_{f_j}}{2} \cdot \left(L_{des} - x_{f_j}\right)$ $\quad V_{swf_j} := \left| w_{sw} \cdot \left(\frac{L_{des}}{2} - x_{f_j}\right) \right|$

$M_{swf} =$

	1
1	0.0
2	16.3
3	23.2
4	41.3
5	54.2
6	62.0
7	64.6
8	62.0
9	54.2
10	41.3
11	23.2
12	16.3
13	0.0

k·ft

$V_{swf} =$

	1
1	10.1
2	8.8
3	8.1
4	6.1
5	4.1
6	2.0
7	0.0
8	2.0
9	4.1
10	6.1
11	8.1
12	8.8
13	10.1

k

$x_f =$

	1
1	0.0
2	1.7
3	2.6
4	5.1
5	7.7
6	10.2
7	12.8
8	15.3
9	17.9
10	20.4
11	23.0
12	23.8
13	25.5

ft

CL bearing
d_v from support
0.1L
0.2L
0.3L
0.4L
midspan
0.6L
0.7L
0.8L
0.9L
d_v from support
CL bearing

Deck Weight:

$w_{d\_int} := t_{sload} \cdot S \cdot w_{ct} + b_f \cdot h_{stload} \cdot w_{ct}$ $\quad w_{d\_ext} := \left[t_{sload} \cdot \left(\frac{S}{2} + Width_{oh}\right) + b_f \cdot h_{stload} + \left(Width_{oh} - \frac{b_f}{2}\right) \cdot \left(\frac{1}{2} \cdot h_{stload} + 1 \cdot in\right) \right] \cdot w_{ct}$

$w_{d\_int} = 0.581 \frac{k}{ft}$ $\quad w_{d\_ext} = 0.529 \frac{k}{ft}$ $\quad w_d := if\left(beam = "interior", w_{d\_int}, w_{d\_ext}\right)$

$M_{deck_j} := \frac{w_d \cdot x_{f_j}}{2} \cdot \left(L_{des} - x_{f_j}\right)$ $\quad V_{deck_j} := \left| w_d \cdot \left(\frac{L_{des}}{2} - x_{f_j}\right) \right|$

$M_{deck} =$

	1
1	0.0
2	11.9
3	17.0
4	30.2
5	39.7
6	45.4
7	47.2
8	45.4
9	39.7
10	30.2
11	17.0
12	11.9
13	0.0

k·ft

$V_{deck} =$

	1
1	7.4
2	6.4
3	5.9
4	4.4
5	3.0
6	1.5
7	0.0
8	1.5
9	3.0
10	4.4
11	5.9
12	6.4
13	7.4

k

Diaphragm Weight: $P_{diaph\_int} := if(N_{dia} > 1, P_{diaph}, 0.5 \cdot P_{diaph})$ $P_{diaph\_ext} := if(N_{dia} > 1, 0.5 \cdot P_{diaph}, 0.25 \cdot P_{diaph})$

$P_{diaph} := if(beam = "interior", P_{diaph\_int}, P_{diaph\_ext})$

$M_{diaph_j} := if\left[x_{f_j} < x_{diaph}, P_{diaph} \cdot x_{f_j}, P_{diaph} \cdot x_{f_j} - P_{diaph} \cdot \left(x_{f_j} - x_{diaph}\right)\right]$ $V_{diaph_j} := if\left(x_{f_j} < x_{diaph}, P_{diaph}, 0 \cdot k\right)$

$M_{diaph} =$

	1
1	0.0
2	0.0
3	0.0
4	0.0
5	0.0
6	0.0
7	0.0
8	0.0
9	0.0
10	0.0
11	0.0
12	0.0
13	0.0

k·ft

$V_{diaph} =$

	1
1	0.0
2	0.0
3	0.0
4	0.0
5	0.0
6	0.0
7	0.0
8	0.0
9	0.0
10	0.0
11	0.0
12	0.0
13	0.0

k

Wearing Course Weight(Composite Dead Load):

$w_{wc} := t_{wc} \cdot \frac{Width_{gtg}}{N_g} \cdot w_{ct}$ $w_{wc} = 0.000 \frac{k}{ft}$

$M_{wc_j} := \frac{w_{wc} \cdot x_{f_j}}{2} \cdot \left(L_{des} - x_{f_j}\right)$ $V_{wc_j} := \left| w_{wc} \cdot \left(\frac{L_{des}}{2} - x_{f_j}\right) \right|$

$M_{wc} =$

	1
1	0.0
2	0.0
3	0.0
4	0.0
5	0.0
6	0.0
7	0.0
8	0.0
9	0.0
10	0.0
11	0.0
12	0.0
13	0.0

k·ft

$V_{wc} =$

	1
1	0.0
2	0.0
3	0.0
4	0.0
5	0.0
6	0.0
7	0.0
8	0.0
9	0.0
10	0.0
11	0.0
12	0.0
13	0.0

k

Barrier Weight (Composite Dead Load): $n := 1 .. 4$

$$w_{barrier} = \begin{pmatrix} 0.396 \\ 0 \\ 0.539 \\ 0.19 \end{pmatrix} \frac{k}{ft}$$

Per beam: $w_b := \frac{\sum_n w_{barrier_n}}{N_g}$ $\quad w_b = 0.0865 \frac{k}{ft}$

$$M_{barrier_j} := \frac{w_b \cdot x_{f_j}}{2} \cdot \left(L_{des} - x_{f_j}\right) \qquad V_{barrier_j} := \left| w_b \cdot \left(\frac{L_{des}}{2} - x_{f_j}\right) \right|$$

$M_{barrier} =$ k·ft

	1
1	0.0
2	1.8
3	2.5
4	4.5
5	5.9
6	6.8
7	7.0
8	6.8
9	5.9
10	4.5
11	2.5
12	1.8
13	0.0

$M_{barrier} :=$ k·ft

$$\begin{pmatrix} -5.50 \\ -2.74 \\ -2.53 \\ -0.21 \\ 1.44 \\ 2.43 \\ 2.76 \\ 2.43 \\ 1.44 \\ -0.21 \\ -2.53 \\ -2.74 \\ -5.50 \end{pmatrix}$$

$V_{barrier} =$ k

	1
1	1.1
2	1.0
3	0.9
4	0.7
5	0.4
6	0.2
7	0.0
8	0.2
9	0.4
10	0.7
11	0.9
12	1.0
13	1.1

$V_{barrier} :=$ k

$$\begin{pmatrix} 1.22 \\ 1.00 \\ 0.98 \\ 0.73 \\ 0.49 \\ 0.24 \\ 0.00 \\ 0.24 \\ 0.49 \\ 0.73 \\ 0.98 \\ 1.00 \\ 1.22 \end{pmatrix}$$

Future Wearing Surface(Composite Dead Load):

$w_{fws} = 0.02 \frac{k}{ft^2}$ $\quad$ Per Beam: $w_f := \frac{Width_{gtg} \cdot w_{fws}}{N_g}$ $\quad w_f = 0.113 \frac{k}{ft}$

$$M_{fws_j} := \frac{w_f \cdot x_{f_j}}{2} \cdot \left(L_{des} - x_{f_j}\right) \qquad V_{fws_j} := \left| w_f \cdot \left(\frac{L_{des}}{2} - x_{f_j}\right) \right|$$

$M_{fws} =$ k·ft

	1
1	0.0
2	2.3
3	3.3
4	5.9
5	7.7
6	8.9
7	9.2
8	8.9
9	7.7
10	5.9
11	3.3
12	2.3
13	0.0

$M_{fws} :=$ k·ft

$$\begin{pmatrix} -5.93 \\ -2.94 \\ -2.72 \\ -0.23 \\ 1.55 \\ 2.62 \\ 2.98 \\ 2.62 \\ 1.55 \\ -0.23 \\ -2.72 \\ -2.94 \\ -5.93 \end{pmatrix}$$

$V_{fws} =$ k

	1
1	1.4
2	1.3
3	1.2
4	0.9
5	0.6
6	0.3
7	0.0
8	0.3
9	0.6
10	0.9
11	1.2
12	1.3
13	1.4

$V_{fws} :=$ k

$$\begin{pmatrix} 1.32 \\ 1.08 \\ 1.06 \\ 0.79 \\ 0.53 \\ 0.26 \\ 0.00 \\ 0.26 \\ 0.53 \\ 0.79 \\ 1.06 \\ 1.08 \\ 1.32 \end{pmatrix}$$

Live Load Moments (HL-93):

Determine Live Load Distribution Factors:

Longitudinal stiffness parameter - (4.6.2.2.1-1) $n_{bd} := \frac{E_{cbeamf}}{E_{cdeck}}$ $n_{bd} = 1.1594$

$e_g := h - y_b + h_{stprop} + \frac{t_{sLL}}{2}$ $e_g = 9.58\,in$ $K_g := n_{bd}\cdot\left(I + A\cdot e_g^{\,2}\right)$ $K_g = 8.8202 \times 10^4\,in^4$

Skew correction factor for moment, interior and exterior beams -

$$c_1 := if\left[\theta < 30, 0, 0.25\cdot\left(\frac{K_g}{12\cdot\frac{L_{des}}{12}\cdot t_{sLL}^{\,3}}\right)^{0.25}\cdot\left(\frac{S}{L_{des}}\right)^{0.5}\right]$$ $c_1 = 0.000000$ $A = 738\,in^2$

$skew_m := 1 - c_1\cdot\tan(if(\theta > 60\cdot deg, 60\cdot deg, \theta\cdot deg))^{1.5}$ $skew_m = 1.000$

Skew correction factor for shear, interior and exterior beams -

$$skew_{sh} := 1 + 0.20\cdot\left(\frac{12\cdot\frac{L_{des}}{12}\cdot t_{sLL}^{\,3}}{K_g}\right)^{0.3}\cdot\tan(\theta\cdot deg)$$ $skew_{sh} = 1.000$

LLDF for moment, interior beams -

One lane loaded -

$$g_{int\_moment_{1,1}} := skew_m\cdot\left[0.06 + \left(\frac{S}{14\cdot ft}\right)^{0.4}\cdot\left(\frac{S}{L_{des}}\right)^{0.3}\cdot\left(\frac{K_g}{12.0\cdot\frac{L_{des}}{12}\cdot t_{sLL}^{\,3}}\right)^{0.1}\right]$$

Two or more lanes loaded -

$$g_{int\_moment_{1,2}} := skew_m\cdot\left[0.075 + \left(\frac{S}{9.5\cdot ft}\right)^{0.6}\cdot\left(\frac{S}{L_{des}}\right)^{0.2}\cdot\left(\frac{K_g}{12.0\cdot\frac{L_{des}}{12}\cdot t_{sLL}^{\,3}}\right)^{0.1}\right]$$ $g_{int\_moment} = (0.535 \quad 0.660)$

ONE LANE TWO+ LANES

$DF_{m\_int} := if\left(g_{int\_moment_{1,1}} > g_{int\_moment_{1,2}}, g_{int\_moment_{1,1}}, g_{int\_moment_{1,2}}\right)$

LLDF for shear, interior beams -

$K_g = 8.8202 \times 10^4\,in^4$ $Check\_K_g := if\left(K_g < 10000\cdot in^4, "NG", if\left(K_g > 7000000\cdot in^4, "NG", "OK"\right)\right)$

$Check\_K_g = "OK"$

One lane loaded -

$$g_{int\_shear_{1,1}} := skew_{sh}\cdot\left(0.36 + \frac{S}{25\cdot ft}\right)$$

Two or more lanes loaded -

$$g_{int\_shear_{1,2}} := skew_{sh}\cdot\left[0.2 + \frac{S}{12\cdot ft} - \left(\frac{S}{35\cdot ft}\right)^{2.0}\right]$$ $g_{int\_shear} = (0.600 \quad 0.671)$

ONE LANE TWO+ LANES

$DF_{sh\_int} := if\left(g_{int\_shear_{1,1}} > g_{int\_shear_{1,2}}, g_{int\_shear_{1,1}}, g_{int\_shear_{1,2}}\right)$

LLDF for moment, exterior beams -

One lane loaded - Lever rule, w/ multiple presence factor -

$$g_{ext\_moment_{1,1}} := skew_m \cdot \left[1.2 \cdot \left[0.5 \cdot \left[\frac{S - (2 \cdot ft - d_e)}{S} + \frac{S - (8 \cdot ft - d_e)}{S} \right] \right] \right]$$

$$g_{ext\_moment_{1,1}} := if\left[S < 8 \cdot ft - d_e, skew_m \cdot \left[1.2 \cdot \left[0.5 \cdot \left[\frac{S - (2 \cdot ft - d_e)}{S} \right] \right] \right], g_{ext\_moment_{1,1}} \right]$$

Two or more lanes loaded

$$e := 0.77 + \frac{d_e}{9.1 \cdot ft} \qquad e = 0.852$$

$$g_{ext\_moment_{1,2}} := e \cdot g_{int\_moment_{1,2}}$$

$$g_{ext\_moment} = (0.474 \quad 0.562)$$

ONE LANE | TWO+ LANES

$$DF_{m\_ext} := if\left(g_{ext\_moment_{1,1}} > g_{ext\_moment_{1,2}}, g_{ext\_moment_{1,1}}, g_{ext\_moment_{1,2}} \right)$$

LLDF for shear, exterior beams -

One lane loaded - Lever rule, w/ multiple presence factor -

$$g_{ext\_shear_{1,1}} := skew_{sh} \cdot \left[1.2 \cdot \left[0.5 \cdot \left[\frac{S - (2 \cdot ft - d_e)}{S} + \frac{S - (8 \cdot ft - d_e)}{S} \right] \right] \right]$$

$$g_{ext\_shear_{1,1}} := if\left[S < 8 \cdot ft - d_e, skew_{sh} \cdot \left[1.2 \cdot \left[0.5 \cdot \left[\frac{S - (2 \cdot ft - d_e)}{S} \right] \right] \right], g_{ext\_shear_{1,1}} \right]$$

Two or more lanes loaded -

$$e := 0.6 + \frac{d_e}{10 \cdot ft} \qquad e = 0.6744$$

$$g_{ext\_shear_{1,2}} := e \cdot g_{int\_shear_{1,2}}$$

$$g_{ext\_shear} = (0.474 \quad 0.452)$$

ONE LANE | TWO+ LANES

$$DF_{sh\_ext} := if\left(g_{ext\_shear_{1,1}} > g_{ext\_shear_{1,2}}, g_{ext\_shear_{1,1}}, g_{ext\_shear_{1,2}} \right)$$

$$DF_m := if\left(beam = "interior", DF_{m\_int}, DF_{m\_ext} \right) \qquad DF_m = 0.660$$

$$DF_v := if\left(beam = "interior", DF_{sh\_int}, DF_{sh\_ext} \right) \qquad DF_v = 0.671$$

Modified Moment and Shear Distribution Factors:

Input the appropriate distribution factors based on slab-span behavior.

$DF_m := 0.507$ $DF_v := 0.507$

(LRFD 3.6.1.2)

Maximum Moments Due to Design Truck or Design Tandem and Design Lane:

Due to the Design Truck:

A closed-form solution for the maximum moment at any point along a simply-supported beam due to the LRFD design truck is given below.

$L := L_{des}$ (purely to condense the expression)

$$M_{truck_j} := \text{if}\left[x_{f_j} \le \frac{L}{3}, \frac{1\cdot k\cdot x_{f_j}}{L}\cdot\left(72\cdot L - 72\cdot x_{f_j} - 672\cdot ft\right), \frac{1\cdot k}{L}\cdot\left[-72\cdot\left(x_{f_j}\right)^2 + 72\cdot x_{f_j}\cdot L - 336\cdot ft\cdot x_{f_j} - 112\cdot ft\cdot L\right]\right]$$

Due to the Design Tandem:

$$M_{tandem_j} := \frac{1\cdot k\cdot x_{f_j}}{L}\cdot\left(50\cdot L - 50\cdot x_{f_j} - 100.0\cdot ft\right)$$

Due to the Design Lane:

$$M_{lane_j} := \frac{w_{lane}\cdot x_{f_j}}{2}\cdot\left(L - x_{f_j}\right)$$

M_{truck} =

	1
1	0.0
2	70.3
3	98.0
4	159.4
5	184.0
6	194.2
7	179.0
8	127.0
9	38.4
10	-87.0
11	-249.2
12	-309.5
13	-448.0

k·ft

M_{tandem} =

	1
1	0.0
2	73.7
3	104.8
4	184.0
5	237.8
6	266.0
7	268.8
8	246.0
9	197.8
10	124.0
11	24.8
12	-12.8
13	-100.0

k·ft

M_{lane} =

	1
1	0.0
2	13.1
3	18.7
4	33.3
5	43.7
6	49.9
7	52.0
8	49.9
9	43.7
10	33.3
11	18.7
12	13.1
13	0.0

k·ft

Live Load Shears:

$$V_{truck_j} := \frac{1\cdot k}{L}\cdot\left(72\cdot L - 72\cdot x_{f_j} - 672\cdot ft\right)$$

$$V_{tandem_j} := \frac{1\cdot k}{L}\cdot\left(50\cdot L - 50\cdot x_{f_j} - 100\cdot ft\right)$$

$$V_{lane_j} := \frac{w_{lane}\cdot\left(L - x_{f_j}\right)^2}{2\cdot L}$$

V_{truck} =

	1
1	45.6
2	40.8
3	38.4
4	31.2
5	24.0
6	16.8
7	9.6
8	2.4
9	-4.8
10	-12.0
11	-19.2
12	-21.5
13	-26.4

k

V_{tandem} =

	1
1	46.1
2	42.7
3	41.1
4	36.1
5	31.1
6	26.1
7	21.1
8	16.1
9	11.1
10	6.1
11	1.1
12	-0.5
13	-3.9

k

V_{lane} =

	1
1	8.2
2	7.1
3	6.6
4	5.2
5	4.0
6	2.9
7	2.0
8	1.3
9	0.7
10	0.3
11	0.1
12	0.0
13	0.0

k

Modified live load moments and shears

Based on continuous beam behavior (Loads taken from BTBEAM run).
These moments will replace the simply-supported moments calculated on the previous page.

$$M_{truck.pos} := \begin{pmatrix} 21.02 \\ 49.77 \\ 52.07 \\ 85.31 \\ 127.57 \\ 148.15 \\ 146.02 \\ 148.15 \\ 127.57 \\ 85.31 \\ 52.07 \\ 49.77 \\ 21.02 \end{pmatrix} \cdot k \cdot ft \qquad M_{tandem.pos} := \begin{pmatrix} 27.11 \\ 33.74 \\ 34.27 \\ 99.39 \\ 148.44 \\ 177.25 \\ 183.49 \\ 177.25 \\ 148.41 \\ 99.39 \\ 34.90 \\ 34.32 \\ 27.13 \end{pmatrix} \cdot k \cdot ft \qquad M_{lane.pos} := \begin{pmatrix} 5.13 \\ 5.44 \\ 5.46 \\ 12.83 \\ 24.05 \\ 31.05 \\ 33.38 \\ 31.04 \\ 24.05 \\ 12.83 \\ 5.46 \\ 5.44 \\ 5.13 \end{pmatrix} \cdot k \cdot ft$$

$$M_{truck.neg} := \begin{pmatrix} -144.19 \\ -88.02 \\ -83.53 \\ -56.84 \\ -47.78 \\ -38.84 \\ -29.90 \\ -38.83 \\ -47.77 \\ -56.84 \\ -83.53 \\ -88.02 \\ -144.20 \end{pmatrix} \cdot k \cdot ft \qquad M_{tandem.neg} := \begin{pmatrix} -113.44 \\ -87.94 \\ -85.90 \\ -73.34 \\ -60.78 \\ -48.22 \\ -35.67 \\ -48.22 \\ -60.78 \\ -73.34 \\ -85.89 \\ -87.93 \\ -113.34 \end{pmatrix} \cdot k \cdot ft \qquad M_{lane.neg} := \begin{pmatrix} -43.57 \\ -24.43 \\ -22.90 \\ -13.94 \\ -13.49 \\ -13.49 \\ -13.49 \\ -13.49 \\ -13.49 \\ -13.94 \\ -22.90 \\ -24.43 \\ -43.57 \end{pmatrix} \cdot k \cdot ft$$

$$V_{truck} := \begin{pmatrix} 47.53 \\ 42.40 \\ 41.96 \\ 35.49 \\ 28.79 \\ 23.25 \\ 19.07 \\ 23.25 \\ 28.79 \\ 35.49 \\ 41.92 \\ 42.37 \\ 47.93 \end{pmatrix} \cdot k \qquad V_{tandem} := \begin{pmatrix} 47.08 \\ 43.15 \\ 42.84 \\ 37.84 \\ 32.33 \\ 26.53 \\ 20.68 \\ 26.53 \\ 32.33 \\ 37.84 \\ 42.83 \\ 43.15 \\ 47.09 \end{pmatrix} \cdot k \qquad V_{lane} := \begin{pmatrix} 9.52 \\ 7.97 \\ 7.85 \\ 6.33 \\ 4.98 \\ 3.81 \\ 2.84 \\ 3.81 \\ 4.98 \\ 6.33 \\ 7.85 \\ 7.97 \\ 9.52 \end{pmatrix} \cdot k$$

Maximum Service Live Load Moments and Shears (HL-93):

The dynamic load allowance (DLA) is applied to the truck or tandem portion only:

$M_{t.pos_j} := if\left(M_{truck.pos_j} > M_{tandem.pos_j}, M_{truck.pos_j}, M_{tandem.pos_j}\right)$ $\quad V_{t_j} := if\left(V_{truck_j} > V_{tandem_j}, V_{truck_j}, V_{tandem_j}\right)$

$M_{LL.pos_j} := DF_m \cdot \left[M_{lane.pos_j} + (1 + DLA) \cdot M_{t.pos_j}\right]$ $\quad V_{LL_j} := DF_v \cdot \left[V_{lane_j} + (1 + DLA) \cdot V_{t_j}\right]$

$M_{t.neg_j} := if\left(M_{truck.neg_j} < M_{tandem.neg_j}, M_{truck.neg_j}, M_{tandem.neg_j}\right)$

$M_{LL.neg_j} := DF_m \cdot \left[M_{lane.neg_j} + (1 + DLA) \cdot M_{t.neg_j}\right]$

$M_{LL.pos} =$

	1
1	20.9
2	36.3
3	37.9
4	73.5
5	112.3
6	135.3
7	140.7
8	135.3
9	112.3
10	73.5
11	37.9
12	36.3
13	20.9

k·ft

$M_{LL.neg} =$

	1
1	-119.3
2	-71.7
3	-69.5
4	-56.5
5	-47.8
6	-39.4
7	-30.9
8	-39.4
9	-47.8
10	-56.5
11	-69.5
12	-71.7
13	-119.3

k·ft

$V_{LL} =$

	1
1	36.9
2	33.1
3	32.9
4	28.7
5	24.3
6	19.8
7	15.4
8	19.8
9	24.3
10	28.7
11	32.9
12	33.1
13	37.1

k

Restraint Moment from Hand Calculations:

Positve restraint moments were calculated 20 years after the continuity pour was made, assuming assuming that the beams were 28 days old when the continuity pour was made.

$$M_{rm.pos} := \begin{pmatrix} 0.0 \\ 0.0 \\ 0.0 \\ 0.0 \\ 0.0 \\ 0.0 \\ 0.0 \\ 0.0 \\ 0.0 \\ 0.0 \\ 0.0 \\ 0.0 \\ 0.0 \end{pmatrix} \cdot k \cdot ft$$

Negative restraint moments were calculated 100 days after the continuity pour was made, assuming that the beams were 90 days old when the continuity pour was made.

$$M_{rm.neg} := \begin{pmatrix} -358.0 \\ -358.0 \\ -358.0 \\ -358.0 \\ -358.0 \\ -358.0 \\ -358.0 \\ -358.0 \\ -358.0 \\ -358.0 \\ -358.0 \\ -358.0 \\ -358.0 \end{pmatrix} \cdot k \cdot ft$$

B.1.4 Strength and Service Limit Checks (B-22 through B-39)

This section of the calculations used the moments that had been calculated previously to calculate the stresses in the top and bottom of the precast section due to the self weight of the precast section, weight of the deck, weight of the barriers, weight of the future wearing surface, live loads, and restraint moments. In addition, prestress losses due to shrinkage, creep, and steel relaxation were calculated and then used to calculate the stresses in the top and bottom of the precast section due to the prestressing force. The calculated stresses were used to check the service limit states; maximum tensile stresses in the bottom of the precast section, and maximum compressive stresses in the top of the precast section. The stresses due to restraint moments were not considered during the service compression checks because it was felt that there was enough reserve capacity to say that each check was okay by inspection.

The remainder of this section used the user inputs and section properties to calculate the design flexural capacity of the composite section. This capacity was compared to the maximum factored moment that would be applied to the section to ensure that the section had adequate flexural strength. An additional check was performed to ensure that there was enough steel reinforcement within the section to guard against abrupt flexural failure immediately after cracking.

Strand Pattern Design

$$Dep\_Pt := Dep\_Frac \cdot L_{des} + \frac{L_{ovr} - L_{des}}{2}$$

$Dep\_Pt = 0.583\,ft$ (distance measured from end of beam)

$$EPat\_n = \begin{pmatrix} 0 \\ 0 \\ 0 \\ 0 \\ 0 \\ 0 \\ 0 \\ 0 \\ 0 \\ 0 \\ 8 \\ 8 \end{pmatrix} \quad EPat\_h = \begin{pmatrix} 0.0 \\ 0.0 \\ 0.0 \\ 0.0 \\ 0.0 \\ 0.0 \\ 0.0 \\ 0.0 \\ 0.0 \\ 0.0 \\ 4.0 \\ 2.0 \end{pmatrix} in \qquad MPat\_n = \begin{pmatrix} 0 \\ 0 \\ 0 \\ 0 \\ 0 \\ 0 \\ 0 \\ 0 \\ 0 \\ 0 \\ 8 \\ 8 \end{pmatrix} \quad MPat\_h = \begin{pmatrix} 0.0 \\ 0.0 \\ 0.0 \\ 0.0 \\ 0.0 \\ 0.0 \\ 0.0 \\ 0.0 \\ 0.0 \\ 0.0 \\ 4.0 \\ 2.0 \end{pmatrix} in$$

End Pattern | Mid Pattern

$$No\_Strands := \sum EPat\_n \qquad i := 1 .. last(EPat\_n)$$

$$y_{end} := \frac{\sum_i \left(EPat\_n_i \cdot EPat\_h_i\right)}{No\_Strands} \qquad y_{end} = 3.00\,in$$

$$y_{mid} := \frac{\sum_i \left(MPat\_n_i \cdot MPat\_h_i\right)}{No\_Strands} \qquad y_{mid} = 3.00\,in$$

$$j := 1 .. 13$$

$$y_{cg_j} := if\left[x_{r_j} \le Dep\_Pt, y_{end} - \left(\frac{x_{r_j}}{Dep\_Pt}\right) \cdot \left(y_{end} - y_{mid}\right), y_{mid}\right]$$

$$ecc_j := y_b - y_{cg_j}$$

$y_{cg} =$

	1
1	3.00
2	3.00
3	3.00
4	3.00
5	3.00
6	3.00
7	3.00
8	3.00
9	3.00
10	3.00
11	3.00
12	3.00
13	3.00

in

$ecc =$

	1
1	2.42
2	2.42
3	2.42
4	2.42
5	2.42
6	2.42
7	2.42
8	2.42
9	2.42
10	2.42
11	2.42
12	2.42
13	2.42

in

Flexural Stresses Due to Loads:

Note: Since for a simple-span structural system of this type, it is unlikely that compression at the top of the deck at a given section would exceed its allowable value, calculation of those stresses will be omitted for simplicity. Only the stresses at the bottom and top of the precast beam itself will be computed. Sign convention is + compression nd - tension.

Beam Self-Weight at Release:

$$f_{swrt_j} := \frac{M_{swr_j}}{S_t}$$

$f_{swrt} =$

	1
1	51.5
2	204.7
3	249.8
4	404.0
5	514.1
6	580.2
7	602.2
8	580.2
9	514.1
10	404.0
11	249.8
12	204.7
13	51.5

psi

$$f_{swrb_j} := -\frac{M_{swr_j}}{S_b}$$

$f_{swrb} =$

	1
1	-44.8
2	-177.8
3	-216.9
4	-350.9
5	-446.5
6	-503.9
7	-523.0
8	-503.9
9	-446.5
10	-350.9
11	-216.9
12	-177.8
13	-44.8

psi

Beam Self-Weight at Final:

$$f_{swt_j} := \frac{M_{swf_j}}{S_t}$$

$f_{swt} =$

	1
1	0.0
2	138.9
3	198.2
4	352.4
5	462.6
6	528.7
7	550.7
8	528.7
9	462.6
10	352.4
11	198.2
12	138.9
13	0.0

psi

$$f_{swb_j} := -\frac{M_{swf_j}}{S_b}$$

$f_{swb} =$

	1
1	0.0
2	-120.7
3	-172.2
4	-306.1
5	-401.8
6	-459.1
7	-478.3
8	-459.1
9	-401.8
10	-306.1
11	-172.2
12	-120.7
13	0.0

psi

Diaphragm Weight:

$$f_{diapht_j} := \frac{M_{diaph_j}}{S_t}$$

$f_{diapht} =$

	1
1	0.0
2	0.0
3	0.0
4	0.0
5	0.0
6	0.0
7	0.0
8	0.0
9	0.0
10	0.0
11	0.0
12	0.0
13	0.0

psi

$$f_{diaphb_j} := -\frac{M_{diaph_j}}{S_b}$$

$f_{diaphb} =$

	1
1	0.0
2	0.0
3	0.0
4	0.0
5	0.0
6	0.0
7	0.0
8	0.0
9	0.0
10	0.0
11	0.0
12	0.0
13	0.0

psi

Deck Weight:

$$f_{deckt_j} := \frac{M_{deck_j}}{S_t}$$

$f_{deckt} =$

	1
1	0.0
2	101.7
3	145.1
4	257.9
5	338.5
6	386.8
7	402.9
8	386.8
9	338.5
10	257.9
11	145.1
12	101.7
13	0.0

psi

$$f_{deckb_j} := \frac{M_{deck_j}}{S_b}$$

$f_{deckb} =$

	1
1	0.0
2	-88.3
3	-126.0
4	-224.0
5	-294.0
6	-336.0
7	-350.0
8	-336.0
9	-294.0
10	-224.0
11	-126.0
12	-88.3
13	0.0

psi

Wearing Course Weight:

$$f_{wct_j} := \frac{M_{wc_j}}{S_{tcbDC2}}$$

$f_{wct} =$

	1
1	0.0
2	0.0
3	0.0
4	0.0
5	0.0
6	0.0
7	0.0
8	0.0
9	0.0
10	0.0
11	0.0
12	0.0
13	0.0

psi

$$f_{wcb_j} := \frac{M_{wc_j}}{S_{bcDC2}}$$

$f_{wcb} =$

	1
1	0.0
2	0.0
3	0.0
4	0.0
5	0.0
6	0.0
7	0.0
8	0.0
9	0.0
10	0.0
11	0.0
12	0.0
13	0.0

psi

Barriers:

$$f_{barriert_j} := \frac{M_{barrier_j}}{S_{tcbDC2}}$$

$f_{barriert} =$

	1
1	-5.6
2	-2.8
3	-2.6
4	-0.2
5	1.5
6	2.5
7	2.8
8	2.5
9	1.5
10	-0.2
11	-2.6
12	-2.8
13	-5.6

psi

$$f_{barrierb_j} := \frac{M_{barrier_j}}{S_{bcDC2}}$$

$f_{barrierb} =$

	1
1	16.8
2	8.4
3	7.7
4	0.6
5	-4.4
6	-7.4
7	-8.4
8	-7.4
9	-4.4
10	0.6
11	7.7
12	8.4
13	16.8

psi

Future Wearing Surface:

$$f_{fwst_j} := \frac{M_{fws_j}}{S_{tcbLL}}$$

$f_{fwst} =$

	1
1	-6.0
2	-3.0
3	-2.8
4	-0.2
5	1.6
6	2.7
7	3.0
8	2.7
9	1.6
10	-0.2
11	-2.8
12	-3.0
13	-6.0

psi

$$f_{fwsb_j} := -\frac{M_{fws_j}}{S_{bcLL}}$$

$f_{fwsb} =$

	1
1	18.1
2	9.0
3	8.3
4	0.7
5	-4.7
6	-8.0
7	-9.1
8	-8.0
9	-4.7
10	0.7
11	8.3
12	9.0
13	18.1

psi

Live Load I (for Service Limit State I):

$$f_{LL\_It.pos_j} := \frac{M_{LL.pos_j}}{S_{tcbLL}}$$

$f_{LL\_It.pos} =$

	1
1	21.2
2	36.8
3	38.4
4	74.5
5	113.8
6	137.0
7	142.5
8	137.0
9	113.7
10	74.5
11	38.4
12	36.8
13	21.2

psi

$$f_{LL\_Ib.neg_j} := -\frac{M_{LL.neg_j}}{S_{bcLL}}$$

$f_{LL\_Ib.neg} =$

	1
1	365
2	219.4
3	212.7
4	172.9
5	146.3
6	120.4
7	94.5
8	120.4
9	146.3
10	172.9
11	212.7
12	219.4
13	365

psi

Live Load III (for Service Limit State III):

$$f_{LL\_IIIb.pos_j} := -\frac{(0.8 \cdot M_{LL.pos})_j}{S_{bcLL}}$$

$f_{LL\_IIIb.pos} =$

	1
1	-51.1
2	-88.9
3	-92.7
4	-179.9
5	-274.8
6	-331.0
7	-344.2
8	-331.0
9	-274.7
10	-179.9
11	-92.7
12	-88.9
13	-51.1

psi

$$f_{LL\_IIIt.neg_j} := \frac{(0.8 \cdot M_{LL.neg})_j}{S_{tcbLL}}$$

$f_{LL\_IIIt.neg} =$

	1
1	-96.7
2	-58.1
3	-56.4
4	-45.8
5	-38.8
6	-31.9
7	-25.0
8	-31.9
9	-38.8
10	-45.8
11	-56.4
12	-58.1
13	-96.7

psi

Restraint Moments:

Stress at bottom of beam due to + RM:

$$f_{rm\_b.pos_j} := \frac{M_{rm.pos_j}}{S_{bcLL}}$$

$f_{rm\_b.pos} =$

	1
1	0
2	0
3	0
4	0
5	0
6	0
7	0
8	0
9	0
10	0
11	0
12	0
13	0

psi

Stress at top of beam due to - RM:

$$f_{rm\_t.neg_j} := \frac{M_{rm.neg_j}}{S_{tcbLL}}$$

$f_{rm\_t.neg} =$

	1
1	-362.7153
2	-362.7153
3	-362.7153
4	-362.7153
5	-362.7153
6	-362.7153
7	-362.7153
8	-362.7153
9	-362.7153
10	-362.7153
11	-362.7153
12	-362.7153
13	-362.7153

psi

Check Initial Prestress Force:

$P_{jack} := Pull \cdot f_{pu} \cdot No\_Strands \cdot A_{strand}$ $P_{jack} = 496\,k$ $Max\_P_{jack} := 2000 \cdot k$

$Check\_Max\_P_{jack} := if(P_{jack} \le Max\_P_{jack}, "OK", "NG")$ $Check\_Max\_P_{jack} = "OK"$

$P_{hdtotal} := (Pull \cdot f_{pu} \cdot No\_Draped \cdot A_{strand}) \cdot \sin\left(\operatorname{atan}\left(\frac{dr\_cg_{end} - dr\_cg_{mid}}{Dep\_Pt}\right)\right)$ $P_{hdtotal} = 0.0\,k$

$Max\_P_{hdtotal} := 25 \cdot k$ $Max\_P_{hdsingle} := 6 \cdot k$

$Chk\_Max\_P_{hdtotal} := if(P_{hdtotal} \le Max\_P_{hdtotal}, "OK", "Use mult. holddowns")$ $Chk\_Max\_P_{hdtotal} = "OK"$

$Chk\_Max\_P_{hdsingle} := if\left(\frac{P_{hdtotal}}{No\_Draped} \le Max\_P_{hdsingle}, "OK", "Use mult. holddowns"\right)$

$Chk\_Max\_P_{hdsingle} = "OK"$

Prestress Losses at Release:

Relaxation: $f_{pj} := Pull \cdot f_{pu}$ $f_{pj} = 202.5\,ksi$ $f_{py} := 0.9 \cdot f_{pu}$ $f_{py} = 243.0\,ksi$ Assume: $t := 18 \cdot hr$

$\Delta f_{pR1} := \frac{\log\left(\frac{t}{hr}\right)}{40.0} \cdot \left(\frac{f_{pj}}{f_{py}} - 0.55\right) \cdot f_{pj}$ $\Delta f_{pR1} = 1800.5\,psi$ (LRFD 5.9.5.4.4b-2)

Elastic Shortening: (LRFD 5.9.5.2.3a)

$E_{ci} := \left(1265 \cdot \sqrt{f_{ci}} + 1000 \cdot \frac{k^{0.5}}{in}\right) \cdot ksi^{0.5}$ $E_{ci} = 3683.5\,ksi$

$\Delta f_{pES} := \frac{\left[No\_Strands \cdot A_{strand} \cdot (f_{pj} - \Delta f_{pR1}) \cdot \left[I + (ecc_7)^2 \cdot A\right]\right] - ecc_7 \cdot M_{swr_7} \cdot A}{\left[No\_Strands \cdot A_{strand} \cdot \left[I + (ecc_7)^2 \cdot A\right]\right] + \frac{A \cdot I \cdot E_{ci}}{E_p}}$

(Alternative Equation C5.9.5.2.3a-1 from LRFD C5.9.5.2.3a)

$\Delta f_{pES} = 5.6966\,ksi$

$f_i := f_{pj} - \Delta f_{pES} - \Delta f_{pR1}$ $f_i = 195.00\,ksi$

$P_i := No\_Strands \cdot A_{strand} \cdot f_i$ $P_i = 477.4\,k$

$S_{cgp} := \frac{I}{y_b - y_{mid}}$ $S_{cgp} = 3465\,in^3$

$f_{cgp} := P_i \cdot \left(\frac{1}{A} + \frac{ecc_7}{S_{cgp}}\right) - \frac{M_{swr_7}}{S_{cgp}}$ $f_{cgp} = 736.25\,psi$

Total Prestress Losses at Release:

$\Delta f_{PTR} := \Delta f_{pES} + \Delta f_{pR1}$ $\Delta f_{PTR} = 7.5\,ksi$

Stresses Due to Prestress at Release:

$f_{per} := f_{pj} - \Delta f_{pES} - \Delta f_{pR1}$ $\quad f_{per} = 195.0\,ksi$

$P_{re} := f_{per} \cdot No\_Strands \cdot A_{strand}$ $\quad P_{re} = 477.4\,k$

$j := 1 .. 13$

$$f_{psrb_j} := if\left[x_{r_j} < 60 \cdot d_{str}, P_{re} \cdot \left(\frac{1}{A} + \frac{ecc_j}{S_b}\right) \cdot \left(\frac{x_{r_j}}{60 \cdot d_{str}}\right), if\left[x_{r_j} > L_{ovr} - 60 \cdot d_{str}, P_{re} \cdot \left(\frac{1}{A} + \frac{ecc_j}{S_b}\right) \cdot \left(\frac{L_{ovr} - x_{r_j}}{60 \cdot d_{str}}\right), P_{re} \cdot \left(\frac{1}{A} + \frac{ecc_j}{S_b}\right)\right]\right]$$

$$f_{psrt_j} := if\left[x_{r_j} < 60 \cdot d_{str}, P_{re} \cdot \left(\frac{1}{A} - \frac{ecc_j}{S_t}\right) \cdot \left(\frac{x_{r_j}}{60 \cdot d_{str}}\right), if\left[x_{r_j} > L_{ovr} - 60 \cdot d_{str}, P_{re} \cdot \left(\frac{1}{A} - \frac{ecc_j}{S_t}\right) \cdot \left(\frac{L_{ovr} - x_{r_j}}{60 \cdot d_{str}}\right), P_{re} \cdot \left(\frac{1}{A} - \frac{ecc_j}{S_t}\right)\right]\right]$$

$f_{psrb} =$

	1
1	317.6
2	1361.1
3	1361.1
4	1361.1
5	1361.1
6	1361.1
7	1361.1
8	1361.1
9	1361.1
10	1361.1
11	1361.1
12	1361.1
13	317.6

psi

$f_{psrt} =$

	1
1	-41.0
2	-175.6
3	-175.6
4	-175.6
5	-175.6
6	-175.6
7	-175.6
8	-175.6
9	-175.6
10	-175.6
11	-175.6
12	-175.6
13	-41.0

psi

Check Stresses at Release:

Top of girder (tension):

$f_{rt_j} := f_{psrt_j} + f_{swrt_j}$

$f_{allow\_rt} := -0.24 \cdot \sqrt{f_{ci}} \cdot \sqrt{ksi}$ (LRFD Table 5.9.4.1.2-1)

$f_{allow\_rt} = -509.1\,psi$

$Status\_ServiceLSrt_j := if\left(f_{rt_j} \geq f_{allow\_rt}, "OK", "NG"\right)$

Note: Normally Mn/DOT assumes that there is no bonded reinforcement in the precompressed tensile zone and limits the initial tension stress to 0.2 ksi. However, 0.2 ksi seems too conservative for this section, so tension reinforcement will be designed in the the top of the section so that the higher allowable tension stress can be used.

$f_{rt} =$ psi

	1
1	10.6
2	29.1
3	74.2
4	228.4
5	338.5
6	404.6
7	426.7
8	404.6
9	338.5
10	228.4
11	74.2
12	29.1
13	10.6

Status_ServiceLSrt =

	1
1	"OK"
2	"OK"
3	"OK"
4	"OK"
5	"OK"
6	"OK"
7	"OK"
8	"OK"
9	"OK"
10	"OK"
11	"OK"
12	"OK"
13	"OK"

Bottom of girder (compression):

$f_{rb_j} := f_{psrb_j} + f_{swrb_j}$

$f_{allow\_rc} := 0.6 \cdot f_{ci}$ (LRFD 5.9.4.1)

$Status\_ServiceLSrc_j := if\left(f_{rb_j} \le f_{allow\_rc}, "OK", "NG"\right)$

$f_{allow\_rc} = 2700.0$ psi

$f_{rb} =$ psi

	1
1	272.8
2	1183.4
3	1144.2
4	1010.3
5	914.6
6	857.2
7	838.1
8	857.2
9	914.6
10	1010.3
11	1144.2
12	1183.4
13	272.8

Status_ServiceLSrc =

	1
1	"OK"
2	"OK"
3	"OK"
4	"OK"
5	"OK"
6	"OK"
7	"OK"
8	"OK"
9	"OK"
10	"OK"
11	"OK"
12	"OK"
13	"OK"

Final Prestress Losses:

Shrinkage:

$\Delta f_{pSR} := (17.0 - 0.150 \cdot H) \cdot ksi$ $\Delta f_{pSR} = 6.05$ ksi (LRFD 5.9.5.4.2-1)

Creep:

$$S_{c\_cg} := \frac{I_{cDC2}}{y_{bcDC2} - y_{mid}} \qquad S_{c\_cg} = 5693\ in^3$$

$$\Delta f_{cdp} := \frac{M_{deck_7} + M_{diaph_7}}{S_{cgp}} + \frac{M_{barrier_7} + M_{wc_7} + M_{fws_7}}{S_{c\_cg}} \qquad \Delta f_{cdp} = 175.7\ psi$$

$\Delta f_{pCR} := 12.0 \cdot f_{cgp} - 7.0 \cdot \Delta f_{cdp}$ $\Delta f_{pCR} = 7.60$ ksi (LRFD 5.9.5.4.3-1)

Steel Relaxation:

For stress-relieved strands:

$\Delta f_{pR2} := 20.0 \cdot ksi - 0.4 \cdot \Delta f_{pES} - 0.2 \cdot (\Delta f_{pSR} + \Delta f_{pCR})$ (LRFD 5.9.5.4.4c-1)

For low-relaxation strands, take 30% of the above value:

$\Delta f_{pR2} := 0.3 \cdot [20.0 \cdot ksi - 0.4 \cdot \Delta f_{pES} - 0.2 \cdot (\Delta f_{pSR} + \Delta f_{pCR})]$ $\Delta f_{pR2} = 4497.1\ psi$

Total Prestress Loss:

$\Delta f_{PT} := \Delta f_{pES} + \Delta f_{pSR} + \Delta f_{pCR} + \Delta f_{pR2}$ $\Delta f_{PT} = 23.8\ ksi$

$\%Loss := \frac{\Delta f_{PT}}{Pull \cdot f_{pu}} \cdot 100$ $\%Loss = 11.78$

Check effective stress after losses:

$f_{pe} := Pull \cdot f_{pu} - \Delta f_{PT}$ $f_{pe} = 178.7\ ksi$

$f_{allow} := 0.80 \cdot f_{py}$ $f_{allow} = 194.4\ ksi$ (LRFD Table 5.9.3-1)

$Status\_ServiceLSsf := if(f_{pe} \le f_{allow}, "OK", "NG")$ Status_ServiceLSsf = "OK"

Stresses Due to Prestress:

$P_f := f_{pe} \cdot No\_Strands \cdot A_{strand}$ $P_f = 437.3\ k$

$j := 1 .. 13$

$$f_{psb_j} := \begin{cases} P_f \cdot \left(\frac{1}{A} + \frac{ecc_j}{S_b}\right) \cdot \left(\frac{\frac{L_{brng}}{2} + x_{f_j}}{60 \cdot d_{str}}\right) & \text{if } x_{f_j} + \frac{L_{brng}}{2} < 60 \cdot d_{str} \\ P_f \cdot \left(\frac{1}{A} + \frac{ecc_j}{S_b}\right) \cdot \left(\frac{L_{ovr} - x_{f_j} - \frac{L_{brng}}{2}}{60 \cdot d_{str}}\right) & \text{if } x_{f_j} + \frac{L_{brng}}{2} > L_{ovr} - 60 \cdot d_{str} \\ P_f \cdot \left(\frac{1}{A} + \frac{ecc_j}{S_b}\right) & \text{otherwise} \end{cases}$$

$f_{psb} =$ psi

	1
1	291.0
2	1151.4
3	1247.0
4	1247.0
5	1247.0
6	1247.0
7	1247.0
8	1247.0
9	1247.0
10	1247.0
11	1247.0
12	1151.4
13	291.0

$$f_{pst_j} := \begin{cases} P_f \cdot \left(\frac{1}{A} - \frac{ecc_j}{S_t}\right) \cdot \left(\frac{\frac{L_{brng}}{2} + x_{f_j}}{60 \cdot d_{str}}\right) & \text{if } x_{f_j} + \frac{L_{brng}}{2} < 60 \cdot d_{str} \\ P_f \cdot \left(\frac{1}{A} - \frac{ecc_j}{S_t}\right) \cdot \left(\frac{L_{ovr} - x_{f_j} - \frac{L_{brng}}{2}}{60 \cdot d_{str}}\right) & \text{if } x_{f_j} + \frac{L_{brng}}{2} > L_{ovr} - 60 \cdot d_{str} \\ P_f \cdot \left(\frac{1}{A} - \frac{ecc_j}{S_t}\right) & \text{otherwise} \end{cases}$$

$f_{pst} =$

	1
1	-37.5
2	-148.5
3	-160.9
4	-160.9
5	-160.9
6	-160.9
7	-160.9
8	-160.9
9	-160.9
10	-160.9
11	-160.9
12	-148.5
13	-37.5

psi

Check Service Limit States:

Service III Limit State (Tensile Stresses in Bottom of Beam):

$f_{allow\_ft} := -0.19 \cdot \sqrt{f_c} \cdot \sqrt{ksi}$

$f_{IIIb.pos_j} := f_{psb_j} + f_{swb_j} + f_{diaphb_j} + f_{deckb_j} + f_{wcb_j} + f_{barrierb_j} + f_{fwsb_j} + f_{rm\_b.pos_j} + f_{LL\_IIIb.pos_j}$

$Status\_ServiceLSft1_j := if\left(f_{IIIb.pos_j} \geq f_{allow\_ft}, "OK", "NG"\right)$ (LRFD Table 5.9.4.2.2-1)

$f_{allow\_ft} = -0.484\ ksi$

$f_{IIIb.pos} =$

	1
1	274.8
2	870.9
3	872.2
4	538.3
5	267.3
6	105.4
7	57.0
8	105.4
9	267.4
10	538.3
11	872.2
12	870.9
13	274.8

psi

$Status\_ServiceLSft1 =$

	1
1	"OK"
2	"OK"
3	"OK"
4	"OK"
5	"OK"
6	"OK"
7	"OK"
8	"OK"
9	"OK"
10	"OK"
11	"OK"
12	"OK"
13	"OK"

Service III Limit State (Tensile Stresses in Top of Beam):

$f_{allow\_ft} := -0.19 \cdot \sqrt{f_c} \cdot \sqrt{ksi}$

$f_{IIIb.neg_j} := f_{pst_j} + f_{swt_j} + f_{diapht_j} + f_{deckt_j} + f_{wct_j} + f_{barriert_j} + f_{fwst_j} + f_{rm\_t.neg_j} + f_{LL\_IIIt.neg_j}$

$Status\_ServiceLSft2_j := if\left(f_{IIIb.neg_j} \geq f_{allow\_ft}, "OK", "NG"\right)$ (LRFD Table 5.9.4.2.2-1)

$f_{allow\_ft} = -0.484\ ksi$

$f_{IIIb.neg} =$ psi

	1
1	-508.5
2	-334.6
3	-241.9
4	40.5
5	241.7
6	365.1
7	410.8
8	365.1
9	241.7
10	40.5
11	-241.9
12	-334.6
13	-508.5

5% over at beam ends
Say OK

$Status\_ServiceLSft2 =$

	1
1	"NG"
2	"OK"
3	"OK"
4	"OK"
5	"OK"
6	"OK"
7	"OK"
8	"OK"
9	"OK"
10	"OK"
11	"OK"
12	"OK"
13	"NG"

Stresses due to restraint moments were not considered in service compression checks. There is enought reserve capacity to say that each check is OK by inspection.

Service I (Compressive Stresses in Top of Beam):

1) Compressive Stress Due to Permanent Loads:

$f_{ldt_j} := f_{pst_j} + f_{swt_j} + f_{diapht_j} + f_{deckt_j} + f_{wct_j} + f_{barriert_j} + f_{fwst_j}$

$f_{allow\_fcd} := 0.45 \cdot f_c$ (LRFD Table 5.9.4.2.1-1)

$Status\_ServiceLSfcd_j := if\left(f_{ldt_j} \leq f_{allow\_fcd}, "OK", "NG"\right)$

$f_{allow\_fcd} = 2925.0\ psi$

$f_{ldt} =$ psi

	1
1	-49.1
2	86.3
3	177.1
4	449.0
5	643.2
6	759.7
7	798.6
8	759.7
9	643.2
10	449.0
11	177.1
12	86.3
13	-49.1

$Status\_ServiceLSfcd =$

	1
1	"OK"
2	"OK"
3	"OK"
4	"OK"
5	"OK"
6	"OK"
7	"OK"
8	"OK"
9	"OK"
10	"OK"
11	"OK"
12	"OK"
13	"OK"

2) Compressive Stress Due to Full Dead Load + Live Load (Top of Beam):

$f_{llt.pos_j} := f_{pst_j} + f_{swt_j} + f_{diapht_j} + f_{deckt_j} + f_{wct_j} + f_{barriert_j} + f_{fwst_j} + f_{LL\_lt.pos_j}$

$Status\_ServiceLSfcl_j := if\left(f_{llt.pos_j} \le f_{allow\_fcl}, "OK", "NG"\right)$

$f_{allow\_fcl} := 0.6 \cdot f_c$

(LRFD Table 5.9.4.2.1-1)

$f_{allow\_fcl} = 3900.0$ psi

$f_{llt.pos} =$

	1
1	-28.0
2	123.1
3	215.5
4	523.5
5	757.0
6	896.8
7	941.1
8	896.8
9	757.0
10	523.5
11	215.5
12	123.1
13	-27.9

psi

Status_ServiceLSfcl =

	1
1	"OK"
2	"OK"
3	"OK"
4	"OK"
5	"OK"
6	"OK"
7	"OK"
8	"OK"
9	"OK"
10	"OK"
11	"OK"
12	"OK"
13	"OK"

2) Compressive Stress Due to Full Dead Load + Live Load (Bottom of Beam):

$f_{llt.neg_j} := f_{psb_j} + f_{swb_j} + f_{diaphb_j} + f_{deckb_j} + f_{wcb_j} + f_{barrierb_j} + f_{fwsb_j} + f_{LL\_lb.neg_j}$

$Status\_ServiceLSfcl_j := if\left(f_{llt.neg_j} \le f_{allow\_fcl}, "OK", "NG"\right)$

$f_{allow\_fcl} := 0.6 \cdot f_c$

(LRFD Table 5.9.4.2.1-1)

$f_{allow\_fcl} = 3900.0$ psi

$f_{llt.neg} =$

	1
1	690.9
2	1179.2
3	1177.6
4	891.2
5	688.4
6	556.8
7	495.7
8	556.8
9	688.4
10	891.2
11	1177.6
12	1179.2
13	690.9

psi

Status_ServiceLSfcl =

	1
1	"OK"
2	"OK"
3	"OK"
4	"OK"
5	"OK"
6	"OK"
7	"OK"
8	"OK"
9	"OK"
10	"OK"
11	"OK"
12	"OK"
13	"OK"

3) Compressive Stress (Top of Beam) Due to Live Load + 0.5(Effective Prestress + Dead Load):

$f_{cfdlt.pos_j} := 0.5 \cdot \left(f_{pst_j} + f_{swt_j} + f_{diapht_j} + f_{deckt_j} + f_{wct_j} + f_{barriert_j} + f_{fwst_j}\right) + f_{LL\_lt.pos_j}$

$f_{allow\_cfdlt} := 0.40 \cdot f_c$

$Status\_ServiceLSfcfdl_j := if\left(f_{cfdlt.pos_j} \le f_{allow\_cfdlt}, "OK", "NG"\right)$

(LRFD Table 5.9.4.2.1-1)

$f_{allow\_cfdlt} = 2600.0\ psi$

$f_{cfdlt.pos} =$ psi

	1
1	-3.4
2	80.0
3	126.9
4	299.0
5	435.4
6	516.9
7	541.8
8	516.9
9	435.4
10	299.0
11	126.9
12	80.0
13	-3.4

$Status\_ServiceLSfcfdl =$

	1
1	"OK"
2	"OK"
3	"OK"
4	"OK"
5	"OK"
6	"OK"
7	"OK"
8	"OK"
9	"OK"
10	"OK"
11	"OK"
12	"OK"
13	"OK"

3) Compressive Stress (Bottom of Beam) Due to Live Load + 0.5(Effective Prestress + Dead Load):

$f_{cfdlt.neg_j} := 0.5 \cdot \left(f_{psb_j} + f_{swb_j} + f_{diaphb_j} + f_{deckb_j} + f_{wcb_j} + f_{barrierb_j} + f_{fwsb_j}\right) + f_{LL\_lb.neg_j}$

$f_{allow\_cfdlt} := 0.40 \cdot f_c$

$Status\_ServiceLSfcfdl_j := if\left(f_{cfdlt.neg_j} \le f_{allow\_cfdlt}, "OK", "NG"\right)$

(LRFD Table 5.9.4.2.1-1)

$f_{allow\_cfdlt} = 2600.0\ psi$

$f_{cfdlt.neg} =$ psi

	1
1	527.9
2	699.3
3	695.1
4	532.0
5	417.3
6	338.6
7	295.1
8	338.6
9	417.3
10	532.0
11	695.1
12	699.3
13	528.0

$Status\_ServiceLSfcfdl =$

	1
1	"OK"
2	"OK"
3	"OK"
4	"OK"
5	"OK"
6	"OK"
7	"OK"
8	"OK"
9	"OK"
10	"OK"
11	"OK"
12	"OK"
13	"OK"

Check Strength Limit State: (LRFD 5.7.3.2)

Restraint moment considered for strength check.

$$M_{u.pos_j} := 1.25\cdot\left(M_{swf_j} + M_{diaph_j} + M_{deck_j} + M_{barrier_j} + M_{wc_j} + M_{fws_j}\right) + 1.75\cdot M_{LL.pos_j} + M_{rm.pos_j}$$

$M_{u.pos}$ =

	1
1	22.3
2	91.7
3	110.0
4	217.6
5	317.6
6	377.2
7	393.1
8	377.2
9	317.6
10	217.6
11	110.0
12	91.7
13	22.3

k·ft

$$\beta_1 := \text{if}\left[f_{ct} \le 4000\cdot(\text{psi}), 0.85, \text{if}\left[f_{ct} \ge 8000\cdot(\text{psi}), 0.65, 0.85 - \left[\frac{f_{ct} - 4000\cdot(\text{psi})}{1000\cdot(\text{psi})}\cdot 0.05\right]\right]\right]$$

$\beta_1 = 0.85$

$A_{ps} := No\_Strands\cdot A_{strand}$ $A_{ps} = 2.45\,in^2$ $b := b_{effLL}$

$f_{pe} = 178.7\,ksi$ $0.5\cdot f_{pu} = 135.0\,ksi$

$Status\_f_{pe} := \text{if}\left(f_{pe} \ge 0.5\cdot f_{pu}, \text{"OK"}, \text{"NG"}\right)$ $Status\_f_{pe} = \text{"OK"}$ (LRFD 5.7.3.1.1)

$$k_1 := 2\cdot\left(1.04 - \frac{f_{py}}{f_{pu}}\right)$$ $k_1 = 0.28$ (LRFD 5.7.3.1.1-2)

$h_f := t_{sLL}$

$$d_{p_j} := h + t_{sLL} + h_{stprop} - y_{cg_j}$$

$$c_i := \frac{A_{ps}\cdot f_{pu}}{0.85\cdot f_{ct}\cdot\beta_1\cdot b + k_1\cdot A_{ps}\cdot\frac{f_{pu}}{d_{p_j}}}$$ (LRFD 5.7.3.1.1-4)

d_p =

	1
1	15.0
2	15.0
3	15.0
4	15.0
5	15.0
6	15.0
7	15.0
8	15.0
9	15.0
10	15.0
11	15.0
12	15.0
13	15.0

(in)

c =

	1
1	3.0
2	3.0
3	3.0
4	3.0
5	3.0
6	3.0
7	3.0
8	3.0
9	3.0
10	3.0
11	3.0
12	3.0
13	3.0

in

if c is > slab thickness, then T-section behavior

$b_{w_j} := if(c_j \le h_f, b, b_f)$

$$c_j := \frac{A_{ps} \cdot f_{pu} - 0.85 \cdot \beta_1 \cdot f_{ct} \cdot (b - b_{w_j}) \cdot h_f}{0.85 \cdot f_{ct} \cdot \beta_1 \cdot b_{w_j} + k_1 \cdot A_{ps} \cdot \frac{f_{pu}}{d_{p_j}}}$$ (LRFD 5.7.3.1.1-3)

$b_w =$

	1
1	72.0
2	72.0
3	72.0
4	72.0
5	72.0
6	72.0
7	72.0
8	72.0
9	72.0
10	72.0
11	72.0
12	72.0
13	72.0

in

$c =$

	1
1	3.0
2	3.0
3	3.0
4	3.0
5	3.0
6	3.0
7	3.0
8	3.0
9	3.0
10	3.0
11	3.0
12	3.0
13	3.0

in

$t_{sLL} + t_f = 9.0\,in$ check that c < ts + tf

$$f_{ps_j} := f_{pu} \cdot \left(1 - k_1 \cdot \frac{c_j}{d_{p_j}}\right)$$

$a_j := \beta_1 \cdot c_j$

$f_{ps} =$

	1
1	254.9
2	254.9
3	254.9
4	254.9
5	254.9
6	254.9
7	254.9
8	254.9
9	254.9
10	254.9
11	254.9
12	254.9
13	254.9

ksi

$a =$

	1
1	2.5
2	2.5
3	2.5
4	2.5
5	2.5
6	2.5
7	2.5
8	2.5
9	2.5
10	2.5
11	2.5
12	2.5
13	2.5

in (LRFD 5.7.3.1.1-1)

$$L_d := 1.6 \cdot \left(f_{ps_1} - \frac{2}{3} \cdot f_{pe}\right) \cdot d_{str} \cdot ksi^{-1}$$

$L_d = 108.6\,in$ (LRFD 5.11.4 and FHWA)

$L_t := 60 \cdot d_{str}$

$L_t = 30.0\,in$

$$dist_j := x_{f_j} + \frac{L_{ovr} - L_{des}}{2}$$

$$df_j := \begin{cases} 1.0 & \text{if } (dist_j > L_d) \vee (dist_j < L_{ovr} - L_d) \\ \frac{dist_j}{L_t} \cdot \frac{f_{pe}}{f_{pu}} & \text{if } dist_j < L_t \\ \frac{f_{pe}}{f_{pu}} + \frac{dist_j - L_t}{L_d - L_t} \cdot \left(1 - \frac{f_{pe}}{f_{pu}}\right) & \text{if } (L_t \le dist_j) \wedge (dist_j \le L_d) \\ \frac{L_{ovr} - dist_j}{L_t} \cdot \frac{f_{pe}}{f_{pu}} & \text{if } dist_j \ge (L_{ovr} - L_d) \\ \frac{f_{pe}}{f_{pu}} + \frac{(L_{ovr} - dist_j) - L_t}{L_d - L_t} \cdot \left(1 - \frac{f_{pe}}{f_{pu}}\right) & \text{otherwise} \end{cases}$$

$$M_{n_j} := df_j \cdot A_{ps} \cdot f_{ps_j} \cdot \left(d_{p_j} - \frac{a_j}{2}\right) + 0.85 \cdot f_c \cdot \left(b - b_{w_j}\right) \cdot \beta_1 \cdot h_f \cdot \left(\frac{a_j}{2} - \frac{h_f}{2}\right) \qquad \text{(LRFD 5.7.3.2.2-1)}$$

dist =

	1
1	7.0
2	27.7
3	37.6
4	68.2
5	98.8
6	129.4
7	160.0
8	190.6
9	221.2
10	251.8
11	282.4
12	292.3
13	313.0

in

df =

	1
1	1.000
2	1.000
3	1.000
4	1.000
5	1.000
6	1.000
7	1.000
8	1.000
9	1.000
10	1.000
11	1.000
12	1.000
13	1.000

(fraction strands are developed)

M_n =

	1
1	713.7
2	713.7
3	713.7
4	713.7
5	713.7
6	713.7
7	713.7
8	713.7
9	713.7
10	713.7
11	713.7
12	713.7
13	713.7

k·ft

$$\phi M_{n_j} := \phi_f \cdot M_{n_j} \qquad M_{r_j} := \phi M_{n_j}$$

$$Status\_StrengthLS_j := if\left(M_{u.pos_j} \le M_{r_j}, \text{"OK"}, \text{"NG"}\right)$$

M_r =

	1
1	713.7
2	713.7
3	713.7
4	713.7
5	713.7
6	713.7
7	713.7
8	713.7
9	713.7
10	713.7
11	713.7
12	713.7
13	713.7

k·ft

$M_{u.pos}$ =

	1
1	22.3
2	91.7
3	110.0
4	217.6
5	317.6
6	377.2
7	393.1
8	377.2
9	317.6
10	217.6
11	110.0
12	91.7
13	22.3

k·ft

Status_StrengthLS =

	1
1	"OK"
2	"OK"
3	"OK"
4	"OK"
5	"OK"
6	"OK"
7	"OK"
8	"OK"
9	"OK"
10	"OK"
11	"OK"
12	"OK"
13	"OK"

Maximum Steel Check: (LRFD 5.7.3.3.1-1)

$c\_d_{p_j} := \frac{c_j}{d_{p_j}}$ limit_c_d_p := 0.42 $Status\_MaxStl_j := if\left(c\_d_{p_j} \le 0.42, "OK", "NG""\right)$

$c\_d_p =$

	1
1	0.1999
2	0.1999
3	0.1999
4	0.1999
5	0.1999
6	0.1999
7	0.1999
8	0.1999
9	0.1999
10	0.1999
11	0.1999
12	0.1999
13	0.1999

Status_MaxStl =

	1
1	"OK"
2	"OK"
3	"OK"
4	"OK"
5	"OK"
6	"OK"
7	"OK"
8	"OK"
9	"OK"
10	"OK"
11	"OK"
12	"OK"
13	"OK"

Minimum Steel Check: (LRFD 5.7.3.3.2)

Compute Cracking Moment at Midspan: $f_r := -0.24 \cdot \sqrt{f_c} \cdot \sqrt{ksi}$ $f_r = -611.9\,psi$

$\Delta f_j := f_{IIIb.pos_j} - f_r$ $\Delta M_j := \Delta f_j \cdot S_{bcLL}$ $M_{cr_j} := M_{swf_j} + M_{diaph_j} + M_{deck_j} + M_{wc_j} + M_{barrier_j} + M_{fws_j} + M_{LL.pos_j} + \Delta M_j$

$\Delta f =$

	1
1	886.7
2	1482.8
3	1484.1
4	1150.2
5	879.2
6	717.3
7	668.9
8	717.3
9	879.3
10	1150.2
11	1484.1
12	1482.8
13	886.7

$\Delta M =$

	1
1	289.9
2	484.8
3	485.2
4	376.0
5	287.4
6	234.5
7	218.7
8	234.5
9	287.4
10	376.0
11	485.2
12	484.8
13	289.9

k·ft

$1.2 \cdot M_{cr} =$

	1
1	359.2
2	652.3
3	669.7
4	624.8
5	596.0
6	578.6
7	572.2
8	578.6
9	596.0
10	624.8
11	669.7
12	652.3
13	359.2

k·ft

$1.33 \cdot M_{u.pos} =$

	1
1	29.6
2	122.0
3	146.4
4	289.4
5	422.5
6	501.7
7	522.8
8	501.7
9	422.4
10	289.4
11	146.4
12	122.0
13	29.6

k·ft

$M_{r\_limit_j} := \text{if}\left(1.2 \cdot M_{cr_j} < 1.33 \cdot M_{u.pos_j},\ 1.2 \cdot M_{cr_j},\ 1.33 \cdot M_{u.pos_j}\right)$

$Status\_MinStl_j := \text{if}\left(M_{r\_limit_j} < M_{r_j},\ \text{"OK"},\ \text{"NG"}\right)$

$M_{r\_limit} =$

	1
1	29.6
2	122.0
3	146.4
4	289.4
5	422.5
6	501.7
7	522.8
8	501.7
9	422.4
10	289.4
11	146.4
12	122.0
13	29.6

k·ft

$M_r =$

	1
1	713.7
2	713.7
3	713.7
4	713.7
5	713.7
6	713.7
7	713.7
8	713.7
9	713.7
10	713.7
11	713.7
12	713.7
13	713.7

k·ft

$Status\_MinStl =$

	1
1	"OK"
2	"OK"
3	"OK"
4	"OK"
5	"OK"
6	"OK"
7	"OK"
8	"OK"
9	"OK"
10	"OK"
11	"OK"
12	"OK"
13	"OK"

B.1.5 Size and Spacing of Transverse Reinforcement (B-41 through B-65)

This section of the calculations was used to determine the size and spacing of reinforcement to satisfy reinforcement requirements for anchorage zone, confinement, vertical shear, and horizontal (i.e., interface) shear. The requirements for anchorage zone were based on the dimensions of the section and the prestressing force, and the requirements for confinement reinforcement were based only on the dimensions of the section. The shear forces that had been calculated previously were used to calculate the maximum vertical shear force that would be exerted on the composite section. Two iterations were needed to accurately predict the vertical shear strength provided by the concrete. Once the design shear strength of the concrete was calculated, it was compared to the vertical shear demand to determine the amount and spacing of vertical shear reinforcement required. The remainder of this section was used to calculate the amount and spacing of horizontal shear reinforcement required.

Following the calculations for transverse reinforcement requirements is a section that was used to calculate the camber and deflections of the composite section. This section is followed by a final design summary for an interior inverted-T precast section of the center span of Mn/DOT Bridge No. 13004.

Anchor Zone Reinforcement:

(LRFD 5.10.10.1)

$P_r := 0.04 \cdot P_{re}$ $P_r = 19.1\,k$

Allowable stress in anchorage steel: $f_s := 20 \cdot ksi$

$A_{s\_anchor} := \frac{P_r}{f_s}$ $A_{s\_anchor} = 1.0\,in^2$

Number of bars which must be placed within h/4 of the end of the beam (assume #16 bars) : $\frac{h}{4} = 3.0\,in$ $Reqd\_bars := \frac{A_{s\_anchor}}{4 \cdot 0.31 \cdot in^2}$

$Reqd\_bars = 0.8$

Confinement Reinforcement:

(LRFD 5.10.10.2)

Not less than No. 10M bars at a spacing of not more than 6 in shall be placed within 1.5d of the end of the girder. These bars shall be shaped to enclose the strands.

Vertical Shear Design

At each section the following must be satisfied for shear:

$V_u \le V_r$ (LRFD 5.8.2.1-2)

$V_r := \phi V_n$

Note: Evaluation has been disabled for these three equations (as indicated by the small boxes) to enable them to be shown without first evaluating their parameters.

$V_n := V_c + V_s + V_p$ (LRFD 5.8.3.3-1)

Critical Section for Shear: (LRFD 5.8.3.2)

The critical section for shear near a support in which the reaction force produces compression in the end of the member is, from the face of support (Fig. 2), the greater of:

a. $0.5 d_v \cot(\theta)$, or

b. d_v

where,

d_v = Effective shear depth.

Note that when $\theta > 26.6^o$, the second equation governs. Since θ is not yet known, for simplicity, assume that this condition is true.

Compute d_v:

d_v = Distance between resultants of tensile and compressive forces.

$d_v = d_e - a/2$.

Thus,

$d_{v_j} := d_{p_j} - \frac{a_j}{2}$

$d_v =$

	1
1	13.7
2	13.7
3	13.7
4	13.7
5	13.7
6	13.7
7	13.7
8	13.7
9	13.7
10	13.7
11	13.7
12	13.7
13	13.7

in

$d_p =$

	1
1	15
2	15
3	15
4	15
5	15
6	15
7	15
8	15
9	15
10	15
11	15
12	15
13	15

in

But d_v need not be taken less than the greater of $0.9d_e$ and $0.72h$. Thus,

$0.72 \cdot h_{cLL} = 13.0\,in$

$Min\_d_{v_j} := if\left(0.9 \cdot d_{p_j} \geq 0.72 \cdot h_{cLL}, 0.9 \cdot d_{p_j}, 0.72 \cdot h_{cLL}\right)$

$d_{v_j} := if\left(d_{v_j} < Min\_d_{v_j}, Min\_d_{v_j}, d_{v_j}\right)$

$Min\_d_v =$

	1
1	13.5
2	13.5
3	13.5
4	13.5
5	13.5
6	13.5
7	13.5
8	13.5
9	13.5
10	13.5
11	13.5
12	13.5
13	13.5

in (LRFD 5.8.2.7)

$d_v =$

	1
1	13.7
2	13.7
3	13.7
4	13.7
5	13.7
6	13.7
7	13.7
8	13.7
9	13.7
10	13.7
11	13.7
12	13.7
13	13.7

in

The original assumption for the critical section for shear was:

$x_{f_2} = 20.7\,in$

Assuming that the distance from the face of support to the centerline of bearing is half the bearing pad length, the critical section for shear is:

$x_{f_2} := d_{v_2} + \frac{L_{brng}}{2}$ $\quad x_{f_2} = 20.7\,in$ (Note: Compare this to original assumption and revise assumption as required)

The factored shears are:

$V_{u_j} := 1.25 \cdot \left(V_{swf_j} + V_{diaph_j} + V_{deck_j} + V_{barrier_j} + V_{fws_j} + V_{wc_j}\right) + 1.75 \cdot V_{LL_j}$

$V_u =$

	1
1	89.6
2	79.5
3	77.6
4	65.3
5	52.6
6	39.7
7	26.9
8	39.7
9	52.6
10	65.3
11	77.6
12	79.5
13	90.1

k

d_v from support

0.1L

0.2L

0.3L

0.4L

midspan

0.6L

0.7L

0.8L

0.9L

d_v from support

Compute the vertical component of the prestressing force, V_p: $P_f = 437.3\,k$ $\alpha := \operatorname{atan}\left(\frac{y_{end} - y_{mid}}{x_{r_6}}\right)$ $\alpha = 0\,deg$

Fix this equation if draped strands are used.

$tfract_j := if\left(dist_j > L_t, 1.0, \frac{dist_j}{L_t}\right)$

tfract =

	1
1	0.233
2	0.923
3	1.000
4	1.000
5	1.000
6	1.000
7	1.000
8	1.000
9	1.000
10	1.000
11	1.000
12	1.000
13	1.000

$_j := if\left(x_{f_j} < Dep\_Frac \cdot L_{des}, tfract_j \cdot P_f \cdot \sin(\alpha), 0 \cdot k\right)$

$V_p =$

	1
1	0.0
2	0.0
3	0.0
4	0.0
5	0.0
6	0.0
7	0.0
8	0.0
9	0.0
10	0.0
11	0.0
12	0.0
13	0.0

k

Compute maximum permissible shear capacity at a section:

$V_{n\_max_j} := \phi_v \cdot \left(0.25 \cdot f_c \cdot b_v \cdot d_{v_j} + V_{p_j}\right)$ (LRFD 5.8.3.3-2)

$Status\_V_{nmax_j} := if\left(V_{u_j} \le V_{n\_max_j}, "OK", "NG"\right)$

$V_{n\_max} =$

	1
1	963.5
2	963.5
3	963.5
4	963.5
5	963.5
6	963.5
7	963.5
8	963.5
9	963.5
10	963.5
11	963.5
12	963.5
13	963.5

k

$Status\_V_{nmax} =$

	1
1	"OK"
2	"OK"
3	"OK"
4	"OK"
5	"OK"
6	"OK"
7	"OK"
8	"OK"
9	"OK"
10	"OK"
11	"OK"
12	"OK"
13	"OK"

The shear contribution from the concrete, V_c, is given by:

$$V_c := 0.0316 \cdot \beta \cdot \sqrt{f'_c}\, b_v \cdot d_v$$ (LRFD 5.8.3.3-3)

To obtain β in the above equation, we need θ and v/f'_c.

First, compute v/f'c:

$$v_j := \frac{V_{u_j} - \phi_v \cdot V_{p_j}}{\phi_v \cdot b_v \cdot d_{v_j}} \qquad v\_fc_j := \frac{v_j}{f'_c}$$ (LRFD 5.8.3.4.2-1)

v =

	1
1	151.2
2	134.2
3	130.9
4	110.2
5	88.7
6	66.9
7	45.4
8	66.9
9	88.7
10	110.2
11	130.9
12	134.2
13	152.0

psi

v_fc =

	1
1	0.0233
2	0.0206
3	0.0201
4	0.0169
5	0.0137
6	0.0103
7	$6.9855 \cdot 10^{-3}$
8	0.0103
9	0.0137
10	0.0169
11	0.0201
12	0.0206
13	0.0234

Compute θ:

Computing θ requires an iterative procedure. The basic steps are as follows:

Step 1: Assume an initial value of θ.

Step 2: Compute ε_x using LRFD 5.8.3.4.2-2.

Step 3: If ε_x is < 0, then factor ε_x by F_ε (LRFD 5.8.3.4.2-3)

Step 4: Knowing v/f'c and ε_x, look up the new θ in LRFD Table 5.8.3.4.2-1.

Step 5: If the new value of θ is not equal to the previous value of θ, go to Step 2.

$j := 1 .. 13$

$M_{u.pos} =$

	1
1	22.3
2	91.7
3	110.0
4	217.6
5	317.6
6	377.2
7	393.1
8	377.2
9	317.6
10	217.6
11	110.0
12	91.7
13	22.3

k·ft

$V_u =$

	1
1	89.6
2	79.5
3	77.6
4	65.3
5	52.6
6	39.7
7	26.9
8	39.7
9	52.6
10	65.3
11	77.6
12	79.5
13	90.1

k

$x_f =$

	1
1	0.000
2	1.727
3	2.550
4	5.100
5	7.650
6	10.200
7	12.750
8	15.300
9	17.850
10	20.400
11	22.950
12	23.775
13	25.500

ft

$x_r =$

	1
1	0.583
2	2.500
3	3.133
4	5.683
5	8.233
6	10.783
7	13.333
8	15.883
9	18.433
10	20.983
11	23.533
12	24.167
13	26.083

ft

Trial 1:

Step 1: Input estimated initial value of θ:

$\theta := \begin{pmatrix} 26.4 \\ 25.9 \\ 27.0 \\ 32.5 \\ 36.0 \\ 38.0 \\ 38.0 \\ 38.0 \\ 36.0 \\ 32.5 \\ 27.0 \\ 25.9 \\ 26.4 \end{pmatrix} \cdot deg$

INPUT INITIAL θ VALUES FOR ITERATION IN VERTICAL SHEAR DESIGN

Step 2: Compute ε_x: using LRFD 5.8.3.4.2-2:

$$\varepsilon_x := \frac{\frac{M_u}{d_v} + 0.5 \cdot (V_u - V_p) \cdot \cot(\theta) - A_{ps\_ft} \cdot f_{po}}{2 \cdot E_p \cdot A_{ps\_ft}}$$

Note: Evaluation has been disabled for this equation to enable it to be shown without first evaluating its parameters.

Compute f_{po}:

This can be estimated by using the following equation:

$$f_{po} := f_{pe} + \frac{f_{pc} \cdot E_p}{E_c} \qquad \text{(LRFD C5.8.3.4.2-1)}$$

$f_{pe} = 178.7\ ksi$

Compute f_{pc}, net stress at c.g. of composite section at final:

$$S_{fpc} := \frac{I}{y_{bcLL} - y_b} \qquad S_{fpc} = 2555.8\ in^3$$

$$y_{cg\_dv_j} := if\left[x_{r_j} > x_{r_6}, y_{mid}, y_{end} - \frac{x_{f_j} + \left(\frac{L_{ovr} - L_{des}}{2}\right)}{x_{r_6}} \cdot (y_{end} - y_{mid})\right]$$

$ecc_{dv} := y_b - y_{cg\_dv}$

$$f_{pc} := P_f \cdot \left(\frac{1}{A} - \frac{ecc_{dv}}{S_{fpc}} \right) + \frac{M_{swf} + M_{diaph} + M_{deck}}{S_{fpc}} \qquad f_{po} := f_{pe} + f_{pc} \cdot \left(\frac{E_p}{E_{cbeamf}} \right)$$

y_{cg_dv} = (in)

	1
1	3.0
2	3.0
3	3.0
4	3.0
5	3.0
6	3.0
7	3.0
8	3.0
9	3.0
10	3.0
11	3.0
12	3.0
13	3.0

ecc_{dv} = (in)

	1
1	2.4
2	2.4
3	2.4
4	2.4
5	2.4
6	2.4
7	2.4
8	2.4
9	2.4
10	2.4
11	2.4
12	2.4
13	2.4

f_{pc} = (ksi)

	1
1	0.178
2	0.310
3	0.367
4	0.514
5	0.619
6	0.682
7	0.703
8	0.682
9	0.619
10	0.514
11	0.367
12	0.310
13	0.178

f_{po} = (ksi)

	1
1	179.9
2	180.7
3	181.1
4	182.1
5	182.8
6	183.3
7	183.4
8	183.3
9	182.8
10	182.1
11	181.1
12	180.7
13	179.9

Compute A_{ps}:

Note that A_{ps} in the equation used to compute ε_x is the area of the prestressing steel on the flexural tension side only. It is not the total area of strands. The variable A_{ps_ft} is introduced below to handle this.

$$slope_i := \frac{EPat\_h_i - MPat\_h_i}{Dep\_Pt}$$

$$\frac{h_{cLL}}{2} = 9\,in$$

$z := 1 .. 13$

$Pat\_ht_{i,1} := EPat\_h_i$

$Pat\_ht_{i,2} := EPat\_h_i - x_{r_2} \cdot slope_i$

$Pat\_ht_{i,3} := EPat\_h_i - x_{r_3} \cdot slope_i$

$Pat\_ht_{i,4} := EPat\_h_i - x_{r_4} \cdot slope_i$

$Pat\_ht_{i,5} := EPat\_h_i - x_{r_5} \cdot slope_i$

$Pat\_ht_{i,6} := MPat\_h_i$

$Pat\_ht_{i,7} := MPat\_h_i$

$Pat\_ht_{i,8} := MPat\_h_i$

$Pat\_ht_{i,9} := MPat\_h_i$

$Pat\_ht_{i,10} := MPat\_h_i$

$Pat\_ht_{i,11} := MPat\_h_i$

$Pat\_ht_{i,12} := MPat\_h_i$

$Pat\_ht_{i,13} := MPat\_h_i$

$$slope = \begin{pmatrix} 0.000000 \\ 0.000000 \\ 0.000000 \\ 0.000000 \\ 0.000000 \\ 0.000000 \\ 0.000000 \\ 0.000000 \\ 0.000000 \\ 0.000000 \\ 0.000000 \end{pmatrix}$$

$$Pat\_ht = \begin{pmatrix} 0.0 & 0.0 & 0.0 & 0.0 & 0.0 & 0.0 & 0.0 & 0.0 & 0.0 & 0.0 & 0.0 & 0.0 & 0.0 \\ 0.0 & 0.0 & 0.0 & 0.0 & 0.0 & 0.0 & 0.0 & 0.0 & 0.0 & 0.0 & 0.0 & 0.0 & 0.0 \\ 0.0 & 0.0 & 0.0 & 0.0 & 0.0 & 0.0 & 0.0 & 0.0 & 0.0 & 0.0 & 0.0 & 0.0 & 0.0 \\ 0.0 & 0.0 & 0.0 & 0.0 & 0.0 & 0.0 & 0.0 & 0.0 & 0.0 & 0.0 & 0.0 & 0.0 & 0.0 \\ 0.0 & 0.0 & 0.0 & 0.0 & 0.0 & 0.0 & 0.0 & 0.0 & 0.0 & 0.0 & 0.0 & 0.0 & 0.0 \\ 0.0 & 0.0 & 0.0 & 0.0 & 0.0 & 0.0 & 0.0 & 0.0 & 0.0 & 0.0 & 0.0 & 0.0 & 0.0 \\ 0.0 & 0.0 & 0.0 & 0.0 & 0.0 & 0.0 & 0.0 & 0.0 & 0.0 & 0.0 & 0.0 & 0.0 & 0.0 \\ 0.0 & 0.0 & 0.0 & 0.0 & 0.0 & 0.0 & 0.0 & 0.0 & 0.0 & 0.0 & 0.0 & 0.0 & 0.0 \\ 0.0 & 0.0 & 0.0 & 0.0 & 0.0 & 0.0 & 0.0 & 0.0 & 0.0 & 0.0 & 0.0 & 0.0 & 0.0 \\ 4.0 & 4.0 & 4.0 & 4.0 & 4.0 & 4.0 & 4.0 & 4.0 & 4.0 & 4.0 & 4.0 & 4.0 & 4.0 \\ 2.0 & 2.0 & 2.0 & 2.0 & 2.0 & 2.0 & 2.0 & 2.0 & 2.0 & 2.0 & 2.0 & 2.0 & 2.0 \end{pmatrix} in$$

$$No_{Aps\_ft}(Pat\_n, Pat\_h, hc\_2, zz) := \begin{| } j \leftarrow last(Pat\_n) \\ N \leftarrow 0 \\ \text{while } Pat\_h_{j,zz} \le \frac{hc\_2}{2} \\ \quad \begin{| } N \leftarrow N + Pat\_n_j \\ \quad j \leftarrow j - 1 \\ \quad \text{break if } j = 0 \\ N \end{|}$$

$$N_{Aps\_ft_z} := No_{Aps\_ft}(EPat\_n, Pat\_ht, h_{cLL}, z) \qquad A_{ps\_ft_z} := df_z \cdot N_{Aps\_ft_z} \cdot A_{strand}$$

$N_{Aps\_ft} =$

	1
1	16
2	16
3	16
4	16
5	16
6	16
7	16
8	16
9	16
10	16
11	16
12	16
13	16

$A_{ps\_ft} =$

	1
1	2.448
2	2.448
3	2.448
4	2.448
5	2.448
6	2.448
7	2.448
8	2.448
9	2.448
10	2.448
11	2.448
12	2.448
13	2.448

in^2

$$\varepsilon_{x_j} := \frac{\frac{M_{u.pos_j}}{d_{v_j}} + 0.5 \cdot \left(V_{u_j} - V_{p_j}\right) \cdot \cot(\theta_j) - A_{ps\_ft_j} \cdot f_{po_j}}{2 \cdot E_p \cdot A_{ps\_ft_j}} \qquad \varepsilon_{x_j} := \min\left(\begin{pmatrix} 0.002 \\ \varepsilon_{x_j} \end{pmatrix}\right) \quad \text{(LRFD 5.8.3.4.2-2)}$$

$\varepsilon_x =$

	1
1	-0.002369
2	-0.002009
3	-0.001942
4	-0.001464
5	-0.000958
6	-0.000669
7	-0.000631
8	-0.000670
9	-0.000958
10	-0.001464
11	-0.001942
12	-0.002009
13	-0.002365

Step 3: If $\varepsilon_x < 0$, use other equation. Thus,

(LRFD 5.8.3.4.2-3)

$$neg_j := \frac{\frac{M_{u.pos_j}}{d_{v_j}} + 0.5 \cdot \left(V_{u_j} - V_{p_j}\right) \cdot \cot\left(\theta_j\right) - A_{ps\_ft_j} \cdot f_{po_j}}{2 \cdot \left(E_{cbeamf} \cdot A_c + E_p \cdot A_{ps\_ft_j}\right)}$$

$$\varepsilon x_j := if\left(\varepsilon_{x_j} < 0, neg_j, \varepsilon_{x_j}\right)$$

neg =

	1
1	-0.000064
2	-0.000054
3	-0.000053
4	-0.000040
5	-0.000026
6	-0.000018
7	-0.000017
8	-0.000018
9	-0.000026
10	-0.000040
11	-0.000053
12	-0.000054
13	-0.000064

$\varepsilon x =$

	1
1	-0.000064
2	-0.000054
3	-0.000053
4	-0.000040
5	-0.000026
6	-0.000018
7	-0.000017
8	-0.000018
9	-0.000026
10	-0.000040
11	-0.000053
12	-0.000054
13	-0.000064

Step 4: Now, knowing v/f'c and ε_x, a new value of θ can be looked up in LRFD Table 5.8.3.4.2-1. This procedure has been automated below using a double interpolation procedure.

Table 1: LRFD Table 5.8.3.4.2-1. Vector C is the column headings (ε_x), vector R is the row headings (v/f'c), θ_x are the θ values, and β_x are the β values corresponding to the θ values.

$$C := \begin{pmatrix} -0.2 \\ -0.10 \\ -0.05 \\ 0 \\ 0.125 \\ 0.25 \\ 0.50 \\ 0.75 \\ 1 \\ 1.5 \\ 2 \end{pmatrix} \quad R := \begin{pmatrix} 0.075 \\ 0.100 \\ 0.125 \\ 0.150 \\ 0.175 \\ 0.200 \\ 0.225 \\ 0.250 \end{pmatrix} \quad \theta x := \begin{pmatrix} 22.3 & 20.4 & 21.0 & 21.8 & 24.3 & 26.6 & 30.5 & 33.7 & 36.4 & 40.8 & 43.9 \\ 18.1 & 20.4 & 21.4 & 22.5 & 24.9 & 27.1 & 30.8 & 34.0 & 36.7 & 40.8 & 43.1 \\ 19.9 & 21.9 & 22.8 & 23.7 & 25.9 & 27.9 & 31.4 & 34.4 & 37.0 & 41.0 & 43.2 \\ 21.6 & 23.3 & 24.2 & 25.0 & 26.9 & 28.8 & 32.1 & 34.9 & 37.3 & 40.5 & 42.8 \\ 23.2 & 24.7 & 25.5 & 26.2 & 28.0 & 29.7 & 32.7 & 35.2 & 36.8 & 39.7 & 42.2 \\ 24.7 & 26.1 & 26.7 & 27.4 & 29.0 & 30.6 & 32.8 & 34.5 & 36.1 & 39.2 & 41.7 \\ 26.1 & 27.3 & 27.9 & 28.5 & 30.0 & 30.8 & 32.3 & 34.0 & 35.7 & 38.8 & 41.4 \\ 27.5 & 28.6 & 29.1 & 29.7 & 30.6 & 31.3 & 32.8 & 34.3 & 35.8 & 38.6 & 41.2 \end{pmatrix}$$

$$\beta x := \begin{pmatrix} 6.32 & 4.75 & 4.10 & 3.75 & 3.24 & 2.94 & 2.59 & 2.38 & 2.23 & 1.95 & 1.67 \\ 3.79 & 3.38 & 3.24 & 3.14 & 2.91 & 2.75 & 2.50 & 2.32 & 2.18 & 1.93 & 1.69 \\ 3.18 & 2.99 & 2.94 & 2.87 & 2.74 & 2.62 & 2.42 & 2.26 & 2.13 & 1.90 & 1.67 \\ 2.88 & 2.79 & 2.78 & 2.72 & 2.60 & 2.52 & 2.36 & 2.21 & 2.08 & 1.82 & 1.61 \\ 2.73 & 2.66 & 2.65 & 2.60 & 2.52 & 2.44 & 2.28 & 2.14 & 1.96 & 1.71 & 1.54 \\ 2.63 & 2.59 & 2.52 & 2.51 & 2.43 & 2.37 & 2.14 & 1.94 & 1.79 & 1.61 & 1.47 \\ 2.53 & 2.45 & 2.42 & 2.40 & 2.34 & 2.14 & 1.86 & 1.73 & 1.64 & 1.51 & 1.39 \\ 2.39 & 2.39 & 2.33 & 2.33 & 2.12 & 1.93 & 1.70 & 1.58 & 1.50 & 1.38 & 1.29 \end{pmatrix}$$

$a := 1 .. 7$

$LB(vector, value) :=$
- $j \leftarrow 1$
- $LB \leftarrow 1$
- $j_{max} \leftarrow last(vector)$
- while $value > vector_j$
  - $j \leftarrow j + 1$
  - $LB \leftarrow j - 1$
  - break if $j > j_{max}$
- LB

$UB(vector, value) :=$
- $j \leftarrow 1$
- $UB \leftarrow 1$
- $j_{max} \leftarrow last(vector)$
- while $value > vector_j$
  - $j \leftarrow j + 1$
  - $UB \leftarrow j$
  - break if $j \geq j_{max}$
- UB

$p_j := LB\left(C, \varepsilon_{x_j} \cdot 1000\right)$

$q_j := UB\left(C, \varepsilon_{x_j} \cdot 1000\right)$

$p =$

	1
1	2
2	2
3	2
4	3
5	3
6	3
7	3
8	3
9	3
10	3
11	2
12	2
13	2

$q =$

	1
1	3
2	3
3	3
4	4
5	4
6	4
7	4
8	4
9	4
10	4
11	3
12	3
13	3

$k_{1_j} := LB\left(R, v\_fc_j\right)$

$l_j := UB\left(R, v\_fc_j\right)$

$k_1 =$

	1
1	1
2	1
3	1
4	1
5	1
6	1
7	1
8	1
9	1
10	1
11	1
12	1
13	1

$l =$

	1
1	1
2	1
3	1
4	1
5	1
6	1
7	1
8	1
9	1
10	1
11	1
12	1
13	1

$$\theta a_j := \text{if}\left[q_j = 1, \theta x_{k1_j, p_j}, \text{if}\left[p_j = \text{last}(C), \theta x_{k1_j, \text{last}(C)}, \theta x_{k1_j, p_j} + \left(\frac{\varepsilon x_j \cdot 1000 - C_{p_j}}{C_{q_j} - C_{p_j}}\right) \cdot \left(\theta x_{k1_j, q_j} - \theta x_{k1_j, p_j}\right)\right]\right]$$

$$\theta b_j := \text{if}\left[q_j = 1, \theta x_{l_j, p_j}, \text{if}\left[p_j = \text{last}(C), \theta x_{l_j, \text{last}(C)}, \theta x_{l_j, p_j} + \left[\frac{\varepsilon x_j \cdot 1000 - C_{p_j}}{\left(C_{q_j}\right) - C_{p_j}}\right] \cdot \left(\theta x_{l_j, q_j} - \theta x_{l_j, p_j}\right)\right]\right]$$

$$CP_j := \text{if}\left[k1_j = l_j, 0, \frac{v\_fc_j - \left(R_{k1_j}\right)}{R_{l_j} - R_{k1_j}}\right] \qquad \theta_j := \theta a_j + CP_j \cdot \left(\theta b_j - \theta a_j\right)$$

$\theta_a =$

	1
1	20.83
2	20.95
3	20.97
4	21.17
5	21.39
6	21.51
7	21.53
8	21.51
9	21.39
10	21.17
11	20.97
12	20.95
13	20.83

$\theta_b =$

	1
1	20.83
2	20.95
3	20.97
4	21.17
5	21.39
6	21.51
7	21.53
8	21.51
9	21.39
10	21.17
11	20.97
12	20.95
13	20.83

$CP =$

	1
1	0.000
2	0.000
3	0.000
4	0.000
5	0.000
6	0.000
7	0.000
8	0.000
9	0.000
10	0.000
11	0.000
12	0.000
13	0.000

$\theta =$

	1
1	20.83
2	20.95
3	20.97
4	21.17
5	21.39
6	21.51
7	21.53
8	21.51
9	21.39
10	21.17
11	20.97
12	20.95
13	20.83

Since the accuracy of the θ values in LRFD Table 5.8.3.4.2-1 is only to the the 0.1 degree, if the looked up value of θ is not within 0.1 degrees of the value from the previous trial (the assumed value for the first trial), then another iteration should be performed.

Trial 2: Recalculate ε_x using the new value of θ calculated in the previous trial:

$$\varepsilon x_j := \frac{\frac{M_{u.pos_j}}{d_{v_j}} + 0.5\cdot\left(V_{u_j} - V_{p_j}\right)\cdot\cot\left(\theta_j\cdot\text{deg}\right) - A_{ps\_ft_j}\cdot f_{po_j}}{2\cdot E_p\cdot A_{ps\_ft_j}} \qquad neg_j := \frac{\frac{M_{u.pos_j}}{d_{v_j}} + 0.5\cdot\left(V_{u_j} - V_{p_j}\right)\cdot\cot\left(\theta_j\cdot\text{deg}\right) - A_{ps\_ft_j}\cdot f_{po_j}}{2\cdot\left(E_{cbeamf}\cdot A_c + E_p\cdot A_{ps\_ft_j}\right)}$$

$$\varepsilon x_j := \min\left(\begin{pmatrix} 0.002 \\ \varepsilon x_j \end{pmatrix}\right) \qquad \varepsilon x_j := \text{if}\left(\varepsilon x_j < 0, neg_j, \varepsilon x_j\right) \qquad p_j := \text{LB}\left(C, \varepsilon x_j\cdot 1000\right) \qquad q_j := \text{UB}\left(C, \varepsilon x_j\cdot 1000\right)$$

$\varepsilon x =$

	1
1	-0.000059
2	-0.000050
3	-0.000048
4	-0.000033
5	-0.000020
6	-0.000013
7	-0.000014
8	-0.000013
9	-0.000020
10	-0.000033
11	-0.000048
12	-0.000050
13	-0.000059

$p =$

	1
1	2
2	2
3	3
4	3
5	3
6	3
7	3
8	3
9	3
10	3
11	3
12	2
13	2

$q =$

	1
1	3
2	3
3	4
4	4
5	4
6	4
7	4
8	4
9	4
10	4
11	4
12	3
13	3

$$\theta a_j := \text{if}\left[q_j = 1, \theta x_{k1_j, p_j}, \text{if}\left[p_j = \text{last}(C), \theta x_{k1_j, \text{last}(C)}, \theta x_{k1_j, p_j} + \left(\frac{\varepsilon x_j\cdot 1000 - C_{p_j}}{C_{q_j} - C_{p_j}}\right)\cdot\left(\theta x_{k1_j, q_j} - \theta x_{k1_j, p_j}\right)\right]\right]$$

$$\theta b_j := \text{if}\left[q_j = 1, \theta x_{l_j, p_j}, \text{if}\left[p_j = \text{last}(C), \theta x_{l_j, \text{last}(C)}, \theta x_{l_j, p_j} + \left[\frac{\varepsilon x_j\cdot 1000 - C_{p_j}}{\left(C_{q_j}\right) - C_{p_j}}\right]\cdot\left(\theta x_{l_j, q_j} - \theta x_{l_j, p_j}\right)\right]\right]$$

$$CP_j := \text{if}\left[k1_j = l_j, 0, \frac{v\_fc_j - \left(R_{k1_j}\right)}{R_{l_j} - R_{k1_j}}\right] \qquad \theta_j := \theta a_j + CP_j\cdot\left(\theta b_j - \theta a_j\right)$$

$\theta_a =$

	1
1	20.90
2	21.00
3	21.04
4	21.27
5	21.48
6	21.59
7	21.58
8	21.59
9	21.48
10	21.27
11	21.04
12	21.00
13	20.90

$\theta_b =$

	1
1	20.90
2	21.00
3	21.04
4	21.27
5	21.48
6	21.59
7	21.58
8	21.59
9	21.48
10	21.27
11	21.04
12	21.00
13	20.90

$CP =$

	1
1	0.000
2	0.000
3	0.000
4	0.000
5	0.000
6	0.000
7	0.000
8	0.000
9	0.000
10	0.000
11	0.000
12	0.000
13	0.000

$\theta =$

	1
1	20.90
2	21.00
3	21.04
4	21.27
5	21.48
6	21.59
7	21.58
8	21.59
9	21.48
10	21.27
11	21.04
12	21.00
13	20.90

With θ now known, the corresponding value of β can now be interpolated:

$$\beta a_j := \text{if}\left[q_j = 1, \beta x_{k1_j, p_j}, \text{if}\left[p_j = \text{last}(C), \beta x_{k1_j, \text{last}(C)}, \beta x_{k1_j, p_j} + \left(\frac{\varepsilon_{X_j} \cdot 1000 - C_{p_j}}{C_{q_j} - C_{p_j}}\right) \cdot \left(\beta x_{k1_j, q_j} - \beta x_{k1_j, p_j}\right)\right]\right]$$

$$\beta b_j := \text{if}\left[q_j = 1, \beta x_{l_j, p_j}, \text{if}\left[p_j = \text{last}(C), \beta x_{l_j, \text{last}(C)}, \beta x_{l_j, p_j} + \left(\frac{\varepsilon_{X_j} \cdot 1000 - C_{p_j}}{C_{q_j} - C_{p_j}}\right) \cdot \left(\beta x_{l_j, q_j} - \beta x_{l_j, p_j}\right)\right]\right]$$

$$\beta j := \beta a_j + CP j \cdot \left(\beta b_j - \beta a_j\right)$$

$\beta_a =$

	1
1	4.21
2	4.10
3	4.08
4	3.98
5	3.89
6	3.84
7	3.85
8	3.84
9	3.89
10	3.98
11	4.08
12	4.10
13	4.21

$\beta_b =$

	1
1	4.21
2	4.10
3	4.08
4	3.98
5	3.89
6	3.84
7	3.85
8	3.84
9	3.89
10	3.98
11	4.08
12	4.10
13	4.21

$\beta =$

	1
1	4.21
2	4.10
3	4.08
4	3.98
5	3.89
6	3.84
7	3.85
8	3.84
9	3.89
10	3.98
11	4.08
12	4.10
13	4.21

j =	$Location_j :=$
1	"0.0Ldes"
2	"Critical Section"
3	"0.1Ldes"
4	"0.2Ldes"
5	"0.3Ldes"
6	"0.4Ldes"
7	"0.5Ldes, Midspan"
8	"0.6Ldes"
9	"0.7Ldes"
10	"0.8Ldes"
11	"0.9Ldes"
12	"Critical Section"
13	"1.0Ldes"

$\theta =$

	1
1	20.9
2	21.0
3	21.0
4	21.3
5	21.5
6	21.6
7	21.6
8	21.6
9	21.5
10	21.3
11	21.0
12	21.0
13	20.9

and $\beta =$

	1
1	4.21
2	4.10
3	4.08
4	3.98
5	3.89
6	3.84
7	3.85
8	3.84
9	3.89
10	3.98
11	4.08
12	4.10
13	4.21

Compute V_c and V_s : $j := 1 .. 13$

$V_{c_j} := 0.0316 \cdot \beta_j \cdot \sqrt{f_c} \cdot \sqrt{ksi} \cdot b_v \cdot d_{v_j}$ (LRFD 5.8.3.3-3)

$V_{s_j} := if\left(\frac{V_{u_j}}{\phi_v} - V_{c_j} - V_{p_j} > 0, \frac{V_{u_j}}{\phi_v} - V_{c_j} - V_{p_j}, 0.1 \cdot k\right)$

$V_u =$

	1
1	89.6
2	79.5
3	77.6
4	65.3
5	52.6
6	39.7
7	26.9
8	39.7
9	52.6
10	65.3
11	77.6
12	79.5
13	90.1

k

$V_c =$

	1
1	223.6
2	217.7
3	216.8
4	211.4
5	206.4
6	204.0
7	204.2
8	204.0
9	206.4
10	211.4
11	216.8
12	217.7
13	223.6

k

$V_p =$

	1
1	0.0
2	0.0
3	0.0
4	0.0
5	0.0
6	0.0
7	0.0
8	0.0
9	0.0
10	0.0
11	0.0
12	0.0
13	0.0

k

$V_s =$

	1
1	0.1
2	0.1
3	0.1
4	0.1
5	0.1
6	0.1
7	0.1
8	0.1
9	0.1
10	0.1
11	0.1
12	0.1
13	0.1

k

Regions NOT Requiring Transverse Reinforcement (LRFD 5.8.2.4)

$Resist_{min} := 0.5 \cdot \phi_v \cdot (V_c + V_p)$

$Resist_{min} =$

	1
1	100.6424
2	97.9548
3	97.5399
4	95.1194
5	92.8966
6	91.7879
7	91.8752
8	91.7881
9	92.8976
10	95.1194
11	97.5404
12	97.9548
13	100.6042

k

$V_u =$

	1
1	89.6331
2	79.5481
3	77.6072
4	65.3235
5	52.6139
6	39.6968
7	26.9231
8	39.6968
9	52.6139
10	65.3235
11	77.5954
12	79.5481
13	90.1051

k

Assuming two vertical legs of No. 16M (#5 bars) stirrups,

$$A_{v_j} := \frac{V_{s_j}}{f_y \cdot d_{v_j} \cdot \cot(\theta_j \cdot \text{deg})} \qquad Spac_j := \frac{2 \cdot 0.31 \cdot in^2}{A_{v_j}} \qquad \text{(LRFD C5.8.3.3-1)}$$

$A_v =$

	1
1	$5.56 \cdot 10^{-4}$
2	$5.59 \cdot 10^{-4}$
3	$5.60 \cdot 10^{-4}$
4	$5.67 \cdot 10^{-4}$
5	$5.73 \cdot 10^{-4}$
6	$5.77 \cdot 10^{-4}$
7	$5.76 \cdot 10^{-4}$
8	$5.77 \cdot 10^{-4}$
9	$5.73 \cdot 10^{-4}$
10	$5.67 \cdot 10^{-4}$
11	$5.60 \cdot 10^{-4}$
12	$5.59 \cdot 10^{-4}$
13	$5.56 \cdot 10^{-4}$

$\frac{in^2}{ft}$ $\quad Spac =$

	1
1	13374.5
2	13302.0
3	13275.6
4	13117.0
5	12974.3
6	12904.2
7	12909.7
8	12904.2
9	12974.4
10	13117.0
11	13275.6
12	13302.0
13	13373.4

in (max stirrup spacing)

Check minimum transverse reinforcement: (LRFD 5.8.2.5-1)

$$A_{v\_min} := 0.0316 \cdot \sqrt{f_c} \cdot \sqrt{ksi} \cdot \frac{b_v}{f_y} \qquad A_{v\_min} = 0.7734 \frac{in^2}{ft} \qquad s_{Avmin} := \frac{0.62 \cdot in^2}{A_{v\_min}} \qquad s_{Avmin} = 9.6\,in$$

Check maximum stirrup spacing: (LRFD 5.8.2.7)

$$V_{spc} := 0.125 \cdot f_c \cdot b_v \cdot d_v$$

$$Max\_spac_j := if\left(V_{u_j} < V_{spc_j}, if\left(0.8 \cdot d_{v_j} < 24 \cdot in, 0.8 \cdot d_{v_j}, 24 \cdot in\right), if\left(0.4 \cdot d_{v_j} < 12 \cdot in, 0.4 \cdot d_{v_j}, 12 \cdot in\right)\right)$$

$$Max\_spac_j := if\left(Max\_spac_j < s_{Avmin}, Max\_spac_j, s_{Avmin}\right)$$

$V_{spc} =$

	1
1	535.3
2	535.3
3	535.3
4	535.3
5	535.3
6	535.3
7	535.3
8	535.3
9	535.3
10	535.3
11	535.3
12	535.3
13	535.3

k $\quad Max\_spac =$

	1
1	9.6
2	9.6
3	9.6
4	9.6
5	9.6
6	9.6
7	9.6
8	9.6
9	9.6
10	9.6
11	9.6
12	9.6
13	9.6

in

$$fmax\_sp\_v_j := \begin{cases} Spac_j & \text{if } \left(Spac_j < Max\_spac_j\right) \wedge \left(V_{u_j} > Resist_{min_j}\right) \\ Max\_spac_j & \text{if } \left(Spac_j \geq Max\_spac_j\right) \wedge \left(V_{u_j} > Resist_{min_j}\right) \\ 999in & \text{otherwise} \end{cases}$$

$$x\_end_j := if\left(j = 1, x_{f_1} + \frac{L_{ovr} - L_{des}}{2}, x_{r_j}\right)$$

final max stirrup spacing based on all criteria ==>

fmax_sp_v =

	1
1	999.0
2	999.0
3	999.0
4	999.0
5	999.0
6	999.0
7	999.0
8	999.0
9	999.0
10	999.0
11	999.0
12	999.0
13	999.0

in

location from end of beam ==>

x_end =

	1
1	0.58
2	2.50
3	3.13
4	5.68
5	8.23
6	10.78
7	13.33
8	15.88
9	18.43
10	20.98
11	23.53
12	24.17
13	26.08

ft

Check Longitudinal Reinforcement: (LRFD 5.8.3.5)

LRFD requires that the longitudinal steel be checked at all locations along the girder. This requirement is made to ensure that the longitudinal reinforcement is sufficient to develop the required tension tie which is required for equilibrium. Equation 5.8.3.5-1 is the general equation, applicable at all sections. However, for the special case of the inside edge of bearing at simple-end supports, the longitudinal reinforcement must be able to resist a tensile force of $(V_u/\phi - 0.5V_s - V_p)\cot(\theta)$. Note that when pretensioned strands are used to develop this force, only a portion of the full prestress force may be available near the support due to partial transfer. Additionally, only those strands on the flexural tension side of the member contribute to the tension tie force.

$$TF_j := \begin{cases} \dfrac{x_{r_j} + \dfrac{L_{brng}}{2} + y_{cg_j} \cdot \cot\left(\theta_j \cdot deg\right)}{60 \cdot d_{str}} & \text{if } x_{r_j} + \dfrac{L_{brng}}{2} + y_{cg_j} \cdot \cot\left(\theta_j \cdot deg\right) < 60 \cdot d_{str} \\ \dfrac{L_{ovr} - x_{r_j} + \dfrac{L_{brng}}{2} + y_{cg_j} \cdot \cot\left(\theta_j \cdot deg\right)}{60 \cdot d_{str}} & \text{if } L_{ovr} - x_{r_j} + \dfrac{L_{brng}}{2} + y_{cg_j} \cdot \cot\left(\theta_j \cdot deg\right) < 60 \cdot d_{str} \\ 1.0 & \text{otherwise} \end{cases}$$

TF =

	1
1	0.729
2	1.000
3	1.000
4	1.000
5	1.000
6	1.000
7	1.000
8	1.000
9	1.000
10	1.000
11	1.000
12	1.000
13	0.729

$Trans\_Fac_j := if(TF_j < 1, TF_j, 1)$ $F_{L\_prov_j} := Trans\_Fac_j \cdot N_{Aps\_ft_1} \cdot A_{strand} \cdot f_{pe}$ $F_{L\_reqd_j} := \left(\frac{V_{u_j}}{\phi_v} - 0.5 \cdot V_{s_j} - V_{p_j}\right) \cdot \cot(\theta_j \cdot deg)$

$Trans\_Fac =$

	1
1	0.729
2	1.000
3	1.000
4	1.000
5	1.000
6	1.000
7	1.000
8	1.000
9	1.000
10	1.000
11	1.000
12	1.000
13	0.729

$F_{L\_prov} =$

	1
1	318.6
2	437.3
3	437.3
4	437.3
5	437.3
6	437.3
7	437.3
8	437.3
9	437.3
10	437.3
11	437.3
12	437.3
13	318.6

k

$F_{L\_reqd} =$

	1
1	260.7
2	230.1
3	224.1
4	186.3
5	148.4
6	111.3
7	75.5
8	111.3
9	148.4
10	186.3
11	224.0
12	230.1
13	262.1

k

$Status\_V_j := if(F_{L\_prov_j} \geq F_{L\_reqd_j}, "OK", "NG")$

$Status\_V_j =$

	1
1	"OK"
2	"OK"
3	"OK"
4	"OK"
5	"OK"
6	"OK"
7	"OK"
8	"OK"
9	"OK"
10	"OK"
11	"OK"
12	"OK"
13	"OK"

Interface Shear:

The ability to transfer shear across the interface between the top of the precast beam and the cast-in-place deck must be checked. This check falls under the interface shear or shear friction section of LRFD (5.8.4).

Applied Factored Shear:

DC2 & DW - $A_{slabDC2} = 372.6\,in^2$ $y_{tcDC2} = 9.3\,in$ $t_{sDC2} = 6.0\,in$

$y_{armDC2} := y_{tcDC2} - \frac{t_{sDC2}}{2}$ $y_{armDC2} = 6.3\,in$

$Q_{DC2} := A_{slabDC2} \cdot y_{armDC2}$ $Q_{DC2} = 2.343534 \times 10^3\,in^3$

$V_{u\_compDC2_j} := 1.25 \cdot V_{barrier_j} + 1.5 \cdot V_{wc_j}$ $V_{u\_compDC2} =$ k

	1
1	1.5
2	1.3
3	1.2
4	0.9
5	0.6
6	0.3
7	0.0
8	0.3
9	0.6
10	0.9
11	1.2
12	1.3
13	1.5

LL & FWS - $A_{slabLL} = 373\,in^2$ $y_{tcLL} = 9.3\,in$ $t_{sLL} = 6.0\,in$

$y_{armLL} := y_{tcLL} - \frac{t_{sLL}}{2}$ $y_{armLL} = 6.3\,in$

$Q_{LL} := A_{slabLL} \cdot y_{armLL}$ $Q_{LL} = 2.343534 \times 10^3\,in^3$

$V_{u\_compLL_j} := 1.5 \cdot V_{fws_j} + 1.75 \cdot V_{LL_j}$ $V_{u\_compLL} =$ k

	1
1	66.5
2	59.6
3	59.1
4	51.5
5	43.4
6	35.1
7	26.9
8	35.1
9	43.4
10	51.5
11	59.1
12	59.6
13	67.0

Strength Approach:

$$v_{uh\_s_j} := \frac{V_{u\_compDC2_j} + V_{u\_compLL_j}}{d_{v_j} \cdot b_f} \qquad v_{uh\_s} = \begin{array}{|c|c|}\hline & 1 \\ \hline 1 & 14.9 \\ 2 & 13.3 \\ 3 & 13.2 \\ 4 & 11.4 \\ 5 & 9.6 \\ 6 & 7.7 \\ 7 & 5.9 \\ 8 & 7.7 \\ 9 & 9.6 \\ 10 & 11.4 \\ 11 & 13.2 \\ 12 & 13.3 \\ 13 & 15.0 \\ \hline \end{array} \frac{k}{ft^2}$$

$$v_{nh\_reqd_j} := \frac{v_{uh\_s_j}}{\phi_v} \qquad v_{nh\_reqd} = \begin{array}{|c|c|}\hline & 1 \\ \hline 1 & 16.5 \\ 2 & 14.8 \\ 3 & 14.7 \\ 4 & 12.7 \\ 5 & 10.7 \\ 6 & 8.6 \\ 7 & 6.5 \\ 8 & 8.6 \\ 9 & 10.7 \\ 10 & 12.7 \\ 11 & 14.6 \\ 12 & 14.8 \\ 13 & 16.6 \\ \hline \end{array} \frac{k}{ft^2}$$

Nominal Shear Resistance of the Interface (Capacity):

$V_n := cA_{cv} + \mu\left(A_{vf} \cdot f_y + P_c\right)$ (LRFD 5.8.4.1-1)

Assume normal density concrete and interface is roughened: (LRFD 5.8.4.2)

$c := 0.1 \cdot ksi \qquad \lambda := 1.00 \qquad \mu := 1.0 \cdot \lambda$

$A_{cv} := b_f \cdot 1.0 \cdot ft \qquad A_{cv} = 576\,in^2$

Since there is no permanent net compressive stress normal to shear plane, $P_c = 0$.

The required amount of horizontal shear steel is thus:

$$A_{vf_j} := \frac{v_{nh\_reqd_j} \cdot A_{cv} - c \cdot A_{cv}}{\mu \cdot f_y} \qquad A_{vf_j} := \text{if}\left(A_{vf_j} < 0, 0, A_{vf_j}\right)$$

$$A_{vf} = \begin{array}{|c|c|}\hline & 1 \\ \hline 1 & 0.1 \\ 2 & 0.0 \\ 3 & 0.0 \\ 4 & 0.0 \\ 5 & 0.0 \\ 6 & 0.0 \\ 7 & 0.0 \\ 8 & 0.0 \\ 9 & 0.0 \\ 10 & 0.0 \\ 11 & 0.0 \\ 12 & 0.0 \\ 13 & 0.1 \\ \hline \end{array} in^2 \quad \text{(per ft)}$$

Check Maximum Allowable Shear:

$V_{nh\_max} := if\left(0.2 \cdot f_{ct} \cdot A_{cv} \le 0.8 \cdot A_{cv} \cdot ksi, 0.2 \cdot f_{ct} \cdot A_{cv}, 0.8 \cdot A_{cv} \cdot ksi\right)$ (LRFD 5.8.4.1-2,3)

$V_{nh\_max} = 460.8\,k$ $V_{nh\_reqd_j} := v_{nh\_reqd_j} \cdot A_{cv}$ $Status\_V_{uh\_max_j} := if\left(V_{nh\_reqd_j} < V_{nh\_max}, "OK", "NG"\right)$

$V_{nh\_reqd} =$ k

	1
1	66.1
2	59.1
3	58.6
4	50.9
5	42.7
6	34.4
7	26.2
8	34.4
9	42.7
10	50.9
11	58.6
12	59.1
13	66.6

$Status\_V_{uh\_max} =$

	1
1	"OK"
2	"OK"
3	"OK"
4	"OK"
5	"OK"
6	"OK"
7	"OK"
8	"OK"
9	"OK"
10	"OK"
11	"OK"
12	"OK"
13	"OK"

Check Minimum Steel:

$A_{vf\_min} := \frac{0.05 \cdot ksi \cdot b_f \cdot 1.0 \cdot ft}{f_y}$ $A_{vf\_min} = 0.48\,in^2$ (per ft) (LRFD 5.8.4.1-4)

Required Horizontal Shear Reinforcement:

$A_{vw_j} := \frac{V_{nh\_reqd_j}}{A_{cv}}$ $A_{vf_j} := if\left(A_{vf_j} < A_{vf\_min}, if\left(A_{vw_j} < 0.1 \cdot ksi, A_{vf_j}, A_{vf\_min}\right), A_{vf_j}\right)$

$A_{vw} =$ psi

	1
1	114.7
2	102.6
3	101.8
4	88.3
5	74.2
6	59.7
7	45.4
8	59.7
9	74.2
10	88.3
11	101.7
12	102.6
13	115.5

$A_{vf} =$ in^2 (per ft)

	1
1	0.48
2	0.48
3	0.48
4	0.00
5	0.00
6	0.00
7	0.00
8	0.00
9	0.00
10	0.00
11	0.48
12	0.48
13	0.48

$$Spac_{hv_j} := if\left[\left(A_{vf_j} = 0 \vee A_{vf_j} \le 0.31in^2\right), 2.0 \cdot ft, \frac{ft}{\frac{A_{vf_j}}{2 \cdot 0.31 \cdot in^2}}\right]$$

$Spac_{hv} =$ in

	1
1	15.5
2	15.5
3	15.5
4	24.0
5	24.0
6	24.0
7	24.0
8	24.0
9	24.0
10	24.0
11	15.5
12	15.5
13	15.5

Final Stirrup Spacing Based on Vertical and Horizontal Shear:

$$Max\_Spac_{v_j} := if\left(fmax\_sp\_v_j \le Spac_{hv_j}, fmax\_sp\_v_j, Spac_{hv_j}\right)$$

max stirrup spacing ==>

$Max\_Spac_v =$ in

	1
1	15.5
2	15.5
3	15.5
4	24.0
5	24.0
6	24.0
7	24.0
8	24.0
9	24.0
10	24.0
11	15.5
12	15.5
13	15.5

location from end of beam ==>

$x\_end =$ ft

	1
1	0.58
2	2.50
3	3.13
4	5.68
5	8.23
6	10.78
7	13.33
8	15.88
9	18.43
10	20.98
11	23.53
12	24.17
13	26.08

Note: Consider Bursting and Confinement Requirements at ends of beam .

Bursting => Reqd_bars = 0.8 $\frac{h}{4} = 3.0$ in (Assumes Double #5 Stirrups)

Confinement => Not less than No. 10M bars at a spacing of not more than 6 in shall be placed within 1.5d of the end of the girder. These bars shall be shaped to enclose the strands.

Note 2: Use, at most, the maximum required spacing for vertical shear a distance three tenths of the beam length from its ends (past DL contraflexure point) to account for the effects of negative moment regions.

Camber and Deflection:

Prestress force at release $P_{re} = 477.4\,k$

Modulus of elasticity at release $E_{ci} = 3683.5\,ksi$

Modulus of elasticity at erection $E_{cbeamf} = 4225.1\,ksi$

Eccentricity @ end of beam $ecc_1 = 2.4\,in$

Eccentricity @ mid span $ecc_7 = 2.4\,in$

Difference $e' := ecc_7 - ecc_1$ $e' = 0.0\,in$

Moment of inertia, beam only $I = 8399\,in^4$

Moment of inertia, comp section for DC2 $I_{cDC2} = 32507\,in^4$

Design length of beam $L_{des} = 25.500\,ft$

Distance from end of beam to hold-down point $x_{r_6} = 10.7833\,ft$

PCI multiplier for prestress at erection $C_1 := 1.8$

PCI multiplier for beam weight at erection $C_2 := 1.85$

Upward camber due to prestress alone

$$\Delta_{ps} := \frac{P_{re}}{E_{ci} \cdot I}\left[\frac{ecc_7 \cdot L_{des}^{\,2}}{8} - \frac{e' \cdot \left(x_{r_6}\right)^2}{6}\right] \qquad \Delta_{ps} = 0.4\,in$$

at erection, $\Delta_{ps\_er} := \Delta_{ps} \cdot C_1$ $\Delta_{ps\_er} = 0.8\,in$

Deflection due to weight of beam alone

$$\Delta_{bm} := \frac{5 \cdot w_{sw} \cdot L_{des}^{\,4}}{384 \cdot E_{ci} \cdot I} \qquad \Delta_{bm} = -0.2\,in$$

at erection, $\Delta_{bm\_er} := \Delta_{bm} \cdot C_2$ $\Delta_{bm\_er} = -0.5\,in$

Initial camber $Camber := \Delta_{ps\_er} + \Delta_{bm\_er}$

initial camber > $Camber = 0.3\,in$

Deflection due to dead load

$$\Delta_{ds} := \frac{5 \cdot w_d \cdot L_{des}^{\,4}}{384 \cdot E_{cbeamf} \cdot I} - \frac{5 \cdot \left(w_{wc} + w_b\right) \cdot L_{des}^{\,4}}{384 \cdot E_{cbeamf} \cdot I_{cDC2}}$$

estimated dead load deflection > $\Delta_{ds} = -0.2\,in$

Residual camber $R\_Camber := Camber + \Delta_{ds}$

residual camber > $R\_Camber = 0.2\,in$

Design Summary

Bridge Number: Bridge_no = "13004"

Description: Description = "Special PS Section for Center Span w/Restraining Moments"

Beam: Section = "MAIN" f_c = 6500 psi f_{ci} = 4500 psi

Span: L_{ovr} = 26.667 ft L_{des} = 25.500 ft

Bridge: N_g = 13 S = 6.000 ft $Width_{oh}$ = 2.410 ft

Strand/Rebar: $Strand_{xx}$ = "0.5 in" d_{str} = 0.5 in Pull = 0.75 f_{pu} = 270 ksi f_y = 60 ksi

Dep_Frac = 0 Dep_Pt = 0.583 ft (distance measured from end of beam)

Approximate Beam Weight: Beam_wt = 10.6 ton

Strand Pattern:

EPat_n = (0, 0, 0, 0, 0, 0, 0, 0, 0, 0, 0, 8, 8)

EPat_h = (0.0, 0.0, 0.0, 0.0, 0.0, 0.0, 0.0, 0.0, 0.0, 0.0, 0.0, 4.0, 2.0) in

MPat_n = (0, 0, 0, 0, 0, 0, 0, 0, 0, 0, 0, 8, 8)

MPat_h = (0.0, 0.0, 0.0, 0.0, 0.0, 0.0, 0.0, 0.0, 0.0, 0.0, 0.0, 4.0, 2.0) in

No_Strands = 16

y_{end} = 3.0 in

y_{mid} = 3.0 in

Δf_{PT} = 23.8 ksi

%Loss = 11.78

P_f = 437.3 k

End Pattern Mid Pattern

Design Results

Service Limit State

top bottom

final: $f_{llt.pos}$ =

	1
1	-28.0
2	123.1
3	215.5
4	523.5
5	757.0
6	896.8
7	941.1
8	896.8
9	757.0
10	523.5
11	215.5
12	123.1
13	-27.9

p f_{allow_fcl} = 3900.0 psi

$f_{lllb.pos}$ =

	1
1	274.8
2	870.9
3	872.2
4	538.3
5	267.3
6	105.4
7	57.0
8	105.4
9	267.4
10	538.3
11	872.2
12	870.9
13	274.8

f_{allow_ft} = −484.4 psi

release: f_{rt} =

	1
1	10.6
2	29.1
3	74.2
4	228.4
5	338.5
6	404.6
7	426.7
8	404.6
9	338.5
10	228.4
11	74.2
12	29.1
13	10.6

psi $f_{allow\_rt} = -5.0912 \times 10^2$ psi f_{rb} =

	1
1	272.8
2	1183.4
3	1144.2
4	1010.3
5	914.6
6	857.2
7	838.1
8	857.2
9	914.6
10	1010.3
11	1144.2
12	1183.4
13	272.8

psi $f_{allow\_rc} = 2700.0$ psi

Strength Limit State

$M_{u.pos}$ =

	1
1	22.3
2	91.7
3	110.0
4	217.6
5	317.6
6	377.2
7	393.1
8	377.2
9	317.6
10	217.6
11	110.0
12	91.7
13	22.3

k· M_r =

	1
1	713.7
2	713.7
3	713.7
4	713.7
5	713.7
6	713.7
7	713.7
8	713.7
9	713.7
10	713.7
11	713.7
12	713.7
13	713.7

k·ft M_{r_limit} =

	1
1	29.6
2	122.0
3	146.4
4	289.4
5	422.5
6	501.7
7	522.8
8	501.7
9	422.4
10	289.4
11	146.4
12	122.0
13	29.6

k·ft c_d_p =

	1
1	0.200
2	0.200
3	0.200
4	0.200
5	0.200
6	0.200
7	0.200
8	0.200
9	0.200
10	0.200
11	0.200
12	0.200
13	0.200

c_dp limit = 0.42

Vertical Shear V_u =

	1
1	89.6
2	79.5
3	77.6
4	65.3
5	52.6
6	39.7
7	26.9
8	39.7
9	52.6
10	65.3
11	77.6
12	79.5
13	90.1

k A_v =

	1
1	0.00
2	0.00
3	0.00
4	0.00
5	0.00
6	0.00
7	0.00
8	0.00
9	0.00
10	0.00
11	0.00
12	0.00
13	0.00

$\frac{in^2}{ft}$ fmax_sp_v =

	1
1	999.0
2	999.0
3	999.0
4	999.0
5	999.0
6	999.0
7	999.0
8	999.0
9	999.0
10	999.0
11	999.0
12	999.0
13	999.0

x_end =

	1
1	0.58
2	2.50
3	3.13
4	5.68
5	8.23
6	10.78
7	13.33
8	15.88
9	18.43
10	20.98
11	23.53
12	24.17
13	26.08

ft

Horizontal Shear

V_{nh_reqd} =

	1
1	66.1
2	59.1
3	58.6
4	50.9
5	42.7
6	34.4
7	26.2
8	34.4
9	42.7
10	50.9
11	58.6
12	59.1
13	66.6

k A_{vf} =

	1
1	0.5
2	0.5
3	0.5
4	0.0
5	0.0
6	0.0
7	0.0
8	0.0
9	0.0
10	0.0
11	0.5
12	0.5
13	0.5

in^2 $Spac_{hv}$ =

	1
1	15.5
2	15.5
3	15.5
4	24.0
5	24.0
6	24.0
7	24.0
8	24.0
9	24.0
10	24.0
11	15.5
12	15.5
13	15.5

in x_end =

	1
1	0.58
2	2.50
3	3.13
4	5.68
5	8.23
6	10.78
7	13.33
8	15.88
9	18.43
10	20.98
11	23.53
12	24.17
13	26.08

ft

$V_{nh\_max} = 460.8\,k$

Anchorage Steel $P_r = 19.1\,k$ $A_{s\_anchor} = 0.95\,in^2$ $\frac{h}{4} = 3.0\,in$ Reqd_bars = 0.8

Camber and Deflection

initial camber > Camber = 0.34 in

estimated dead load deflection > $\Delta_{ds} = -0.16\,in$

residual camber > R_Camber = 0.17 in

B.2 Design of Reinforcement within Negative Moment Region

Sheet No: 1/14
Bridge No: 13004
Made By: KRH/JMF
Date: 4/4/2006

Interior Strip Design

NOTE: Concrete slab will be designed based on a 1-foot strip width.

Custom Units

$k \equiv 1000 \cdot lb$ $\quad psf \equiv 1 \cdot \frac{lb}{ft^2}$ $\quad pcf \equiv 1 \cdot \frac{lb}{ft^3}$ $\quad ORIGIN \equiv 1$

$ksi \equiv 1000 \cdot \frac{lb}{in^2}$ $\quad ksf \equiv 1000 \cdot \frac{lb}{ft^2}$ $\quad kcf \equiv 1000 \cdot \frac{lb}{ft^3}$

General Input

$L_{out} := 22.0ft$	length of outer spans	$f'_c := 4ksi$	concrete strength at 28 days
$L_{in} := 27.0ft$	length of inner spans	$f_y := 60ksi$	rebar yield strength
$t_s := 18.0in$	structural slab thickness	$E := 29000ksi$	rebar modulus of elasticity
$D_{ws} := 0in$	overlay thickness	$n := 8$	steel-concrete modular ratio
$b := 12in$	design width	$\phi := 0.9$	flexural resistance factor

$Z := 130 \frac{k}{in}$ crack width parameter (severe exposure)

Service Moments (From BTBeam)

$M_{DC2} := -1.9k \cdot ft$	Service DL Moment
$M_{LL} := -19.9k \cdot ft$	Service LL Moment
$M_{RM} := -59.7k \cdot ft$	Restraining Moment

Fatigue Moments (From BTBeam)

$M_{fat\_max} := -8.30k \cdot ft$	Max Fatigue Moment
$M_{fat\_min} := 1.32k \cdot ft$	Min Fatigue Moment

Reinforcement

$A'_s := 1.99in^2$	R/F area over piers (#8's @ 4")	$A'_{s3} := 0.79in^2$	R/F area in spans (#8's @ 12")
$Sp := 4in$	R/F spacing over piers	$Sp_3 := 12in$	R/F spacing in spans
$r_{bar} := 0.5in$	R/F radius over piers	$r_{bar3} := 0.5in$	R/F radius in spans

$A'_{s2} := 1.39in^2$ R/F area in transition (~#8's @ 6")

$Sp_2 := 6in$ ~R/F spacing in transition

$r_{bar2} := 0.5in$ R/F radius in transition

$cover_{top} := 3.0in$ clear cover to top bar

I) Strength Design

1) Flexure

$M_u := 1.25 \cdot M_{DC2} + 1.75 \cdot M_{LL} + 1.0 \cdot M_{RM}$ $\quad M_u = -96.900\ k \cdot ft$

$d := t_s - cover_{top} - r_{bar}$ $\quad d = 14.500\ in$

$M_n := A'_s \cdot f_y \cdot \left(d - \frac{A'_s \cdot f_y}{1.7 \cdot f'_c \cdot b} \right)$ $\quad M_n = 129.716\ k \cdot ft$

$\phi \cdot M_n = 116.744\ k \cdot ft$

$Status_{FLEX} := if\left(|\phi \cdot M_n| \geq |M_u|, \text{"OK"}, \text{"NO GOOD"} \right)$ $\quad Status_{FLEX} = \text{"OK"}$

$PR_{flexure} := \left| \frac{\phi \cdot M_n}{M_u} \right|$ $\quad PR_{flexure} = 1.205$

II) Service Limit Checks

1) Crack Control

$M_{serv} := 1.0 \cdot M_{DC2} + 1.0 \cdot M_{LL} + 1.0 \cdot M_{RM}$ $\quad M_{serv} = -81.500\ k \cdot ft$

- **Calculate location of crack ignoring compression steel**

By simply taking moments of the steel and concrete areas about the bottom of the crack, the following equation is obtained:

$\left(b \cdot \frac{x^2}{2} \right) - A'_{sT} \cdot (d - x) := 0$ (x is the depth of uncracked concrete from the bottom of the slab)

Transform steel area into concrete area

$A'_s = 1.990\ in^2$ (full negative moment reinforcement)

$A'_{sT} := A'_s \cdot n$ $\quad A'_{sT} = 15.920\ in^2$

Solve the quadratic equation:

$$Coefs := \begin{bmatrix} -(A'_{sT} \cdot d) \cdot \frac{1}{in^3} \\ (A'_{sT}) \cdot \frac{1}{in^2} \\ \left(\frac{b}{2}\right) \cdot \frac{1}{in} \end{bmatrix} \qquad polyroots(Coefs) = \begin{pmatrix} -7.670 \\ 5.016 \end{pmatrix}$$

$x := if\left(polyroots(Coefs)_1 < 0, polyroots(Coefs)_2 \cdot in, polyroots(Coefs)_1 \cdot in \right)$

$x = 5.016\ in$

- **Calculate cracked moment of inertia ignoring compression steel**

$$I_{CR} := \frac{b\cdot\left(x^3\right)}{3} + A'_{sT}\cdot(d - x)^2 \qquad I_{CR} = 1936.760\,in^4$$

- **Negative Moment Steel Stress**

$$\sigma_{st\_T} := \frac{M_{serv}\cdot(d - x)}{I_{CR}}$$ (With transformed steel area) $\sigma_{st\_T} = -4.789\,ksi$

Calculate actual steel stress

$\sigma_{st} := \sigma_{st\_T}\cdot n$ $\sigma_{st} = -38.312\,ksi$

- **Negative moment limiting stress** 5.7.3.4

$d_c := if\left(cover_{top} + D_{ws} \le 2in, cover_{top} + D_{ws} + r_{bar}, 2in + r_{bar}\right)$

$d_c = 2.500\,in$ (extreme tension fiber to cener of bar)

$A := \left(2\cdot d_c\cdot Sp\right) - \pi\cdot r_{bar}^2$ (Area of concrete with same centroid as tensile reinforcement around each bar)

$A = 19.215\,in^2$

$$f_{sa} := if\left[\frac{Z}{\left(d_c\cdot A\right)^{\frac{1}{3}}} \le 0.6\cdot f_y, \frac{Z}{\left(d_c\cdot A\right)^{\frac{1}{3}}}, 0.6\cdot f_y\right]$$ $f_{sa} = 35.762\,ksi$

$Status_{CR} := if\left(\left|f_{sa}\right| \ge \left|\sigma_{st}\right|, "OK", "NO\ GOOD"\right)$ $Status_{CR} = "NO\ GOOD"$

$$PR_{cr} := \left|\frac{f_{sa}}{\sigma_{st}}\right|$$ $PR_{cr} = 0.933$

This check fails because of the restraint moment at the pier. The true magnitude of the this moment is uncertain, and indications are that this moment is usually overestimated. "Proposed Revisions to the AASHTO LRFD Bridge Design Specifications on the subject of Precast/Prestressed Concrete Girders Made Continuous for Live Load," Section C5.14.1.2.7b (see attached) states that:

- "...the consequences of negative restraint moments on these bridges are not generally as for positive moments."
- "...it is questionable whether negative moments due to differential shrinkage form to the extent predicted by analysis" (Shrinkage was used in the analysis to obtain the moments that were used in the above analysis.)
- "...designers should be aware that these [published] methods [for computing restraint moments] may overestimate the restraint moments - both positive and negative."

For this structure, the effect of negative restraint moments has been accounted for to a reasonable extent by placing #8's @ 4" over the pier. The crack control check still fails by 9.3%, but based on guidance from the proposed code and engineering judgement, it is believed that restraint moments (which control) will not develop to the extent predicted. **Therefore, the Crack Control Check is OK.**

2) Minumum Reinforcement 5.7.3.3.2

a) Calculate M_{cr}

- **Modulus of Rupture**

$f_r := 0.24 \cdot \sqrt{f_c \cdot ksi}$ $f_r = 0.480\ ksi$ 5.4.2.6

- **Gross Moment of Inertia and Cracking Moment**

$I_{Gr} := \frac{1}{12} \cdot b \cdot t_s^3$ $I_{Gr} = 5832.000\ in^4$

$y := \frac{t_s}{2}$ $y = 9.000\ in$

$M_{cr} := \frac{f_r \cdot I_{Gr}}{y}$ $M_{cr} = 25.920\ ft \cdot k$

b) Determine limits

$limit_{min} := if\left(\left|1.2 \cdot M_{cr}\right| < \left|1.33 \cdot M_n\right|, \left|1.2 \cdot M_{cr}\right|, \left|1.33 \cdot M_n\right|\right)$

$limit_{min} = 31.104\ k \cdot ft$

c) Moment capacities with steel used (ignoring compression steel)

$\phi \cdot M_n = 116.744\ k \cdot ft$

$Status_{MIN} := if\left(\left|\phi \cdot M_n\right| \geq \left|limit_{min}\right|, "OK", "NOT\ OK"\right)$ $Status_{MIN} = "OK"$

3) Maximum Reinforcement

a) Determine β_1

$\beta_1 := 0.85 - \left[0.05 \cdot \left(\frac{f_c}{ksi} - 4\frac{ksi}{ksi}\right)\right]$ $\beta_1 = 0.850$

b) Check Negative Reinforcement

$c := \frac{A'_s \cdot f_y}{\beta_1 \cdot 0.85 \cdot f_c \cdot b}$ $c = 3.443\ in$

$Status_{MAX} := if\left(\frac{c}{d} \leq 0.42, "OK", "NOT\ OK"\right)$ $Status_{MAX} = "OK"$

III) Fatigue Limit Checks 5.5.3.1

2) Negative Reinforcement

a) Calculate σ_{min} using I_{Gr}

$\sigma_{min} := \frac{\left(M_{DC2} + M_{RM} + 2.0 \cdot M_{fat\_min}\right) \cdot y}{I_{Gr}}$ $\sigma_{min} = -1.092\ ksi$ 5.5.3.1

$0.095 \cdot \sqrt{f_c \cdot ksi} = 0.190\ ksi$

b) σ_{min} exceeds 0.19 ksi tension so use I_{CR} to calculate f'_{min}

$$f_{min} := \begin{cases} \dfrac{(M_{DC2} + M_{RM} + M_{fat\_min})\cdot(d - x)}{I_{CR}} & \text{if } \sigma_{min} < 0\cdot ksi \wedge |\sigma_{min}| > 0.095\cdot\sqrt{f_c\cdot ksi} \\ \dfrac{(M_{DC2} + M_{RM} + M_{fat\_min})\cdot(y)}{I_{Gr}} & \text{otherwise} \end{cases}$$

$f_{min} = -3.542\ ksi$

c) Transform Stress

$f_{min\_T} := f_{min}\cdot n$ $\qquad f_{min\_T} = -28.336\ ksi$

d) Calculate σ_{max} using I_{Gr}

$$\sigma_{max} := \frac{(M_{DC2} + M_{RM} + 2.0\cdot M_{fat\_max})\cdot y}{I_{Gr}} \quad \sigma_{max} = -1.448\ ksi \qquad 5.5.3.1$$

$0.095\cdot\sqrt{f_c\cdot ksi} = 0.190\ ksi$

e) σ_{max} exceeds 0.19 ksi tension so use I_{CR} to calculate f'_{min}

$$f_{max} := \begin{cases} \dfrac{(M_{DC2} + M_{RM} + M_{fat\_max})\cdot(d - x)}{I_{CR}} & \text{if } \sigma_{max} < 0\cdot ksi \wedge |\sigma_{max}| > 0.095\cdot\sqrt{f_c\cdot ksi} \\ \dfrac{(M_{DC2} + M_{RM} + M_{fat\_max})\cdot(y)}{I_{Gr}} & \text{otherwise} \end{cases}$$

$f_{max} = -4.107\ ksi$

f) Transform Stress

$f_{max\_T} := f_{max}\cdot n$ $\qquad f_{max\_T} = -32.859\ ksi$

g) Stress Range

$Range := f_{max\_T} - f_{min\_T}$ $\qquad Range = -4.522\ ksi$

h) Calculate Maximum Allowable Stress Range

$f_f := 21ksi - 0.33\cdot f_{min\_T} + 8\cdot(0.3)\cdot ksi$ $\qquad f_f = 32.751\ ksi$ $\qquad 5.5.3.2$

$Status_{FAT} := if(|Range| \le |f_f|, "OK", "NOT OK")$ $\qquad Status_{FAT} = "OK"$

NOTE: Additional fatigue checks must be made when bars are terminated.

IV) Bar Cutoffs

1) Calculate Strength Capacity in Negative Moment Regions, Ignore Compression Steel

- **Strength Capacity with Negative Moment Steel Over Piers**

$$M_r := \phi \cdot A'_s \cdot f_y \cdot \left(d - \frac{A'_s \cdot f_y}{2 \cdot 0.85 \cdot f'_c \cdot b} \right) \qquad \boxed{M_r = 116.744\,k \cdot ft}$$

- **Strength Capacity with Negative Moment Steel in Transition Regions**

$$d_2 := t_s - cover_{top} - r_{bar2} \qquad d_2 = 14.500\,in$$

$$M_{r2} := \phi \cdot A'_{s2} \cdot f_y \cdot \left(d_2 - \frac{A'_{s2} \cdot f_y}{2 \cdot 0.85 \cdot f'_c \cdot b} \right) \qquad \boxed{M_{r2} = 84.305\,k \cdot ft}$$

- **Strength Capacity with Negative Moment Steel in Span**

$$d_3 := t_s - cover_{top} - r_{bar3} \qquad d_3 = 14.500\,in$$

$$M_{r3} := \phi \cdot A'_{s3} \cdot f_y \cdot \left(d_3 - \frac{A'_{s3} \cdot f_y}{2 \cdot 0.85 \cdot f'_c \cdot b} \right) \qquad \boxed{M_{r3} = 49.482\,k \cdot ft}$$

2) Calculate Service Capacity in Negative Moment Regions, Ignore Compression Steel

- **Service Capacity over Piers (based on service steel stress - 5.7.3.4)**

$$M_{servMAX} := \frac{f_{sa} \cdot I_{CR}}{(d - x) \cdot n} \qquad \boxed{M_{servMAX} = 76.076\,k \cdot ft}$$

- **Service Capacity in Transition Region (based on service steel stress - 5.7.3.4)**

Calulate I_{CR} for the section ignoring compression steel (-Moment)

- **Calculate location of crack ignoring compression steel**

By simply taking moments of the steel and concrete areas about the bottom of the crack, the following equation is obtained:

$$\left(b \cdot \frac{x_2^2}{2} \right) - A'_{s2T} \cdot (d_2 - x_2) := 0$$

(x is the depth of uncracked concrete from the top of the slab)

Transform steel area into concrete area

$A'_{s2} = 1.390\,in^2$ (area of negative reinforcement in span)

$A'_{s2T} := n \cdot A'_{s2}$ $A'_{s2T} = 11.120\,in^2$

Solve the quadratic equation:

$$Coefs := \begin{bmatrix} -(A'_{s2T} \cdot d_2) \cdot \frac{1}{in^3} \\ (A'_{s2T}) \cdot \frac{1}{in^2} \\ \left(\frac{b}{2}\right) \cdot \frac{1}{in} \end{bmatrix} \qquad polyroots(Coefs) = \begin{pmatrix} -6.193 \\ 4.339 \end{pmatrix}$$

$x_2 := if\left(polyroots(Coefs)_1 < 0, polyroots(Coefs)_2 \cdot in, polyroots(Coefs)_1 \cdot in\right)$

$x_2 = 4.339\,in$

- **Calculate cracked moment of inertia ignoring compression steel**

$$I_{CR2} := \frac{b \cdot \left(x_2^{\,3}\right)}{3} + A'_{s2T} \cdot (d_2 - x_2)^2$$

$I_{CR2} = 1474.855\,in^4$

Maximum Negative Service Moment With Steel in Transition Regions

$d_{c2} := if\left(cover_{top} + D_{ws} \le 2in, cover_{top} + D_{ws} + r_{bar2}, 2in + r_{bar2}\right)$

$d_{c2} = 2.500\,in$ (extreme tension fiber to cener of bar)

$A_2 := \left(2 \cdot d_c \cdot Sp_2\right) - \pi \cdot r_{bar2}^{\,2}$ (Area of concrete with same centroid as tensile reinforcement around each bar)

$A_2 = 29.215\,in^2$

$$f_{sa2} := if\left[\frac{Z}{(d_{c2} \cdot A_2)^{\frac{1}{3}}} \le 0.6 \cdot f_y, \frac{Z}{(d_{c2} \cdot A_2)^{\frac{1}{3}}}, 0.6 \cdot f_y\right] \qquad 5.7.3.4\text{-}1$$

$f_{sa2} = 31.100\,ksi$

$M_{servMAX} = 76.076\,k \cdot ft$

$$M_{servMAX2} := \frac{f_{sa2} \cdot I_{CR2}}{(d_2 - x_2) \cdot n}$$

$\boxed{M_{servMAX2} = 47.025\,k \cdot ft}$

- **Service Capacity in Spans (based on service steel stress - 5.7.3.4)**

Calulate I_{CR} for the section ignoring compression steel (-Moment)

- **Calculate location of crack ignoring compression steel**

By simply taking moments of the steel and concrete areas about the bottom of the crack, the following equation is obtained:

$$\left(b\cdot\frac{x_3^{\,2}}{2}\right) - A'_{s3T}\cdot(d_3 - x_3) := 0$$

(x is the depth of uncracked concrete from the top of the slab)

Transform steel area into concrete area

$A'_{s3} = 0.790\,in^2$ (area of negative reinforcement in span)

$A'_{s3T} := n\cdot A'_{s3}$ $A'_{s3T} = 6.320\,in^2$

Solve the quadratic equation:

$$Coefs := \begin{bmatrix} -(A'_{s3T}\cdot d_3)\cdot\frac{1}{in^3} \\ (A'_{s3T})\cdot\frac{1}{in^2} \\ \left(\frac{b}{2}\right)\cdot\frac{1}{in} \end{bmatrix} \qquad polyroots(Coefs) = \begin{pmatrix} -4.470 \\ 3.417 \end{pmatrix}$$

$x_3 := if\left(polyroots(Coefs)_1 < 0, polyroots(Coefs)_2\cdot in, polyroots(Coefs)_1\cdot in\right)$

$x_3 = 3.417\,in$

- **Calculate cracked moment of inertia ignoring compression steel**

$$I_{CR3} := \frac{b\cdot\left(x_3^{\,3}\right)}{3} + A'_{s3T}\cdot(d_3 - x_3)^2$$

$I_{CR3} = 935.890\,in^4$

Maximum Negative Service Moment With Steel in Span

$d_{c3} := if\left(cover_{top} + D_{ws} \le 2in, cover_{top} + D_{ws} + r_{bar3}, 2in + r_{bar3}\right)$

$d_{c3} = 2.500\,in$ (extreme tension fiber to cener of bar)

$A_3 := \left(2 \cdot d_c \cdot Sp_3\right) - \pi \cdot r_{bar3}^2$ (Area of concrete with same centroid as tensile reinforcement around each bar)

$A_3 = 59.215\,in^2$

$$f_{sa3} := if\left[\frac{Z}{\left(d_{c3} \cdot A_3\right)^{\frac{1}{3}}} \le 0.6 \cdot f_y, \frac{Z}{\left(d_{c3} \cdot A_3\right)^{\frac{1}{3}}}, 0.6 \cdot f_y\right]$$ 5.7.3.4-1

$f_{sa3} = 24.575\,ksi$

$M_{servMAX} = 76.076\,k \cdot ft$

$M_{servMAX3} := \frac{f_{sa3} \cdot I_{CR3}}{\left(d_3 - x_3\right) \cdot n}$

$M_{servMAX3} = 21.616\,k \cdot ft$

Summary of Capacities:

Strength Capacities	Service Capacities (Based on Cracking)
$M_r = 116.744\,k \cdot ft$	$M_{servMAX} = 76.076\,k \cdot ft$
$M_{r2} = 84.305\,k \cdot ft$	$M_{servMAX2} = 47.025\,k \cdot ft$
$M_{r3} = 49.482\,k \cdot ft$	$M_{servMAX3} = 21.616\,k \cdot ft$

Use the above capacities to draw capacity diagram in Excel.

3) Cut Locations

Cut locations may be governed by one of three criteria:

1) Location where STR-1 moment is equal to moment capacity of steel in span plus greatest of (L/20, d, or 15*d_b) [LRFD 5.11.1.2.1]

2) Location where steel in span is adequate for service requirements

3) Location where cut is at least one development length from peak moment

Moment capacities with minimum steel:

$M_{r3} = 49.482\,k \cdot ft$

Calculate required extension past theoretical cut:

$L := if\left(L_{out} \ge L_{in}, L_{out}, L_{in}\right)$ $L = 27.000\,ft$

$d_2 = 14.500\,in$

$d_{b2} := 2 \cdot r_{bar2}$

$d_{b2} = 1.000\,in$ $\quad \frac{L}{20} = 16.200\,in$ $\quad d_2 = 14.500\,in$ $\quad 15 \cdot d_{b2} = 15.000\,in$

$Cut_{ext} := \max\left(\frac{L}{20}, d_2, 15 \cdot d_{b2}\right)$ $\quad Cut_{ext} = 16.200\,in$

Use Excel Spreadsheet to determine cut locations based on the above 3 criteria.

4)Service Checks at Critical Cut Locations (Crack Control not checked since used for cutoffs)

a) Negative Reinforcement

- **Check Fatigue of Continuing Bars**

Moment values at max fatigue range

$M_{fat\_max\_cut} := 23.07k \cdot ft$ $\quad M_{fat\_min\_cut} := -8.43k \cdot ft$

$M_{DL\_cut} := 0.83k \cdot ft$

Calculate f'_{min} using I_{Gr} at mid span

$f_{min} := \frac{\left(M_{DL\_cut} + 2.0 \cdot M_{fat\_min\_cut}\right) \cdot y}{I_{Gr}}$ $\quad f_{min} = -0.297\,ksi$ $\quad 5.5.3.1$

$0.095 \cdot \sqrt{f_c \cdot ksi} = 0.190\,ksi$

f'_{min} doesn't exceeds 0.19 ksi tension but conservatively use I_{CR3} to calculate f'_{min}

$f_{min} := \frac{\left(M_{DL\_cut} + M_{fat\_min\_cut}\right) \cdot \left(d_3 - x_3\right)}{I_{CR3}}$ $\quad f_{min} = -1.080\,ksi$

Transform Stress

$f_{min\_T} := f_{min} \cdot n$ $\quad f_{min\_T} = -8.640\,ksi$

Calculate f'_{max} using I_{posCR}

Calulate I_{CR} for the section ignoring compression steel (+Moment)

- **Calculate location of crack ignoring compression steel**

By simply taking moments of the steel and concrete areas about the top of the crack, the following equation is obtained:

$\frac{b \cdot x_{pos}^2}{2} - \frac{1}{2} A_{sT} \cdot \left(d_{pos} - x_{pos}\right) := 0$ $\quad$ (x is the depth of uncracked concrete from the top of the slab)

$A_s := 0.833\,in^2$ assume 4-#9 bars for every 6 feet for +Mom R/F

$r_{bar\_pos} := 0.564in$

$cover_{bot} := 8.0in$

Transform steel area into concrete area

$A_s = 0.833\,in^2$ (half positive reinforcement)

$A_{sT} := A_s \cdot n$ $A_{sT} = 6.664\,in^2$

$d_{pos} := t_s - cover_{bot} - r_{bar\_pos}$ $d_{pos} = 9.436\,in$

Solve the quadratic equation:

$$Coefs := \begin{bmatrix} -\left(\frac{1}{2} A_{sT} \cdot d_{pos}\right) \cdot \frac{1}{in^3} \\ \left(\frac{1}{2} A_{sT}\right) \cdot \frac{1}{in^2} \\ \left(\frac{b}{2}\right) \cdot \frac{1}{in} \end{bmatrix} \qquad polyroots(Coefs) = \begin{pmatrix} -2.584 \\ 2.028 \end{pmatrix}$$

$x_{pos} := if\left(polyroots(Coefs)_1 < 0, polyroots(Coefs)_2 \cdot in, polyroots(Coefs)_1 \cdot in\right)$

$x_{pos} = 2.028\,in$

- **Calculate cracked moment of inertia ignoring compression steel**

$$I_{posCR} := \frac{b \cdot \left(x_{pos}^{\,3}\right)}{3} + \frac{1}{2} A_{sT} \cdot \left(d_{pos} - x_{pos}\right)^2$$

$I_{posCR} = 216.218\,in^4$

$$f_{max} := \frac{\left(M_{DL\_cut} + M_{fat\_max\_cut}\right) \cdot \left(x_{pos} - cover_{top}\right)}{I_{posCR}} \qquad f_{max} = -1.289\,ksi$$

Transform Stress

$f_{max\_T} := f_{max} \cdot n$ $f_{max\_T} = -10.312\,ksi$

Stress Range

$Range := f_{min\_T} - f_{max\_T}$ $Range = 1.672\,ksi$

Calculate Maximum Allowable Stress Range

$f_f := 21ksi - 0.33 \cdot f_{min\_T} + 8 \cdot (0.3) \cdot ksi$ $f_f = 26.251\,ksi$ 5.5.3.2

$Status_{FATcut} := if(|Range| \le |f_f|, "OK", "NO GOOD")$ $Status_{FATcut} = "OK"$

This check was very conservative as positive moment cracked section properties were used to calculate the maximum steel stress. Since the bottom half of the section is prestressed, the section properties calculated above are probably too conservative. However, the check works with no problem so do not revise.

- **Check Minimum Reinforcement**

$M_{u\_cut} := -15.79\,ft \cdot k$

$\phi M_{n\_cut} \ge M_{u\_cut}$ $M_{n\_cut} := \frac{M_{u\_cut}}{\phi}$ $M_{n\_cut} = -17.544\,ft \cdot k$

a) Determine limits

$limit_{cut} := if(|1.2 \cdot M_{cr}| < |1.33 \cdot M_{n\_cut}|, |1.2 \cdot M_{cr}|, |1.33 \cdot M_{n\_cut}|)$

$limit_{cut} = 23.334\,k \cdot ft$

b) Check Section

$M_{r3} = 49.482\,k \cdot ft$

$Status_{MINcut} := if(|M_{r3}| \ge |limit_{cut}|, "OK", "NO GOOD")$ $Status_{MINcut} = "OK"$

- **Check Maximum Reinforcement**

$c_{cut} := \frac{A'_{s3} \cdot f_y}{\beta_1 \cdot 0.85 \cdot f'_c \cdot b}$ $c_{cut} = 1.367\,in$

$Status_{MAXcut} := if\left(\frac{c_{cut}}{d_3} \le 0.42, "OK", "NO GOOD"\right)$ $Status_{MAXcut} = "OK"$

The controlling cutoff location is OK so all other cut locations are OK by inspection.

V) Temperature and Shrinkage Steel

Minimum area of reinforcement in each direction to control temperature change and shrinkage cracking: 5.10.8.2

$A_{g\_slab} := b \cdot t_s$ $A_{g\_slab} = 216.000\,in^2$

$A_s \geq 0.11ksi \cdot \frac{A_{g\_slab}}{f_y}$

$A_{s\_slab} := 0.11ksi \cdot \frac{A_{g\_slab}}{f_y}$ $A_{s\_slab} = 0.396\,in^2$

Equally Distributed on Both Faces:

$A_{s\_slab} := \frac{A_{s\_slab}}{2}$ $A_{s\_slab} = 0.198\,in^2$

For Transverse T&S steel:

Use #5's at 12" (= 0.31 in^2/ft) in span

VI) Distribution Reinforcement

Transverse load distribution steel must be provided on the bottom of the slab: 5.14.4.1

$$\%_{primary\_out} := \begin{cases} \frac{100 \cdot \sqrt{ft}}{\sqrt{L_{out}}} & \text{if } \frac{100 \cdot \sqrt{ft}}{\sqrt{L_{out}}} \leq 50 \\ 50 & \text{otherwise} \end{cases} \qquad \%_{primary\_out} = 21.320$$

$$\%_{primary\_in} := \begin{cases} \frac{100 \cdot \sqrt{ft}}{\sqrt{L_{in}}} & \text{if } \frac{100 \cdot \sqrt{ft}}{\sqrt{L_{in}}} \leq 50 \\ 50 & \text{otherwise} \end{cases} \qquad \%_{primary\_in} = 19.245$$

Use only the controlling percentage

$\%_{primary} := \text{if}(\%_{primary\_out} > \%_{primary\_in}, \%_{primary\_out}, \%_{primary\_in})$

$\%_{primary} = 21.320$

For this structure, the primary reinforcement consists of prestressing strands. Use the average prestressing strand area per foot width of the bridge to calculate the required distribution steel. Look at a 6'-0" wide interior section:

$A_{strand} := 0.153\,in^2$ $n_{strand} := 16$ $w_{beam} := 6 \cdot ft$

$$A_{ps} := \frac{A_{strand} \cdot n_{strand}}{w_{beam}} \cdot ft \qquad A_{ps} = 0.408\ in^2$$

Since the modulus of elasticities for mild reinforcement and prestressing strands are similar, the above prestressing area will not be transformed.

Main Reinforcing:

$A_{ps} = 0.408\ in^2$

$$A_{s\_dr} := \frac{\%_{primary}}{100} \cdot A_{ps} \qquad A_{s\_dr} = 0.087\ in^2$$

#6's @ 12" (A_s = 0.44in^2/ft) are provided transversely near the bottom of the slab. From the above calculations, this will be adequate for distribution.

Longitudinal Reinforcement Summary:

Over Piers => 1-#8 & 2-#7's per ft. width (4" sp)
In Spans => #8's @ 12"

Transverse Reinforcement Summary:

Top => #5's @ 12"
Bottom => #6's @ 12"

Appendix C

Instrumentation and Data Acquisition System Components

C.1 Instrumentation

The instrumentation of this bridge consisted of embedment strain gages and spot-weldable strain gages. Both of these strain gages use the vibrating wire principle to obtain strain measurements within the structure. A length of steel wire is tensioned between two end blocks within the gage which expand and contract with the element (e.g., concrete, steel) altering the tension in the steel wire. This change in tension is measured as a change in the resonant frequency of vibration of the wire. Electromagnetic coils that are located close to the wire provide the excitation and readout of the gage frequency. Portable read-outs or dataloggers used in conjunction with these gages, provide the necessary voltage pulses to pluck the wire and convert the measured frequencies so as to display or record the reading directly in microstrain units.

C.1.1 Geokon® Model VCE-4200 Vibrating Wire Embedment Strain Gage

The Geokon® Model VCE-4200 Vibrating Wire (VW) Strain Gage is designed for long-term strain measurements in mass concrete, for use in structures such as foundations, piles, bridges, dams, containment vessels, tunnel liners, etc. This gage has an active gage length of 6 in. and a sensitivity of 1.0 microstrain. The temperature range for this gage is -20° C to 80° C. Figure C.1 shows a diagram of the Model VCE-4200 Vibrating Wire Embedment Strain Gage and its components. A photograph of this strain gage tied to reinforcement is provided in Figure C.2.

C.1.2 Geokon® Model VW-4150 Vibrating Wire Spot-weldable Strain Gage

The VK-4150 VW Spot-weldable Strain Gage is designed for measuring strains on structural steel members such as bridges, piles, tunnel linings, buildings, etc. This gage consists of a VW gage element and integral coil assembly and has an active gage length of 2 in. and a sensitivity of 1.0 microstrain. The temperature range for this gage is -20° C to 80° C. Figure C.3 shows a diagram of the Model VK-4150 Vibrating Wire Spot-weldable Strain Gage and its components. A photograph of this strain gage installed on steel reinforcement is provided in Figure C.4.

C.2 Data Acquisition System Components

C.2.1 CR-10X Measurement and Control Module

The datalogger generally serves as the central processing unit of the data acquisition system. Programs are downloaded into the CR-10X which enable it to read numerous different electrical instruments. These programs control the type of measurements to be taken (i.e., temperature, vibrating wire strain), the frequency at which measurements are taken, and the location where the collected data is to be stored (i.e., storage modules). Once a program is downloaded into the datalogger it will continue to run that program until the datalogger is shut off or a new program is downloaded in which case the previous program is erased. When the datalogger is powered on it will run the latest program that was downloaded. All communication with the datalogger, including the downloading of programs, was done using a computer via an SC929 to RS-232 interface cable.

The CR-10X datalogger has 12 single-ended or 6 differential channels used to obtain readings. It also has 8 ports that are used to control the operation of up to 8 AM 16/32 relay multiplexers. The CR-10X requires 12 V of DC power provided by a PS100 12 V rechargeable battery. The CR-10X supplies power to each of the peripherals connected to it. A photograph of a CR-10X Measurement and Control Module is provided in Figure C.5.

C.2.2 AM 16/32 Relay Multiplexer

The main function of a multiplexer is to increase the capacity of instruments that can be read by each datalogger allowing the system to monitor an increased number of instruments. The capacity of the AM 16/32 relay multiplexer depends primarily on the type of instrument to be read. For the purpose of this project, each multiplexer had the capacity for 16 differential sensors that require excitation, i.e., 16 VW strain gages, along with the differential thermistor of each gage. Therefore using three multiplexers for each datalogger increased the capacity of each datalogger to 48 VW strain gages and the capacity of the entire system to 96 VW strain gages.

The program that was downloaded to the datalogger controlled the data collection from the multiplexer. The data was read from each channel of the multiplexer sequentially then the process was repeated for the next multiplexer. The AM 16/32 multiplexer required 12 V of DC power that was supplied by the datalogger. A photograph of an AM 16/32 relay multiplexer is provided in Figure C.6.

C.2.3 AVW4 Vibrating Wire Interface

A VW interface is located between the multiplexers and the dataloggers in systems that include VW sensors. These interfaces convert the strain and temperature measurements obtained from the VW strain gage to single-ended measurements which can be read by a datalogger. The AVW4 interface had the capacity to read four VW gages or four multiplexers with VW gages attached to them.

The AVW4 VW interface required 5 V of power that was supplied by the datalogger. A photograph of an AVW4 Vibrating Wire Interface is provided in Figure C.7.

C.2.4 SM16M Storage Module

All of the data that the dataloggers collect was sent to the SM16M Storage Modules. Each module could hold up to 8 million low-resolution data values. The use of these modules allowed for more data storage and easier data retrieval than if the data was stored in the dataloggers. The storage module would stop storing data in the case that the storage module had become full and would not over-write old data. A photograph of an SM16M Storage Module is provided in Figure C.8.

These storage modules required 5 V of DC power that was supplied through the SC12 cable that connected the storage module to the datalogger. All communication with the storage modules from a computer, including data retrieval, was done using an SC532A to RS-232 interface cable along with LoggerNet software which was downloaded from the Campbell Scientific, Inc. website (www.campbellscientific.com).

C.2.5 PS100 12V DC Power Supply with Charging Regulator and Battery

The PS100 12 V DC Power Supply was used to supply 12 V of DC power to the dataloggers. These batteries included a charging regulator. Long-term charging power was supplied by a CSI Model 9591 AC transformer plugged into the permanent AC power source. A photograph of a PS100 12 V Power Supply is provided in Figure C.9.

C.2.6 PC400 Software

The PC400 datalogger support software program was used to write programs and to communicate with the dataloggers. One of the main features of this software was the EZSetup Wizard which was used to setup the dataloggers. In addition, this software simplified the writing and editing of programs with Short Cut, Edlog, and CRBasic programming tools. The programs for this project were written using the Edlog tool. When using this tool, the user types in a command and then fills in the variables (i.e, execution interval, delay, etc.). The programs that were downloaded into the dataloggers at the beginning of the field testing to collect data are provided in Appendix E of this report.

The minimum computer requirements for this software were a 300 MHz Pentium II processor with 64 Mbytes of RAM and a screen resolution of 800x600. The recommended operating systems were Windows® 98, NT, 2000, or XP.

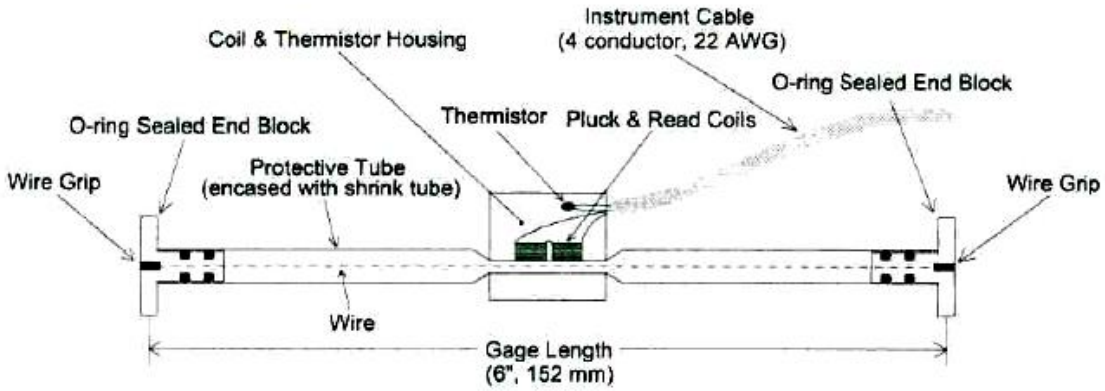

Figure C.1 Diagram of VCE-4200 VW Embedment Strain Gage

Figure C.2 Photograph of VCE-4200 VW Embedment Strain Gage tied to uncoated rebar

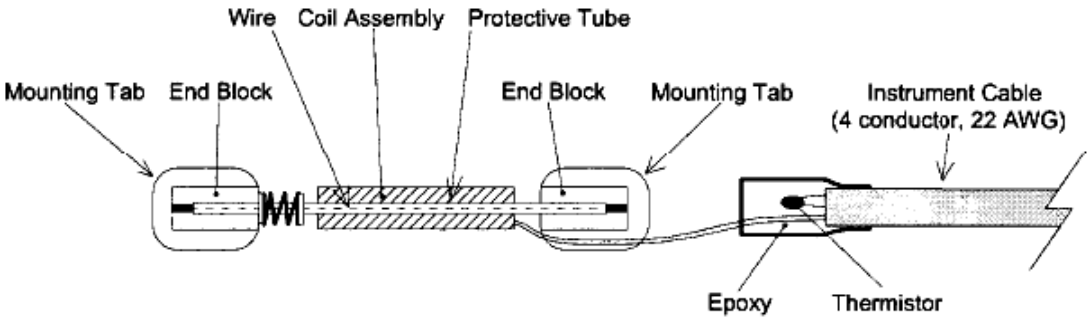

Figure C.3 Diagram of VK-4150 VW Spot-weldable Strain Gage

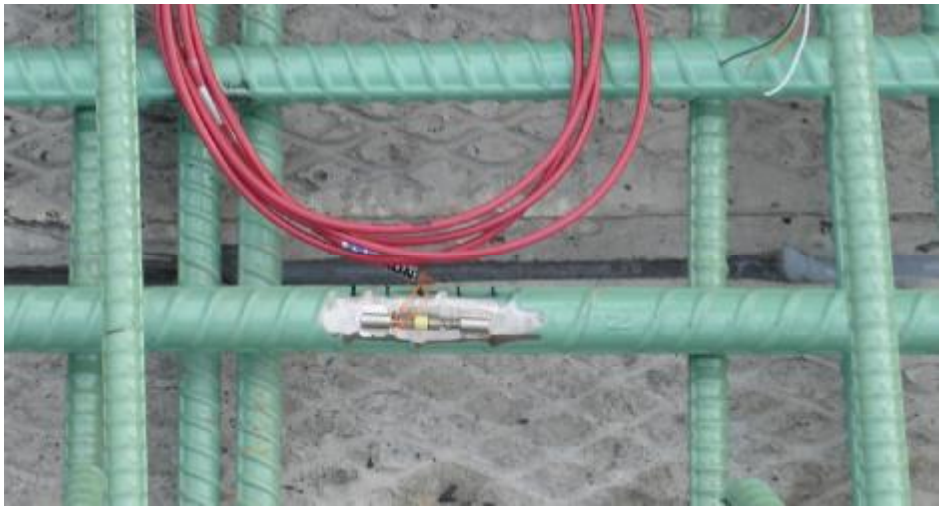

Figure C.4 Photograph of VK-4150 VW Spot-weldable Strain Gage

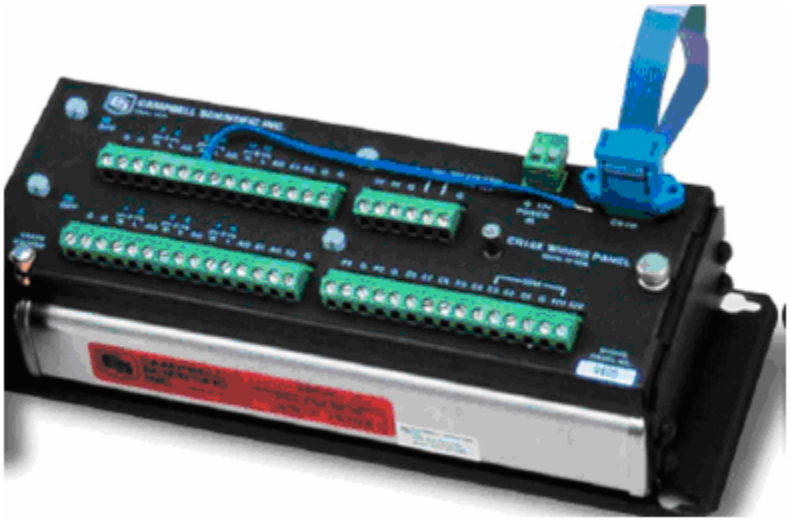

Figure C.5 CR-10X Measurement and Control Module

Figure C.6 AM 16/32 Relay Multiplexer

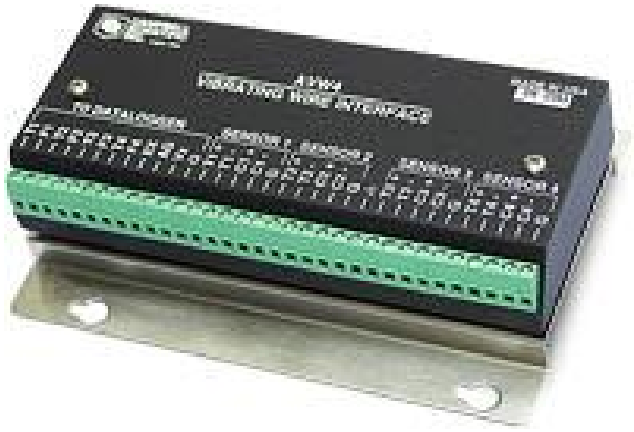

Figure C.7 AVW4 Vibrating Wire Interface

Figure C.8 SM16M Storage Module

Figure C.9 PS100 12 V DC Power Supply with Charging Regulator and Battery

Appendix D

Installation Log

D.1 Mn/DOT Bridge No. 13004 in Center City, MN

September 2, 2005- Friday
Charles Bell II, Catherine French, Carol Shield, Matthew Smith

All 21 precast sections of Stage 1 of the bridge construction were erected in-place during the morning. The age of the precast sections ranged from 4 to 15 days when they were delivered to the site. In the afternoon, once the precast sections were in place, 21 VW spot-weldable strain gages were installed on the transverse hooks of the precast sections. Initially, difficulties were encountered with properly welding the gages to the transverse hooks. It was determined that these difficulties could be avoided by grinding a smooth flat surface for the welding pads of the gages and grinding a groove for the coil between the flat surfaces for the welding pads.

September 6, 2005- Tuesday
Charles Bell II, Scott Nesvold, Justin Ocel, Carol Shield

The iron workers were at the site to tie and place the reinforcement cages above the longitudinal joints between adjacent precast sections as well as place the No. 8 bars above the piers. In addition, the construction workers set up formwork for the CIP concrete railing. VW spot-weldable strain gages were installed on the reinforcement cage after they were tied together but prior to setting the cages in place above the longitudinal joints. After all of the gages were installed on a reinforcement cage, the cage was dropped in place above the joint. The No. 8 bars were set in place over the piers after the reinforcement cages were placed in the joints on both the center and east spans. At this point gages were installed on the No. 8 bars. A total of ten VW spot-weldable strain gages were installed on the longitudinal steel of the reinforcement cage and the No. 8 bars above the piers on this day. Three gages could not be installed because one of the reinforcement cages on the east span was not set in place above the joints and therefore the No. 8 bars within this joint were not yet in place.

September 12, 2005- Monday
Charles Bell II, Paul Bergson, Justin Ocel, Carol Shield, Matthew Smith

The remaining 3 VW spot-weldable strain gages that could not be installed on Tuesday, September 6, 2005 were installed on the No. 8 bar over the pier. In addition, five VW embedment strain gages were installed directly above Joint #1 (Figure D.1). The portion of the conduit that would be in the CIP concrete topping was erected in-place. Cables were run through the conduit to the multiplexer boxes below the bridge deck. Four VW spot-weldable strain gages were soldered to the cables within the conduit. Readings were taken and recorded for the gages that were soldered to the cables on this day using a Geokon® GK-403 read-out box to ensure they were working properly. The date of installation for each gage and the initial reading obtained for each gage once the gage was soldered to a cable are provided in Tables D.1 through D.3. The construction workers set up formwork for the construction joint along the center of the bridge. Work was cut short due to inclement weather.

September 13, 2005- Tuesday
Charles Bell II, Paul Bergson, Cathy French, Carol Shield

Five VW embedment strain gages were installed in both Joints #2 and #3 (Figure D.1) directly above the longitudinal joints. All of the gages that had been installed at the midspan of the center span and the end and midspan of the east span were soldered to the cables that had previously been run through the conduit. Readings were taken and recorded for the gages soldered to the cables on this day using a Geokon® GK-403 read-out box to ensure they were working properly. The construction workers set up the formwork for the deck at the ends of the bridge.

September 15, 2006- Thursday
Charles Bell, Scott Nesvold, Brian Runzel, Carol Shield

Ten VW embedment strain gages were tied to the bottom of the longitudinal steel above Joints #1, #2, and #3 (Figure D.1). Eighteen VW spot-weldable strain gages were installed on the longitudinal deck steel at the midspan of both the center and eastern spans and adjacent to the pier cap. A number of the longitudinal reinforcing bars had to be untied in order to rotate the bars after the gages had been installed so that the gages were then located on the underside of the bar. This was done to protect the gages during casting of the CIP concrete deck. Many of these gages were soldered to the cables that had previously been run through the conduit. Readings were taken and recorded for all gages soldered to the cables to date using a Geokon® GK-403 read-out box to ensure they were working properly. The construction workers finished setting up formwork for the deck and worked on the formwork for the east approach panel. The iron workers finished placing and tying the deck steel, including the bars that had to be untied, and started to place and tie reinforcement for the east approach panel.

September 16, 2005- Friday
Charles Bell II, Carol Shield, Matthew Smith

One additional VW spot-weldable strain gage was installed on the longitudinal deck steel. The remaining gages at the instrumented locations above Joints #1, #2, and #3 (Figure D.1) were soldered to the cables that had previously been run through the conduit. In addition a number of the gages that were installed near the pier caps had to be soldered to supplementary cables to reach the multiplexer boxes. The wiring from the remaining gages was run down to the multiplexer boxes. Readings were taken and recorded for all gages using a Geokon® GK-403 read-out box to ensure they were working properly. The boxes of the conduit that would be covered with CIP concrete were closed and sealed using duct seal and mastic tape. The iron workers finished placing and tying the reinforcement for the east approach panel.

September 19, 2005- Monday
Charles Bell II, Matthew Smith

Readings were taken and recorded for all gages using a Geokon® GK-403 read-out box to ensure they were working properly. The portions of the reinforcement that had been ground during installation were painted with epoxy. The areas around the installed gages were painted pink to bring them to the attention of the concrete workers during the concrete casting process. The concrete workers poured and finished the concrete deck. Special attention was paid to the areas surrounding instrumentation to make sure that vibration did not occur too close to the gages. Readings were taken and recorded for all gages using a Geokon® GK-403 read-out box after the concrete pour to ensure they were still working properly. All of the gages survived the concrete pour. The age of the precast sections ranged from 32 to 21 days at the time the CIP concrete of the deck was poured.

September 21, 2005- Wednesday
Charles Bell II, Matthew Smith

Readings were taken and recorded using a Geokon® GK-403 read-out box between the times of 1:30 and 2:30 pm.

September 23-26, 2005
Charles Bell II, Matthew Smith

Readings were taken and recorded using a Geokon® GK-403 read-out box between the times of 7:30 and 8:30 am.

September 26, 2005- Monday
Charles Bell II, Matthew Smith

After readings were taken and recorded using a Geokon® GK-403 read-out box, cables were run through the conduit from the multiplexer boxes to the cabinet that was used to temporarily house the dataloggers near the abutment. The multiplexers were mounted on plywood within the multiplexer boxes. The cables that were attached to the instruments were stripped and then partially connected to the multiplexers.

September 27, 2005- Tuesday
Charles Bell II, Matthew Smith

The remaining cables were connected to the multiplexers. The temporary cabinet was set up and the multiplexer cables were connected to the dataloggers housed in the temporary cabinet. Programs were downloaded to the dataloggers, but the dataloggers were not working properly. Work was halted due to darkness.

September 28, 2005- Wednesday
Charles Bell II, Matthew Smith

Modifications were made to the programs and connections to get the dataloggers working properly. The readings obtained from the gages matched the readings taken through the installation process using the Geokon® GK-403 read-out box. However, eight of the gages did not record temperature readings.

November 18, 2005- Friday
Charles Bell II, Matthew Smith

An effort was made to obtain temperature readings from the eight gages that were not providing temperature readings. Five of the gages were fixed by adjusting the connection at the multiplexers to ensure that there was not an electrical shortage. Three of the gages still did not give temperature readings. The following gages were still not giving temperature readings: SJ1-11-1, SJ2-5T-6, and SJ3-5T-1.

Table D.1 Installation date and initial readings for all gages installed between September 2 and September 12, 2005

Gage #	Date Installed	Date of Initial Reading	Strain Reading (με)	Temp. Reading (ºC)
SJ1-5T-1	9/2/2005	9/12/2005	3180	19.9
SJ1-5T-2	9/2/2005	9/12/2005	2810	20.3
SJ1-5T-3	9/2/2005	9/12/2005	2678	20.0
SJ1-5T-4	9/2/2005	9/12/2005	2863	21.4
SJ1-5T-5	9/2/2005	9/13/2005	2420	20.4
SJ1-5T-6	9/2/2005	9/13/2005	2609	21.1
SJ1-5T-7	9/2/2005	9/13/2005	2408	20.7
SJ2-5T-1	9/2/2005	9/13/2005	4060	22.7
SJ2-5T-2	9/2/2005	9/13/2005	3201	22.7
SJ2-5T-3	9/2/2005	9/13/2005	3194	23.0
SJ2-5T-4	9/2/2005	9/13/2005	1453	23.7
SJ2-5T-5	9/2/2005	9/13/2005	2757	23.2
SJ2-5T-6	9/2/2005	9/13/2005	2012	25.5
SJ2-5T-7	9/2/2005	9/13/2005	3320	23.8
SJ3-5T-1	9/2/2005	9/13/2005	1243	23.6
SJ3-5T-2	9/2/2005	9/13/2005	3300	24.5
SJ3-5T-3	9/2/2005	9/13/2005	2992	24.3
SJ3-5T-4	9/2/2005	9/13/2005	3335	24.9
SJ3-5T-5	9/2/2005	9/13/2005	2793	24.6
SJ3-5T-6	9/2/2005	9/13/2005	2998	25.7
SJ3-5T-7	9/2/2005	9/13/2005	2372	25.4
SJ1-51-1	9/6/2005	9/13/2005	1956	24.9
SJ1-52-1	9/6/2005	9/13/2005	3226	25.9
SJ2-51-1	9/6/2005	9/13/2005	1739	31.4
SJ2-52-1	9/6/2005	9/13/2005	2201	29.3
SJ2-41-1	9/6/2005	9/13/2005	2683	25.4
SJ3-41-1	9/6/2005	9/16/2005	2486	26.0
SJ1-21-1	9/6/2005	9/13/2005	2492	27.3
SJ1-22-1	9/6/2005	9/13/2005	3308	27.5
SJ1-11-1	9/6/2005	9/13/2005	2907	25.6
SJ1-12-1	9/6/2005	9/13/2005	2624	26.8
SJ1-41-1	9/12/2005	9/13/2005	2795	24.9
SJ1-C1-1	9/12/2005	9/13/2005	2491	25.3
SJ1-31-1	9/12/2005	9/13/2005	3294	24.6
CJ1-51-1	9/12/2005	9/13/2005	2652	21.0
CJ1-51-2	9/12/2005	9/13/2005	2776	22.1
CJ1-51-3	9/12/2005	9/13/2005	2881	21.3
CJ1-51-4	9/12/2005	9/13/2005	2889	23.4
CJ1-51-5	9/12/2005	9/13/2005	2818	22.7

Table D.2 Installation date and initial readings for the VW embedment strain gages installed between September 13 and September 15, 2005

Gage #	Date Installed	Date of Initial Reading	Strain Reading (με)	Temp. Reading (ºC)
CJ2-51-1	9/13/2005	9/13/2005	2908	22.7
CJ2-51-2	9/13/2005	9/13/2005	2848	24.7
CJ2-51-3	9/13/2005	9/13/2005	2913	25.0
CJ2-51-4	9/13/2005	9/13/2005	2921	27.1
CJ2-51-5	9/13/2005	9/13/2005	2855	25.5
CJ3-51-1	9/13/2005	9/13/2005	2915	24.6
CJ3-51-2	9/13/2005	9/13/2005	2828	25.7
CJ3-51-3	9/13/2005	9/13/2005	2771	25.9
CJ3-51-4	9/13/2005	9/13/2005	2895	26.0
CJ3-51-5	9/13/2005	9/13/2005	2858	25.6
CJ1-53-1	9/15/2005	9/15/2005	2897	22.7
CJ1-53-2	9/15/2005	9/15/2005	2878	23.6
CJ1-53-3	9/15/2005	9/15/2005	2804	23.1
CJ1-53-4	9/15/2005	9/15/2005	2797	23.8
CJ1-53-5	9/15/2005	9/15/2005	2661	23.2
CJ1-53-6	9/15/2005	9/15/2005	2938	23.8
CJ1-53-7	9/15/2005	9/15/2005	2787	23.8
CJ1-53-8	9/15/2005	9/15/2005	2822	23.7
CJ1-53-9	9/15/2005	9/15/2005	2965	24.2
CJ1-53-10	9/15/2005	9/15/2005	2914	24.9
CJ2-53-1	9/15/2005	9/15/2005	2959	27.0
CJ2-53-2	9/15/2005	9/15/2005	2896	26.2
CJ2-53-3	9/15/2005	9/15/2005	2843	25.3
CJ2-53-4	9/15/2005	9/15/2005	2895	26.5
CJ2-53-5	9/15/2005	9/15/2005	2842	25.9
CJ2-53-6	9/15/2005	9/15/2005	2860	26.4
CJ2-53-7	9/15/2005	9/15/2005	2942	26.7
CJ2-53-8	9/15/2005	9/15/2005	2768	26.1
CJ2-53-9	9/15/2005	9/15/2005	2022	26.8
CJ2-53-10	9/15/2005	9/15/2005	2865	26.6
CJ3-53-1	9/15/2005	9/15/2005	2804	26.2
CJ3-53-2	9/15/2005	9/15/2005	2843	26.6
CJ3-53-3	9/15/2005	9/15/2005	2878	25.5
CJ3-53-4	9/15/2005	9/16/2005	2877	25.2
CJ3-53-5	9/15/2005	9/16/2005	2814	25.6
CJ3-53-6	9/15/2005	9/16/2005	2890	25.8
CJ3-53-7	9/15/2005	9/16/2005	2917	25.6
CJ3-53-8	9/15/2005	9/16/2005	2805	25.5
CJ3-53-9	9/15/2005	9/16/2005	2875	26.3
CJ3-53-10	9/15/2005	9/16/2005	2834	23.4

Table D.3 Installation date and initial readings for the VW spot-weldable strain gages installed between September 15 and September 16, 2005

Gage #	Date Installed	Date of Initial Reading	Strain Reading (με)	Temp. Reading (ºC)
SJ1-53-2	9/15/2005	9/15/2005	2827	25.8
SJ1-53-1	9/15/2005	9/15/2005	2726	26.2
SJ1-43-2	9/15/2005	9/15/2005	1995	24.9
SJ1-43-1	9/15/2005	9/15/2005	2801	27.8
SJ1-33-2	9/15/2005	9/15/2005	2120	25.6
SJ1-33-1	9/15/2005	9/15/2005	2988	27.5
SJ1-23-1	9/15/2005	9/15/2005	2731	26.0
SJ1-13-1	9/15/2005	9/15/2005	2287	26.6
SJ2-53-1	9/15/2005	9/15/2005	2616	27.6
SJ2-43-1	9/15/2005	9/16/2005	2697	28.6
SJ3-43-1	9/15/2005	9/16/2005	1965	26.4
SW1-43-1	9/15/2005	9/16/2005	3090	29.2
SW1-43-2	9/15/2005	9/16/2005	3083	28.8
SW1-43-3	9/15/2005	9/16/2005	2766	27.7
SW2-43-1	9/15/2005	9/16/2005	2902	27.0
SW2-43-2	9/15/2005	9/16/2005	3057	27.5
SW2-43-3	9/15/2005	9/16/2005	3144	26.6
SJ1-C3-1	9/15/2005	9/16/2005	2691	25.7
SJ1-C3-2	9/16/2005	9/16/2005	2541	28.3

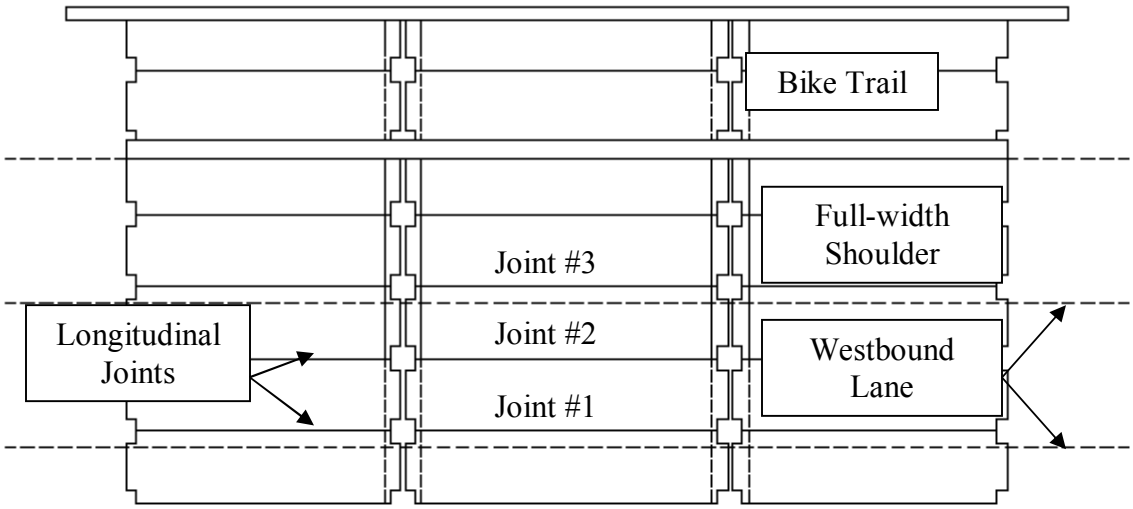

Figure D.1 Plan View of Stage 1 of the Bridge Construction of Mn/DOT Bridge No. 13004 highlighting the Instrumented Joints

Appendix E

Datalogger Programs

E.1 Datalogger Programs

A program was downloaded into each CR-10X datalogger to administer the collection of data. These programs controlled when data was collected, what type of reading was recorded (i.e, temperature reading, strain reading, etc.), and where this data was stored. The programs that were initially downloaded into the dataloggers instructed the dataloggers to take strain and temperature readings from each strain gage every two hours and to store those readings in the SM16M storage modules.

The programs of the two dataloggers differed slightly because of the number and order of VW embedment and VW spot-weldable strain gages that were connected to each datalogger. For instance, the program for Datalogger #1 starts with a loop that reads the gages connected to Multiplexer #1, which were six VW embedment strain gages followed by ten VW spot-weldable strain gages. In order to do this an inner loop must run six times to take readings from the six VW embedment strain gages and after that is complete a second inner loop runs ten times to take readings from the ten VW spot-weldable strain gages. At this point the program is done taking readings from Multiplexer #1 and it is the end of that loop. Then a second loop starts that takes readings from Multiplexer #2, but this multiplexer has a different number of each gage connected to it and they are in a different order, therefore the inner loops must be modified to read the correct sequence of gages. The program for Datalogger #1 is annotated below to explain the loops in more detail.

E.1.1 Datalogger #1

```
;{CR10X}
;
*Table 1 Program
  01: 7200.0    Execution Interval (seconds)

;Multiplexer 1

1:  Do (P86)
 1: 41       Set Port 1 High


;Embedment

2:  Beginning of Loop (P87)
 1: 0000     Delay
 2: 6        Loop Count


   3:  Do (P86)
    1: 72       Pulse Port 2
```

The first command tells the program how often to take readings. The maximum execution interval is 7200 seconds.

This starts the loop for Multiplexer #1. "Set Port 1 High" tells the datalogger to open Port 1 which is the where the reset wire from Multiplexer #1 connects to Datalogger #1.

This starts the inner loop for VW embedment strain gages. The loop count is set at 6 because there are 6 VW embedment strain gages connected to Channels 1 through 6 of Multiplexer #1.

Port 2 is where the clock wire from Multiplexer #1 is connected to Datalogger #1. The pulse repeatedly changes the channel on the multiplexer so as to read each gage.

; 20ms Pause

4: Excitation with Delay (P22)
1: 1 Ex Channel
2: 10 Delay W/Ex (0.01 sec units)
3: 10 Delay After Ex (0.01 sec units)
4: 0000 mV Excitation

This command creates a 20 ms pause. This ensures sufficient settling time for relay contacts.

5: Excite-Delay (SE) (P4)
1: 1 Reps
2: 15 2500 mV Fast Range
3: 1 SE Channel
4: 1 Excite all reps w/Exchan 1
5: 1 Delay (0.01 sec units)
6: 2500 mV Excitation
7: 1 -- Loc [TM1CE_1]
8: .001 Multiplier
9: 0.0 Offset

This command tells the datalogger to obtain a voltage reading for temperature from the first gage. It stores that reading at the input location given in "Loc". The multiplier puts the voltage reading in the correct units to be converted to a temperature reading. SE Channel 1 is the channel that the temperature wires from Multiplexer #1 are connected to Datalogger #1.

6: Polynomial (P55)
1: 1 Reps
2: 1 -- X Loc [TM1CE_1]
3: 1 -- F(X) Loc [TM1CE_1]
4: -104.78 C0
5: 378.11 C1
6: -611.59 C2
7: 544.27 C3
8: -240.91 C4
9: 43.089 C5

This command uses a polynomial to convert the voltage reading obtained above to a temperature reading and then stores it back in the input location in "Loc". C0-C5 are the constants used in the polynomial.

7: Vibrating Wire (SE) (P28)
1: 1 Reps
2: 5 SE Channel
3: 1 Excite all reps w/Exchan 1
4: 4 Starting Freq. (100 Hz units)
5: 12 End Freq. (100 Hz units)
6: 250 No. of Cycles
7: 50 Rep Delay (0.01 sec units)
8: 49 -- Loc [M1CE_1]
9: 3304 Multiplier

This command tells the data logger to obtain a reading from the VW embedment strain gage. The multiplier is a gage factor that is used to convert this reading to a strain reading in microstrain units. SE Channel 5 is where the gage wires from Multiplexer #1 are connected to Datalogger #1.

```
   10: 0.0      Offset

8:  End (P95)

;Spot Weldable

9:  Beginning of Loop (P87)
 1: 0000     Delay
 2: 10       Loop Count


   10:  Do (P86)
    1: 72       Pulse Port 2

;20ms Pause

   11:  Excitation with Delay (P22)
    1: 1        Ex Channel
    2: 10       Delay W/Ex (0.01 sec units)
    3: 10       Delay After Ex (0.01 sec units)
    4: 0000     mV Excitation


   12:  Excite-Delay (SE) (P4)
    1: 1        Reps
    2: 15       2500 mV Fast Range
    3: 1        SE Channel
    4: 1        Excite all reps w/Exchan 1
    5: 1        Delay (0.01 sec units)
    6: 2500     mV Excitation
    7: 7     -- Loc [ TM1SW_1   ]
    8: .001     Multiplier
    9: 0.0      Offset


   13:  Polynomial (P55)
    1: 1        Reps
    2: 7     -- X Loc [ TM1SW_1   ]
    3: 7     -- F(X) Loc [ TM1SW_1   ]
    4: -104.78  C0
    5: 378.11   C1
    6: -611.59  C2
    7: 544.27   C3
    8: -240.91  C4
    9: 43.089   C5
```

This ends the inner loop for the VW embedment strain gages connected to Multiplexer #1. After Datalogger #1 has performed this loop 6 times it moves on to the next inner loop.

This starts the inner loop for VW spot-weldable strain gages. The loop count is set at 10 because there are 10 VW spot-weldable strain gages connected to Channels 7 through 16 of Multiplexer #1.

This starts the inner loop for VW spot-weldable strain gages. The loop count is set at 10 because there are 10 VW spot-weldable strain gages connected to Channels 7 through 16 of Multiplexer #1. The rest of this loop follows the same pattern as the first inner loop.

14: Vibrating Wire (SE) (P28)
1: 1 Reps
2: 5 SE Channel
3: 1 Excite all reps w/Exchan 1
4: 14 Starting Freq. (100 Hz units)
5: 35 End Freq. (100 Hz units)
6: 250 No. of Cycles
7: 50 Rep Delay (0.01 sec units)
8: 55 -- Loc [M1SW_1]
9: 391 Multiplier
10: 0.0 Offset

The multiplier was changed because the gage factor for VW spot-weldable strain gages is different from the embedment gages.

15: End (P95)

16: Do (P86)
1: 51 Set Port 1 Low

This ends the loop for Multiplexer #1.

;Multiplexer 2

This starts the loop for Multiplexer #2.

17: Do (P86)
1: 43 Set Port 3 High

;Spot Weldable

This starts the inner loop to read the VW spot-weldable strain gages connected to channels 1 through 7 of Multiplexer #2. The rest of the program follows the same pattern as the first loop, until the end of the program.

18: Beginning of Loop (P87)
1: 0000 Delay
2: 7 Loop Count

19: Do (P86)
1: 74 Pulse Port 4

;20ms Pause

20: Excitation with Delay (P22)
1: 1 Ex Channel
2: 10 Delay W/Ex (0.01 sec units)
3: 10 Delay After Ex (0.01 sec units)
4: 0000 mV Excitation

21: Excite-Delay (SE) (P4)

1: 1 Reps
2: 15 2500 mV Fast Range
3: 2 SE Channel
4: 1 Excite all reps w/Exchan 1
5: 1 Delay (0.01 sec units)
6: 2500 mV Excitation
7: 17 -- Loc [TM2SW_1]
8: .001 Multiplier
9: 0.0 Offset

22: Polynomial (P55)
1: 1 Reps
2: 17 -- X Loc [TM2SW_1]
3: 17 -- F(X) Loc [TM2SW_1]
4: -104.78 C0
5: 378.11 C1
6: -611.59 C2
7: 544.27 C3
8: -240.91 C4
9: 43.089 C5

23: Vibrating Wire (SE) (P28)
1: 1 Reps
2: 6 SE Channel
3: 1 Excite all reps w/Exchan 1
4: 14 Starting Freq. (100 Hz units)
5: 35 End Freq. (100 Hz units)
6: 250 No. of Cycles
7: 50 Rep Delay (0.01 sec units)
8: 65 -- Loc [M2SW_1]
9: 391 Multiplier
10: 0.0 Offset

24: End (P95)

;Embedment

25: Beginning of Loop (P87)
1: 0000 Delay
2: 9 Loop Count

26: Do (P86)

```
  1: 74       Pulse Port 4

;20ms Pause

 27:  Excitation with Delay (P22)
  1: 1        Ex Channel
  2: 10       Delay W/Ex (0.01 sec units)
  3: 10       Delay After Ex (0.01 sec units)
  4: 0000     mV Excitation


 28:  Excite-Delay (SE) (P4)
  1: 1        Reps
  2: 15       2500 mV Fast Range
  3: 2        SE Channel
  4: 1        Excite all reps w/Exchan 1
  5: 1        Delay (0.01 sec units)
  6: 2500     mV Excitation
  7: 24    -- Loc [ TM2CE_1   ]
  8: .001     Multiplier
  9: 0.0      Offset


 29:  Polynomial (P55)
  1: 1        Reps
  2: 24    -- X Loc [ TM2CE_1   ]
  3: 24    -- F(X) Loc [ TM2CE_1   ]
  4: -104.78  C0
  5: 378.11   C1
  6: -611.59  C2
  7: 544.27   C3
  8: -240.91  C4
  9: 43.089   C5


 30:  Vibrating Wire (SE) (P28)
  1: 1        Reps
  2: 6        SE Channel
  3: 1        Excite all reps w/Exchan 1
  4: 4        Starting Freq. (100 Hz units)
  5: 12       End Freq. (100 Hz units)
  6: 250      No. of Cycles
  7: 50       Rep Delay (0.01 sec units)
  8: 72    -- Loc [ M2CE_1    ]
  9: 3304     Multiplier
```

10: 0.0 Offset

31: End (P95)

32: Do (P86)
1: 53 Set Port 3 Low

;Multiplexer 3

33: Do (P86)
1: 45 Set Port 5 High

;Embedment

34: Beginning of Loop (P87)
1: 0000 Delay
2: 6 Loop Count

35: Do (P86)
1: 76 Pulse Port 6

;20ms Pause

36: Excitation with Delay (P22)
1: 1 Ex Channel
2: 10 Delay W/Ex (0.01 sec units)
3: 10 Delay After Ex (0.01 sec units)
4: 0000 mV Excitation

37: Excite-Delay (SE) (P4)
1: 1 Reps
2: 15 2500 mV Fast Range
3: 3 SE Channel
4: 1 Excite all reps w/Exchan 1
5: 1 Delay (0.01 sec units)
6: 2500 mV Excitation
7: 33 -- Loc [TM3CE_1]
8: .001 Multiplier
9: 0.0 Offset

38: Polynomial (P55)

```
 1: 1        Reps
 2: 33    -- X Loc [ TM3CE_1   ]
 3: 33    -- F(X) Loc [ TM3CE_1   ]
 4: -104.78  C0
 5: 378.11   C1
 6: -611.59  C2
 7: 544.27   C3
 8: -240.91  C4
 9: 43.089   C5


39:  Vibrating Wire (SE) (P28)
 1: 1        Reps
 2: 7        SE Channel
 3: 1        Excite all reps w/Exchan 1
 4: 4        Starting Freq. (100 Hz units)
 5: 12       End Freq. (100 Hz units)
 6: 250      No. of Cycles
 7: 50       Rep Delay (0.01 sec units)
 8: 81    -- Loc [ M3CE_1    ]
 9: 3304     Multiplier
10: 0.0      Offset


40:  End (P95)

;Spot Weldable

41:  Beginning of Loop (P87)
 1: 0000     Delay
 2: 10       Loop Count


42:  Do (P86)
 1: 76       Pulse Port 6

;20ms Pause

43:  Excitation with Delay (P22)
 1: 1        Ex Channel
 2: 10       Delay W/Ex (0.01 sec units)
 3: 10       Delay After Ex (0.01 sec units)
 4: 0000     mV Excitation


44:  Excite-Delay (SE) (P4)
```

1: 1 Reps
2: 15 2500 mV Fast Range
3: 3 SE Channel
4: 1 Excite all reps w/Exchan 1
5: 1 Delay (0.01 sec units)
6: 2500 mV Excitation
7: 39 -- Loc [TM3SW_1]
8: .001 Multiplier
9: 0.0 Offset

45: Polynomial (P55)
1: 1 Reps
2: 39 -- X Loc [TM3SW_1]
3: 39 -- F(X) Loc [TM3SW_1]
4: -104.78 C0
5: 378.11 C1
6: -611.59 C2
7: 544.27 C3
8: -240.91 C4
9: 43.089 C5

46: Vibrating Wire (SE) (P28)
1: 1 Reps
2: 7 SE Channel
3: 1 Excite all reps w/Exchan 1
4: 14 Starting Freq. (100 Hz units)
5: 35 End Freq. (100 Hz units)
6: 250 No. of Cycles
7: 50 Rep Delay (0.01 sec units)
8: 87 -- Loc [M3SW_1]
9: 391 Multiplier
10: 0.0 Offset

47: End (P95)

48: Do (P86)
1: 55 Set Port 5 Low

49: Batt Voltage (P10)
1: 97 Loc [Battery]

This command tells the program to take a battery voltage reading.

```
50:  Do (P86)
 1: 10       Set Output Flag High (Flag 0)

51:  Real Time (P77)^10788
 1: 110      Day,Hour/Minute (midnight = 0000)

52:  Resolution (P78)
 1: 1        High Resolution

53:  Sample (P70)^1767
 1: 97       Reps
 2: 1        Loc [ TM1CE_1    ]

54:  Serial Out (P96)
 1: 71       Storage Module

*Table 2 Program
  02: 0.0000    Execution Interval (seconds)

*Table 3 Subroutines

End Program
```

This command tells the datalogger to prepare to send the data to be stored.

This command prepares the reading to be stored in its final form with day and time information.

This command tells the datalogger to send the readings to the storage module.

```
-Input Locations-
1 TM1CE_1    5 2 2
2 TM1CE_2    9 1 0
3 TM1CE_3    9 1 0
4 TM1CE_4    9 1 0
5 TM1CE_5    9 1 0
6 TM1CE_6    9 1 0
7 TM1SW_1    9 2 2
8 TM1SW_2    9 1 0
9 TM1SW_3    9 1 0
```

10 TM1SW_4 9 1 0
11 TM1SW_5 9 1 0
12 TM1SW_6 9 1 0
13 TM1SW_7 9 1 0
14 TM1SW_8 9 1 0
15 TM1SW_9 9 1 0
16 TM1SW_10 9 1 0
17 TM2SW_1 9 2 2
18 TM2SW_2 9 1 0
19 TM2SW_3 9 1 0
20 TM2SW_4 9 1 0
21 TM2SW_5 9 1 0
22 TM2SW_6 9 1 0
23 TM2SW_7 9 1 0
24 TM2CE_1 9 2 2
25 TM2CE_2 9 1 0
26 TM2CE_3 9 1 0
27 TM2CE_4 9 1 0
28 TM2CE_5 9 1 0
29 TM2CE_6 9 1 0
30 TM2CE_7 9 1 0
31 TM2CE_8 9 1 0
32 TM2CE_9 9 1 0
33 TM3CE_1 9 2 2
34 TM3CE_2 9 1 0
35 TM3CE_3 9 1 0
36 TM3CE_4 9 1 0
37 TM3CE_5 9 1 0
38 TM3CE_6 9 1 0
39 TM3SW_1 9 2 2
40 TM3SW_2 9 1 0
41 TM3SW_3 9 1 0
42 TM3SW_4 9 1 0
43 TM3SW_5 9 1 0
44 TM3SW_6 9 1 0
45 TM3SW_7 9 1 0
46 TM3SW_8 9 1 0
47 TM3SW_9 9 1 0
48 TM3CE_10 9 1 0
49 M1CE_1 9 1 1
50 M1CE_2 9 1 0
51 M1CE_3 9 1 0
52 M1CE_4 9 1 0
53 M1CE_5 9 1 0
54 M1CE_6 9 1 0
55 M1SW_1 9 1 1

56 M1SW_2 9 1 0
57 M1SW_3 9 1 0
58 M1SW_4 9 1 0
59 M1SW_5 9 1 0
60 M1SW_6 9 1 0
61 M1SW_7 9 1 0
62 M1SW_8 9 1 0
63 M1SW_9 9 1 0
64 M1SW_10 9 1 0
65 M2SW_1 9 1 1
66 M2SW_2 9 1 0
67 M2SW_3 9 1 0
68 M2SW_4 9 1 0
69 M2SW_5 9 1 0
70 M2SW_6 9 1 0
71 M2SW_7 9 1 0
72 M2CE_1 9 1 1
73 M2CE_2 9 1 0
74 M2CE_3 9 1 0
75 M2CE_4 9 1 0
76 M2CE_5 9 1 0
77 M2CE_6 9 1 0
78 M2CE_7 9 1 0
79 M2CE_8 9 1 0
80 M2CE_9 9 1 0
81 M3CE_1 9 1 1
82 M3CE_2 9 1 0
83 M3CE_3 9 1 0
84 M3CE_4 9 1 0
85 M3CE_5 9 1 0
86 M3CE_6 9 1 0
87 M3SW_1 9 1 1
88 M3SW_2 9 1 0
89 M3SW_3 9 1 0
90 M3SW_4 9 1 0
91 M3SW_5 9 1 0
92 M3SW_6 9 1 0
93 M3SW_7 9 1 0
94 M3SW_8 9 1 0
95 M3SW_9 9 1 0
96 M3SW_10 17 1 0
97 Battery 1 0 1
-Program Security-
0000
0000
0000

-Mode 4-
-Final Storage Area 2-
0
-CR10X ID-
0
-CR10X Power Up-
3
-CR10X Compile Setting-
3
-CR10X RS-232 Setting-
-1
-DLD File Labels-
0
-Final Storage Labels-
0,Day_RTM,10788
0,Hour_Minute_RTM
1,TM1CE_1~1,1767
1,TM1CE_2~2
1,TM1CE_3~3
1,TM1CE_4~4
1,TM1CE_5~5
1,TM1CE_6~6
1,TM1SW_1~7
1,TM1SW_2~8
1,TM1SW_3~9
1,TM1SW_4~10
1,TM1SW_5~11
1,TM1SW_6~12
1,TM1SW_7~13
1,TM1SW_8~14
1,TM1SW_9~15
1,TM1SW_10~16
1,TM2SW_1~17
1,TM2SW_2~18
1,TM2SW_3~19
1,TM2SW_4~20
1,TM2SW_5~21
1,TM2SW_6~22
1,TM2SW_7~23
1,TM2CE_1~24
1,TM2CE_2~25
1,TM2CE_3~26
1,TM2CE_4~27
1,TM2CE_5~28
1,TM2CE_6~29
1,TM2CE_7~30

1,TM2CE_8~31
1,TM2CE_9~32
1,TM3CE_1~33
1,TM3CE_2~34
1,TM3CE_3~35
1,TM3CE_4~36
1,TM3CE_5~37
1,TM3CE_6~38
1,TM3SW_1~39
1,TM3SW_2~40
1,TM3SW_3~41
1,TM3SW_4~42
1,TM3SW_5~43
1,TM3SW_6~44
1,TM3SW_7~45
1,TM3SW_8~46
1,TM3SW_9~47
1,TM3CE_10~48
1,M1CE_1~49
1,M1CE_2~50
1,M1CE_3~51
1,M1CE_4~52
1,M1CE_5~53
1,M1CE_6~54
1,M1SW_1~55
1,M1SW_2~56
1,M1SW_3~57
1,M1SW_4~58
1,M1SW_5~59
1,M1SW_6~60
1,M1SW_7~61
1,M1SW_8~62
1,M1SW_9~63
1,M1SW_10~64
1,M2SW_1~65
1,M2SW_2~66
1,M2SW_3~67
1,M2SW_4~68
1,M2SW_5~69
1,M2SW_6~70
1,M2SW_7~71
1,M2CE_1~72
1,M2CE_2~73
1,M2CE_3~74
1,M2CE_4~75
1,M2CE_5~76

1,M2CE_6~77
1,M2CE_7~78
1,M2CE_8~79
1,M2CE_9~80
1,M3CE_1~81
1,M3CE_2~82
1,M3CE_3~83
1,M3CE_4~84
1,M3CE_5~85
1,M3CE_6~86
1,M3SW_1~87
1,M3SW_2~88
1,M3SW_3~89
1,M3SW_4~90
1,M3SW_5~91
1,M3SW_6~92
1,M3SW_7~93
1,M3SW_8~94
1,M3SW_9~95
1,M3SW_10~96
1,Battery~97

E.1.2 Datalogger #2

;{CR10X}
;
*Table 1 Program
 01: 7200 Execution Interval (seconds)

;Multiplexer 4

1: Do (P86)
 1: 41 Set Port 1 High

;Spot Weldable

2: Beginning of Loop (P87)
 1: 0000 Delay
 2: 7 Loop Count

 3: Do (P86)
  1: 72 Pulse Port 2

```
;20ms Pause

   4:  Excitation with Delay (P22)
    1: 1        Ex Channel
    2: 10       Delay W/Ex (0.01 sec units)
    3: 10       Delay After Ex (0.01 sec units)
    4: 0000     mV Excitation


   5:  Excite-Delay (SE) (P4)
    1: 1        Reps
    2: 15       2500 mV Fast Range
    3: 1        SE Channel
    4: 1        Excite all reps w/Exchan 1
    5: 1        Delay (0.01 sec units)
    6: 2500     mV Excitation
    7: 1     -- Loc [ TM4SW_1   ]
    8: .001     Multiplier
    9: 0.0      Offset


   6:  Polynomial (P55)
    1: 1        Reps
    2: 1     -- X Loc [ TM4SW_1   ]
    3: 1     -- F(X) Loc [ TM4SW_1   ]
    4: -104.78  C0
    5: 378.11   C1
    6: -611.59  C2
    7: 544.27   C3
    8: -240.91  C4
    9: 43.089   C5


   7:  Vibrating Wire (SE) (P28)
    1: 1        Reps
    2: 5        SE Channel
    3: 1        Excite all reps w/Exchan 1
    4: 14       Starting Freq. (100 Hz units)
    5: 35       End Freq. (100 Hz units)
    6: 250      No. of Cycles
    7: 50       Rep Delay (0.01 sec units)
    8: 49    -- Loc [ M4SW_1    ]
    9: 391      Multiplier
   10: 0.0      Offset
```

8: End (P95)

;Embedment

9: Beginning of Loop (P87)
 1: 0000   Delay
 2: 9   Loop Count

    10: Do (P86)
     1: 72   Pulse Port 2

; 20ms Pause

    11: Excitation with Delay (P22)
     1: 1   Ex Channel
     2: 10   Delay W/Ex (0.01 sec units)
     3: 10   Delay After Ex (0.01 sec units)
     4: 0000   mV Excitation

    12: Excite-Delay (SE) (P4)
     1: 1   Reps
     2: 15   2500 mV Fast Range
     3: 1   SE Channel
     4: 1   Excite all reps w/Exchan 1
     5: 1   Delay (0.01 sec units)
     6: 2500   mV Excitation
     7: 8   -- Loc [TM4CE_1   ]
     8: .001   Multiplier
     9: 0.0   Offset

    13: Polynomial (P55)
     1: 1   Reps
     2: 8   -- X Loc [TM4CE_1   ]
     3: 8   -- F(X) Loc [TM4CE_1   ]
     4: -104.78 C0
     5: 378.11   C1
     6: -611.59 C2
     7: 544.27   C3
     8: -240.91 C4
     9: 43.089   C5

14: Vibrating Wire (SE) (P28)
1: 1 Reps
2: 5 SE Channel
3: 1 Excite all reps w/Exchan 1
4: 4 Starting Freq. (100 Hz units)
5: 12 End Freq. (100 Hz units)
6: 250 No. of Cycles
7: 50 Rep Delay (0.01 sec units)
8: 56 -- Loc [M4CE_1]
9: 3304 Multiplier
10: 0.0 Offset

15: End (P95)

16: Do (P86)
1: 51 Set Port 1 Low

;Multiplexer 5

17: Do (P86)
1: 43 Set Port 3 High

;Embedment

18: Beginning of Loop (P87)
1: 0000 Delay
2: 6 Loop Count

19: Do (P86)
1: 74 Pulse Port 4

;20ms Pause

20: Excitation with Delay (P22)
1: 1 Ex Channel
2: 10 Delay W/Ex (0.01 sec units)
3: 10 Delay After Ex (0.01 sec units)
4: 0000 mV Excitation

21: Excite-Delay (SE) (P4)
1: 1 Reps
2: 15 2500 mV Fast Range

```
 3: 2        SE Channel
 4: 1        Excite all reps w/Exchan 1
 5: 1        Delay (0.01 sec units)
 6: 2500     mV Excitation
 7: 17    -- Loc [ TM5CE_1   ]
 8: .001     Multiplier
 9: 0.0      Offset


22:  Polynomial (P55)
 1: 1        Reps
 2: 17    -- X Loc [ TM5CE_1   ]
 3: 17    -- F(X) Loc [ TM5CE_1   ]
 4: -104.78  C0
 5: 378.11   C1
 6: -611.59  C2
 7: 544.27   C3
 8: -240.91  C4
 9: 43.089   C5


23:  Vibrating Wire (SE) (P28)
 1: 1        Reps
 2: 6        SE Channel
 3: 1        Excite all reps w/Exchan 1
 4: 4        Starting Freq. (100 Hz units)
 5: 12       End Freq. (100 Hz units)
 6: 250      No. of Cycles
 7: 50       Rep Delay (0.01 sec units)
 8: 65    -- Loc [ M5CE_1    ]
 9: 3304     Multiplier
10: 0.0      Offset


24:  End (P95)

;Spot Weldable

25:  Beginning of Loop (P87)
 1: 0000     Delay
 2: 10       Loop Count


26:  Do (P86)
 1: 74       Pulse Port 4
```

```
;20ms Pause

   27:  Excitation with Delay (P22)
    1: 1        Ex Channel
    2: 10       Delay W/Ex (0.01 sec units)
    3: 10       Delay After Ex (0.01 sec units)
    4: 0000     mV Excitation


   28:  Excite-Delay (SE) (P4)
    1: 1        Reps
    2: 15       2500 mV Fast Range
    3: 2        SE Channel
    4: 1        Excite all reps w/Exchan 1
    5: 1        Delay (0.01 sec units)
    6: 2500     mV Excitation
    7: 23    -- Loc [ TM5SW_1   ]
    8: .001     Multiplier
    9: 0.0      Offset


   29:  Polynomial (P55)
    1: 1        Reps
    2: 23    -- X Loc [ TM5SW_1   ]
    3: 23    -- F(X) Loc [ TM5SW_1   ]
    4: -104.78  C0
    5: 378.11   C1
    6: -611.59  C2
    7: 544.27   C3
    8: -240.91  C4
    9: 43.089   C5


   30:  Vibrating Wire (SE) (P28)
    1: 1        Reps
    2: 6        SE Channel
    3: 1        Excite all reps w/Exchan 1
    4: 14       Starting Freq. (100 Hz units)
    5: 35       End Freq. (100 Hz units)
    6: 250      No. of Cycles
    7: 50       Rep Delay (0.01 sec units)
    8: 71    -- Loc [ M5SW_1    ]
    9: 391      Multiplier
   10: 0.0      Offset
```

31: End (P95)

32: Do (P86)
 1: 53   Set Port 3 Low

;Multiplexer 6

33: Do (P86)
 1: 45   Set Port 5 High

;Spot Weldable

34: Beginning of Loop (P87)
 1: 0000   Delay
 2: 7   Loop Count

35: Do (P86)
 1: 76   Pulse Port 6

;20ms Pause

36: Excitation with Delay (P22)
 1: 1   Ex Channel
 2: 10   Delay W/Ex (0.01 sec units)
 3: 10   Delay After Ex (0.01 sec units)
 4: 0000   mV Excitation

37: Excite-Delay (SE) (P4)
 1: 1   Reps
 2: 15   2500 mV Fast Range
 3: 3   SE Channel
 4: 1   Excite all reps w/Exchan 1
 5: 1   Delay (0.01 sec units)
 6: 2500   mV Excitation
 7: 33   -- Loc [TM6SW_1   ]
 8: .001   Multiplier
 9: 0.0   Offset

38: Polynomial (P55)
 1: 1   Reps
 2: 33   -- X Loc [TM6SW_1   ]
 3: 33   -- F(X) Loc [TM6SW_1   ]

```
 4: -104.78  C0
 5: 378.11   C1
 6: -611.59  C2
 7: 544.27   C3
 8: -240.91  C4
 9: 43.089   C5


39:  Vibrating Wire (SE) (P28)
 1: 1        Reps
 2: 7        SE Channel
 3: 1        Excite all reps w/Exchan 1
 4: 14       Starting Freq. (100 Hz units)
 5: 35       End Freq. (100 Hz units)
 6: 250      No. of Cycles
 7: 50       Rep Delay (0.01 sec units)
 8: 81    -- Loc [ M6SW_1    ]
 9: 391      Multiplier
10: 0.0      Offset


40:  End (P95)

;Embedment

41:  Beginning of Loop (P87)
 1: 0000     Delay
 2: 9        Loop Count


42:  Do (P86)
 1: 76       Pulse Port 6

;20ms Pause

43:  Excitation with Delay (P22)
 1: 1        Ex Channel
 2: 10       Delay W/Ex (0.01 sec units)
 3: 10       Delay After Ex (0.01 sec units)
 4: 0000     mV Excitation


44:  Excite-Delay (SE) (P4)
 1: 1        Reps
 2: 15       2500 mV Fast Range
 3: 3        SE Channel
```

4: 1 Excite all reps w/Exchan 1
5: 1 Delay (0.01 sec units)
6: 2500 mV Excitation
7: 40 -- Loc [TM6CE_1]
8: .001 Multiplier
9: 0.0 Offset

45: Polynomial (P55)
1: 1 Reps
2: 40 -- X Loc [TM6CE_1]
3: 40 -- F(X) Loc [TM6CE_1]
4: -104.78 C0
5: 378.11 C1
6: -611.59 C2
7: 544.27 C3
8: -240.91 C4
9: 43.089 C5

46: Vibrating Wire (SE) (P28)
1: 1 Reps
2: 7 SE Channel
3: 1 Excite all reps w/Exchan 1
4: 4 Starting Freq. (100 Hz units)
5: 12 End Freq. (100 Hz units)
6: 250 No. of Cycles
7: 50 Rep Delay (0.01 sec units)
8: 88 -- Loc [M6CE_1]
9: 3304 Multiplier
10: 0.0 Offset

47: End (P95)

48: Do (P86)
1: 55 Set Port 5 Low

49: Batt Voltage (P10)
1: 97 Loc [Battery]

50: Do (P86)
1: 10 Set Output Flag High (Flag 0)

```
51:  Real Time (P77)^10788
 1: 110      Day,Hour/Minute (midnight = 0000)


52:  Resolution (P78)
 1: 1        High Resolution


53:  Sample (P70)^1767
 1: 97       Reps
 2: 1        Loc [ TM4SW_1    ]


54:  Serial Out (P96)
 1: 71       Storage Module



*Table 2 Program
  02: 0.0000    Execution Interval (seconds)

*Table 3 Subroutines

End Program




-Input Locations-
1 TM4SW_1    1 2 2
2 TM4SW_2    1 1 0
3 TM4SW_3    1 1 0
4 TM4SW_4    1 1 0
5 TM4SW_5    1 1 0
6 TM4SW_6    1 1 0
7 TM4SW_7    1 1 0
8 TM4CE_1    1 2 2
9 TM4CE_2    1 1 0
10 TM4CE_3    1 1 0
11 TM4CE_4    1 1 0
12 TM4CE_5    1 1 0
13 TM4CE_6    1 1 0
14 TM4CE_7    1 1 0
```

15 TM4CE_8 1 1 0
16 TM4CE_9 1 1 0
17 TM5CE_1 1 2 2
18 TM5CE_2 1 1 0
19 TM5CE_3 1 1 0
20 TM5CE_4 1 1 0
21 TM5CE_5 1 1 0
22 TM5CE_6 1 1 0
23 TM5SW_1 1 2 2
24 TM5SW_2 1 1 0
25 TM5SW_3 1 1 0
26 TM5SW_4 1 1 0
27 TM5SW_5 1 1 0
28 TM5SW_6 1 1 0
29 TM5SW_7 1 1 0
30 TM5SW_8 1 1 0
31 TM5SW_9 1 1 0
32 TM5SW_10 0 0 0
33 TM6SW_1 1 2 2
34 TM6SW_2 1 1 0
35 TM6SW_3 1 1 0
36 TM6SW_4 1 1 0
37 TM6SW_5 1 1 0
38 TM6SW_6 1 1 0
39 TH6SW_7 1 0 0
40 TM6CE_1 1 2 2
41 TM6CE_2 1 1 0
42 TM6CE_3 1 1 0
43 TM6CE_4 1 1 0
44 TM6CE_5 1 1 0
45 TM6CE_6 1 1 0
46 TM6CE_7 1 1 0
47 TM6CE_8 1 1 0
48 TM6CE_9 1 1 0
49 M4SW_1 1 1 1
50 M4SW_2 1 1 0
51 M4SW_3 1 1 0
52 M4SW_4 1 1 0
53 M4SW_5 1 1 0
54 M4SW_6 1 1 0
55 M4SW_7 0 0 0
56 M4CE_1 1 1 1
57 M4CE_2 1 1 0
58 M4CE_3 1 1 0
59 M4CE_4 1 1 0
60 M4CE_5 1 1 0

61 M4CE_6 1 1 0
62 M4CE_7 1 1 0
63 M4CE_8 1 1 0
64 M4CE_9 1 1 0
65 M5CE_1 1 1 1
66 M5CE_2 1 1 0
67 M5CE_3 1 1 0
68 M5CE_4 1 1 0
69 M5CE_5 1 1 0
70 M5CE_6 1 1 0
71 M5SW_1 1 1 1
72 M5SW_2 1 1 0
73 M5SW_3 1 1 0
74 M5SW_4 1 1 0
75 M5SW_5 1 1 0
76 M5SW_6 1 1 0
77 M5SW_7 1 1 0
78 M5SW_8 1 1 0
79 M5SW_9 1 1 0
80 M5SW_10 0 0 0
81 M6SW_1 1 1 1
82 M6SW_2 1 1 0
83 M6SW_3 1 1 0
84 M6SW_4 1 1 0
85 M6SW_5 1 1 0
86 M6SW_6 1 1 0
87 M6SW_7 0 0 0
88 M6CE_1 1 0 1
89 M6CE_2 1 1 0
90 M6CE_3 1 1 0
91 M6CE_4 1 1 0
92 M6CE_5 1 1 0
93 M6CE_6 1 1 0
94 M6CE_7 1 1 0
95 M6CE_8 1 1 0
96 M6CE_9 1 1 0
97 Battery 1 0 1
-Program Security-
0000
0000
0000
-Mode 4-
-Final Storage Area 2-
0
-CR10X ID-
0

-CR10X Power Up-
3
-CR10X Compile Setting-
3
-CR10X RS-232 Setting-
-1
-DLD File Labels-
0
-Final Storage Labels-
0,Day_RTM,10788
0,Hour_Minute_RTM
1,TM4SW_1~1,1767
1,TM4SW_2~2
1,TM4SW_3~3
1,TM4SW_4~4
1,TM4SW_5~5
1,TM4SW_6~6
1,TM4SW_7~7
1,TM4CE_1~8
1,TM4CE_2~9
1,TM4CE_3~10
1,TM4CE_4~11
1,TM4CE_5~12
1,TM4CE_6~13
1,TM4CE_7~14
1,TM4CE_8~15
1,TM4CE_9~16
1,TM5CE_1~17
1,TM5CE_2~18
1,TM5CE_3~19
1,TM5CE_4~20
1,TM5CE_5~21
1,TM5CE_6~22
1,TM5SW_1~23
1,TM5SW_2~24
1,TM5SW_3~25
1,TM5SW_4~26
1,TM5SW_5~27
1,TM5SW_6~28
1,TM5SW_7~29
1,TM5SW_8~30
1,TM5SW_9~31
1,TM5SW_10~32
1,TM6SW_1~33
1,TM6SW_2~34
1,TM6SW_3~35

1,TM6SW_4~36
1,TM6SW_5~37
1,TM6SW_6~38
1,TH6SW_7~39
1,TM6CE_1~40
1,TM6CE_2~41
1,TM6CE_3~42
1,TM6CE_4~43
1,TM6CE_5~44
1,TM6CE_6~45
1,TM6CE_7~46
1,TM6CE_8~47
1,TM6CE_9~48
1,M4SW_1~49
1,M4SW_2~50
1,M4SW_3~51
1,M4SW_4~52
1,M4SW_5~53
1,M4SW_6~54
1,M4SW_7~55
1,M4CE_1~56
1,M4CE_2~57
1,M4CE_3~58
1,M4CE_4~59
1,M4CE_5~60
1,M4CE_6~61
1,M4CE_7~62
1,M4CE_8~63
1,M4CE_9~64
1,M5CE_1~65
1,M5CE_2~66
1,M5CE_3~67
1,M5CE_4~68
1,M5CE_5~69
1,M5CE_6~70
1,M5SW_1~71
1,M5SW_2~72
1,M5SW_3~73
1,M5SW_4~74
1,M5SW_5~75
1,M5SW_6~76
1,M5SW_7~77
1,M5SW_8~78
1,M5SW_9~79
1,M5SW_10~80
1,M6SW_1~81

1,M6SW_2~82
1,M6SW_3~83
1,M6SW_4~84
1,M6SW_5~85
1,M6SW_6~86
1,M6SW_7~87
1,M6CE_1~88
1,M6CE_2~89
1,M6CE_3~90
1,M6CE_4~91
1,M6CE_5~92
1,M6CE_6~93
1,M6CE_7~94
1,M6CE_8~95
1,M6CE_9~96
1,Battery~97